



THE UNIVERSITY OF ADELAIDE

The effect of clinical polishing protocols on
ceramic surface texture and wear rate of opposing
enamel: A laboratory study

MICHAEL ZANINOVICH

Thesis submitted for the degree of Doctor of Clinical Dentistry (Prosthodontics)

School of Dentistry

The University of Adelaide

TABLE OF CONTENTS

TABLE OF CONTENTS	II
PREFACE	VIII
ABSTRACT	IX
DECLARATION	X
ACKNOWLEDGEMENTS	XI
SECTION ONE	1
CHAPTER 1 MASTICATORY SYSTEM	2
1.1. Physical and mechanical properties of human teeth	2
1.2. Biomechanical process of mastication.....	4
CHAPTER 2 TOOTH WEAR	6
2.1. Historical background	6
2.2. Clinical importance of wear of teeth and dental materials	7
2.3. Wear behaviour of enamel and dentine	8
2.4. Aetiology, mechanisms and definitions of tooth wear processes	8
2.5. Attrition	9
2.6. Abrasion	12
2.7. Adhesion.....	16
2.8. Erosion.....	17
2.9. Saliva and tooth wear	20
2.10. Prevalence of tooth wear	21
2.11. Tooth wear and Quality of Life	21
CHAPTER 3 WEAR & SURFACE TEXTURE ANALYSIS	22
3.1. Methods of assessment of tooth and restorative material wear	22
3.2. Qualitative wear assessment methods	22
3.2.1. Tooth Wear Index	22
3.2.2. United States Public Health Services criteria	23
3.2.3. Clinical comparative scales	23
3.2.4. Hardness and erosive wear	24

3.3.	Quantitative methods of wear analysis	24
3.3.1.	Chemical analysis	25
3.3.2.	Microradiography	25
3.3.3.	Digital image analysis.....	25
3.3.4.	Surface profilometry and mapping	26
3.3.4.1.	Mechanical contact profilometer	26
3.3.4.2.	Non-contact profilometer	27
3.3.4.2.1.	Engineering principles of non contacting optical profilometer	28
3.3.5.	Scanning Electron Microscopy	29
3.3.6.	Secondary ion mass spectroscopy.....	31
3.4.	Importance of surface texture analysis in dentistry	32
3.5.	Amplitude parameters	33
3.5.1.	Roughness Amplitude Parameters	34
CHAPTER 4 TRIBOLOGY		41
4.1.	Adhesive wear	43
4.2.	Abrasive wear	43
4.3.	Fatigue wear	46
4.4.	Erosive wear	48
4.5.	Fretting wear.....	48
CHAPTER 5 CERAMICS.....		50
5.1.	Historical background	50
5.2.	Modern Dental Ceramics.....	51
5.3.	Chemical structures of dental ceramics	51
5.4.	Classifications of dental ceramics	54
5.5.	Predominately Glass Ceramics	56
5.6.	Particle Filled Glass Ceramics.....	57
5.6.1.	Glass Ceramics (subgroup of Particle Filled Glass Ceramics)	57
5.6.1.1.	Leucite-reinforced glass ceramic- IPS Empress CAD	58
5.6.1.1.1.	Microstructure.....	58
5.6.1.1.2.	Chemical composition.....	59
5.6.1.1.3.	Physical	59
5.6.1.2.	Lithium disilicate glass ceramic- IPS e.max Pressed and CAD blocks.....	60
5.6.1.2.1.	Standard chemical composition	60
5.6.1.2.2.	Physical properties	61
5.6.1.2.3.	Processing and manufacturing	62
5.6.1.2.4.	Microstructure lithium disilicate IPS e.max CAD Blocks	62
5.6.1.2.5.	Microstructure IPS e.max Press	65
5.7.	Polycrystalline ceramics.....	66
5.7.1.	Alumina-based ceramic	67

5.7.2.	Zirconia-based ceramic	68
CHAPTER 6 IN-VITRO CERAMIC WEAR TESTING		71
6.1.	Considerations of <i>in vitro</i> ceramic wear testing	71
6.2.	Quantification of wear	71
6.3.	Standardising wear simulation research protocols.....	72
6.4.	<i>In vitro</i> ceramic wear research test parameters.....	73
6.4.1.	Chewing simulators	73
6.4.1.1.	Willytec chewing simulator	73
6.4.2.	Loads applied to specimens	74
6.4.3.	The force actuator	74
6.4.4.	Number of cycles.....	74
6.4.5.	Exogenous abrasive materials.....	75
6.4.6.	Lubrication and pH variations	75
6.4.7.	Specimen geometry	76
6.5.	The outcome of <i>in vitro</i> test parameter variation.....	77
6.6.	Factors influencing enamel wear when opposed by ceramic.....	77
6.6.1.	Ceramic Physical Microstructural Properties	78
6.6.2.	Hardness	78
6.6.3.	Frictional resistance	79
6.6.4.	Fracture toughness	79
6.6.5.	Porosity.....	80
6.6.6.	Crystals	81
6.6.7.	Ceram Layer	82
6.6.8.	Effect of surface finish.....	83
6.7.	Ceramic surface texture and tooth wear	83
CHAPTER 7 MINIMISING SURFACE ROUGHNESS		87
7.1.	Ceramic Clinical Polishing	87
7.1.1.	Polishing Engineering Principles.....	87
7.2.	Glaze Process	89
7.3.	Ceramic surface texture and different surface finishing protocols	90
7.4.	Ceramic surface texture and mechanical properties	96
SECTION TWO		99
CHAPTER 8 RATIONALE, AIMS AND HYPOTHESIS.....		100
8.1.	Rationale.....	100
8.2.	Study Aims	100
8.3.	Hypothesis	101

CHAPTER 9 MATERIALS AND METHODS.....	102
9.1. STUDY A.....	102
9.1.1. Sample preparation	102
9.1.2. Ceramic samples.....	102
9.1.3. Surface texture altitude parameters.....	104
9.1.3.1. Double Determinations for surface texture analysis.....	105
9.1.3.2. Programat CS Furnace	105
9.1.3.3. Slow speed Saw.....	106
9.1.3.4. Finishing diamonds	108
9.1.3.5. Optrafine polishing system.....	108
9.1.3.6. Sof-Lex discs.....	109
9.1.3.7. Glazing.....	110
9.2. STUDY B.....	110
9.2.1. Preparation of tooth specimens.....	110
9.2.2. Mounting specimens of Scanning Electron Microscopy (SEM) studs.....	111
9.2.3. Assessment of tooth and ceramic wear	114
9.2.3.1. Optical Microscope 3D assessment: Leica MZ16FA stereo microscope	114
9.2.3.2. Three Dimensional Scanning and quantitative results	115
9.2.3.2.1. 3D PIX-4 scanner.....	116
9.2.3.2.2. “Dr.PICZA” software.....	116
9.2.3.2.3. Matlab 6.5	117
9.2.3.2.4. Validity and reliability of 3D Scanning and quantitative results.....	120
9.2.3.3. Scanning Electron Microscopy (SEM) and qualitative results.....	120
9.2.3.3.1. Fabrication of specimen replicas.....	120
9.2.3.3.2. Scanning Electron Microscopy (SEM) observations	120
9.2.4. Tooth wear simulator protocol.....	122
9.2.4.1. Willytec tooth wear design.....	123
9.2.4.1.1. Method of lubrication.....	127
9.2.5. Statistical analysis.....	128
9.2.5.1. Double Determinations for volumetric analysis.....	128
CHAPTER 10 RESULTS STUDY A – SUFACE ROUGHNESS	130
10.1. SEM analysis.....	130
10.2. Leica MC 90 light microscope surface texture analysis	135
10.2.1. Surface characteristics before wear simulation	135
10.2.1.1. Leucite-reinforced ceramic	135
10.2.1.2. Lithium disilicate ceramic	137
10.3. Surface finishing protocols and glass ceramics	139
CHAPTER 11 RESULTS STUDY B - WEAR.....	140
11.1. SEM analysis.....	140

11.2.	Leica MC 90 light microscope surface texture post wear analysis.....	140
11.2.1.	Leucite-reinforced ceramic	140
11.2.2.	Lithium disilicate ceramics	141
11.2.3.	Surface texture comparison between ceramics after wear simulation.....	142
11.2.4.	Enamel specimens.....	143
11.3.	Volumetric analysis of enamel opposing leucite-reinforced ceramic	144
11.4.	Volumetric analysis of enamel opposing lithium disilicate ceramic	146
11.5.	Volumetric analysis of enamel when abraded against an enamel specimen.....	147
11.6.	Volumetric loss of enamel when abraded against enamel, leucite-reinforced and lithium disilicate ceramic specimens.....	147
SECTION THREE.....		149
CHAPTER 12 DISCUSSION		150
12.1.	Importance of ceramic surface texture and effectiveness of finishing methods	150
12.2.	Visual appearance of the effect of different finishing protocols.....	150
12.3.	Efficacy of Optrafine finishing system and leucite-reinforced ceramics.....	151
12.4.	Efficacy of Optrafine finishing system and lithium disilicate ceramics	151
12.5.	Efficacy of Sof-Lex finishing method	152
12.6.	Efficacy of diamond polishing paste finishing method	153
12.7.	Surface texture comparison of leucite-reinforced and lithium disilicate ceramic before after wear simulation	153
12.8.	Comparison of enamel specimen surface texture before and after wear simulation.....	153
12.9.	Limitations of <i>in vitro</i> wear studies	154
12.10.	Current <i>in vitro</i> study parameters	155
12.11.	Influence of ceramic initial surface texture and, finishing methods on opposing enamel wear rate	155
12.12.	Influence of ceramic hardness on opposing enamel wear rate	157
12.13.	Influence of the ceramic material on opposing enamel wear	158
12.14.	Influence of the ceramic microstructure porosity and flaws on opposing enamel wear	159
CHAPTER 13 CONCLUSIONS		161
SECTION FOUR.....		162
CHAPTER 14 REFERENCES		163
SECTION FIVE.....		189
CHAPTER 15 APPENDICES		190

FIGURES.....212

PREFACE

This thesis reports on research completed during my Doctorate of Clinical Dentistry at the School of Dentistry, The University of Adelaide, from January 2010 to December 2012. There were two aims of the research project. Firstly to determine the polishability of modern CAD glass ceramic restorative material and secondly to investigate what influence the surface texture of modern CAD glass ceramics had on the wear rate of opposing enamel tooth structure.

ABSTRACT

There has been a significant increase in the delivery of all ceramic restorations especially with the global explosion of CAD CAM technology. Frequently, the ceramic restorations require refinements to the surfaces with abrasives prior to or after cementation. If adjustments are made to a glazed or non-glazed surface after cementation, only mechanical polishing is an option to restore the surface texture.

Surface roughness of ceramic restorations influences the aesthetics, functional and biological parameters of the restoration [1, 2]. A relatively rough surface can negatively influence the strength [3, 4] and longevity of a restoration [5, 6], increase friction [7] and rate of wear of the restoration [8] and opposing tooth structure [9], promote gingival inflammation [10], adverse soft tissue reactions [11], and the accumulation of stains and plaque on the surface [12-14]. Recent low fusing ceramics have properties which improve the surface characteristics and allows a relatively smoother surface to be achieved either by glazing or polishing [15, 16].

The aim of this study is to increase the understanding of the surface characteristics produced from either glazing or polishing and what impact the surface texture produced from such finishing methods has on the wear rate of opposing enamel. Clinically this will assist with decision making regarding the most effective method to achieve an optimal ceramic surface finish.

DECLARATION

This work contains no material which has been accepted for the award of any other degree or diploma in any other university or other tertiary institution to Michael Zaninovich and, to the best of my knowledge and belief, contains no material previously published or written by another person, except where due reference has been made in the text.

I certify that no part of this work will, in the future, be used in a submission for any other degree or diploma in any university of other tertiary institution without the prior approval of the University of Adelaide.

I give consent to this copy of my thesis when deposited in the University library, being made available for loan and photocopying, subject to the provisions of the Copyright Act 1968.

I also give permission for the digital version of my thesis to be made available on the web, via the University's digital research repository, the Library catalogue, the Australasian Digital Theses Program (ADTP) and also through the web search engines, unless permission has been granted by the University to restrict access for a period of time.

MICHAEL ZANINOVICH

Dated this.....day of2013

ACKNOWLEDGEMENTS

I take this opportunity to express my thanks to many people who have provided their assistance in the production of this report and throughout my time at the School of Dentistry, The University of Adelaide.

I would like to sincerely thank my supervisors Professor Lindsay Richards, Dr Tom Berekally and Dr Vladimir Hotinski for their wise and thoughtful advice and support. My benefit from their broad experience and knowledge is greatly appreciated.

My thanks also extends to Winthrop Professor Paul Abbott from the University of Western Australia for allowing me the opportunity to the use of the Willytec chewing simulator, Mr Angus Netting from the Centre of Electron Microscopy and Microstructure Analysis at The University of Adelaide and Geoff Staples and Mr Peter Lobo from Ivoclar Vivadent.

I would like to thank my friends and fellow prosthodontic students Dr Amal Mamdouh Bakey and Dr Sofie Diem Bui for their wonderful friendship. It has been a great pleasure to study with you both.

SECTION ONE

CHAPTER 1

MASTICATORY SYSTEM

1.1. Physical and mechanical properties of human teeth

Human teeth have a unique structure composed of the anisotropic parts: enamel, dentine-enamel junction, dentine, cementum, cemento-enamel junction and pulp. Dental enamel consists of about 94% inorganic substance, mainly hydroxyapatite and fluorapatite, 2% organic material and 4% water by weight [17, 18]. Enamel is comprised of long, thin rod like prisms, 2-3 μ m in diameter, arranged in a parallel order to the longitudinal side of the rods and roughly perpendicular to the dentine-enamel junction (Figure 1.1). The only areas where the enamel rods are arranged vertically to the tooth surface are the cusp tips and proximal edges [19]. As a unit the crystal structure forms a complex and complicated three-dimensional pattern [18]. The enamel prisms do not run a straight course from the dentine-enamel junction to the outer surface. Groups of prisms make a series of bends along the course. This gives rise to what is known as the Hunter-Schreger bands. Thus, the enamel is characterized by a subtle, intricate substructure. This well-ordered structure is also responsible for the typical etching pattern, which forms in the course of etching the enamel with acid. The organic components of enamel are composed of short peptide fragments, which are breakdown products of amelogenin, the enamel matrix protein [20]. The mechanical properties vary with the location on the tooth, local prism orientation and chemical composition [21, 22]. The high mineral content of enamel contributes to a high hardness, and the tensile strength reflects the brittleness of the enamel [21].

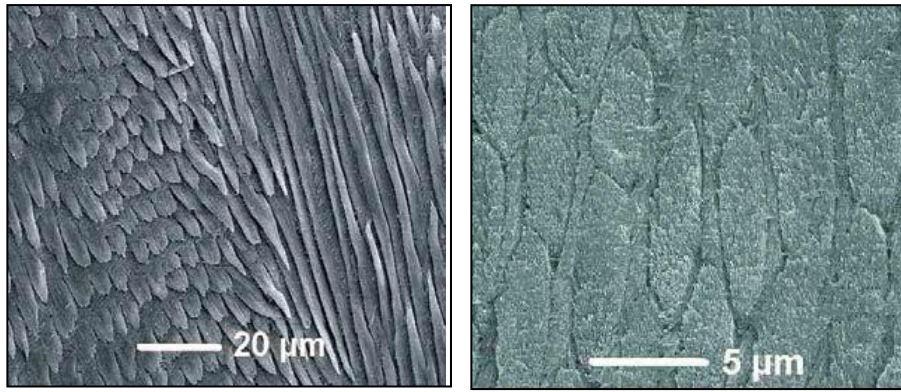


Figure 1.1 Scanning electron micrograph of etched enamel. The enamel rods have been cut longitudinally (left). The enamel rods have been cut diagonally (right) [23].

Dentine consists of about 70% inorganic material, 18% organic matrix and 12% water by weight [17, 24]. On a microscopic level, highly mineralised dentine material surrounds dentinal tubules which run through the entire dentinal substance. Densely arranged dentine tubules traverse the entire thickness of the dentine. A density of 59,000 to 76,000 tubules per mm^2 exists in the vicinity of the pulp [25]. The diameter of dentine tubules is approximately 2.5mm near the pulp and 0.9mm at the dentine-enamel junction [26]. The mechanical properties of dentine maintain the integrity of the overlying enamel and this relationship is most reflected at the junction between the enamel and dentine. Specifically, the biological dentine-enamel interface exhibits a high fracture toughness, thus making it possible to dissipate stresses and prevent crack propagation throughout the enamel hard tissues [21]. The mean physical and mechanical properties of enamel and dentine are outlined in Table 1.1. The values should only be regarded as estimations and general guidelines, as the data is compiled from different studies and textbooks, and the study design of the experiments that provided the data might have differed from one study to the other [17, 21, 22].

Table 1.1: Physical parameters (mean value) of enamel and dentine. [17,21, 22]

Physical Parameters (units)	Enamel	Dentine
Hardness (Gpa)	3.03	0.58
Flexural strength (Mpa)	141	172
Compressive strength (Mpa)	384	297
Tensile strength (Mpa)	10	52
Fracture toughness (Mpa m ^{1/2})	0.77	3.4
Young's modulus (Gpa)	94	20
Coefficient of thermal expansion (µm/m ^o K)	11.4	8.3
Density (g/cm ⁻³)	2.97	2.14
Thermal conductivity (Wm ⁻¹ K ⁻¹)	0.93	0.57
Friction coefficient µ	0.14	0.31

1.2. Biomechanical process of mastication

The biomechanical process of mastication is very complex. It is regulated by trigger zones in the brain stem and submitted to multiple feedback mechanisms, some of which are located in the periodontal ligament [27]. Mastication reduces the food bolus to a few square millimetres, which facilitates swallowing and aids digestion. The typical masticatory cycle can be divided into phases [28, 29]. Initially the mandible opens and slides into a lateral position to achieve physical contact with the food bolus. The second phase commences when the dentition contacts the food bolus and an occlusal load is applied. This load compresses the food bolus and essentially prepares the food for swallowing. In the final phase, the teeth move back to their original position.

The entire masticatory movement is further complicated because it is completed in two planes: the horizontal (lateral) and frontal planes [30]. In the horizontal plane, the movement line is an arc formed by rotation around the working condyle of the temporomandibular joint. When the working condyle is moving to a lateral position, the teeth on the balancing side lose contact in most patients. The profile of the force curve corresponds to the positive half of a sine curve and is therefore also called Haversine Wave Form [30].

The masticatory force depends on the texture of the food as well as on the location within the oral cavity. Higher forces are exerted in the posterior region and when grinding hard food. However, the biting force varies substantially between different individuals. The magnitude of biting force is in the range of 10 to 20 N in the initial biting phase and in the range of 100 to 140 N in the molars and 25 to 45 N in the incisor teeth at the end of the chewing cycle [31].

The mean duration of a typical masticatory cycle is approximately 0.8 seconds. The mean duration of occlusion is only approximately 0.4 to 0.6 seconds [27, 31] and the sliding distance is less than 1mm with a speed of 0.25 to 0.5 mm/sec [32]. Despite these averages there are many influencing factors that can alter the duration of a cycle [32].

Tooth contact periods add up to 15 to 30 minutes per day, depending on the eating frequencies and habits, not including the tooth contact during swallowing, which, however is only of a lower magnitude. If a mean chewing frequency of approximately 1.5 Hz and a chewing time of approximately 20 minutes per day are assumed, an individual carries out 4.87 million chewing cycles per year [32].

CHAPTER 2 TOOTH WEAR

2.1. Historical background

Tooth wear and friction mechanisms have been an area of scientific interest for many centuries [33], and tooth wear observations derived from human skulls were first published by Hunter [34] in one of the first text books dedicated to dentistry, '*The Natural History of Human teeth. Explaining their Structure, Use, Formation, Growth and Diseases.*' Since these modest beginnings of scientific tooth wear investigations, many diverse populations have been studied by an extensive list of researchers, and the wisdom attained concludes tooth wear to be a normal physiological process when the worn teeth remain functional throughout one's life [35]. It is apparent that there is variation of tooth wear in relation to its severity and pattern between various populations and this variation is hypothesized to be associated with the abrasiveness of the diet, the use of the teeth as tools, the environment, culture and gender of an individual [36].

Anthropological studies documenting historic populations report wear to occur mostly on the occlusal and interproximal surfaces. Anthropologists postulated this was advantageous from an evolutionary perspective for numerous reasons. Firstly, wear leads to flattening of the occlusal and interproximal surfaces causing an increased degree of lateral tooth contact. This leads to increased efficiency of mastication by increasing the degree of shearing force [36].

Secondly, the accompanying compensatory changes facilitated continued stability and function of the masticatory system [37]. Specifically, compensatory stomatognathic and dentoalveolar changes consist of continued tooth eruption, coronal migration and up-righting of anterior dentition, mesial drift and forward shifting of the mandibular teeth [38].

Clinical investigations report wear to historically be due to two main factors. The first factor being the increased number of chewing strokes necessary to adequately 'prepare' less refined and tougher foods into a bolus ready to swallow, and secondly due to the friction of the exogenous materials forced over the tooth surfaces [39, 40]. The correlation of hard and more abrasive food with advanced tooth wear has also been shown in more recent times by studying modern day indigenous populations who share coarse diets similar to historical populations such as Australian Aborigines [33].

The extent and severity of tooth wear on a population level has reduced in modern times. This has been postulated to be due to a softer, more refined and processed diet [39]. Despite the overall reduction of excessive or pathological tooth wear on a population level, it still remains to be a clinical problem in modern times.

2.2. Clinical importance of wear of teeth and dental materials

Wear of the enamel and dentine tissues of human teeth can result in various changes in the stomatognathic system. Such changes and outcomes, of which the degree of severity can be variable, include the following. Negative aesthetical effects, negative biological outcomes, such as increased risk of pulpitis, remodelling of the temporomandibular joints, ingestion or inhalation of potentially harmful artificial materials [41, 42] and negative functional effects including pathological opposing and adjacent teeth relationships, and a reduction of occlusal vertical height [43].

The evidence that occlusal wear leads to biological consequences on the stomatognathic system including dysfunction of the temporomandibular joint (TMJ), muscle pain or periodontal disease is limited and studies are conflicting [44-47]. Due to the highly adaptive capacity of the stomatognathic system, severe wear of the occlusal surfaces is not correlated with deteriorating oral health, and the loss of posterior support does not necessarily lead to increased wear of anterior teeth [48]

nor lead to an increased risk of temporomandibular disorder [49].

2.3. Wear behaviour of enamel and dentine

Dental enamel is highly resistant to wear with an annual wear rate of approximately 30-40mm [50, 51]. This quality is attributed to the intricate crystallite orientation of the enamel prisms, which give the enamel unparalleled hardness. The wear of enamel is mainly resulting from microfracture processes and characterised by delamination and microploughing. It does not appear to increase on a linear basis and is independent of the tooth type. With all other factors being equal, the wear rate of enamel is higher during the first two years with contact with the opposing teeth (running-in phase) and decreases thereafter (steady-state phase). This is likely due to the increase in surface area, resulting in a reduction in occlusal stress per unit area of tooth structure. The surface hardness of enamel and its wear depth varies with age and consequently, lower hardness and higher wear depths were observed in patients belonging to older age groups compared with patients belonging to young or middle aged groups [52]. The wear rate of enamel is defined as pathological when it is greater than 40 microns per year [53], however other definitions and criteria have been documented [54].

2.4. Aetiology, mechanisms and definitions of tooth wear processes

The Institution of Mechanical Engineers defines wear as “the progressive and destructive loss of a substance or material from the surface of a body brought about by mechanical action” [56]. More specifically to dentistry, tooth wear is defined as a macro-level oral manifestation [57] from at least five underlying aetiological processes, which seldom act mutually exclusively [58] but instead occur either synergistically, sequentially or alternately, and their influence can commonly be additive resulting in a much greater rate of tooth surface loss compared to if there was only one mechanism of tooth wear occurring [59].

The definition of processes associated with tooth wear such as “attrition”, “abrasion”,

“abfraction”, “corrosion” and “erosion” historically was often interchangeable and has contributed to confusion amongst colleagues. This may be due to the fact that such terms have slightly different meanings whether used by dental material scientists, oral biologists, pathologists, epidemiologists or tribologists when describing tooth wear. More recently, the definitions describing the general mechanisms of tooth wear have become more clearly described [60, 61].

2.5. Attrition

Attrition is originally a Latin word which means ‘rubbing against’ [33] however in modern times the definition has been expanded to describe the loss of tooth surface structure or ‘wear’ due to frictional and shear forces that occurs between opposing tooth contacts, without a food bolus or anything between them [62]. The characteristics and presentation of tooth wear due to attrition mainly include lustrous wear facets in opposing arches which correlate in a specific jaw relationship. With an increasing severity of attrition, tooth surfaces including cusp tips, incisal edges, occlusal and palatal surfaces are affected [50, 63], and the exposure of dentine is more likely which is a common characteristic of advanced wear [64]. Attrition does not clinically present with cupping of the dentine since the rate of dentine wear remains equal to the rate of enamel wear [33] (Figure 2.1).



Figure 2.1.1: Clinical image of male patient, 22 years of age. Severe attrition associated with parafunctional habit.



Figure 2.1.2: Occlusal view of upper teeth. Note loss of cusp tips and flattened occlusal surfaces.

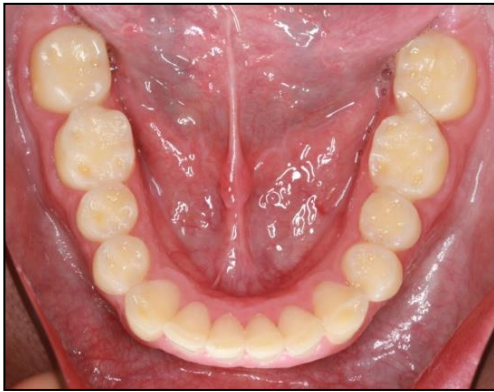


Figure 2.1.3: Occlusal view of lower teeth.



Figure 2.1.4: Right lateral view. Note equal dentine and enamel tissue height and communication of opposing teeth wear facets in lateral mandibular movement



Figure 2.1.5: Left lateral view.

Attrition-affected enamel examined under light microscopy and scanning electron microscope presents as intricate parallel striations within the borders and confines of the wear facets (Figure 2.2).

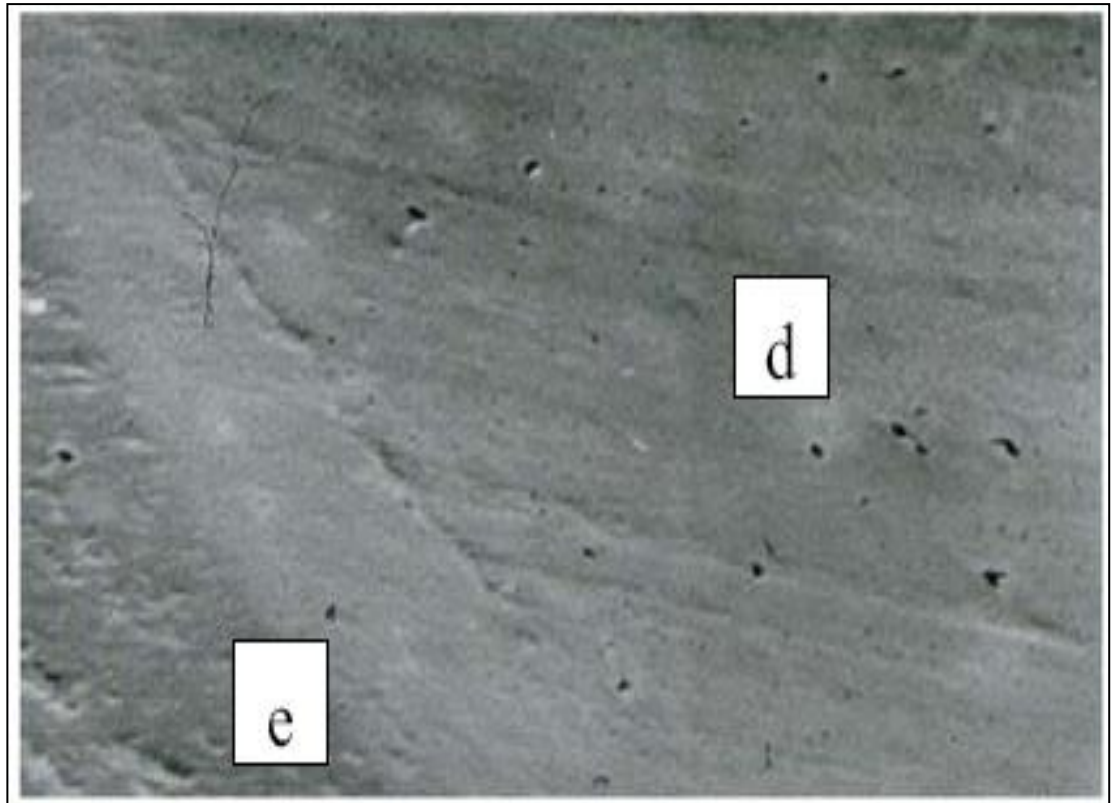


Figure 2.2: Scanning electron microscope image of wear facet showing parallel striations. The dentine (d) is not scooped out and is at the same level as the enamel (e)[33].

Opposing teeth contact during the conscious activity of chewing food and as a side effect during other processes, such as swallowing and speaking. Tooth contacts other than these are attributed to parafunctional or pathological actions or habits, namely bruxism [65].

The underlying mechanisms of parafunctional activity are multifactorial however largely unclear [66]. Parafunction has been thought to be associated with sleep disorders or a natural habitual process which is a characteristic of not only humans but other mammalian species. Based on several cross-sectional studies, estimates assume that the prevalence of parafunction in the industrialised countries is in the range of 20% with physiological stress factors being the most important aetiological

factor [67].

Parafunctional tooth contacting habits effectively increase the duration of frictional contact between teeth, resulting in a greater loss of tooth structure due to attrition [68, 69]. Longitudinal prospective studies show annual enamel loss in bruxers to be three or four times greater than that in non-bruxers [64]. The masticatory muscle forces and resultant bite force generated during normal and parafunctional activity may influence the rate of wear due to attrition [65], however clinical studies to support this hypothesis are unclear [70, 71]. Furthermore there is evidence to suggest muscle activity does not correlate with an increased maximal bite force and there is no difference in maximal bite force between people with pathologic attrition and people with healthy dentitions [67, 72]. Overloading and subjecting the teeth to excessively high occlusal forces is controlled by the protective feedback mechanism from the periodontal ligament nociceptors which are more sensitive to forces along the long axis of the tooth compared to lateral forces.

Attempts have been made to assess if there is a correlation between the number of occlusal contacts and the resulting amount of wear. The number of occluding contacts has been found to be proportional to the increase of attrition [71] however there are reports stating no relationship between missing posterior teeth and incisal tooth wear [73].

2.6. Abrasion

Abrasion wear (from Latin *abrasio* = wear or *abradere* = to scratch off) is the term to describe the mechanism of wear as a result of frictional forces between a tooth and an exogenous material. The location of wear often reflects its causative factors. Buccal and lingual tooth surfaces are more likely to be abraded when exposed to mechanical oral hygiene procedures, while occlusal surfaces are subject to both attrition and abrasive wear, which occurs almost simultaneously or in short subsequent episodes. Abrasion is linearly associated with age and diet [74]. It is more prevalent in cultures with a hard and abrasive diet than in cultures who ingest

refined and soft consistency food [33, 62]. Other common exogenous materials that have been known to cause abrasive wear include overzealous tooth brushing, incorrect use of floss and toothpicks, detrimental oral habits such as chewing tobacco, biting on hard objects such as pens, pencils or pipe stems; opening hair pins with teeth; and biting fingernails. Less common causes specific to certain occupations may occur among tailors or seamstresses who sever thread with their teeth, shoemakers and upholsterers who hold nails between their teeth, and glassblowers, and musicians who play wind instruments [33].

Light microscopy and scanning electron microscope studies reveal tooth surfaces affected by abrasion are pitted and gouged. Exposed dentine is likely to wear at a higher rate than surrounding enamel and will appear to be scooped out (Figure 2.3). Unlike wear by attrition which shows parallel striations, abrasive worn surfaces show irregular random scratch marks.



Figure 2.3: An example showing the effect of an abrasive diet on the teeth of a pre-contemporary Australian Aboriginal. Note the gouged and pitted enamel and the scooping of the dentine [33].

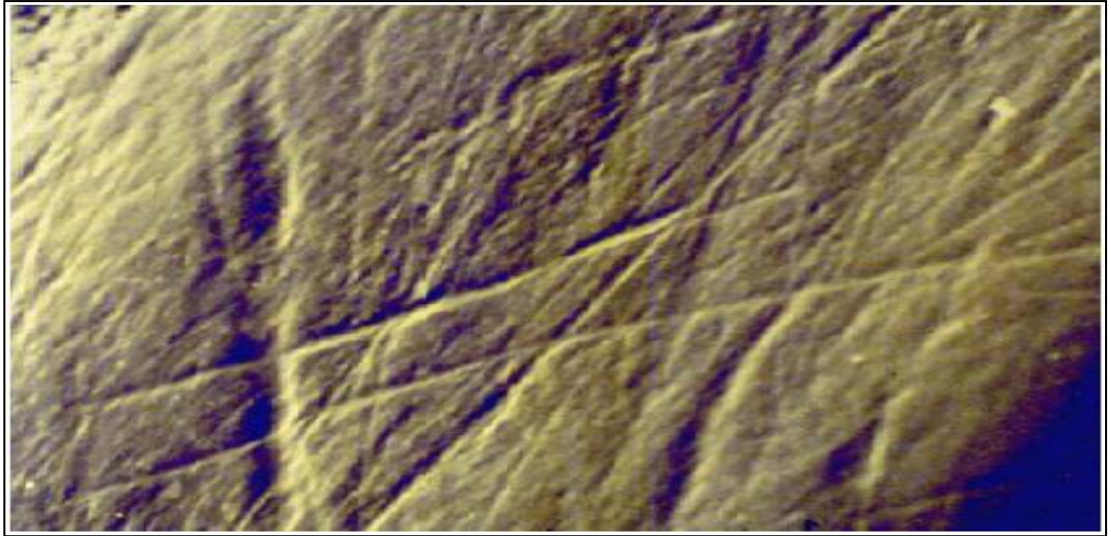


Figure 2.4: Microwear detail of an abrasion area showing haphazard scratch marks [33].



Figure 2.5: Clinical image of abrasion lesions on occlusal surfaces. Patient is 43 years old with history of gastric oesophageal reflux disease, severe parafunctional activity and hard bristle tooth brush. Note striations of enamel and scooping of the dentine.

Non carious cervical lesions (NCCL's) is a term to describe the clinical presentation of an abrasion or abfraction lesion on the buccal cervical region of a tooth. This type of lesion has become more prevalent in modern times [75]. The aetiology of NCCLs is multifactorial [76] and there are numerous aetiological, predisposing and perpetuating factors [55]. Risk factors include tooth brushing techniques, frequency, duration, bristle design, hardness and dentrifice abrasiveness [77]. The presence of an acidic environment dramatically increases the rate and severity of these types of wear lesions [55] (Figure 2.6).



Figure 2.6: Clinical image of 65 year old patient with non carious cervical lesions. Self-performed plaque control with hard bristle toothbrush.

Abfraction is a term used to describe the loss of tooth structure which is not due to wear but instead is the result of high tensile stress concentration from non-axial occlusal forces at the fulcrum point which is consistent with the most coronal point of the alveolar bone [78].

It has been hypothesised that this flexure causes fatigue and leads to breaking away of thin layers of enamel rods, and microfracture of cementum and dentine, frequently leading to a crescent form along the cervical line [79, 80]. Based on the clinical presentation of a non carious cervical lesion, it is difficult to determine the aetiological factors (Figure 2.7).



Figure 2.7: Multifactorial aetiology of NCCLs resulting in variation in NCCL morphology.

2.7. Adhesion

Adhesion wear (from Latin *adhaesio* =adherence) occurs when two solid surfaces slide over one another under pressure. Surface projections or asperities are plastically deformed and eventually joined together by the high local pressure. In the process, material may be transferred from the artificial material on one tooth to the artificial material on the opposing tooth or to the tooth enamel. Likewise, a similar transfer of material may happen on the proximal surfaces of neighbouring or adjacent teeth [81, 82].

2.8. Erosion

According to the American Society for Testing and Materials Committee on Standards, erosion is defined as “the progressive loss of a material from a solid surface due to mechanical interaction between that surface and a fluid, a multicomponent fluid, impinging liquid or solid particles” [83]. This definition does not correlate precisely with the definition of dental erosion popularised in dental journals over the last few decades.

In dentistry, erosion describes the wear process due to the chemical dissolution of tooth surface from the action of acid not produced by bacteria [84]. This chemical process of tooth loss may be exacerbated by the superimposing mechanical factors [85] and may produce defects that are sharply defined, wedge-shaped depressions often in facial and cervical areas [86].

Due to the variation of the definitions of the term erosion, the term ‘corrosion’ may be more appropriate than the term ‘erosion’ [87]. It has been suggested “erosion” should be deleted from the dental lexicon and supplanted by the term “corrosion” to denote the tooth surface loss due to acidic chemical dissolution where the origin of acid is not from bacteria.

At an early stage, the clinical presentation of a corrosive lesion is a smooth, glazed unstained appearance. Dentinal scooping is commonly seen with some degree of sensitivity because dentinal tubules remain patent [88]. Loss of enamel makes the incisal edges and proximal surfaces of anterior teeth become more translucent and the teeth appearing darker because of the translucency of the underlying dentine [89]. At high magnification, lesions appear smooth and clean (Figure. 2.8).

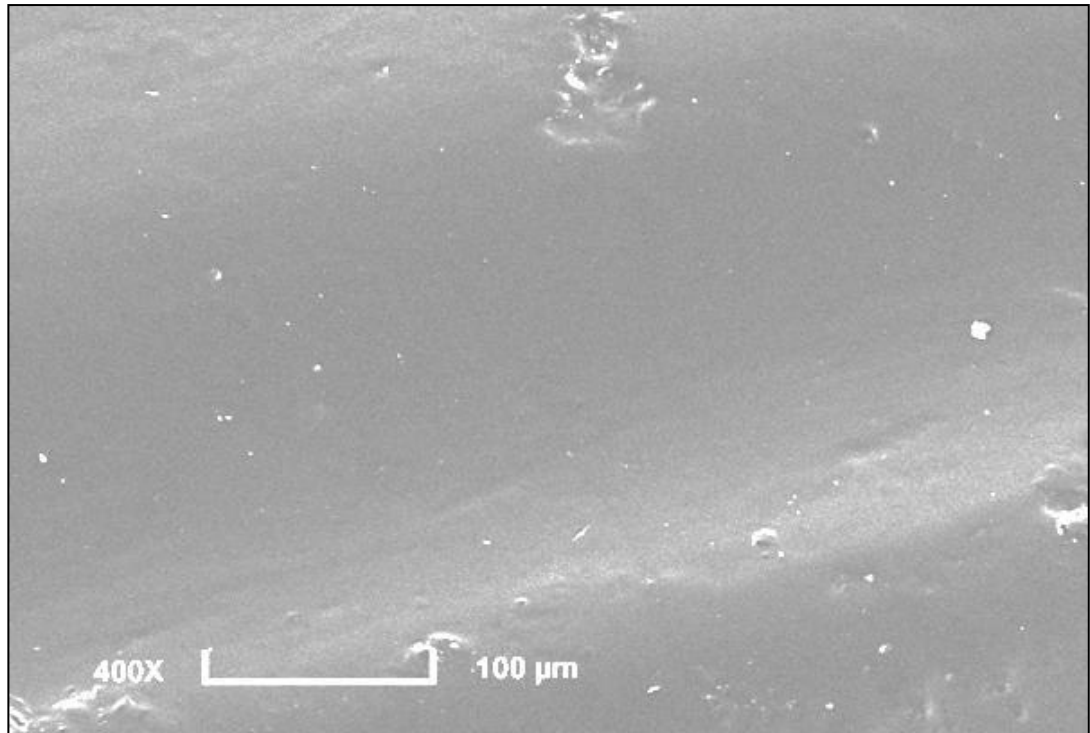


Figure 2.8: Micrograph of erosion lesion (courtesy of Dr S. Ranjitkar). Note the lack of mechanical wear.

The acids which contribute to corrosion of tooth surfaces originate externally or internally. Internal or endogenous sources of acid specifically include gastric acids which communicate with the oral cavity [90]. *Bulimia nervosa* and gastric oesophageal reflux disease are known causes of dental corrosion which arise from stomach acids. The tooth surface loss associated with these conditions can in many cases be unique. In regards to *bulimia nervosa*, dental corrosion is most marked on the palatal surfaces of maxillary anterior teeth and, in more severe cases, on the buccal surfaces of posterior teeth [91].

Gastroesophageal reflux disease is associated with slower movement of gastric acids into the oral cavity from the stomach compared to the gastric acid movement of bulimia. The corrosive tooth wear pattern of gastroesophageal reflux disease has been suggested to be different from patients suffering from bulimia. Typical sites of corrosion include the posterior occlusal, anterior palatal and cervical regions [68, 69, 92]. Such areas correlate to where gastric reflux fluid may pool during sleeping

periods. Enamel appears thin and translucent in the affected areas, and invaginated areas develop where dentine has been exposed on the occlusal or incisal surfaces. This dentinal cupping results from the joint digestive action of hydrochloric acid and the proteolytic enzyme pepsin that is contained in gastric juice [90]. Dentine is significantly more susceptible to dental corrosion in relation to enamel essentially due to its physical and chemical properties [93] (Figure 2.9).

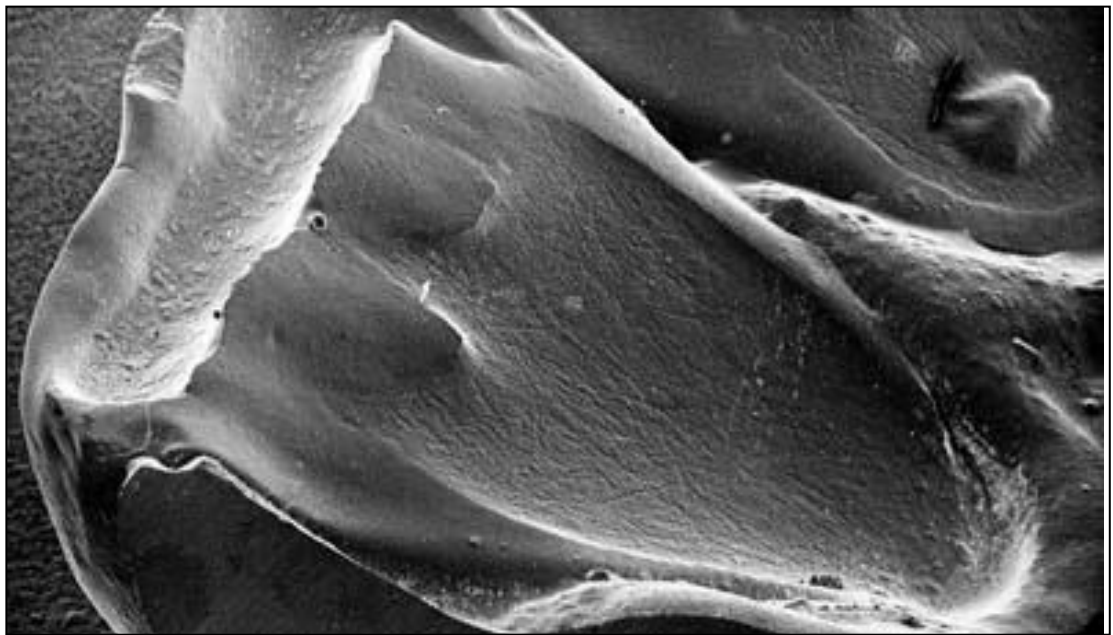


Figure 2.9: Maxillary left first incisor showing erosion on the incisal edge and on the palatal surface. Palatal enamel is mostly eroded, even into the gingival sulcus. Palatal dentine is finely striated. This tooth was from a patient with *Bulimia nervosa* [59].

Exogenous sources of corrosion include any acidic food or liquid substance with a critical pH value of less than 5.5 [94, 95]. Patients who ingest large volumes of exogenous low pH acids at a higher frequency are at a greater risk of tooth surface loss due to corrosion than patients who limit their intake of such exogenous acidic food and beverages. Citrus fruits, drinking carbonated soft drinks, alcoholic drinks, chewing vitamin C tablets and sucking sour candies greatly increase the risk of corrosion. Acidulated carbonated soft drinks are strong corrosive agents due to the presence of added citric and phosphoric acids and citrate ions rather than from the carbon dioxide they contain. More specifically, the corrosive potential of an acidic drink does not depend exclusively on its pH value, but is also strongly influenced by

its buffering capacity, the chelation properties of the acid and by the frequency and duration of ingestion [95, 96]. Acids not only chelate and dissolve the mineral content of the tooth but also soften the tooth surface rendering it more susceptible to the harmful effects of attrition and abrasion.

Certain occupations can increase the risk of corrosion. The main cause of environmental corrosion is the presence of acidic materials in the work place. Characteristically, the erosion lesions are localised to the labial surfaces of the maxillary and mandibular incisors [68, 70, 97]. The prevalence of corrosive lesions is higher in wine tasters, competitive swimmers [98] and miners in dusty environments [70].

Dental caries is a dynamic bio-corrosive process resulting in the loss of tooth structure due to the accumulation of acidic by-products produced by commensal bacterial species colonising in undisturbed dental plaque [96]. While dental corrosion involves degradation of the surface, dental caries initiates demineralisation at the subsurface of the tooth structure [75].

2.9. Saliva and tooth wear

Saliva plays a vital role in the protection of tooth structure from all mechanisms of tooth wear, especially corrosion. Its relevant functions to minimising tooth wear include lubrication due to the presence of glycoproteins and mucopolysaccharides, the formation of the acquired pellicle due to the absorption of salivary proteins to hard dental tissue, controlling the balance of mineral loss and gain by acting as a reservoir for ions such as calcium, phosphate and possibly fluoride that are needed for the remineralisation process, and finally it is responsible for cleansing, buffering and neutralising potentially harmful acids [70, 92, 99].

2.10. Prevalence of tooth wear

The lack of documentation of the type of tooth wear [66] analysed and the difficulty in comparing *in vitro* and *in vivo* studies with different methodologies and epidemiological research tools designed to assess, measure and document tooth wear [39, 100] has contributed to the lack of clear understanding on the prevalence and severity of tooth wear in modern societies [79-82].

2.11. Tooth wear and Quality of Life

A study was completed to determine if tooth wear had any impact or correlation to daily living, quality of life and the patient's satisfaction with their own dentition [101]. From a pool of 76 patients with tooth wear and based on various biological, functional and aesthetic parameters, 36% of tooth wear patients were not satisfied with their dentition. This was in comparison to only 3.9% of the control group (n=76), which composed of subjects with tooth wear that was considered within normal limits for their particular age group. The study also noted that when wear was moderate to severe in relation to the patient's age, eating ability was compromised and oral discomfort was more common [101].

CHAPTER 3

WEAR & SURFACE TEXTURE ANALYSIS

3.1. Methods of assessment of tooth and restorative material wear

There are various qualitative and quantitative methods of tooth surface and wear assessment which provide different insights into tooth wear processes *in vivo* and *in vitro* [102]. They range from two dimensional simple descriptive and imaging techniques for describing macro- and microscopic wear to complex three dimensional elemental analyses. Each method has its own advantages and limitations depending on its mode of action and this makes a particular method or instrument more suitable for some applications compared to others. To improve precision, reliability and validity of surface measurements, more than one method of assessment is desirable. Recent publications have emphasised the importance of 3D surface topography in science and engineering applications.

3.2. Qualitative wear assessment methods

Qualitative *in vivo* tooth wear can be assessed by visually documenting the clinical appearance of a tooth or restorative surface, and comparing changes that have occurred over a period of time to a standardised series of models or photographs or by using tooth wear indices such as the Tooth Wear Index (TWI) and United States Public Health Services (USPHS) criteria.

3.2.1. Tooth Wear Index

The Tooth Wear Index (TWI), developed in 1984, assesses the wear of enamel [57]. Each visible tooth surface (buccal, lingual, occlusal/incisal) together with a separate score for the buccal cervical area is recorded and categorised into one of the four scoring groups. It does not take into consideration the aetiological factors, nor does it

detect minor changes in wear. It is more suitable for epidemiology studies [102].

3.2.2. United States Public Health Services criteria

The United States Public Health Services (USPHS) criteria is a scoring system to provide a standardised and structured tool to evaluate, assess and compare the clinical work of general practitioners and collect data for insurance companies [103].

Among many other criteria, wear of material is evaluated as part of the USPHS scoring system. Initially the evaluation of wear was subjective, limiting the validity [104]. Recently, a group of renowned scientists have further developed the USPHS criteria by systematically structuring them based on evidence and normative and subjective guidelines, acknowledging, however, that wear can only be quantified by sophisticated equipment [105].

3.2.3. Clinical comparative scales

Various clinical comparative scales of wear have been developed. Historically, clinical wear used to be quantified by comparing cast replicas with a set of standards, known as scales. Two evaluators would compare the replica with the standards by means of loupes and assign a wear value [106]. The scales were based on the concept that material loss at the restoration margin was indicative of the loss of material over the entire restoration surface.

Mainly three different scales were propagated at that time. The Leinfelder scale [107], which used 6 calibrated die stone standards from clinical restorations, exhibiting approximately 100–500 μm of occlusal loss; the Moffa–Lugassy (M–L) scale [108], which used 18 standard dies with cylindrical incremental defects ranging from 25 μm to 1000 μm ; and the Vivadent scale (modification of M–L scale) which used tooth sized dies with restoration-like incremental defects.

All scales involved problems with internal and external validity. By applying the standard scales, the agreement among different evaluators can vary tremendously, especially amongst inexperienced evaluators [109]; the Vivadent scale, however, consistently achieved the highest level of agreement. Yet, even the Vivadent scale was shown to lacking in accuracy, as it was proven that the actual wear is systematically underestimated when the results obtained with the Vivadent scale were compared with those obtained with sophisticated laser equipment [110].

3.2.4. Hardness and erosive wear

Hardness measurements can provide information about enamel erosive lesions because the erosive process weakens and softens the enamel surface [111, 112]. Commonly used measurement methods are microindentation and nanoindentation or ultra-microindentation. While microindentation gives the results in Knoop hardness number (KHN) or Vickers hardness number (VHN), nanoindentation results can be read in the SI unit of Pascals (Nm^{-2}). An advantage of nanoindentation is that it can measure enamel erosion lesions at an earlier stage because the measurement can detect a lesion that is as small as 200nm [113]. Also, nanoindentation can explore both the plastic and elastic deformation for the surface while microindentation investigates only plastic deformation [111, 112]. However, microindentation is less expensive and the process is faster and simpler. Both techniques require the specimens to be polished flat before subjected to experiment.

3.3. Quantitative methods of wear analysis

Mechanical and electro-optical sensors derived from industry are available for the quantification of clinical wear. These quantitative methods include: chemical analysis, microradiography, digital image analysis, surface profilometry and mapping, scanning electron microscopy, atomic force microscopy, and secondary ion mass spectroscopy [102]. These are mainly used for *in vitro* investigations [114].

To correctly assess wear with such instrumentation it is necessary to take an accurate light-body polyvinylsiloxane impression and measure the wear extra-orally. This allows the researcher to transfer longitudinal research information from the *in vivo* setting to the *in vitro* laboratory setting which allows more efficient assessment of tooth wear. A comparative analysis of accuracy of clinical wear measurement using replica models revealed no difference between individually fitted and conventional trays [115].

3.3.1. Chemical analysis

Erosion studies often use chemical methods to measure the degree of demineralisation. Here, the concentration of calcium and phosphate in the solution is quantified after apatite dissolution in acid [102, 112]. The technique is sensitive and accurate and provides information on the concentration of ions released [111].

3.3.2. Microradiography

Microradiography determines a volume change due to the loss of minerals and a change in sample lesion depth. This assessment is based on the attenuation of X-rays by dental hard tissues. The mineral density of enamel and dentine can be recorded based on the amount of radiation that penetrates through the dental hard tissue onto a photo counting and X- ray recording detector [102, 111, 112].

3.3.3. Digital image analysis

With digital image analysis, images generated by computers can be compared to measure erosive or abrasive lesions. However, there exists a potential for errors with the method [102].

3.3.4. Surface profilometry and mapping

Methods appropriate for surface profilometry and mapping include: mechanical contact profilometers, noncontact laser profilometers, interference microscopy, confocal laser scanning-microscopy, atomic force microscopy, laser specular reflectance and scanning tunnel microscopy [102, 116, 117]. All the mentioned quantitative techniques have limitations in range and resolution and they are scale dependent, i.e. information on measurement scale and cut-off filters are needed when discussing measurement results [118].

3.3.4.1. Mechanical contact profilometer

A mechanical contact profilometer or stylus instrument traces the specimen surface to record two or three dimensional coordinates [102, 116, 117]. Stylus instruments are based on the principle of running a probe across a surface in order to detect variations in height as a function of distance [119, 120]. Early stylus instruments employed a system of levers to magnify the vertical displacement of the stylus and recorded the profile on a smoked-glass plate however with technological advances; transducers were incorporated into stylus instruments which converted vertical displacement into an electrical signal. This signal can then be processed by the instrument electronics to calculate a suitable roughness parameter.

Modern mechanical contact stylus instruments have a diameter tip of 0.1mm or larger and loaded with a pre-determined force in the milli-newton range [112, 116]. Mechanical contact profilometer produces more accurate results compared to non-contacting profilometry and is not affected by differences in surface material properties such as colour or transparency. The degree of precision of contact profilometry is 2.2µm and it has an accuracy of 10µm [117]. To ensure optimal accuracy of mechanical contact profilometry, a high degree of precision in specimen orientation and positioning during analysis is necessary [102].

Some error can be introduced in roughness measurements when a stylus instrument is used because of several factors. Some of these factors include the size of the stylus, stylus load, stylus speed, and lateral deflection by asperities. The effect of stylus size is illustrated in Figure 3.1, which is a schematic comparison of an actual profile against the traced profile [119]. The effect of stylus size becomes more significant as the curvature of the peaks and valleys decreases, or the magnitude of the slope increases [119]. Studies show that stylus speed and lateral deflection are only minor sources of error [119]. The contacting stylus may also damage the surface of specimen especially if the surface is dematerialised or has a low hardness [112, 116].

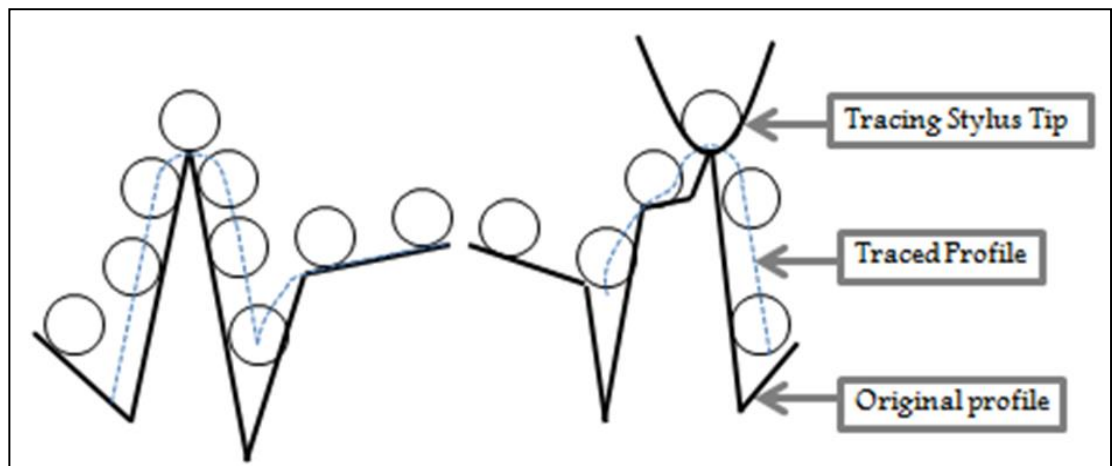


Figure 3.1: Distortion of a surface profile due to the effect of stylus size [119].

3.3.4.2. Non-contact profilometer

A non-contact light or laser sensor traces the surface to record two or three dimensional coordinates [102, 116, 117]. Non-contacting profilometers are optical instruments and use lasers or lights of different colours. The advantages of the laser profilometers include the fact that they do not contact the surface and the scanning time is much shorter than systems using contacting sensors [102, 116, 121]. However, laser systems require an opaque, diffuse reflecting surface and the laser stylus may produce “overshoots” at the sharp edges, resulting in artefacts [112, 116].

3.3.4.2.1. Engineering principles of non contacting optical profilometer

A beam of electromagnetic radiation can be reflected off a surface in three different ways: specular, diffusely, or both [119]. This is illustrated in Figure 3.2. Depending on the surface roughness, radiation of a certain wavelength may be reflected specularly, while radiation of another wavelength may be reflected diffusely. Thus, the amount of specular and diffuse reflection can be used to determine surface roughness [120]. Light section microscopes that employ specular reflection to characterise roughness, work as follows. An image of a slit is projected onto the surface and the objective lens captures the image at the specular reflection angle. If the surface is smooth, the image obtained will be straight; however, if the surface is rough, an undulating pattern will be observed [119].

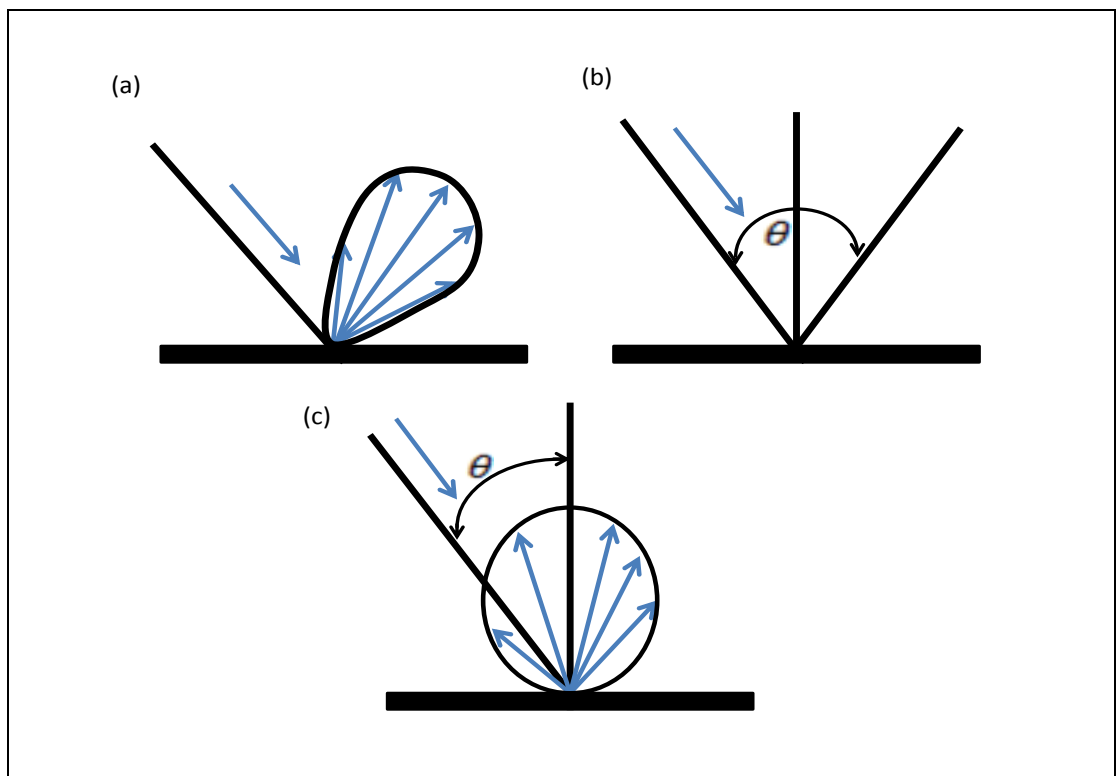


Figure 3.2: Modes of Reflection[119]: (a) Combined Specular and Diffuse; (b) Specular Only; (c) Diffuse Only.

The interaction of polarised light with a surface can also be employed to evaluate surface roughness. Such is the case of the long-path length optical profiler, which

focuses a laser beam onto a surface by means of an arrangement of mirrors [119]. Before reaching the specimen, the laser goes through a Wollaston prism that polarises the beam into two orthogonal components. The beams are then focused onto the surface where they reflect back to the prism. Finally, the reflected beams are directed to a beam splitter, which sends each beam to a different detector. The phase difference of the polarised beams, which is related to the height difference at the surface, results in a voltage difference that can be measured [119].

3.3.5. Scanning Electron Microscopy

Scanning electron microscopy (SEM) characterizes surface-topography qualitatively and has a high lateral resolution as well as a large depth of focus. When two SEM micrographs are studied, e.g. stereo-SEM, quantitative assessments can also be performed [118]. There are two methods of SEM specimen preparation. The most common method is when the specimens are coating with graphite/carbon/ and assessed in the SEM under vacuum. This technique however may lead the crack formation and propagation in specimens fabricated from certain materials. Such crack would negatively influence the results of a study. To overcome this limitation, another technique “environmental SEM”, involves uncoated samples viewed in a pressurised container instead of a vacuum [118].

3.3.6 Atomic Force Microscopy

Atomic force microscopy (AFM) uses a cantilever probe tip to detect weak forces on a specimen. It is essentially an example of a scanning probe microscope. It is useful in studies of abrasion, binding, cleansing, corrosion, acidification, friction, lubrication, and coating. The system uses a topographic surface view at the nanometer level to measure the forces between molecules [76].

While the specimen sample moves in the x-y direction the pointed end of the cantilevered probe can either make contact with the specimen surface or function in a

non-contact mode. The scanning moves along the x-y direction and detects the extremely small repulsion forces from the probe and the surface of the specimen, and moves up and down vertically following the shape of the surface. All of the data can be collected by using lasers, piezo electric sensors or photoelectric sensors. The piezo electric sensors send a voltage to a transducer whenever a movement from the cantilever is made. The photoelectric sensor is able to measure movement based on changes in the incident angle made by changes cantilevers movement. The principle of the laser works in the same manner as the photoelectric sensor. Only in contact mode or in a state of strong repulsive forces can the highest resolution be achieved [120]. Figure 3.3 is a representation of the three different sensors on the AFM Machine.

AFM delivers an accurate three dimensional high resolution quantitative assessment [111]. It specifically provides accurate surface altitude parameters including various details including densely located elevations or valleys; tiny, small, and spiny juts; smooth and flat parts; cracks, breaches, craters, or holes; wide-angled and round elevations and valleys; deteriorated surface images; asymmetric or parallel areas; and shiny, smooth surfaces [122-124].

Compared with profilometry and visual assessment, the advantage of AFM is mainly greater detail of surface texture. It also does not require the specimens to be hydrated, coated or vacuumed, therefore avoiding artefacts and damage due to sample preparation. Although this system has high running costs and is time consuming, its main disadvantage is that its 3D topographic view and numerical parameters of surface smoothness are difficult to repeat because the scanning field is smaller than in other methods [125, 126].

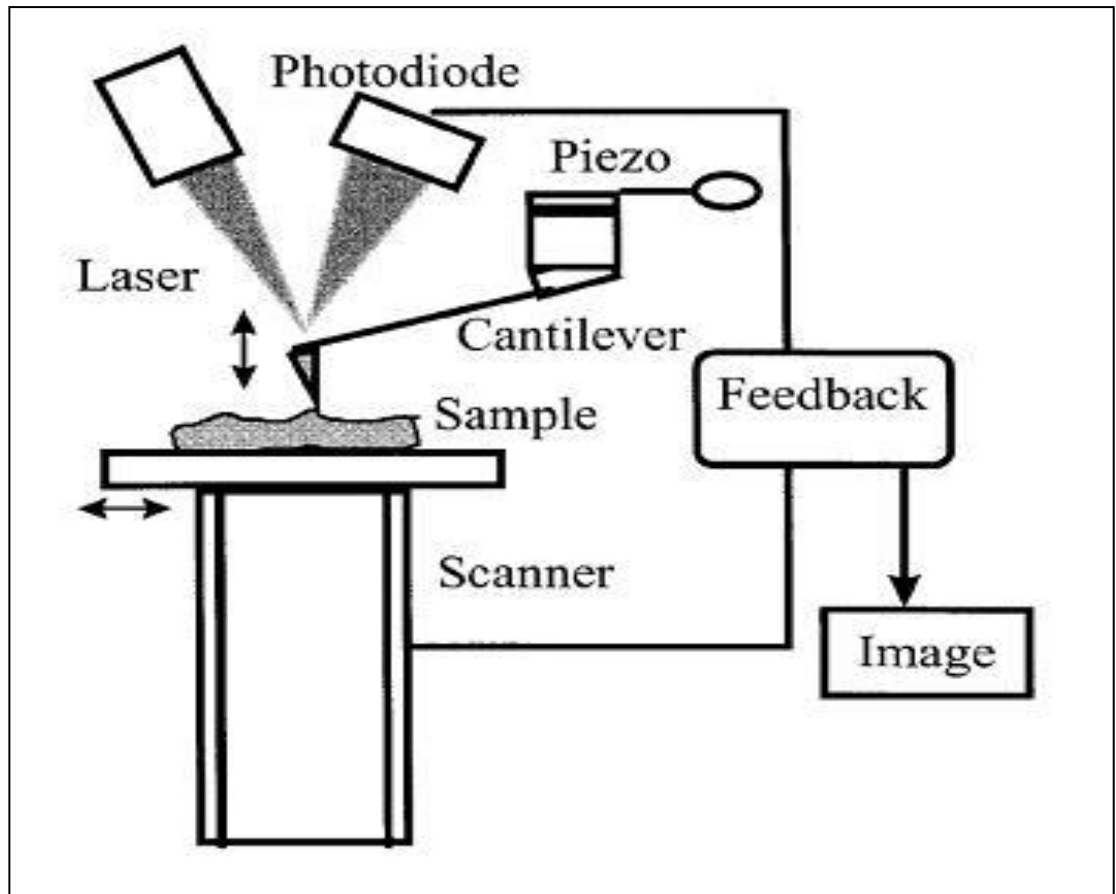


Figure 3.3: Working principles of AFM[120].

3.3.6. Secondary ion mass spectroscopy

Secondary ion mass spectroscopy “is a form of mass spectroscopy in which a beam of ions is incident on a surface, causing the ejection of secondary ions which are spectroscopically analysed” [111]. The technique is extremely sensitive and is used as an effective tool to analyse major and trace elements in dental hard tissues [127].

A review of the literature revealed that usually SEM and profilometry [3, 128-130] or rarely SEM and visual assessment [131] or AFM and profilometry [124] are used together. There are also studies that used a single method to analyse the surface smoothness of dental ceramics, for example, SEM [132] visual assessment [133], AFM [122], laser specular reflectance system [134], or profilometry [135, 136].

3.4. Importance of surface texture analysis in dentistry

Characterisation of surface topography is important in applications involving friction, lubrication, and wear [119]. In general, it has been found that friction increases with average roughness and therefore roughness parameters of ceramics and dental hard tissue is important since it plays a major factor in the process of wear.

The characterisation of surface topography, texture or roughness can be done in two principal planes [119]. Using a sinusoidal curve as a simplified model of the surface profile, roughness can be measured at right angles to the surface in terms of the wave amplitude, and parallel to the surface in terms of the surface wavelength. The latter one is also recognised as texture. The technique used to measure roughness in any of these two planes will inevitably have certain limitations. The smallest amplitude and wavelength that the instrument can detect corresponds to its vertical and horizontal resolution, respectively. Similarly, the largest amplitude and wavelength that can be measured by the instrument are the vertical and horizontal range.

In statistical terms, the parameters used to characterise surface topography are divided into central, second, third and fourth moments. Central moments include parameters which assess the altitude of the surface or the distribution of heights such as centre average line (CLA) or average surface roughness (Ra) and root mean square (RMS) [137]. The second moment is known as the *variance* and represents the deviation of the distribution from its mean. The third moment is the *skewness* and is a measure of the asymmetry of the distribution. The fourth moment is known as the *kurtosis* and represents the shape of the distribution curve [119].

In addition to amplitude parameters, there are other parameters that are used to characterise texture. One of them is the high-spot count (HSC), which is the number of peaks per unit length. Its reciprocal, Sm , is the mean spacing between peaks.

Another parameter used to evaluate texture is the profile length ratio RL , which is the length of the profile divided by its nominal length. Currently there are more than 100 2D parameters that have been described in the literature [119]. Common surface texture parameters are listed in Figure 3.4.

Parameter	Name
Ra	Roughness Average (Ra)
Rq	Root Mean Square (RMS) Roughness
Rt	Maximum Height of the Profile
Rv, Rm	Maximum Profile Valley Depth
Rp	Maximum Profile Peak Height
Rpm	Average Maximum Profile Peak Height
Rz	Average Maximum Height of the Profile
Rmax	Maximum Roughness Depth
Rc	Mean Height of Profile Irregularities
Rz(iso)	Roughness Height
Ry	Maximum Height of the Profile
Wt, W	Waviness Height
S	Mean Spacing of Local Peaks of the Profile
Sm, RSm	Mean Spacing of Profile Irregularities
D	Profile Peak Density
Pc	Peak Count (Peak Density)
HSC	High Spot Count
λ_a	Average Wavelength of the Profile
λ_q	Root Mean Square (RMS) Wavelength of the Profile
Δa	Average Absolute Slope
Δq	Root Mean Square (RMS) Slope
Lo	Developed Profile Length
Ir	Profile Length Ratio
Rsk,Sk	Skewness

Figure 3.4: Surface texture parameter [119]

3.5. Amplitude parameters

Amplitude parameters are the most important parameters to characterise surface topography. They are used to measure the vertical characteristics of the surface deviations [138].

3.5.1. Roughness Amplitude Parameters

Average Roughness (Ra) describes the overall mean roughness of a surface and is the area between the roughness profile and its mean line over a sampling length or the integral of the absolute value of the roughness profile height over the evaluation length. It is also known as arithmetic average (AA), centre line average (CLA), and arithmetical mean deviation of the profile [139].

When evaluated from digital data, the integral is normally approximated by a trapezoidal rule: Graphically, the average roughness is the area (shown below) between the roughness profile and its centre line divided by the evaluation length (normally five sample lengths with each sample length equal to one cut-off).

Average roughness (Ra) is one of the most effective and common surface roughness measures. It is easy to define, easy to measure, requires the least sophisticated instruments and gives a good general description of the height variations of a surface. Average roughness (Ra) however provides limited information on the assessed profile and the interpretation of the given value is difficult. This is because it is a true amplitude parameter and gives no information of the profile data. Specifically it does not give any information on the spatial structure such as the wavelength, does not differentiate between peaks/valleys [138] and is not sensitive to small changes in profile [119] (Figure 3.5).

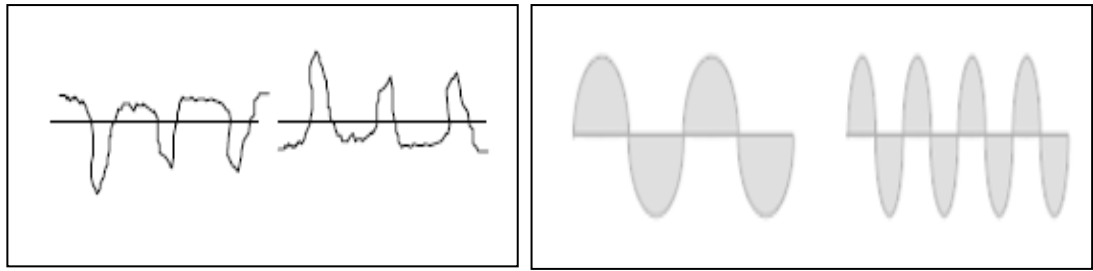


Figure 3.5: the limitations of Average mean roughness. Variations in wavelength are not evident with surface texture parameter 'Average mean roughness.' All graphical representations showing surface roughness have the same Ra value.

The mathematics definition and the digital implementation of the arithmetic average height parameter are shown respectively in Figure 3.6 and correlate with the graphical representation shown in Figure 3.7.

$$R_a = \frac{1}{l} \int_0^l |y(x)| dx$$

$$R_a = \frac{1}{n} \sum_{i=1}^n |y_i|$$

Figure 3.6: Mathematical definition and the digital implementation of arithmetic average height parameter (Ra). L = evaluation length, y = height, x = distance along measurement, Z(x) = profile ordinates of roughness profile.

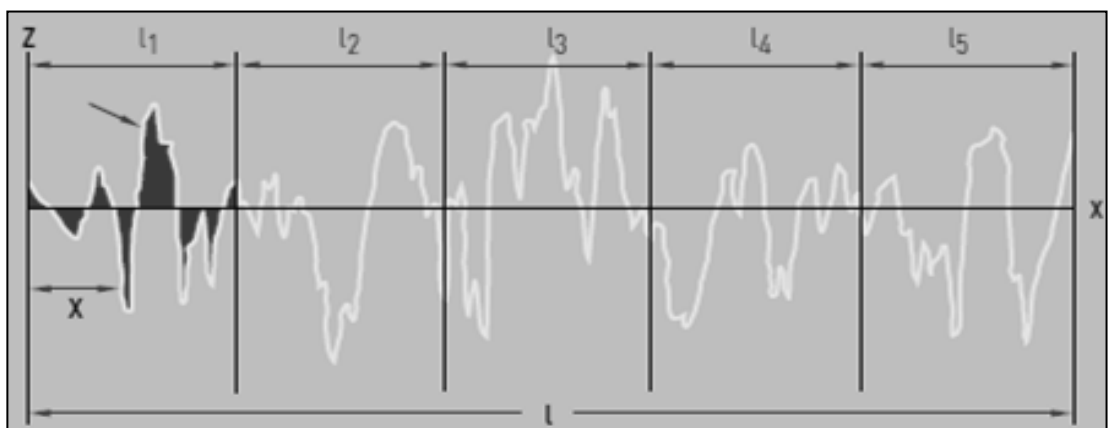


Figure 3.7: Ra is the arithmetic mean of the absolute departures of the roughness profile from the mean line. It is universally recognised as the most often used international parameter of roughness [137].

The Root Mean Square roughness (RMS or Rq) is the root mean square average of the roughness profile ordinates. It represents the standard deviation of the distribution of surface heights, so it is an important parameter to describe the surface roughness by statistical methods. This parameter is more sensitive than the arithmetic average surface roughness (Ra) to large deviation from the mean line. The mathematical definition and the digital implementation of this parameter are as follows [140] (Figure 3.8).

$$R_q = \sqrt{\frac{1}{l} \int_0^l \{y(x)\}^2 dx}$$
$$R_q = \sqrt{\frac{1}{n} \sum_{i=1}^n y_i^2}$$

Figure 3.8: Mathematical definition and the digital implementation of the Root Mean Square roughness (RMS or Rq) L = evaluation length, y = height, x = distance along measurement, Z(x) = profile ordinates of roughness profile [140].

It provides information on the symmetry of the surface distribution on a statistical basis but similar to average roughness average (Ra), its disadvantages are that it provides no spatial structure information and does not differentiate differences between peaks and valleys.

The RMS mean line is the line that divides the profile so that the sum of the squares of the deviations of the profile height from it is equal to zero [140] (Figure 3.9).

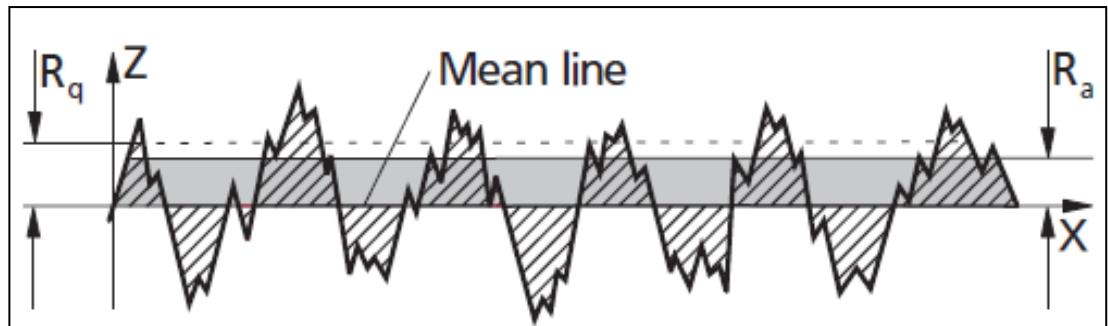


Figure 3.9: RMS mean line divides the profile so that the sum of the squares of the deviations of the profile height from it is equal to zero [140].

The mean roughness depth parameter (R_z) is a surface texture parameter which is more sensitive to occasional high peaks or deep valleys than average surface roughness (R_a). This is because maximum profile heights and not just the averages are taken into consideration. The Single Roughness depth (R_{zi}) is the vertical distance between the highest peak and the deepest valley within a sampling length. The Mean Roughness Depth (R_z) is the arithmetic mean value of the single roughness depths of consecutive sampling lengths. Mean roughness depth is defined by two methods according to the definition system. The international ISO system defines this parameter as the difference in height between the average of the five highest peaks and the five lowest valleys along the assessment lengths of the profile. The German DIN system defines R_z as the average of the summation of the five highest peaks and the five lowest valleys along the assessment length of the profile [114, 140]. The mathematical and graphical definition is shown in Figure 3.10. The Maximum Roughness Depth (R_{max}) is the largest single roughness depth within the evaluation length. The R_{max} parameter is useful for surfaces where a single defect is not permissible, e.g. a seal with a single scratch. R_z and R_{max} are used together to monitor the variations of surface finish in a production process. Similar values of R_z and R_{max} indicate a consistent surface finish, while a significant difference indicates a surface defect in an otherwise consistent surface [119].

lengths: $R_z = \frac{1}{n} (R_{z1} + R_{z2} + \dots + R_{zn})$

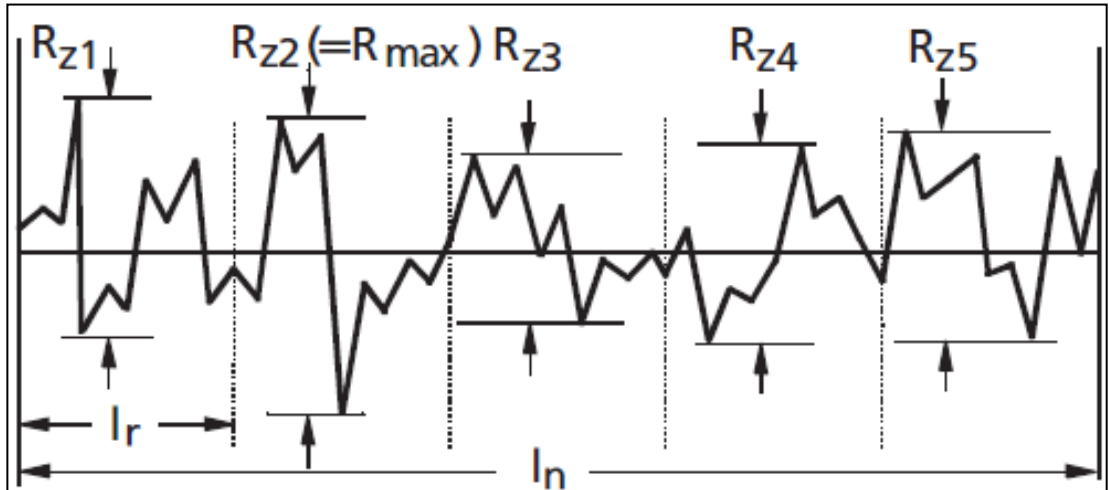


Figure 3.10: The mathematical and graphical definition of mean roughness parameter R_z where n is the number of samples along the assessment line [140].

Parameters which describe the roughness profile slope include the mean width of profile elements and the root mean square slope [139]. The mean width of profile elements (RSm) is the arithmetic mean value of the widths of the profile elements of the roughness profile, where a profile element is a peak and valley in the roughness profile. The root mean square slope (Rsq) is the root mean square average of all local profile slopes (Figure 3.11). Each slope is calculated using a smoothing algorithm to reduce the effect of random noise on the value of Rsq [140].

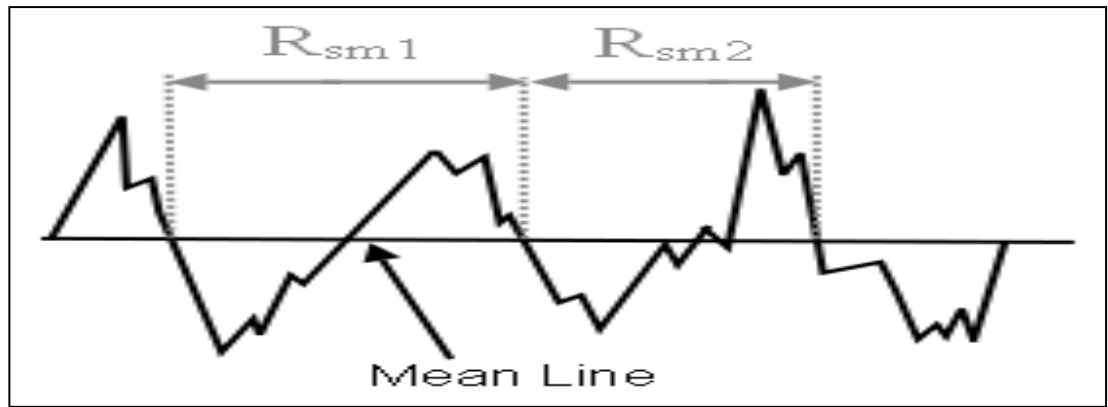


Figure 3.11: The mean width of profile elements (R_{Sm}) is the arithmetic mean value of the widths of the profile elements of the roughness profile, where a profile element is a peak and valley in the roughness profile [139].

The Mean Levelling Depth parameter (R_{pm}) measures the mean value of the levelling depths of five consecutive sampling lengths. Exceptional profile peaks are thus only partly considered. By contrast to the surface parameters already described such as R_a and R_z , the R_{pm} parameter gives reliable information on the profile shape. Small R_{pm} values characterise a surface featuring wide peaks and narrow valleys whilst greater R_{pm} values indicate a spiky, sharp ridge profile [139]. The ratio $R_{pm}:R_z$ is of special interest because the value quantifies the asymmetry of a profile [62, 141] and also gives valuable information on profile shape. A ratio higher than 0.5 indicates a sharp ridge profile, a ratio smaller than 0.5 indicates that the profile is rounded [142]. The levelling depth (R_p) is also the largest of the five levelling depths. The maximum roughness depth, (R_t) peak to valley height is the vertical distance between the highest peak and the lowest valley of the roughness profile R within the evaluation length L (Figure 3.12).

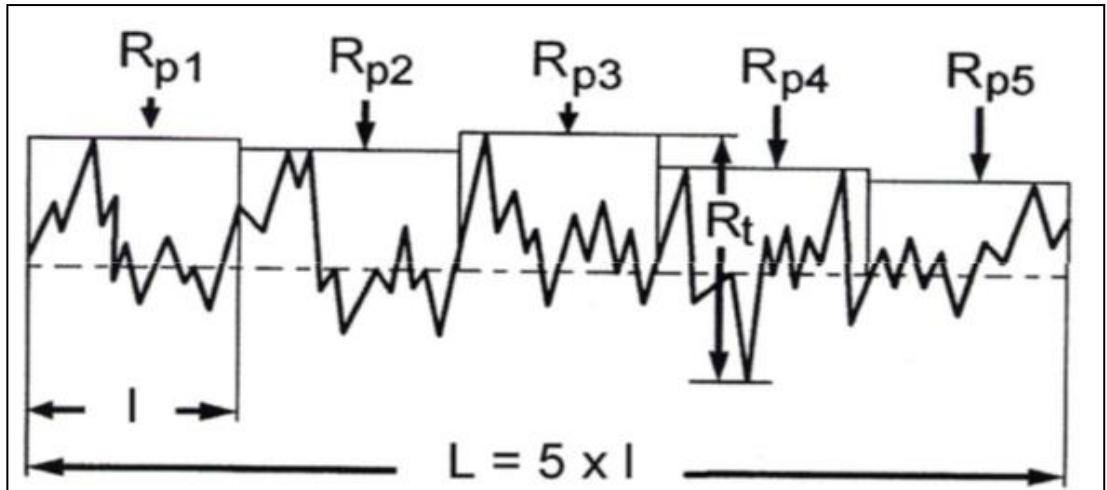


Figure 3.12: Mean levelling depth parameter measures the mean value of the levelling depths of five consecutive sampling lengths. The levelling depth (R_p) is also the largest of the five levelling depths. The maximum roughness depth (R_t), peak to valley height is the vertical distance between the highest peak and the lowest valley of the roughness profile R within the evaluation length L . [139, 141] $R_{pm} = 1/5 (R_{p1} + R_{p2} + R_{p3} + R_{p4} + R_{p5})$.

CHAPTER 4 TRIBOLOGY

Tribology is the science and engineering of interacting surfaces in relative motion and of related subjects and practices [56]. It includes the study and application of the principles of friction, lubrication and wear [141]. Historically, Leonardo da Vinci was the first to formulate two laws of friction and centuries later, observations were made by Charles-Augustin de Coulomb [56].

The word *tribology*, coined in 1969 by the International Research Group on Wear of Engineering Materials, is derived from the Greek word *tribos* meaning "rubbing," so the literal translation would be the science of rubbing [143]. The tribological interactions of a solid surface with interfacing materials and the environment may result in loss of material from the surface. The process leading to loss of material is known as "wear" and there are several mechanisms of wear [56]. Wear includes six distinct mechanisms that have only one thing in common: the removal of solid material from rubbing surfaces. These mechanisms include; adhesive, abrasive, fatigue, impact by erosion or percussion, corrosive and electrical arc-induced wear [144, 145] (Figure 4.1). Other commonly encountered wear types are fretting and fretting corrosion. These are not distinct mechanisms, but rather combinations of the adhesive, corrosive, and abrasive forms of wear [58]. Surface loss can also occur in static situations as a result of chemical degradation (e.g. rust), but this should be regarded as a separate aspect of damage [146].

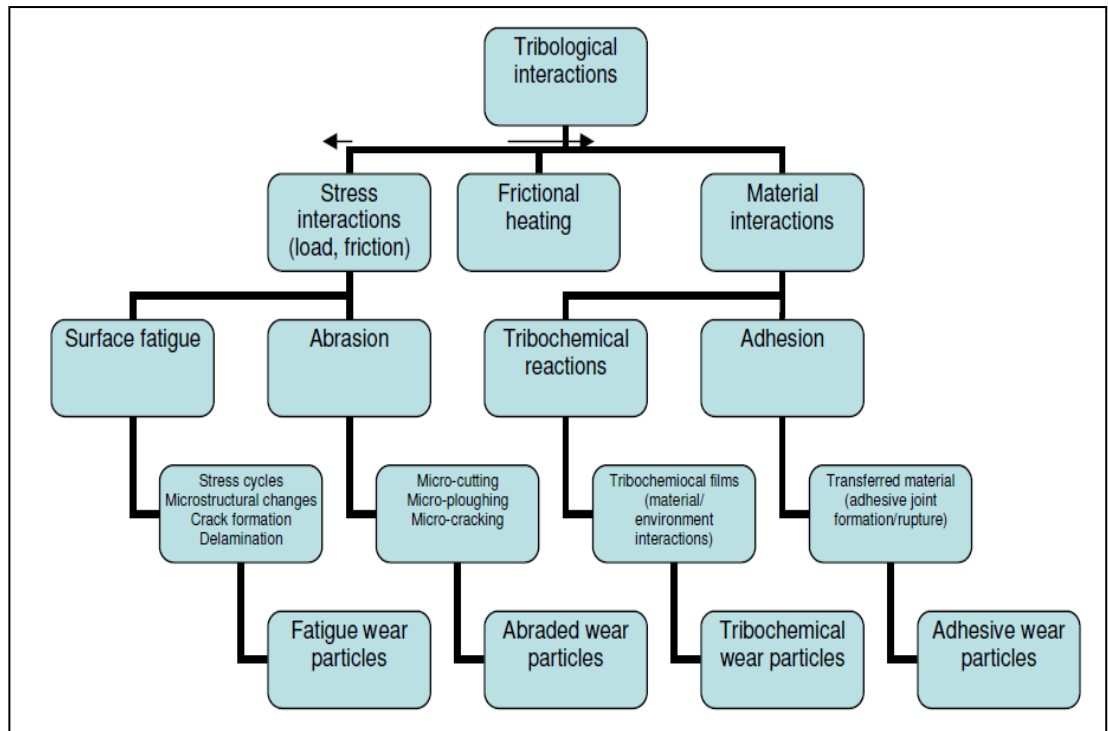


Figure 4.1: Tribological interactions and wear mechanisms [147].

A fundamental principle of tribology is that no solid surface is perfectly smooth regardless of the preparation method and this inherent roughness, results in point-to-point contact between opposing surface asperities [148]. This fundamental principle of tribology is particularly important in dentistry [148]. The risk of wear can be minimised by surface ‘finishing’ to minimise the disparities on the surface and by the use of lubricants. These methods minimise frictional and adhesive wear [55].

The interaction of two solid surfaces results in two manifestations. Firstly there is resistance to the motion which is indicated by the coefficient of friction. This frictional energy results in heat release and sometimes noise. Secondly, during the sliding process all surfaces are to a greater or lesser extent changed in their basic characteristics. They may become smoother or rougher, have physical properties such as their hardness altered, and some material may be lost in the so-called wear process [55, 59].

4.1. Adhesive wear

Adhesive wear occurs when two solid surfaces rub against each other. The friction between the moving surfaces causes cold welding of the protuberances of the contacting surfaces resulting in adhesive wear [56, 149-151]. Further movement of the surfaces fractures these welds. The line of separation is not necessarily coincident with the original weld [146]. The overall result is the transfer of material from one surface to another. The geometry of surface particle transfer defines the different types of adhesive wear. These types include *galling*, *scuffing*, *scoring*, or *smearing* [58]. This transfer element is repeatedly passed from one surface to the other and grows quickly to a large size, absorbing many of the transfer elements so as to form a flake like particle from materials of both rubbing elements. Rapid growth of this transfer particle finally accounts for its removal as a wear particle by a fatigue process resulting in three body wear (Figure 4.2).

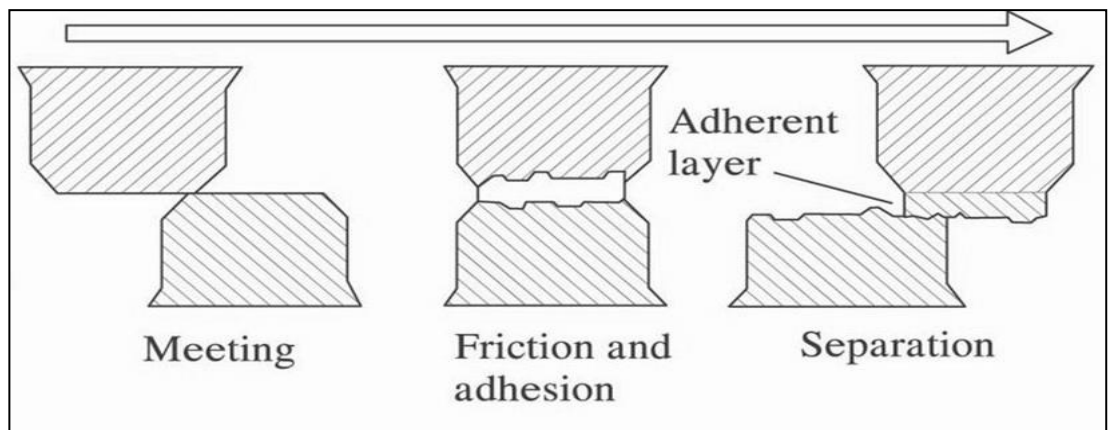


Figure 4.2: Adhesive wear process. Note the transfer of material from one surface to another [62].

4.2. Abrasive wear

Abrasive wear is defined by the American Society for Testing and Materials as the loss of material when a rough, hard surface slides on a softer surface and ploughs a series of grooves in it [83]. The surface can be ploughed and plastically deformed and then fracture by a low-cycle fatigue mechanism (Figure 4.3) [58]. The two modes of abrasive wear are known as two-body and three-body abrasive wear. Two

body abrasion is when the hard or sharper surface is the harder of two rubbing surfaces such as Sof-Lex aluminium dioxide polishing discs (Figure 4.4). Three body abrasion is when the hard surface is a third body, generally a small particle of grit or abrasive, caught between the two other surfaces and sufficiently harder that it is able to abrade either one or both of the mating surfaces, for example dental polishing pastes (Figure 4.5).

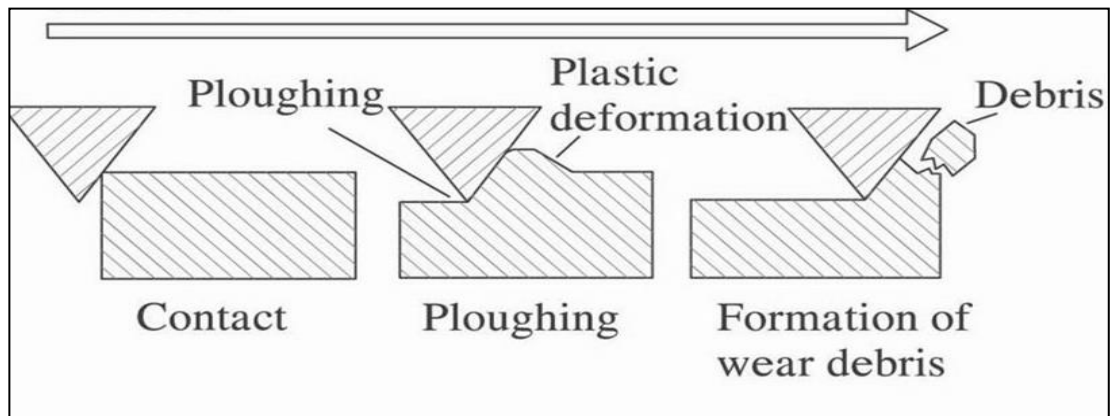


Figure 4.3: Abrasive wear. The surface can be ploughed and plastically deformed without removal of material or removal can occur by a low-cycle fatigue mechanism [62].

Factors which influence type of abrasive wear which occurs and hence the manner of material removal include: the hardness of the materials in contact, the geometry of the abrasive particles, and the load and the sliding distance [56]. Three commonly identified mechanisms of abrasive wear which describe the manner in which the material is removed are; plowing, cutting and fragmentation.

Plowing occurs when material is displaced to the side, away from the wear particles, resulting in the formation of grooves that do not involve direct material removal. The displaced material forms ridges adjacent to grooves, which may be removed by subsequent passage of abrasive particles. Ploughing may lift a 'chip' on the softer surface which may subsequently be cut by the continued sliding of the surfaces [152]. Cutting occurs when material is separated from the surface in the form of primary debris, or microchips, with little or no material displaced to the sides of the

grooves. This mechanism closely resembles conventional machining [141, 152]. Fragmentation occurs when material is separated from a surface by a cutting process and the indenting abrasive causes localised fracture of the wear material. These cracks then freely propagate locally around the wear groove, resulting in additional material removal by spalling [153].

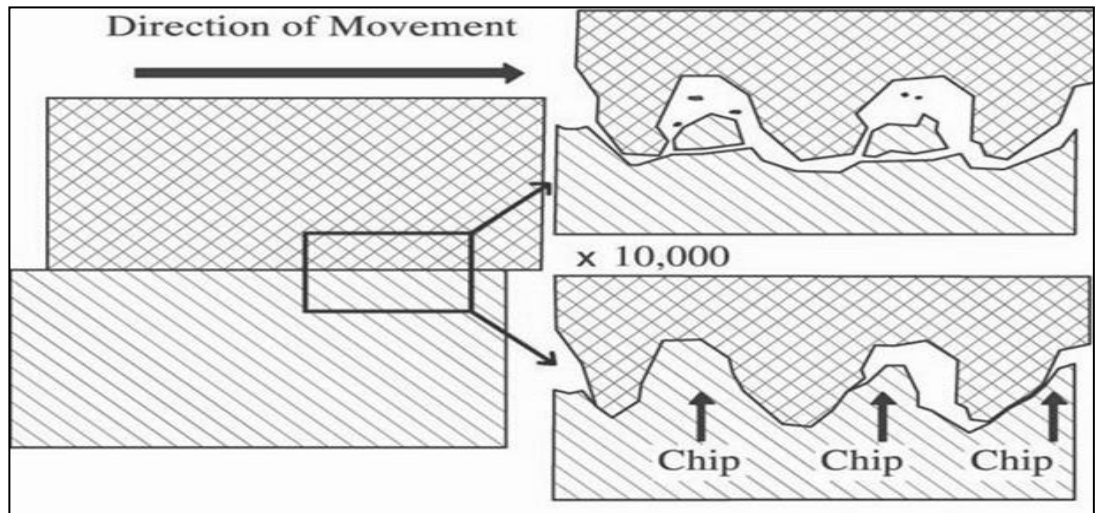


Figure 4.4: Two-body abrasive wear. If both surfaces are brittle, there is fracture of the asperities (upper right diagram). If one surface is harder than the other, the harder surface ‘plows’ into the softer surface (lower right image) [141].

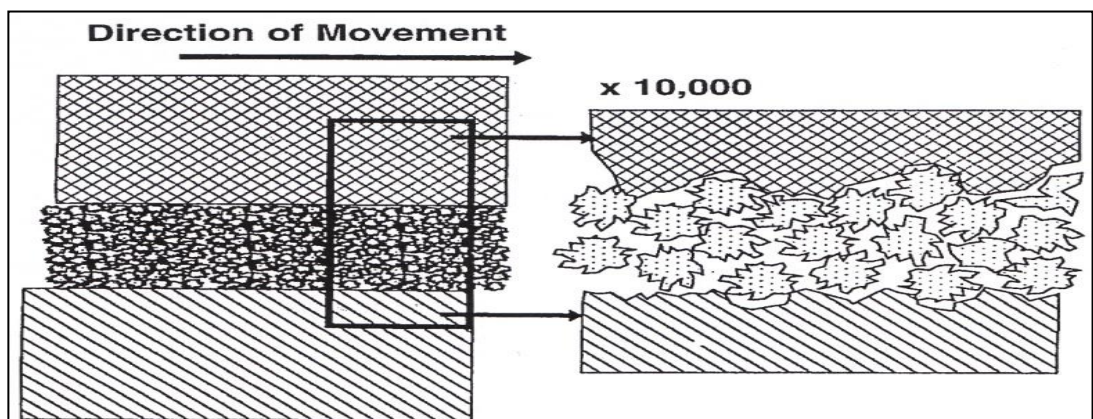


Figure 4.5: Three-body abrasive wear. As the abrasive particles in the slurry flow under pressure, they cut away the surfaces [141].

4.3. Fatigue wear

Fatigue wear is when there is a rolling action of the two surfaces in relation to one another [58]. The rolling condition results in the accumulation of shear stress at a subsurface level. This stress accumulation dissipates the plastic deformation energy of the asperities and is responsible for nucleation of cracks. An applied frictional force at the interface results in the propagation of subsurface cracks towards the surface resulting in delamination [58, 82]. Delamination is the formation of chips or fractured surface material and occurs after a critical number of loading cycles when the surface material becomes surrounded by a network of linked cracks. The breakup of the surface then increases risk of the formation of larger fragments and will lead to larger pits on the surface [81, 82].

The rate of fatigue wear is non-linear and prior to the point of surface fracturing, negligible wear takes place, which is in marked contrast to the wear caused by adhesive or abrasive mechanisms, where wear causes a gradual deterioration of the surface. Time to fatigue failure is dependent on the amplitude of the reversed shear stresses, the interface lubrication conditions, and the fatigue properties of the rolling materials [150, 154] (Figure 4.6). Adhesive wear can exacerbate surface fracturing and delamination by weakening the subsurface, allowing adhesive forces to pluck out the surface fragments [82].

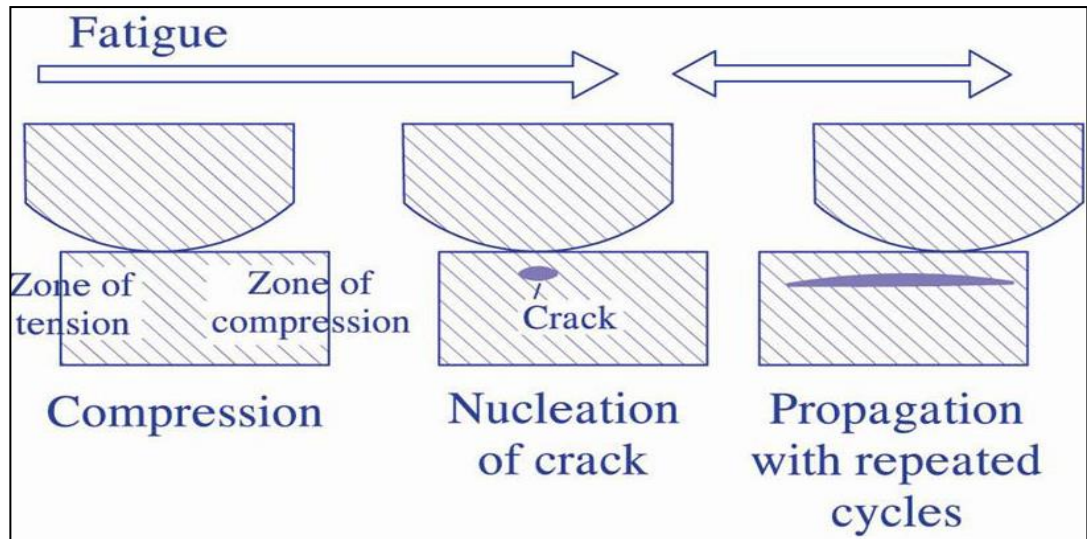


Figure 4.6: The process of fatigue wear [62]. Rolling action of two surfaces results in shear stress at the subsurface which result in nucleation of cracks. Cracks propagate laterally to surface with repeated rolling action resulting in delamination and fatigue failure.

4.4 Corrosive wear

Corrosive wear requires both corrosion and rubbing and therefore occurs when sliding takes place in a corrosive environment. If there is no abrasion or attrition occurring, the products of the corrosion form a barrier film which tends to slow down or even arrest the corrosion [146]. With the presence of rubbing and sliding, the protective oxide barrier is worn away and the corrosive attack can continue [62] (Figure 4.7).

Chemical corrosion occurs in a highly corrosive environment and in high temperature and high humidity environments. Electrochemical corrosion or tribochemical wear [146] is a chemical reaction accompanied by the passage of an electric current, and for this to occur, a potential difference must exist between two regions [56, 149, 150].

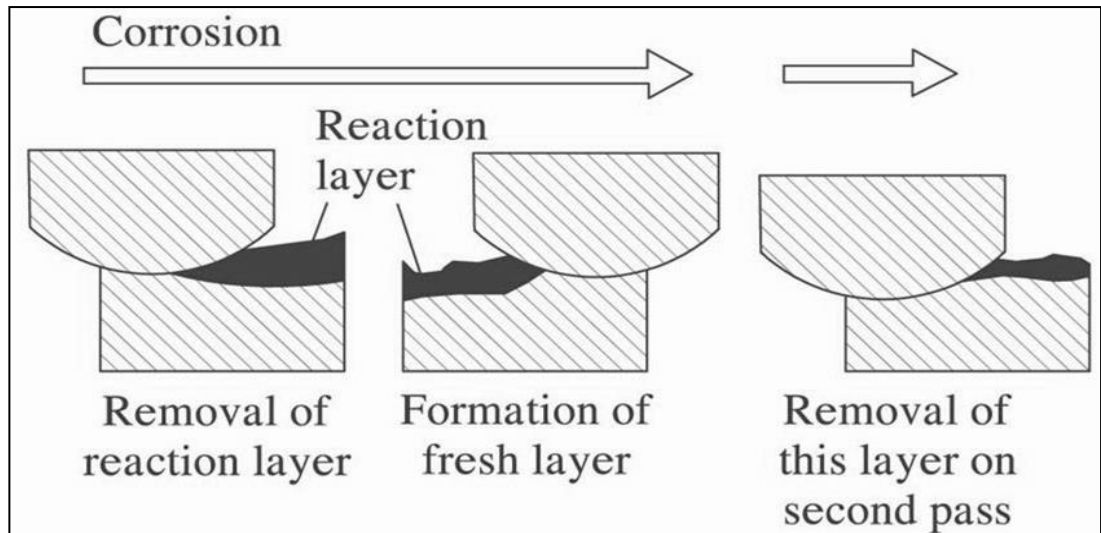


Figure 4.7: Corrosive wear occurs when there is sliding movement in a corrosive environment. The layer of protective oxides formed due to the effects of corrosion are worn away with sliding movement [62].

4.4. Erosive wear

Erosive wear results from the impact of external particle or fluid under pressure [58]. The essential feature of erosion is that the wear medium which may include particles or fluid such as sand or water acts like the second surface. This can therefore be distinguished from three-body abrasion where the particles are compressed between two separate surfaces [58, 62].

4.5. Fretting wear

Fretting wear occurs as a result of prolonged slow slipping between surfaces under load. These conditions do not occur in the mouth therefore this process does not feature in dental wear [56].

Tribology concepts are based on micro and nano-scale observations. The understanding of the mechanical and chemical engineering principles of the wear process, aids the interpretation and understanding of macro-level observations of dental tissue wear. In this project the dental terminology has generally been used

other than when the alternative, more specific tribology terminology allows a clearer explanation of an observation or process.

CHAPTER 5 CERAMICS

5.1. Historical background

Ceramics were initially developed to help solve specific problems and increase the restorative versatility of dental clinicians. In the early 1700s, Europeans began intensive research in developing porcelain to match the quality hard and translucent porcelain they were importing from China and Japan which was developed a thousand years earlier [155].

In 1774, Alexis Duchateau was the first patient to receive porcelain dentures from Parisian dentist Nicholas Dubois de Che´mant. Porcelain dentures represented a huge step forward in personal hygiene because they did not absorb oral fluids, and were not porous like ivory dentures which were the norm. The advancement of this dental technology led to public honours for de Che´mant from the Academy of Sciences and the Academy of Medicine of Paris University [156-158].

In 1808 an Italian dentist, Giuseppangelo Fonzi, significantly improved the versatility of ceramics by firing individual denture teeth, each containing a platinum pin. This invention allowed teeth to be fixed to metal frameworks enabling partial denture fabrication, reparability and modest improvements in aesthetics [159].

The porcelain used to fabricate dentures was initially described as an opaque white material. In 1838, American dentist Dr Elias Wildman improved the formula, bringing both translucency and tooth colours to porcelain. Specifically the formula was altered to increase the amount of feldspar and eliminated kaolin. The next major advancement in the enhancement of translucency and colour development was in

1949 with the introduction of vacuum firing by the Dentist Supply Company [160].

A Detroit dentist, Dr Charles H Land, patented the concept of fusing porcelain to a thin platinum foil. Dr Land is considered the ‘father of porcelain dental art’ and the techniques and discoveries led to the development of modern day porcelain jacket crowns and also guided the profession toward wider applications for porcelain, preservation of tooth structure, improved aesthetics and the need to protect and preserve the periodontal tissue [161].

5.2. Modern Dental Ceramics

The word ceramics originates from the Greek word “keramos”, which means “burnt material” [162, 163]. In dentistry, the term ‘ceramics’ refers to inorganic crystalline materials which are fired at high temperatures to achieve desirable properties [156, 162]. It applies equally to products that veneer a metal substructure and to those that comprise an entire restoration [164].

Dental ceramic materials exhibit many desirable material properties. The variability of properties between the different categories of ceramics is considerable however generalisations can be made. Favourable properties include their biocompatibility, aesthetics, high compressive strength, diminished plaque accumulation, low thermal conductivity and diffusivity, abrasion resistance, and colour stability [165-168]. Limitations of ceramics include brittleness, low fracture toughness, and low tensile strength [169-171].

5.3. Chemical structures of dental ceramics

Fundamental dental porcelain constituents include a crystalline silicon-oxygen network such as feldspar, quartz, and alumina and an amorphous glass-forming matrix. The amount of crystal and glass varies in different types of porcelain

formulations [172]. The fusion of the principle constituents forms a large three-dimensional network of silica tetrahedral, connected by oxygen atoms (Figure 5.1) [173].

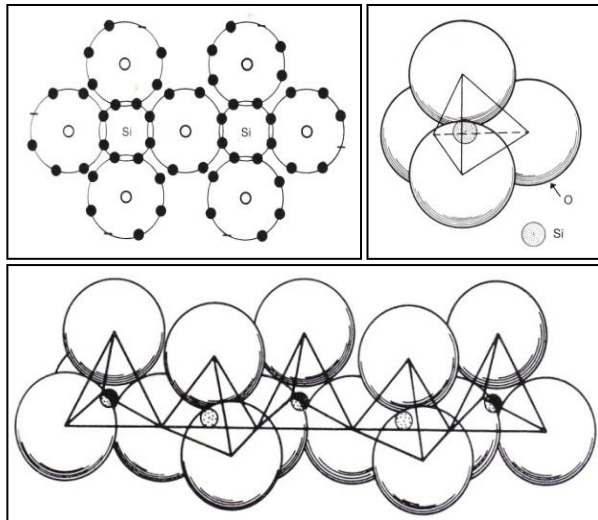


Figure 5.1: Diagram of a silicate unit with each SiO tetrahedral sharing an oxygen atom (upper left). Three dimensional drawing of a silicate unit in which the silicon atom Si is surrounded by four oxygen atoms (upper right). Three dimensional drawing of linked silicate units which form the continuous network in glass (lower) [165].

Each phase of the ceramics contributes to the optical and mechanical properties of the material. The glassy phase gives porcelain properties of glass such as brittleness, a non-directional fracture pattern and translucency. Metal oxides such as potassium, sodium, calcium, aluminium and boric oxides are incorporated to give additional beneficial properties such as, improved handling and manipulation [158], low-fusing temperature, high viscosity, resistance to devitrification and tooth-like colour [172].

Feldspar is the ingredient responsible for forming the glass matrix and is lends itself to the fritting and colouring process. It exists in nature as a mixture of two substance including potassium aluminium silicate (Potash feldspar) and sodium aluminium silicate (Sodium feldspar). These two types of feldspar have different characteristics and properties [164].

Sodium feldspar is not favourable in modern ceramic formulations since it is more susceptible to pyroplastic flow, does not contribute to translucency and is considered less attractive than potash feldspar.

Potash feldspar is favoured in formulations because of the natural translucent aesthetics it adds to the fired restorations, the improved hardness, increased viscosity of the molten glass, the improved chemical durability and the improved control of the porcelain pyroplastic flow during sintering [165, 171]. When melted between 1250-1500°C, potash fuses with quartz, transforming the mass into a molten glass phase and a leucite phase [171]. On cooling, the precipitated refractory leucite potassium aluminium silicate tetragonal structured crystals (KAlSi_2O_6 or $\text{K}_2\text{O} \cdot \text{Al}_2\text{O}_3 \cdot 4\text{SiO}_2$) form and are interspersed throughout the amorphous glass matrix. As much as 75% to 85% of the total volume is comprised of the glass matrix. The volume of leucite may range from 10% to 35%. This process in which a material melts to create a liquid and a different crystalline material is referred to as 'incongruent melting' [171, 174]. The leucite crystals are formed by 'surface crystallisation' when the porcelain is fired between 700°C and 1200°C, which means the crystals grow slowly along the grain boundaries towards the centre of the grain. If necessary, additional leucite ceramic may be added artificially.

The feldspathic leucite crystalline phase determines the thermal and mechanical behaviour of the porcelain depending on the distribution and size of the crystals. It elevates porcelain strength, fracture toughness, and hardness. Improves the optical properties and additionally the high thermal expansion of leucite helps to control the thermal expansion coefficient of the porcelain, depending on the amount present (10-20%) [156, 162]. Improving the homogeneity of thermal contraction between metal copings and overlaying porcelain helps avoid internal stress, a common cause for cracking and failure of metal ceramic and veneered all ceramic restorations. There are limitations in the properties of leucite because it is a relatively unstable phase and subsequently, repeated firing, slow cooling and extended heat soaks can affect the leucite content and overall mechanical properties of porcelain [175].

Factors such as the amount of potash, the firing temperature and the length of time the porcelain is held at high temperature also affect the extent of leucite crystal formation [176]. Repeated firings and slow cooling can either increase or decrease the leucite content in the glassy matrix. A process called secondary crystallisation is when the quantity of leucite crystals increases with subsequent firings, resulting in a higher coefficient of thermal expansion with each firing. Conversely, firing at a temperature too high can cause the leucite crystals to dissolve into the glass matrix. Such a change reduces the volume of crystallisation phase, lowering the coefficient of thermal expansion and consequently weakening the ceramic [171].

Quartz (SiO_2) also known as silica, has a high fusion temperature and serves as the framework around which the other ingredients can flow. By stabilising the porcelain build-up at high temperatures, quartz along with potash feldspar helps prevent the porcelain from undergoing pyroplastic flow on the metal substructure during sintering and strengthens the fired porcelain [177].

Alumina (Al_2O_3) is the hardest and strongest component of porcelain. The water molecules naturally attached to alumina are removed by a calcinations process resulting in alpha alumina which is ground into a fine powder [165]. Alumina increases the overall strength and viscosity of the melt.

5.4. Classifications of dental ceramics

There are several ways to classify dental ceramics. These methods include; fusion temperature, fabrication method, crystalline composition and phase and finally clinical application.

Fusion temperature refers to the temperature range over which ceramic particles fuse together because the melting process does not occur at a discrete temperature. Four

categories exist when classifying ceramics based on the fusion temperature. These categories include high fusing, medium fusing and low fusing and ultralow fusing. There are three subcategories within the traditional low-fusing porcelain category. These subcategories are also labelled high, medium and low fusing and differentiation again is based on the firing temperature range [164]. Specifically, the high fusing range within the low fusing category includes ceramics that are fired above a temperature of 900°C, medium fusing ceramics firing temperature is between 850°C -900°C and the low fusing ceramic group has a firing temperature below 850°C. Ultralow fusing porcelains were designed to veneer a metal substructure at very low temperatures [156].

If ceramics are classified according to the composition, the three ceramic categories include; predominantly glass; particle-filled glass; polycrystalline (Figure 5.2 and Figure 5.3) [176]. The particle filled glass category has a subgroup of ceramics called ‘glass ceramics’ [176, 178].

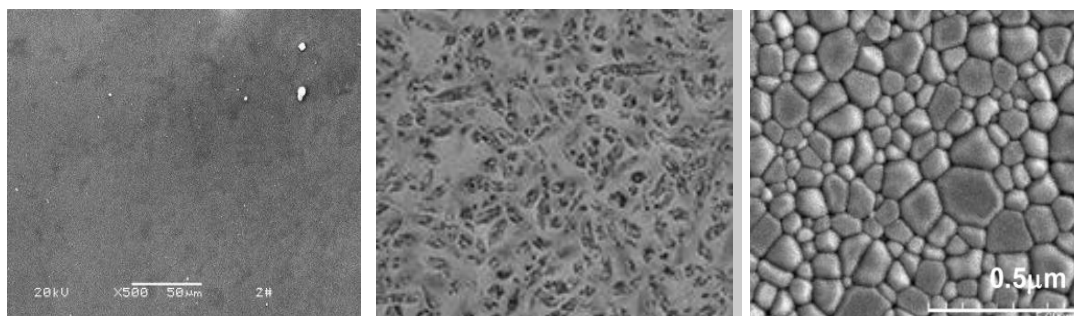


Figure 5.2: Schematic representation of three basic classes of dental ceramics. Predominantly glass-based ceramics are lightly filled with colorants and opacifiers to mimic natural aesthetics and are the weakest ceramics (left). Glasses containing 35 to 70 percent filler particles for strength can be moderately aesthetic as full-thickness restorations (middle). Completely polycrystalline ceramics (no glass), which are used to create strong substructures and frameworks via computer-aided design/computer-aided manufacturing processes (right).

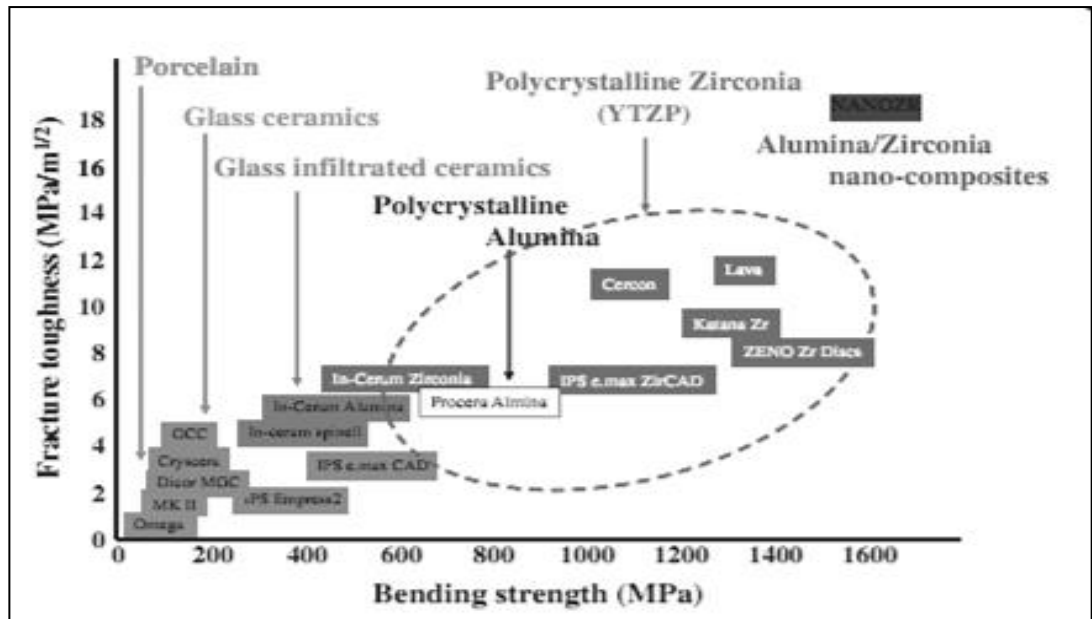


Figure 5.3: Classification of ceramics based on physical properties- fracture toughness and bending strength [176].

5.5. Predominately Glass Ceramics

Glass ceramics are an amorphous 3-D network of atoms having no regular pattern of their spacing and arrangement. They are derived principally from feldspar and are based on silica (silicon oxide) and alumina (aluminum oxide). Therefore these feldspathic porcelains (or glass ceramics) belong to a family called aluminosilicate glasses. These types of dental ceramics best mimic the optical properties of enamel and dentine [176].

Glass feldspathic ceramics are resistant to crystallisation which is called devitrification during firing, have long firing ranges so they resist slumping if temperatures rise above optimal and they are extremely biocompatible.

Devitrification and crystallisation during firing is not desirable since it can lead to increasing opacities and a whitish scum on the surface of a ceramic when it is fired for too long. Severe devitrification can cause deterioration and cracking [179].

5.6. Particle Filled Glass Ceramics

Particle-filled glasses are an example of why ceramics are composites. These ceramics contain filler particles. The filler particles are added to the base glass composition in order to improve mechanical properties through dispersion strengthening and to control optical effects such as opalescence, colour and opacity. They are usually crystalline such as leucite or they can be particles of a higher melting glass.

5.6.1. Glass Ceramics (subgroup of Particle Filled Glass Ceramics)

Glass ceramics are a group of ceramics and are a special subset of particle-filled glasses. Essentially this group of ceramics is characterised by mixing together crystalline and glass powders then after a special heat treatment, precipitation and growth of filler particles occurs [176]. Since these fillers are derived chemically from atoms of the glass itself, the composition of the remaining glass is altered as well during this process (termed 'ceraming') [180]. Therefore the final crystalline phases which determines the glass ceramics overall properties depend on the composition of glass, species of nucleating agent and the heating methods. Such particle-filled composites called glass-ceramics include IPS Empress CAD, IPS e.max Press and CAD (Ivoclar Vivadent).

Regarding the kinetics, when glassy phases transform to crystalline phase(s), it is necessary to overcome a certain energy barrier, which is called the activation energy of crystallisation (E). E is one of the important kinetics parameters to judge crystallisation capability of any glasses. If this energy were lower, it would be easier for the glasses to crystallise. Similarly, the crystal growth index (n) can also be applied to describe the capability of crystallisation of any glasses. The higher the crystal growth index (n), the easier the crystallisation. When the index (n) is less than three, the surface crystallisation mechanism will be dominated; when n is more than three, it is expected to have bulk crystallisation mechanism [164].

5.6.1.1. Leucite-reinforced glass ceramic- IPS Empress CAD

Since 1990, the IPS Empress glass-ceramic has been used to fabricate veneers, inlays, onlays, anterior and posterior crowns [181]. The material however is not suitable for the fabrication of bridges, mainly due to the low flexural strength of the ceramic [182].

5.6.1.1.1. Microstructure

IPS Empress CAD (Ivoclar Vivadent, Schaan, Liechtenstein) is a leucite-reinforced glass-ceramic consisting mainly of silica (SiO_2) and aluminum oxide (Al_2O_3) Table 5.5. The ceramic ingots have a homogenous composition, consisting of 35-45% evenly distributed leucite crystals which have a diameter of 1-5 μm . Etching the surface with hydrofluoric acid exposes the microstructure (Figure 5.4) and results in surface ideal for micromechanical retention with a resin cementation system [183, 184]. As leucite is the result of surface crystallisation, the leucite crystals are predominately located along the grain boundaries. The small leucite crystals that are arranged like strings of beads show the former grain boundaries prior to tempering/sintering. The physical properties are shown in Table 5.6.

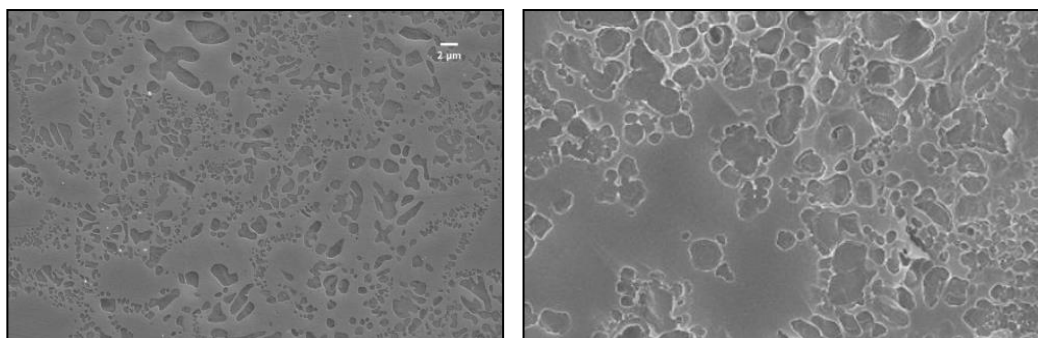


Figure 5.4: The SEM images of polished and etched surfaces reveal the microstructure of IPS Empress CAD (left). Etching technique using 40% HF vapour, 20 seconds, dissolves the leucite crystals more quickly than the glass (right). Typical leucite structure of IPS Empress Esthetic Veneer exposed when etched with 3% HF for 10 seconds. Source: R&D Ivoclar Vivadent AG, Schaan, Liechtenstein.

5.6.1.1.2. Chemical composition

Table 5.5: Standard chemical composition in percentage by weight of leucite-reinforced glass ceramic, IPS Empress CAD. (Ivoclar Vivadent, Schaan, Liechtenstein) Source: R&D Ivoclar Vivadent AG, Schaan, Liechtenstein

IPS Empress CAD	
Blocks	
<u>Standard Composition:</u>	(in weight %)
SiO ₂	60.0 - 65.0
Al ₂ O ₃	16.0 - 20.0
K ₂ O	10.0 - 14.0
Na ₂ O	3.5 - 6.5
Other oxides	0.5 - 7.0
Pigments	0.2 - 1.0

5.6.1.1.3. Physical

Table 5.6: Physical properties of IPS Empress CAD (Ivoclar Vivadent AG, Schaan, 2005/2006)

Physical Properties of IPS Empress	CAD
CTE (100-400°C [10^{-6} /K])	16.6
CTE (100-500°C [10^{-6} /K])	17.5
Flexural strength (biaxial) [MPa]	160
Fracture toughness [MPa M ^{1/2}]	1.3
Modulus of elasticity [GPa]	62
Vickers hardness [MPa]	6200
Chemical resistance [$\mu\text{g}/\text{cm}^3$]	25
Transformation temperature °C	625

5.6.1.2. Lithium disilicate glass ceramic- IPS e.max Pressed and CAD blocks

Milled and pressable lithium disilicate material is indicated for any restorative non-metal indirect prosthesis that is desired which is less than 3 units in total. Such prosthetics include inlays, onlays, veneers, crowns, 3-unit and implant restorations [185].

5.6.1.2.1. Standard chemical composition

The crystals of both the IPS e.max Press and IPS e.max CAD are the same in composition. Both microstructures are 70% crystalline lithium disilicate, $\text{Li}_2\text{Si}_2\text{O}_5$, but the size and length of these crystals are different (Table 5.7).

Table 5.7: Standard chemical composition in % by weight of lithium disilicate glass ceramic, IPS e.max press (left) and CAD block (right). (Ivoclar Vivadent, Schaan, Liechtenstein) Source: R&D Ivoclar Vivadent AG, Schaan, Liechtenstein

IPS e.max Press	
Ingots for the ceramic press technique	
<u>Standard composition:</u>	(in wt %)
SiO_2	57.0 – 80.0
Li_2O	11.0 – 19.0
K_2O	0.0 – 13.0
P_2O_5	0.0 – 11.0
ZrO_2	0.0 – 8.0
ZnO	0.0 – 8.0
+ other oxides	0.0 – 10.0
+ coloring oxides	0.0 – 8.0

IPS e.max CAD	
Ceramic blocks for the CAD/CAM technique	
<u>Standard Composition:</u>	(in wt %)
SiO_2	57.0 – 80.0
Li_2O	11.0 – 19.0
K_2O	0.0 – 13.0
P_2O_5	0.0 – 11.0
ZrO_2	0.0 – 8.0
ZnO	0.0 – 8.0
Other and colouring oxides	0.0 – 12.0

5.6.1.2.2. Physical properties

Material properties such as coefficient of thermal expansion, modulus of elasticity, and chemical solubility are the same, yet the flexural strength and fracture toughness are slightly higher for the IPS e.max Press material (Table 5.8) [186]. The glass ingots or blocks are then processed using the lost-wax hot pressing techniques or milling procedures.

Table 5.8: Physical Properties of IPS e.max Press and CAD Blocks

Physical Properties of IPS e.Max	Press	CAD
CTE (100-400°C [$10^{-6}/K$])	10.2	10.2
CTE (100-500°C [$10^{-6}/K$])	10.5	10.5
Flexural strength (biaxial) [MPa]	400	360
Fracture toughness [$MPa M^{1/2}$]	2.75	2.25
Modulus of elasticity [GPa]	95	95
Vickers hardness [MPa]	5800	5800
Chemical resistance [$\mu g/cm^3$]	40	40
Press temperature EP 600 [°C]	920	

Lithium disilicate ceramics have a high flexural strength and modest fracture toughness relative to leucite-reinforced and feldspathic porcelain [187]. The higher fracture toughness and flexural strength of lithium disilicate ceramics is attributed to the dispersed interlocking crystal arrangement which hinders crack propagation by means of energy-absorbing processes, such as crack deflection and branching. The

lithium disilicate glass-ceramic displays a considerably lower coefficient of thermal expansion compared to leucite-reinforced [188] which subsequently yields a highly thermal shock resistant glass ceramic when processed [187].

5.6.1.2.3. Processing and manufacturing

IPS e.max lithium disilicate is predominately composed of quartz, lithium dioxide, phosphor oxide, alumina and potassium oxide. These powders are combined to produce a glass melt. Once the proper viscosity is achieved, similar to that of honey, the glass melt is poured into a separable steel mould of the proper shape and left to cool. This process produces minimal internal defects due to the glass flow process. The translucency aids ease of quality control since porosities can be easily detected [182, 185] (Figure 5.9).



Figure 5.9: The translucency of IPS e.max. (Ivoclar Vivadent, Schaan, Liechtenstein) aids ease of quality control since porosities can be easily detectedSource: R&D Ivoclar Vivadent AG, Schaan, Liechtenstein.

5.6.1.2.4. Microstructure lithium disilicate IPS e.max CAD Blocks

During processing, the IPS e.max CAD material has two crystal types and two microstructures that provide its unique properties during each phase of its use. The

microstructure of intermediate crystallised IPS e.max CAD lithium disilicate consists of 40% platelet-shaped lithium metasilicate (Li_2SiO_3) crystals embedded in a glassy phase. These crystals range in length from 0.2 to 1.0 μm . The intermediate lithium meta-silicate crystal structure allows the material to be easily milled without excessive bur wear. The post crystallisation microstructure of IPS e.max CAD lithium disilicate material consists of 70% fine-grain lithium disilicate crystals embedded in a glassy matrix. The millable intermediate crystallised IPS e.max CAD blocks are coloured using colouring ions but unlike the pressed lithium disilicate, the colouring elements, are in a different oxidation state during the intermediate phase than in the fully crystallised state. As a result, the lithium metasilicate exhibits a blue colour. The material achieves its desired tooth colour and opacity when the lithium metasilicate is transformed into lithium disilicate during the post milling firing process.

The IPS e.max CAD “blue block” (Figure 5.10) uses a two-stage crystallisation process. The two-stage crystallisation uses a controlled double nucleation process where lithium meta-silicate crystals are precipitated during the first step. A second heat treating step at approximately 840-850°C is performed after the milling process has occurred. During the heat treatment, the meta-silicate phase is completely dissolved and the lithium disilicate ($\text{Li}_2\text{Si}_2\text{O}_5$) crystallises, giving a fine 1.5 μm grain glass ceramic with 70% crystal volume incorporated a glass matrix (Figure 5.11). This provides the ceramic with favourable mechanical properties such as high strength.

Polyvalent ions that are dissolved in the glass are utilised to provide the desired colour to the lithium disilicate material. These colour-controlling ions are homogeneously distributed in the single-phase material, thereby eliminating colour-pigment imperfections in the microstructure (Figure 5.12) [178].

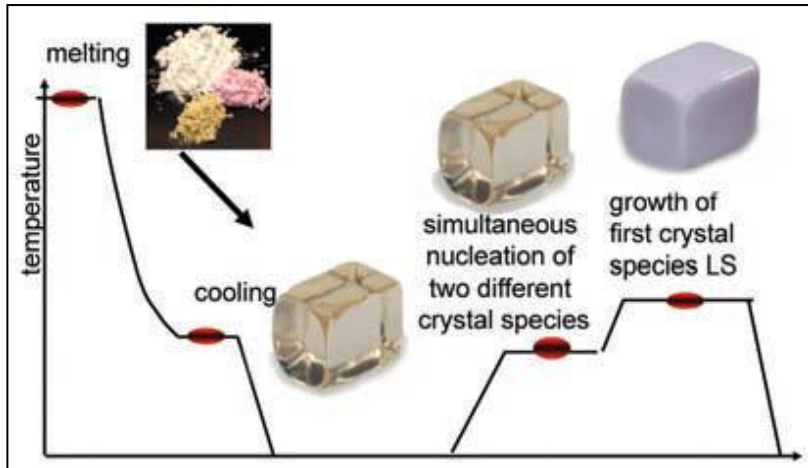


Figure 5.10: The IPS e.max CAD “blue block” uses a two-stage crystallisation process. Source: R&D Ivoclar Vivadent AG, Schaan, Liechtenstein.

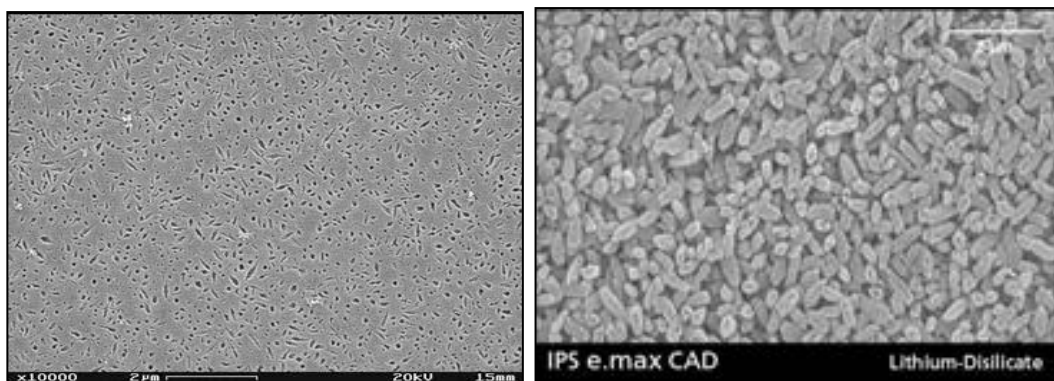


Figure 5.11. SEM image of partially crystallised lithium metasilicate IPS e.max CAD (Ivoclar Vivadent) etched with 0.5% HF for 10 sec. The etched-out areas represent the lithium metasilicate crystals (left). Fully crystallised lithium disilicate IPS e.max CAD (Ivoclar Vivadent) etched with 0.5% HF vapour for 30 sec (right). Source: R&D Ivoclar Vivadent AG, Schaan, Liechtenstein.

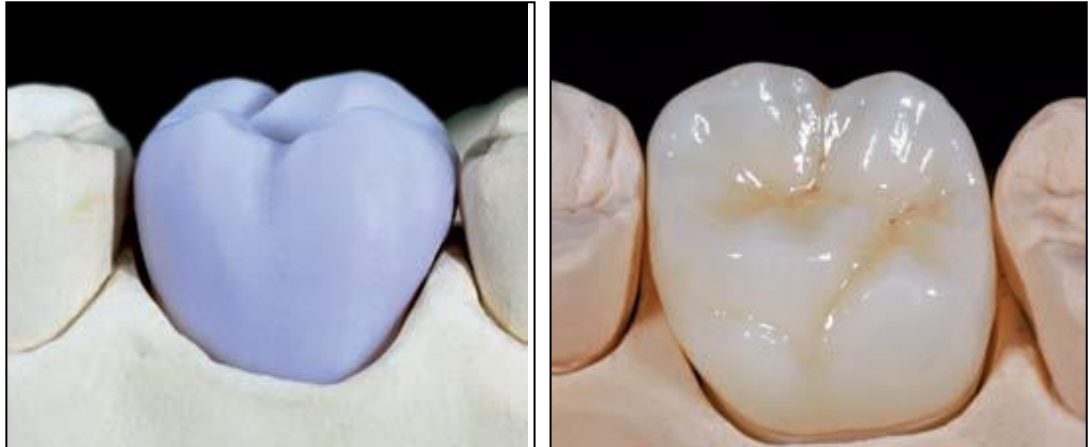


Figure 5.12: IPS e.max CAD “blue block” (Ivoclar Vivadent) (right), IPS e.max CAD completely crystallised lithium disilicate ceramic (left). Source: R&D Ivoclar Vivadent AG, Schaan, Liechtenstein.

5.6.1.2.5. Microstructure IPS e.max Press

The IPS e.max Press material is produced similarly to the IPS e.max CAD as far as the formation of the initial glass ingots, as they are composed of different powders that are melted and cooled to room temperature to produce glass ingots. Following the glass formation, the ingots are then nucleated and crystallised in one heat treatment to produce the final ingots (Figure 5.13). These ingots are then pressed at approximately 920°C for five to fifteen minutes to form a 70% crystalline lithium disilicate restoration. This process is constantly optimized in order to prevent the formation of defects. The microstructure of the pressable lithium disilicate ($\text{Li}_2\text{Si}_2\text{O}_5$) material consists of approximately 70% volume of needle-like lithium disilicate crystals that are crystallised in a glassy matrix (Figure 5.14). These crystals measure approximately 3µm to 6µm in length [181].

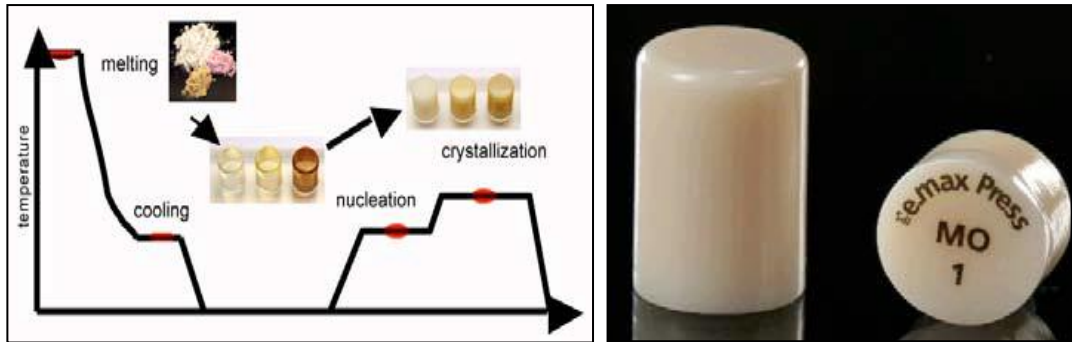


Figure 5.13: Following the glass formation, the ingots are then nucleated and crystallised in one heat treatment to produce the final ingots (left). The ingots are available in two degrees of opacity (right). Source: R&D Ivoclar Vivadent AG, Schaan, Liechtenstein.

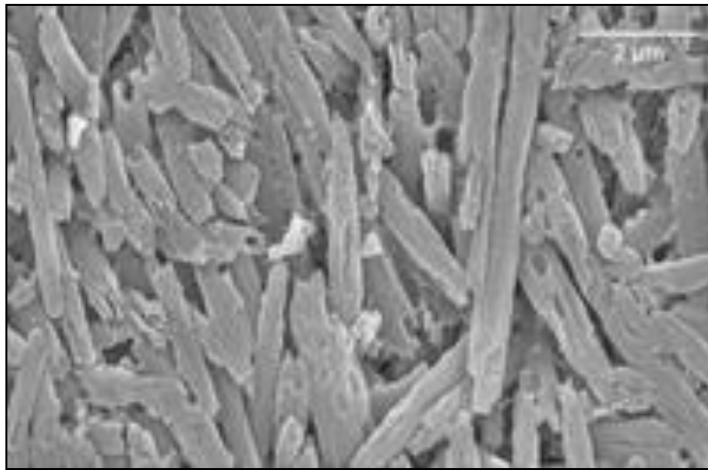


Figure 5.14: Microstruture of IPS e.max Press glass ceramic. Note the long (3-6 μ m) lithium disilicate crystalline structure (Ivoclar Vivadent, Schaan, Liechtenstein) Source: R&D Ivoclar Vivadent AG, Schaan, Liechtenstein.

5.7. Polycrystalline ceramics

Two developments allowed us to use polycrystalline ceramics in dentistry since the 1980s. These technological advances include: the availability of highly controlled starting powders; and the application of computers to ceramics processing [178]. Unlike glassy ceramics, polycrystalline ceramics cannot be simply pressed as a fully dense material into slightly oversized moulds. Polycrystalline ceramics instead are formed from powders that can only be packed to around 70% of their theoretical density and because of this they shrink by around 30% by volume (10% linear) when made fully dense during firing. For this reason the powders need to be well characterised so that we can predict the shrinkage that will occur and allow the

prosthesis to fit accurately. Polycrystalline ceramics are either alumina or zirconia based.

Polycrystalline ceramics have no glassy components and all of the atoms are densely packed [189]. This composition results in a very strong and tougher ceramic material and thus makes it more difficult to drive a crack through when compared to ceramics where the atoms are less dense and have an irregular network (Figure 5.15).

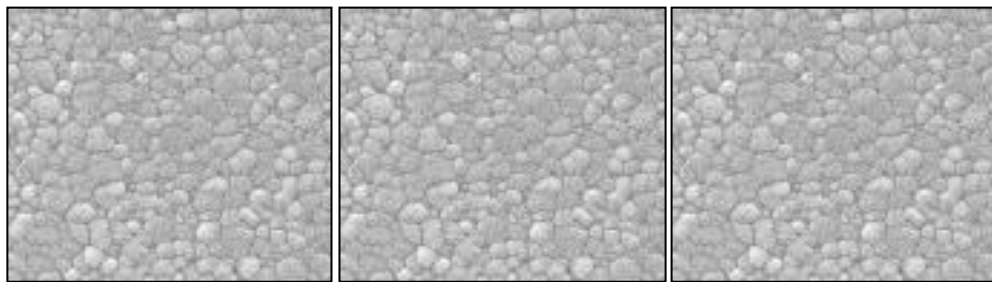


Figure 5.15: Polycrystalline 3Y TZP ceramic. Note the dense array of atoms, irregular network and absence of glass matrix [176].

Polycrystalline ceramics are very strong and opaque and are commonly the substructure material of all ceramic restorations. Due to their high strength and fracture toughness, they are able to resist crack propagation better than other ceramics [190].

5.7.1. Alumina-based ceramic

The first all-ceramic system In-Ceram Alumina (VITA Zahnfabrik, Bad Säckingen, Germany), an alumina-based ceramic, was introduced in 1989. It is an opaque core, fabricated through the slip-casting technique and veneered with feldspathic porcelain [163, 191]. In 1994, In-Ceram Spinell (VITA Zahnfabrik, Bad Säckingen, Germany) was launched, with a specific crystalline structure referred to as “spinell” (magnesium aluminate- $MgAl_2O_4$) in the composition. The spinell core has a better translucency but reduced flexural strength, allowing it to be used directly or to be veneered with a feldspathic porcelain [163, 191]. The In-Ceram Alumina was later

modified with the addition of 35% zirconium oxide to strengthen the core, forming In-Ceram Zirconia (VITA Zahnfabrik, Bad Säckingen, Germany). However, this core is also opaque and lacks translucency [163].

Another alumina-based product that has been more commonly used lately is the Procera All-ceramic System (Procera-Snadvik, Stockholm, Sweden). Copings produced from this system composed of a very high purity aluminum oxide (>99.9%) [183, 192], giving the porcelain optimal strength.

5.7.2. Zirconia-based ceramic

Three types of zirconia-containing ceramics are used in dentistry are; yttrium cation-doped tetragonal zirconia polycrystals (3Y-TZP), magnesium cation-doped partially stabilized zirconia (Mg-PSZ) and zirconia-toughened alumina (ZTA) [189]. 3Y-TZP has the most favourable properties [190]. A summation of the mechanical properties of 3Y-TZP Zirconia is shown in Table 5.16.

Table 5.16: Tetragonal Zirconia Polycrystals 3Y-TZP: Mechanical and Physical Properties.

Equiaxed grains $\mu\text{m D}$	0.2-0.5
Flexural strength MPa	800-1200
Fracture toughness $\text{MPa m}^{1/2}$	6.1-8.5
Weibull modulus	10-18
Porosity %	8.1-11.5
Threshold Intensity factor $\text{MPa m}^{1/2}$	3.1
Critical crack Intensity $\text{MPa m}^{1/2}$	7.4
Thermal Conductivity $\text{Wm}^{-1}\text{K}^{-1}$	2

Transformation toughening properties are unique to zirconia based polycrystalline ceramics. This favourable property was first noted in the 1970s by Garvie and was published in the Nature Journal in 1975 [193]. Garvie was an Australian working for CSIRO in Melbourne. Transformation toughened zirconia or partially stabilised Zirconia or metastable zirconia involves an additional mechanism not found in other polycrystalline ceramics which increases its fracture toughness. The resulting fracture toughness of the zirconia ceramic is twice that of alumina ceramics [190].

At ambient pressure, unalloyed zirconia can assume three crystallographic forms depending on the temperature. These phases are cubic (c), tetragonal (t) and monoclinic (m). At firing temperature, the crystalline zirconia is tetragonal and at room temperature the symmetry is monoclinic [189]. The phase is cubic when above 2370°C. Interestingly a unit cell of monoclinic occupies about 4.4% more volume than when tetragonal, and this important physical property is what is harnessed and responsible for its very favourable strengthening properties. Interestingly, the phase change from (c) to (t) t is associated with a 2.31% volume increase [194, 195]. Zirconia based ceramics partially stabilise the (t) phase at room temperature. Full stabilisation is not desired as it does not improve the ceramic physical properties [189, 196].

The stabilisation of the (t) phase at room temperature is due to influences of particle size, particle morphology, and the amount and type of dopant used. Partial stabilisation involves dopants, such as with CaO, MgO, La₂O₃, and Y₂O₃, in concentrations lower than that required for full c-ZrO₂ stabilization [176, 187, 190]. A concentration of 2 to 5 mol has been tested to be most beneficial for ideal partial stabilisation.

Transformation mechanisms from the (t) to the (m) phase results in a reduced local stress intensity, compressive stress in the crack region which is associated with the 4.4% volume increase as the t crystals upright themselves, this shields and limits the crack propagation and overall increases the flexural strength and fracture toughness since now, a greater amount of stress is necessary to overcome this compressive

stress and cause more crack propagation [197]. This toughening mechanism does however increase the rate of ageing and risk of fatigue failure [178, 194]. Surface treatment such as grinding or sandblasting can trigger the phase transformation from tetragonal to monoclinic, which could be harmful to the long-term performance of the material [189].

CHAPTER 6

IN-VITRO CERAMIC WEAR TESTING

6.1. Considerations of *in vitro* ceramic wear testing

Investigating the wear process that occurs between dental ceramics and dental hard tissue is complex for many reasons. The process of wear of dental hard tissue is influenced by multiple factors and these factors are extremely difficult to control in laboratory based wear simulation studies. *In vitro* studies are a valuable research procedure because a large amount of data and information can be attained within a short period of time and this type of research design is able to investigate individual factors that cause tooth wear.

A limitation with *in vitro* studies arises when comparing *in vitro* studies with one another and when trying extrapolate data from *in vitro* studies to clinical situations [198]. This is of concern because there is significant variability in the research instrumentation, materials and protocol and each of these parameters is capable of altering the wear mechanism [81, 199, 200]. For example the different types of wear machines, contact geometry and pressures, loading protocols, chemistry and flow of lubricants used in dental wear *in vitro* studies [4, 201-206] as well as variables such as contact pressure; friction, material microstructures and physical properties; food characteristics; and, chemicals all appear to influence the degree of variation and mechanism of wear [39, 207-209].

6.2. Quantification of wear

The quantification of tooth wear can be undertaken using a variety of instruments. Recent ISO technical specification recommendations relating to wear by two-and/or three body contact describe eight different wear assessment methods [210]. Using different instruments may cause inaccuracies and reduces the validity when

comparing different studies and when determining material rankings.

In the early experimental studies involving enamel specimens, wear was assessed by the change in weight of specimens between experimental time points. Over time more accurate methods were developed to overcome the errors associated with the uptake and loss of moisture by dentine and restorative materials. These methods involved the microscopic measurement of specimen height reduction and, more recently, scanning specimens and the use of purpose-written software to quantify specimen volumes. The more common assessment methods in the literature include height loss [198, 211-219], volume loss [198, 220-222], weight loss [223] and wear surface area [224]. Measurements of height or volume loss have been performed with a stereoscopic microscope with a micrometer-calibrated movable platform [222] or a Reflex microscope [211]. The most common and effective technique used to measure height and volume loss is with a scanning profilometry [198, 212-214, 216-221, 224].

6.3. Standardising wear simulation research protocols

The standardisation of *in vitro* study protocols would improve the quality of dental wear studies by resulting in more effective comparisons and extrapolations to the clinical setting and this would ultimately improve our overall body of scientific knowledge. Despite the dental scientific community efforts, the International Standards Organization Technical Committee 106 (Dentistry) was unable to reach consensus to standardise dental related wear testing protocols. The committee stated that despite many wear tests being proposed for dentistry, there is no generally accepted method and none of the *in vitro* wear simulators have been developed based on direct observations of mechanisms of damage accumulation occurring intra-orally [225]. The committee further reported that due to the extensive variability in research methodologies, it is not surprising that differences in results and outcomes are probable even when studies are examining the same materials [203, 226, 227].

6.4. *In vitro* ceramic wear research test parameters

In vitro studies testing wear between dental hard tissue and materials such as ceramics commonly use prepared enamel from extracted molars and premolars as the antagonist and flat ceramic specimens in which the surfaces are abraded, polished or glazed. Other research and test parameters however lack such standardisation and subsequently no comprehensive analysis or meta-analysis has been able to be completed on a specific category of ceramic materials. The test parameters in relation to the instrumentation and material set up which demonstrate considerable variation in the literature includes the type of chewing simulators, applied force, force actuator, number and frequency of cycles, lubricating medium force, the force actuator, the use of lubricants and the pH of the lubricant and surrounding medium, exogenous abrasive materials, as well as the number of specimens and the geometry of the specimens analysed [147, 174, 227].

6.4.1. Chewing simulators

In the literature there are a large number of various chewing or wear simulators described. The various simulators include; Pin on disc simulator [228-231], University of Alabama [216], Oregon Health Sciences University [224, 232], Willytec [233], Leinfelder [220] [218], the closed loop servohydraulics [234], and different custom made chewing simulators [211].

6.4.1.1. Willytec chewing simulator

A good compromise with regard to costs, practicability and robustness is the Willytec chewing simulator [52], which uses weights as the force actuator and stepping motors for vertical and lateral movements [235]. Force measurements have revealed that in the beginning of the stylus/specimen contact phase the force impulse is three to four times higher during dynamic loading than during static loading [52]. When the antagonist hits the flat specimen with a mass of 5 kg, a force of 150–200N is generated within the first 25–30 ms, then fluctuating between 40 and 60N for the

following 100ms and then varying between 20 and 100N for about 50 ms [52] The full contact time is 200 ms. As this variation occurs in all eight-test chambers, the coefficient of variation for material wear is relatively low and has been calculated to be on average 12.5% if ten materials have been tested [236].

6.4.2. Loads applied to specimens

The loads applied in previous wear studies are variable and have been reported in either grams, kilograms or Newtons, and ranged broadly from as small as 180g or 1.8N to 160N [212, 237, 238]. A range of loads that have been used in studies of wear of ceramics are as follows: 0.75N [218, 219, 230], 4.5N [202, 239], 6N [221], 10N, 13.5N [234, 240], 20N for the cycles and direct contact with a static load of 70N at the end [229], 30N [200], 40N [53], 49N [233], 76-80N [228]. Loads greater than 160N are not usually considered because they frequently resulted in catastrophic failure of the specimens. A loading force of approximately 50N can be regarded as a mean value of the physiological biting forces of non-bruxist patients [241]. Higher forces during *in vitro* simulation lead to higher wear rates [242].

6.4.3. The force actuator

Force generation is a highly variable parameter in the *in vitro* wear systems. There are different force generating principles called actuators, which all have their advantages and disadvantages. Even if the wear parameters are identical, the use of different force actuators can generate different levels of quantitative wear and therefore when the same wear method is repeated using a different device and force actuator, different results may be obtained [233].

6.4.4. Number of cycles

The duration of *in vitro* experimentation is planned to give sufficient wear to allow reliable measurement of the amount of tooth reduction and comparison of wear rates

between consecutive experimental intervals. Wear testing between enamel and ceramic specimens commonly run for a period of 5000 and 300000 cycles depending on the protocol. Experiments involving dentine however were continued for as long as possible to assess the change in wear rate as tooth reduction progressed deeper into the dentine. The following are some examples of studies with different protocols for number of cycles. 10 000 cycles [200, 231, 239, 243, 244], 25 000 cycles [53, 245, 246], 43200 cycles [104, 202, 205], 100000 cycles [230, 233], 172800 cycles [247], 250000 cycles [228], 300000 cycles [234]. As far as the number of loading cycles is concerned, wear increases with the increasing number of cycles. Most *in vitro* wear test methods demonstrate a running-in phase with a steep increase in wear in the initial phase and a flattening of the curve thereafter. From a certain point onwards, wear increases in an even linear pattern [202], but this is not always the case [248].

6.4.5. Exogenous abrasive materials

To test the wear of dental hard tissue and restorative materials against masticatory forces, a third body slurry of various components is incorporated into the chewing simulator machine to simulate the food bolus during the chewing cycle. The composition of the slurry aims to replicate the modern diet acidity, consistency and abrasiveness. Slurry materials can include a multitude of substances, however poly methyl methacrylate (PMMA) slurry [216] and non-plasticized PMMA powders with a mean particle size of 40 μ m are commonly used [233]. Less common slurries may consist of materials such as a mixture of glass pearls, aluminum oxide powder (105 μ m) and water [249] or a mixture of cornmeal grit and wholemeal flour in distilled water [250].

6.4.6. Lubrication and pH variations

The most popular lubricating medium used in studies on wear rates of porcelain and enamel has been distilled water [198, 211, 215, 218, 219, 221, 222, 251]. Some researchers have used artificial saliva [217, 223] or tap water [212, 216]. Fresh,

natural saliva as a lubricant has also been used but not as commonly as the other methods for lubrication [252] [253]. All these approaches have their advantages and disadvantages. Distilled water appears to be favourable due to its low cost, ease of use and minimal corrosive influence on the metallic materials and adhesives used, however this disadvantage of distilled and tap water for that matter is that they do not mimic the lubricating properties of saliva. Artificial saliva does not mimic natural saliva and also adds another variable, that of remineralisation, which potentially changes the results. Natural saliva, on the other hand, although seemingly a good approach denatures within minutes and makes the results of long experiments skewed and reduced the correlation with the oral environment.

Most of the wear studies between enamel and porcelain have been carried out in neutral or near neutral pH and only two papers by the same group of authors were found to address the wear in lower pH [254, 255]. Their experiments investigated wear of three types of porcelain (Vitadur Alpha (Vita Zahnfabrik, Germany), Duceram-LFC (Ducera Dental GmbH, Germany) and Vita Mark II (Vita Zahnfabrik, Germany)) against enamel in Coca-Cola (pH in the range of 2.28 to 2.37). It was found that exposure to the carbonated beverage increased the amount of enamel wear by 19% against Alpha porcelain, 13% against Vita Mark II and 74% against Duceram-LFC compared with enamel wear produced in water [233, 234].

6.4.7. Specimen geometry

The majority of *in vitro* studies analyse flat ceramic specimens mounted on an SEM platform. Flat ceramic specimens are favourable due to their ease of fabrication and standardisation. The analysis of the surface texture and wear of the ceramic specimens is also easier and more efficient when light microscopes are necessary. *In vitro* studies have demonstrated material wear of flat specimens to be higher than that of crown specimens and flat specimens compared to crown specimens were associated with more wear on the opposing dentition [43]. This is possibly due to a greater surface area of contact between the ceramic and enamel and also because the strain distribution in flat specimens is higher than in anatomically formed specimens

like crowns or inlays, thus causing more material wear in flat specimens.

6.5. The outcome of *in vitro* test parameter variation

Despite efforts to standardise test parameters, methodologies, materials and sample preparations, the large degree of variation accounts for the lack of consistency between studies testing similar or the same materials. This has led to a lack of agreement of ranking of specific ceramic materials for enamel and material wear because it is difficult to determine what influence, if any that it had on the outcomes of the results. In regards to surface finish, there is limited consistency between *in vitro* studies. However the most recent studies suggest that both procedures, either polishing or glazing are effective methods in reducing the surface roughness and optimising the surface texture of a material [43, 227, 256-258].

6.6. Factors influencing enamel wear when opposed by ceramic

Ceramic materials are generally resistant to wear and are abrasiveness to enamel. The extent of enamel wear was more of an issue in the earlier decades when our understanding of ceramic properties and enamel wear was limited and the importance of polishing and reducing surface texture of ceramic occlusal surfaces was not appreciated. The severity of tooth surface wear can be influenced by a number of dental material and patient related factors [43]. Firstly, ceramic material factors which influence the rate of enamel wear include physical, micro structural, chemical and surface characteristics [259, 260]. For example, a polycrystalline ceramic such as a 3Y-TZP zirconia core which has a much higher hardness and surface roughness than a glass ceramic may result in more opposing tooth wear. Low fusing ceramics appear to be more protective to the opposing enamel compared to older types of ceramics. Manufacturers claim that this is due to their lower hardness, lower concentrations of the crystal phase and smaller crystal sizes [261]. Patient factors including highly acidic and erosive diets, dysfunctional occlusion, high biting force and parafunctional habits may also increase the rate of dental hard tissue loss [43].

No specific physical parameter of ceramic materials has been identified to be a predictor of wear of the opposing enamel. Surface hardness of ceramics was thought to determine enamel wear in the 1980's [199] however studies in the 1990's demonstrated that surface hardness is not a reliable predictor for wear of the opposing enamel [43, 81, 262]. The most recent studies strongly suggest surface texture and specifically surface roughness to have the most influence on opposing tooth wear compared to all other ceramic physical factors considered [212, 223, 263]. It is important to keep in mind that reported 'influencing' factors are derived from *in vitro* chewing simulation studies which as discussed are often inconsistent, contradictory, lack external validity and overall do not highly correlate clinically [259, 260].

6.6.1. Ceramic Physical Microstructural Properties

The physical properties of ceramic materials can influence the polishability of the surface and also the wear of the opposing material, whether it be a ceramic of dental hard tissues [264]. The exact influence of physical properties including hardness, frictional resistance, fracture toughness leucite content, crystal size, porosities, creaming and surface texture is still debated [265].

6.6.2. Hardness

Hardness is a term to describe the degree of resistance a material has to plastic deformation. It was previously assumed that a greater hardness was associated with an increased rate of enamel wear however more recent studies have shown that there is not a strong correlation between the hardness of ceramic and the wear rate of enamel [266]. Instead, the wear process appears to be more closely related to the ceramic microstructure, the surface roughness of contacting surfaces, and environmental influences such as lubrication pH [173, 234]. There are several explanations to explain the weak correlation between hardness and enamel wear.

Firstly it is because when ceramic slides against ceramic or enamel, wear does not occur by plastic deformation, as with metals, but by fracturing [43, 243]. Secondly, the micro-hardness of the crystalline ceramics varies depending on the orientation of the indenter to the crystals, and finally it is due to the variability in the hardness between the glass matrix and the crystals [201]. For these reasons, it is not surprising that relatively soft ceramics exhibit more abrasive action against human enamel than harder ceramics [201].

6.6.3. Frictional resistance

Frictional resistance is the term used to describe the resistance two materials in contact with one another have to lateral sliding. This characteristic depends on the relative motion, the properties and structures of the contacting materials, and the surrounding environment. For example, friction between porcelain-to-porcelain contacts has been reported as nearly twice that of porcelain-to-acrylic resin contacts and almost three times that of enamel-to enamel contacts [170]. Rough surfaces, high loads, and high sliding speeds have been shown to increase the coefficient of friction, resulting in greater wear [170]. Even the most meticulously polished surfaces have microscopic irregularities, and it is the interaction between the microscopic peaks and valleys that determines the friction between two opposing surfaces. Because the surface hardness of ceramic decreases in an aqueous environment, the friction between the two materials can increase due to adhesion at a microscopic level especially in the presence of saliva or lubricating medium. For these reasons the outcomes of *in vitro* tooth wear studies can be influenced by the lubrication medium and may possibly obscure the relevance to what actually is likely to occur *in vivo* [169].

6.6.4. Fracture toughness

Fracture toughness describes the resistance of a material has to rapid crack propagation under tensile stress [173]. It is an intrinsic material property that depends on two factors. The first factor it depends on is the stress intensity at a crack tip in the

material, and the second factor is the size of the crack relative to the micro structural features of the material (such as crystal size, aspect ratio, and orientation; distribution of the glass phase; and porosity). Fracture of a ceramic material starts when the applied load produces a stress at the tip of a flaw or crack. Because ceramic failure occurs without any noticeable plastic deformation, the importance of fracture toughness in the ceramic wear process can be significant. This type of characteristic wear can start with crack formation, and then slow crack propagation over time and then eventual catastrophic failure and fracture of the material [169, 170, 173].

If the restorative ceramic material does not have sufficient toughness to resist fracture, then brittle chipping may occur leading to an increase in the surface roughness. Brittle chips formed during the abrasive process can cause resharpener of the edge of the particles with a further increase in the wear rate. The sharp edges of broken glass do not dull rapidly because of their higher hardness. Brittle fracture of ceramics may be more pronounced when they are situated adjacent to processing defects such as porosity and impurity inclusions and they can all further increase the probability of crack propagation under loading and over time.

Lithium disilicate and leucite-reinforced ceramic has a higher Vickers hardness and fracture toughness compared to enamel [43]. The lower hardness of enamel compared to the leucite-reinforced and lithium disilicate ceramic materials cause the enamel antagonist to wear more than the ceramic material. The wear of the opposing enamel is further accelerated by the rough ceramic surface that is created during the simulation and chipped pieces may act as an abrasive medium. In addition, when the fracture toughness of the enamel is significantly lower than that of the ceramic material, even more pronounced antagonist wear may occur [43].

6.6.5. Porosity

Sintered porcelain is produced when a powder is mixed with a liquid which is then

condensed and sintered. The main problem with this process is the accumulation of porosities which is difficult to completely remove from the porcelain structure. These porosities can promote undesirable characteristics such as reduced strength and aesthetics. Air entrapment can be minimised however by casting or pressing ceramic ingots supplied by manufacturers [267]. If a subsurface porosity is exposed during the wear process, the sharp edge of the defect presents as an area of stress concentration and produces more wear against the opposing dentition [169]. Industrially manufactured ceramic CAD blocks are more homogenous and less likely to have porosities within the ceramic.

6.6.6. Crystals

Dental porcelain is composed of silica glass that is modified by fluxes such as CaO, K₂O, Na₂O, B₂O₃, and Al₂O₃. With an appropriate composition of the oxides, leucite crystals (K₂O.Al₂O₃.4SiO₂) are formed to improve mechanical and optical properties and control the coefficient of thermal expansion of the ceramic. Ceramics used in metal-ceramic restorations contain 15 to 25 vol% leucite as their major crystalline phase whereas all-ceramic restorations contain up to 90 vol% leucite as their major crystalline phase. The leucite crystals consist primarily of alumina, magnesia, zirconia, or lithia in a glassy matrix [178].

These crystals which are commonly about 5 to 7 microns in diameter are incorporated into a glassy matrix are responsible for the greater wear of the opposing dentition because of their higher hardness. The potential abrasiveness of the crystals also varies depending on the type, content, morphology, and distribution of the crystalline particles. Nevertheless it may be inappropriate to correlate the wear characteristics of a ceramic material only on the crystal qualities and amount in the glassy matrix since studies show that crystals in the glassy matrix do not necessarily have a negative impact on the wear of the enamel [267, 268].

Care must be taken in interpreting data from *in vitro* tests because the wear behaviour of a ceramic with low fusing crystal content, which was developed to achieve better wear characteristics, may be characterised differently by different wear tests. For example, enamel loss against low-fusing porcelain was reported as significantly lower than that against conventional feldspathic porcelain in a sliding wear test [269] and greater than conventional porcelain in a sliding and impact loading test [270]. The wear resistance of the low-fusing porcelain was consistently lower than that of conventional porcelain for both of the test methods, supporting the theory that crystals in a glassy matrix improve the fracture resistance of ceramic [267, 270]. To clarify this debate in the literature, better standardisation of *in vitro* test methods has been recommended.

It has been suggested that ceramic materials with a higher leucite percentage may be more difficult to polish [271], thus needing more polishing time compared to materials with less leucite and more glassy matrix [272].

6.6.7. Ceram Layer

Ceramming is the controlled crystallisation of the glass resulting in formation of crystals evenly distributed throughout the glass structure. The size, amount and rate of growth of crystals are determined by the time and temperature of the ceramming heat treatment. This ceramming process results in crystals orientated perpendicular to the external surface of the glass-ceramic. The most outer layer of the ceramic which is called the ceram layer is reported to be up to twice as abrasive to the opposing natural dentition and four times less wear resistant than a polished ceramic [270].

6.6.8 Chemical degradation by acid attack

The wear rate of enamel and ceramic is significantly higher in a highly acidic environment than in a less acidic environment [267]. This observation is attributed due to two reasons. Firstly the acidic environment affects the solubility of tooth

structure and by decreasing the oral pH from 6.5 to a more acidic 5.5 increases the solubility by a factor of seven to eight times of enamel. Secondly, forms of chemical degradation such as glass corrosion, etching, and crystal deposition increase the degree of surface roughness and lower the wear resistance of ceramics against opposing teeth by continuously exposing a rough surface. If a degraded ceramic surface is further subjected to dysfunctional occlusion or parafunctional habits such as clenching and bruxism, the wear process may be accelerated [273].

6.6.8. Effect of surface finish

The uneven distribution of pressed ceramic crystals in the glassy matrix may lead to flaws in their internal structure. These defects, which can be further enhanced during the ceramic processing in the dental laboratory can reduce the material strength and increase the wear of enamel [247]. Sealing or reducing flaws and porosities at the surface by polishing or glazing the surface may reduce the abrasiveness of the ceramic material towards the opposing tooth structure. The treatment of the ceramic surface, whether it is glazed or polished, may possibly only influence the early stages of the wear process [205].

6.7. Ceramic surface texture and tooth wear

The surface texture of dental ceramics should be as smooth as possible to enhance the function, aesthetics, and biologic compatibility of a restoration [274, 275]. Rough surfaces can decrease the flexural strength of material [276], abrade antagonistic hard tissues [245, 277], and accumulate stain, plaque, and tartar [124, 278]. As a result, the susceptibility to infection in oral soft tissues and caries increases [279, 280], because the free surface energy is lower at uneven surfaces than at smooth ones, microorganisms can easily adhere and colonise [257, 281]. Such factors and outcomes subsequently reduce the aesthetic quality of the restoration [133]. The surface roughness of ceramic restorations can be minimised by polishing or glazing.

There are a limited number of *in vivo* studies of wear rates of enamel and porcelain, largely because clinical studies are time-consuming and difficult to conduct [198]. Furthermore, there is a lack of the clinical relevance of *in vitro* wear studies since prospective studies correlating *in vitro* with long-term *in vivo* results with identical materials are not available [208].

One study evaluated the wear of IPS Empress ceramic (Ivoclar-Vivadent, Licheinstein) inlays, onlays, enamel and luting cement over eight years of clinical service [282]. It was found that the opposing enamel wore significantly faster than ceramic inlays regardless of the location of inlays and antagonists in the oral cavity [282].

Another *in vivo* study evaluated the wear of enamel opposing a new heat-pressed core ceramic IPS e.max Press (Ivoclar Vivadent) over a period of one year [213]. This core ceramic was made of lithium disilicate with high fracture toughness. The result showed that the mean occlusal wear rate of enamel was 88.4 μm for premolars and 88.3 μm for molars, with a range of 29 to 255 μm [213]. This wear rate was faster than the reported annual normal enamel wear rate of 18 μm for premolars and 38 μm for molars [283].

The most recent *in vivo* study assessing the wear of enamel opposing metal (Simidur S2, Panadent, a high noble ceramo-metal alloy composing gold, platinum, palladium and silver used for metal-ceramic crown), a metal ceramic material (IPS Classic, Ivoclar Vivadent), an experimental hot-pressed ceramic with lithium disilicate crystals (Ivoclar Vivadent) and Procera Allceram (Nobel Biocare) was reported in 2008 [214]. It was found that the Procera AllCeram produced more wear on the opposing enamel and the material itself was worn down more than other selected materials over a period of 24 months.

Many long-term studies on leucite-reinforced ceramic (IPS Empress) posterior crowns (up to 12 years) did not report on excessive wear of the opposing enamel and concluded that the material is “tooth-friendly” [146, 203, 209, 284]. However, these studies did not quantify the enamel wear.

Although *in vitro* conditions can never simulate completely the complicated oral environment, they offer some advantages such as being inexpensive and not requiring a follow up on patients over an extended period of time and despite the difficulty in comparing results between *in vitro* wear studies due to different wear conditions and tested materials, some important conclusions have been generated. First, porcelain has a potential to induce wear to the opposing enamel, with effects correlated more with the surface roughness than with the material hardness [212, 223, 263]. Furthermore, low-fusing temperature porcelain was not less abrasive than the traditional feldspathic porcelain [224], and porcelain denture teeth would cause more vertical loss to the opposing enamel compared to those made from acrylic resin or nano-filled composite [285]. Interestingly, the wear in a two-body condition is significantly higher than that in a three-body environment for both porcelain and opposing materials (gold, composite resin and enamel) [216].

In the dental literature papers on surface roughness measurements have often been presented in which a certain roughness quantity or parameter has been used without any discussion of its properties or any explanation of why it was preferred. Roughness can also be conceived in various ways. In general a surface is considered rough if it is characterised by protrusions and recesses of high amplitudes and short wavelengths. If the wavelengths are long, the surface may be thought of as being smooth, but wavy [286]. The roughness of dental enamel surfaces can be measured in such a way that the perikymata, appearing in numbers of 10-30 per millimeter, contribute to the roughness value. However, this undulation of the enamel surface can also be considered as a base line and the roughness measured as the deviations from this base. When calculating roughness in this case the roughness meter must be adjusted to exclude long-waved oscillations and to use only the short-waved

deviations, superimposed on the curved base line. In studying surface roughness, a distinction must often be made between roughness and curvature. In modern roughness meters this can usually be done since the equipment offers a possibility of filtering away some of the long-waved oscillations. In the dental literature filtration as a means of distinguishing between shape and roughness has only been very briefly mentioned in a few papers. The technical literature, on the other hand, contains papers which discuss filtration and the separating of roughness from curvature [138]. The results obtained in the measuring of roughness depends on several factors. Some of these pertain to the material itself, its softness, the presence of voids. Others refer to equipment design, in particular to the design of the surface tracer [286].

CHAPTER 7

MINIMISING SURFACE ROUGHNESS

7.1. Ceramic Clinical Polishing

The surface texture, lustre and contour of ceramics after a period of intra-oral service should be reviewed and refined if necessary [128]. This is because the surface roughness may increase with time due to contact with opposing dental materials, exogenous materials, acidulated phosphate fluoride applications, and carbonated beverages and air-powder abrasion processes. Periodic clinical mechanical polishing aims to restore the surface roughness to an optimum value, thereby decreasing the abrasion on teeth, reduce the risk of porcelain fracture, and provide the continuity of biologic and aesthetic criteria by avoiding accumulation of tartar [128, 274, 287, 288].

7.1.1. Polishing Engineering Principles

Polishing is the mechanical process involving friction which produces a smooth and glossy finish [289]. Specifically the mechanism of polishing is a chip-removal process. The cutting tool is an individual abrasive grain in the polishing wheel. A straight grinding wheel of diameter D removes a layer of material to a depth d . An individual grain on the periphery of the wheel moves at an angular velocity. This polishing process and its parameters are illustrated in Figure 7.1 [290].

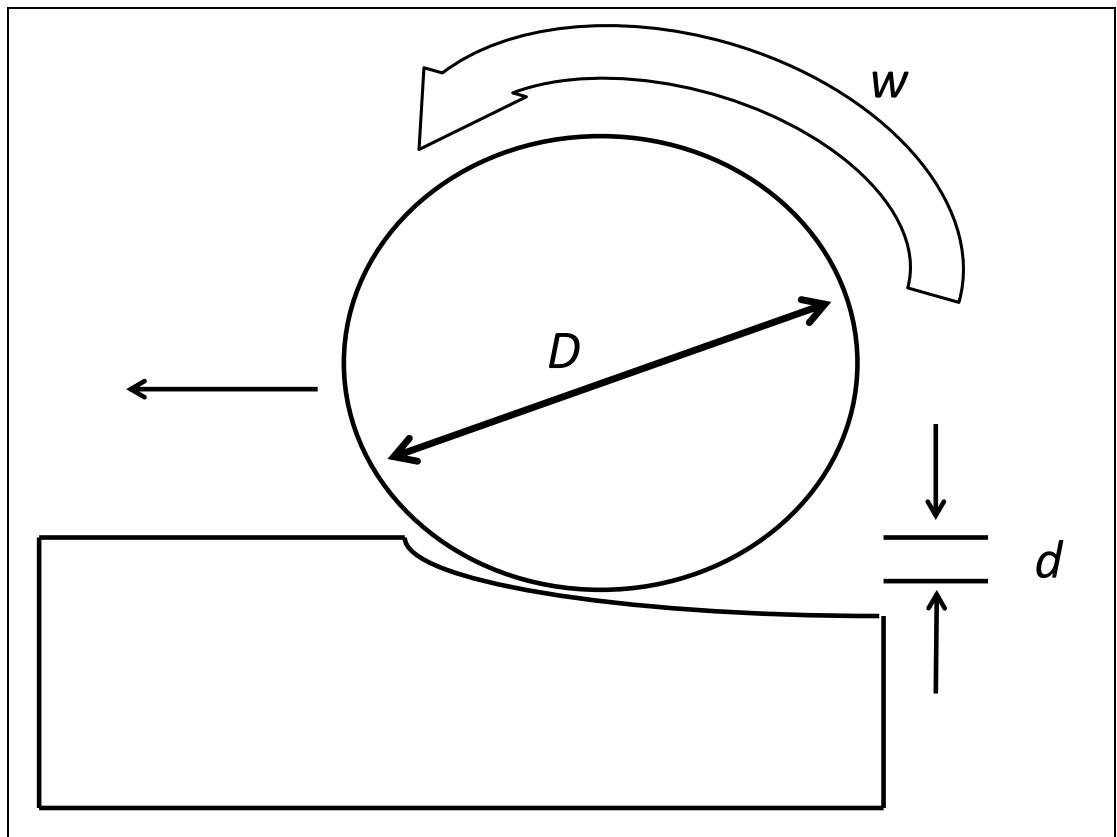


Figure 7.1: Schematic illustration of the polishing process showing process variables. The figure depicts conventional grinding. A straight grinding wheel of diameter D removes a layer of material to a depth d . An individual grain on the periphery of the wheel moves at an angular velocity [290].

Grain force increases with increasing work piece velocity and depth of cut; and decreases with increasing wheel speed, number of cutting points per unit area of the periphery of the wheel and wheel diameter. The workpiece speed, number of cutting points per unit area and wheel speeds have greater influence on grain force than depth of cut and wheel diameter. The energy dissipated in producing a chip consists of the energy required for: chip formation, ploughing and friction caused by rubbing of the grain along the surface. The grain develops a wear flat as a result of the polishing operation. The wear flat rubs along the polished surface and, because of friction, dissipates energy mainly in the form of heat. This temperature rise during polishing is an important consideration because it can adversely affect the surface properties by inducing residual stresses on the workpiece. Residual stresses are induced by non-uniform plastic deformation near the workpiece surface. Mechanical interactions of abrasive grains with the workpiece produce predominantly residual compressive stresses as a result of localized plastic flow (Figure 7.2). Since dental

ceramics are much weaker in tension than in compression, residual compressive stresses are considered beneficial, whereas residual tensile stresses adversely affect strength. The compressive layer can act to partially close an existing surface crack. This in turn increases the stress required for crack propagation and effectively increases the strength of the material [291]. Temperature increases with increasing depth of cut, wheel diameter, and wheel speed; and decreases with increasing specimen speed. It can be seen that the depth of cut, d has the greatest influence on temperature. Because of the deleterious effect of residual tensile stresses on mechanical properties, the process variables should be carefully selected so that residual compression stress at the surface is more likely. Lowering wheel speed and increasing specimen speed (gentle grinding) can usually reduce the temperature and this reduces residual tensile stresses and increases residual compressive stresses [286]. Gentle grinding however may prolong the polishing procedure and expose the ceramic surface to elevated temperature for a longer period of time leading to an increased risk of residual tensile stress at the surface [291].

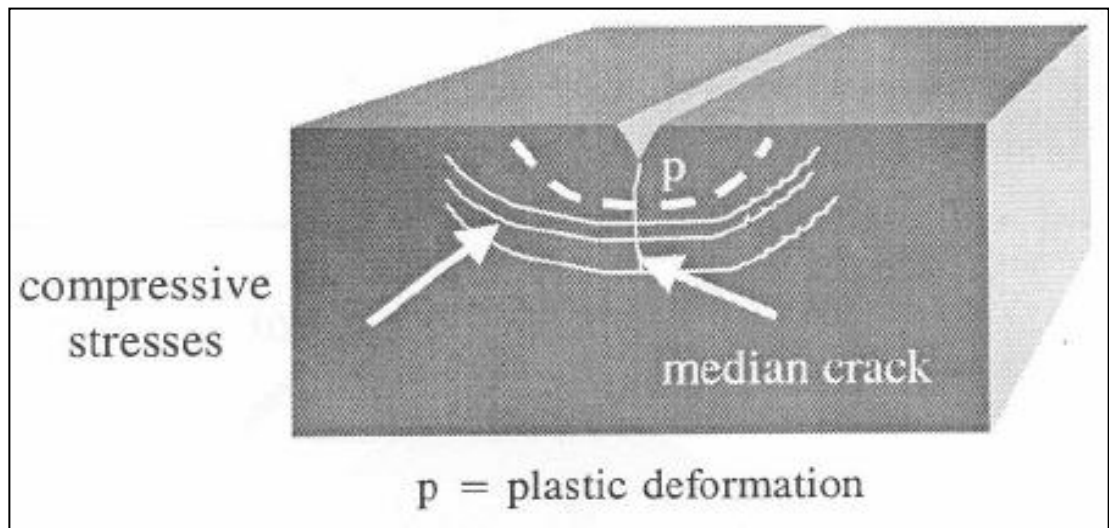


Figure 7.2: Schematic representation of compressive stress as a result of mechanical interactions of abrasive grains with the workpiece. For cracks to propagate, energy must be consumed to overcome the compressive stresses [290].

7.2. Glaze Process

There are two glaze methods which produce a smooth ceramic surface. These

methods are called ‘overglaze’ and ‘natural glaze’ [164]. Glazing produces a very smooth and hygiene surface [292], and increases the functional strength and aesthetics [166, 293, 294].

Overglaze is the addition of glass material that is vitrified at a low temperature and decreases the heat of fusion. When external stains need to be applied or a labial margin needs to be created, the porcelain should not be exposed to high temperatures, ruling out a natural glazing. Overglazing should be used to prevent damage to the stains or labial margin [295, 296]. Overglaze is generated by exposing a low-temperature porcelain to a temperature that is 20°C to 60°C below the firing temperature [292].

Natural glaze keeps the surface of material at the temperature of its last firing without adding other materials [164]. The restoration is fired to a temperature that is usually equal to or slightly higher than the original firing temperature. If the crown is to have a natural glaze, it will be fired after the stains are applied. The restoration should first be allowed to dry at the entrance of the furnace muffle until the stain medium has evaporated completely, leaving a dry, chalky surface. Then, the crown is inserted into the furnace slowly and fired to the manufacturer’s recommended glazing temperature for a short period, usually 1 to 2 minutes, until the outer surface of the porcelain develops the desired level of gloss. The porcelain surface of the restoration is exposed to temperatures high enough to permit the porcelain to fuse together and create a smooth, glossy outer “skin.” This process is performed at atmospheric pressure [164, 295, 297] (Naylor 1992, Sarac 2006, Tamaura 1987).

7.3. Ceramic surface texture and different surface finishing protocols

Glazing and polishing protocols aim to reduce the surface texture of a ceramic material [298-302], thereby minimising the potential of negative clinical outcomes associated with an unfavourable surface texture [1, 2, 303]. Polishing is a mechanical

process and involves the use of diamond burs and points, flexible diamond discs , fluted carbide, mounted points, abrasive stones and discs, sandpaper discs, rubber wheels, and abrasive diamond pastes [3, 124, 131, 133, 234, 304]. Glazing is a temperature dependant physicochemical process which may or may not involve the use of additional ceramic glaze material.

Glazing has in the past decades generally been favoured since the popular, traditional metal ceramic restorations could be assessed, adjusted and then returned to the laboratory for any refinements and reglazing [302, 305, 306]. The disadvantage of a glazed surface is that it can be removed after an occlusal adjustment or after a short period in function and also if it has been cemented then glazing is obviously not an option in the future [1, 8]. Due to the increase in popularity of all ceramic restorations, effective polishing protocols have become suitable to reduce the surface texture of ceramic surfaces chair side before and also after cementation or bonding procedures.

Glazing has been traditionally stated to be the gold standard in terms of surface finish [307], producing the smoothest ceramic surface possible [9, 265, 308-311] when compared to polishing protocols [312, 313]. Other studies have concluded that various polishing protocols can produce ceramic surfaces to be equally smooth than glazed surfaces [308, 314, 315] and there are also other studies which state that polishing can result in even less abrasive and more aesthetic surface textures than glazed ceramic surfaces [264, 272, 302, 315-320]. The studies analysed all focused on determining the best method for creating a smooth ceramic surface. Tholt et al [124] assessed the surface roughness of Allceram, IPS Empress 2 and Vitadur Alpha ceramics when modified by five different finishing methods. The samples were initially glazed, then abraded with diamond burs followed by various finishing methods. The finishing methods included diamond polish paste (Eve), rubber points (Identoflex), and the Shofu polishing kit. There was no statistical difference in the surface roughness between IPS Empress 2 (lithium disilicate) glazed surface (Ra 0.65µm) and a IPS Empress 2 surface polished with either rubber points (Ra 0.6µm)

or Shofu porcelain polish kits (Ra 0.65 μ m). The Vitadur and Allceram glazed surface was also statistically similar to a Shofu polished and diamond polished surface. The study concluded that glazed surfaces tend to produce the lowest Ra values (0.4 μ m-0.6 μ m) consistently regardless of the ceramic materials whereas the polishing protocol seems to aid some ceramics more than other ceramics.

Ai Hiyasat et al [245] studied the effects of different finishing methods in relation to surface roughness and opposing tooth wear under various pH conditions. The study reported that both glazed (Ra 0.68 μ m) and polished surfaces (Ra 0.73 μ m) were smoother than unglazed surfaces (Ra 0.1.5 μ m) and statistically, the differences between the glazed and polished samples were not significant [321].

Martinex-Gomis et al [280] completed a study which assessed the surface roughness of forty IPS classic shade guide ceramic after abrasion with a 120 μ m grit bur and then polished by four different methods. The polishing methods included white silicon and black rubber, Shofu rubbers, diamond burs, and Sof-Lex disks. All samples were then polished by Yeti diamond paste. All polishing methods produced smooth ceramic surfaces which were not statistically different. The study stated that overall the efficacy of the diamond polishing paste was questionable.

In the earlier studies, the polishing parameters used, handpiece speed, abrasive characteristic, and polishing load were not controlled or standardised. Only more recently, some effort have been made by the researchers to control the handpiece speed and polishing load used [130, 290]. Due to the lack of comprehensive research examining these issues, is very difficult to draw a meaningful conclusion when comparing studies done to evaluate the effect of polishing on ceramic. Since the polishing parameters used were not quantified, the contradicting study results between various studies may in fact be due to the polishing process itself.

Scurria and Powers [322] compared the roughness produced by five different

combinations of intraoral instrumentation on feldspathic porcelain and machinable glass ceramic. The relative speed used was reported as pounds per square inch of air pressure delivered to the handpiece. No attempt was made, however, to confirm the speed used. Force applied to the handpiece was measured by performing all polishing on samples stabilised on a special balance designed to weigh laboratory animals (Mettler Balance PM4600, Mettler Instrument AG, Hightstown, N.J). They found that feldspathic porcelain could be polished smoother than glazed, and Dicor (Dicor MGC, Dentsply, York,PA) ceramic could be polished smoother than Ceramco II (Ceramco Inc, Burlington N.J) ceramic. In this study the use of a 30-fluted carbide bur did not improve smoothness as reported by Haywood et al [323].

Glavina et al [324] assessed the surface roughness of Vitamark II cerec blocks after various polishing methods. The study concluded that Sof-Lex discs resulted in a statistically significantly smoother surface compared to other polishing methods such as the Hawe brush and diamond polish paste, and politip-P rubber cups. A study by Stoll et al [325] evaluated the Sof-Lex system against four industrially sintered feldspathic ceramics including Vitamark II ceramic and stated that the Ra after polishing with the Sof-Lex disc system and found similar results. Karapetian et al [326], Mörmann [327] and Jung [328] all reported similar Ra values of ceramics after polishing with Sof-Lex polishing system .

Elmaria et al [243] evaluated three different ceramic substrates and compared the surface roughness to a type III gold alloy. The ceramics were glazed or polished with Dialite polishing system. They included pressed ceramic IPS Empress, condensable Finesse and All-Ceram. The Ra of glazed IPS Empress was 0.46 μ m and the Ra of polished IPS Empress was 0.15 μ m. Glazed Finesse ceramic Ra was 0.72 μ m, polished Ra 0.37 μ m and All-ceram Ra was 0.17 μ m for both polished and glazed surfaces [329]. The SEM analysis of all ceramic substrates revealed increased porosity of the polished surfaces when compared with the glazed surfaces [329].

An in vitro study by Flury et al [330] assessed the performance of two CAD CAM ceramic materials after polishing with various protocols. The ceramics tested were included Vitamark II (lithium disilicate crystalline ceramic) and IPS Empress CAD (leucite reinforced crystalline ceramic). The five polishing methods included EVE diacera ceramic polishing set (diamond stones), JOTA ceramic polishing kit (diamond stones), Optrafine HP paste and brushes, Sof-Lex discs and finally Shofu brown and greenie silicone polishers and Occlubrush. The glazed surfaces exhibit significantly lower Rz values but higher Ra values compared to the polishing groups. For IPS Empress CAD, Sof-Lex polishing produced the lowest Ra value of 0.154 μ m followed by JOTA which was Ra 0.342 μ m. The Ra for glazing IPS Empress CAD was 0.433 μ m. For Vitamark II, the Sof-Lex discs also produced a smoother surface than the glazed specimens. These results are similar to and supported by Martines Gomis et al [264]. The study stated the medium Sof-Lex was sufficient to reduce the surface roughness and that the Al₂O₃ particles of the super fine (1-7 μ m) and fine discs (9-3 μ m) were not able to additionally smooth the hard ceramic material [331].

Haywood et al [207] investigated the effects of water, speed, and experimental instrumentation on finishing and polishing porcelain intraorally. They reported that the best results were obtained when diamond instruments were used wet at moderate speed, and when carbide instruments were used dry at high speed. The relative speeds used were characterised by the amount of air pressure delivered to the handpiece. No effort to control polishing load was made [207].

A study by Olivera et al [332] tested five ceramic materials. The ceramics included IPS Empress 2, IPS Empress (Ivoclar Vivadent), Duceram Plus (Degussa, Dentsply), Duceram LFC (Degussa), and Symbio (Degussa). The Ra value of glazed or polished ceramics was comparable and not statistically significant. This study is supported by Jacobi et al [333] but not by Al-Hiyasat et al [321]. The study concluded there was no correlation between glazed and polished ceramics and enamel wear, and secondly that there was no statistical difference in the surface roughness of either finishing method.

Sarikaya et al [258] evaluated the effects of eleven different finish techniques on four commonly used dental porcelains. The porcelains evaluated included feldspathic porcelain (Vita WMK 95, Ceramco III) a low fusing porcelain (matchmaker MC) and machinable (Vitamark I) porcelain. The polishing systems included pastes of Zircate silica or Al₂O₃, porcelain polish kits or Sof-Lex discs or a combination of these materials. No differences in the Ra were noted between the Glaze, Sof-Lex and porcelain polish system groups. The Ra values were between 0.6 -0.7µm for the feldspathic and low fusing porcelain for all polishing protocols and the Ra value of the machinable ceramics was significantly lower with values of 0.3 to 0.4µm for all polishing systems. No polishing system produced significantly lower Ra values compared to the other polishing systems for any ceramic used.

Yilmaz et al [334] aimed to determine the best method for smoothing surface roughness in various dental ceramics. Classic IPS ceramic, Empress 2 and Empress aesthetic ceramics were tested. Regardless of the ceramic material, the glaze, then natural glaze then mechanical polishing produced the lowest Ra values. These results are not consistent with other studies by Brewer et al [133], Ward et al [335], and Wright et al [320] but they are supported by Campbell [132] and Patterson et al [315].

On the basis of an SEM visual examination, Riamondo et al [131] compared the finishes of porcelain samples. It was noted that glazing produce a better surface than the other polishing methods. The scientific weighting of SEM results may to subject to criticism since it has been shown that the surface roughness parameters such as Ra values do not necessarily correlate to relative smoothness as noted by SEM or the relative shine and when a ceramic is glazed [131].

Hulterstrom and Bergman [336] evaluated the thirteen polishing systems against eight ceramic materials *in vitro*. Glazed surface and polished surfaces had similar Ra values which were between 0.5um-0.8um. The Sof-Lex system and Shofu porcelain

lamine polishing kit produced the best polishing results compared to other polish systems. There was no difference in Ra with respect to time of polishing. A study by Sulik et al [337] found no differences clinically or by means of SEM between polished and naturally glazed surfaces.

The effectiveness of a final polishing with diamond paste is variable depending on the initial polishing system and ceramic material used [338] [339] [340]. Hulterstrom and Bergman [336] stated diamond paste did not statistically improve the smoothness of the ceramic surface when polished with the Sof-Lex system, but did have some benefit when used after the Shofu system. This additional step can therefore be omitted in intraoral polishing [338]. These recommendations are supported by Sarac et al [272], Klausner et al [130] and Al Wahadni et al [265] who tested pressed IPS empress ceramic and stated that polishing with the Shofu system followed by diamond polish paste was equivalent to reglazing and reduced the surface roughness [265]. Studies by Flurry et al [330] and Martinez and Gomis et al [280] both stated that diamond polishing paste might round the profile shape and lower the height of maximum roughness peaks which leads to a reduction in the arithmetic mean height of the surface profile (Rz) but would not influence the average surface roughness (Ra) [264, 331].

A table outlining the various methods used by authors and researchers is presented in Appendix 8

7.4. Ceramic surface texture and mechanical properties

There are a number of studies in the dental and ceramic literature on the strengthening effects of grinding and polishing, as well as heat treatment of ceramics. The effectiveness of these strengthening mechanisms is not well established and may not be applicable to clinical dentistry. Previous studies both support and refute the strengthening effect of surface and heat treatments. Levy [341] evaluated the effect of polishing with pumice and etching on the flexural strength of dental ceramics after air, and vacuum glazing, and over glazing. It was reported that no significant

difference among treatments; however, polished glazed specimens had higher strength values. Brackett et al [342] tested the effects of auto glaze, overglaze, and auto glaze plus polish on the strength of five dental ceramics. Polishing was done with a Shofu Polishing Kit. The authors reported that the flexural strength of the specimens tested with an overglaze was significantly greater than specimens treated with auto glaze and those treated with autoglaze and polish. Unfortunately, the polishing parameters used in these studies were not quantified and the difference in polishing may have affected the results. Results that contradicted these studies were reported by Fairhurst et al [343]. He investigated the strengthening of feldspathic porcelain by analysing the effect of various polishing and firing procedures on four groups (n = 50) of Jelenko body porcelains (Jelenko Gingival, Jelenko Dental Health Products, Armonk, NY). The specimens that were fired, polished to 1 μ m surface finish, and not glazed were significantly higher in flexural strength compared to the other groups. The other three groups that received additional firing recorded a significant decrease in strength. The study concluded that self-glazing did not increase flexural strength and that some glazing techniques can be detrimental to the fracture properties of leucite-containing porcelains.

Griggs et al [344] repeated the study by Fairhurst et al [343] with a larger average flaw size and a wider distribution in flaw sizes. It was thought that the effects of glazing might be more obvious if the initial flaw size were bigger. The same type body porcelain was used in their study. The firing schedules and type of furnace used were different. The results indicated that re-firing of porcelain did not significantly increase the flexural strength regardless of the size of the surface flaws.

Giordano et al [19] reported that overglazing, grinding, and polishing all significantly increased the flexural strength of dental ceramics by 15% to 30 %, and re-firing of the ground and polished samples decreased the flexural strength significantly from 11% to 18%.

Chen [345] conducted a study comparing the flexural strength of dental ceramics polished manually and by a machine (Buehler Ecomet III). The results indicated that the flexural strength of machine-polished samples was higher but not statistically significantly higher compared to manually polished and control (self-glaze) groups. Surface roughness was evaluated quantitatively by surface profilometry, and specimens polished with the Buehler machine had the best surface finish.

SECTION TWO

CHAPTER 8

RATIONALE, AIMS AND HYPOTHESIS

8.1. Rationale

Understanding the relationship between ceramic surface characteristics and in particular altitude parameters to opposing enamel wear will outline to clinicians the necessity to polish and in some circumstances, repolish ceramics after a certain period of time *in situ* to prevent excessive enamel wear.

Due to rapid advancements in dental ceramic technology, there are limited studies addressing the various polishing methods, resulting surface texture and risk of wear to opposing enamel of contemporary dental ceramic materials.

There has been a significant increase in the delivery of ceramic inlays and onlays especially with the global explosion of CAD CAM technology. Frequently, the ceramic restorations require refinements to the surfaces with abrasives prior to or after cementation. If adjustments are made to a glazed or non-glazed surface after cementation, only mechanical polishing is an option to restore the surface texture. This study will increase understanding of the surface characteristics produced from glazing and polishing and will assist with clinical decision making regarding the most effective method for restorative ceramic surface.

8.2. Study Aims

The specific aims of this study are to:

- Investigate and compare the surface characteristics of leucite-reinforced (IPS Empress CAD, Ivoclar Vivadent) and lithium disilicate ceramic (IPS e.max

CAD, Ivoclar vivadent) after chair-side polishing using Optra Fine polishing system (Ivoclar Vivadent), and Sof-Lex discs (3M ESPE) and after overglazing using In-Ceram glaze paste (Ivoclar Vivadent).

- Investigate the influence of surface roughness of ceramic specimens on the wear rate of opposing enamel.

8.3. Hypothesis

Increasing the surface texture of lithium disilicate and leucite reinforced ceramics will statistically increase the wear rate of opposing tooth surface enamel under standardised laboratory conditions

CHAPTER 9

MATERIALS AND METHODS

9.1. STUDY A

9.1.1. Sample preparation

Ceramic specimens were prepared by sectioning IPS e.max CAD and IPS Empress CAD ceramic blocks into 2mm thick specimens using a slow speed saw (Buehler, Chicago, IL, USA). To simulate clinical procedure, the grinding and polishing steps were carried out manually by a single operator similar to previous studies [328, 335, 346-348]. Abrasion of the ceramic surface was completed with a high speed dental handpiece to simulate the adjustment and refinement of an occlusal surface of a ceramic restoration. Various mechanical polishing procedures were then completed simulating the effort to re-establish an ideal ceramic surface texture. To eliminate the risk of three body wear and the accumulation of heat and negative surface effects such as surface crack initiation and propagation from occurring, all grinding and polishing abrasion was completed under high speed water cooling. To further standardise specimen preparation, one operator applied uniform pressure in consistent three different planes and uniform application time of thirty seconds for each grinding and polishing surface treatment.

9.1.2. Ceramic samples

The two low fusing ceramic materials manufactured by Ivoclar-Vivadent were tested. These included homogenous IPS e.max CAD lithium disilicate (Figure 9.1.1) and IPS Empress I CAD leucite-reinforced ceramic (Figure 9.1.2).



Figure 9.1.1: IPS e.max CAD partially crystallised blocks (Ivoclar-Vivadent).



Figure 9.1.2: IPS Empress CAD blocks (Ivoclar Vivadent).

A total of 150 ceramic specimens were prepared. Seventy specimens of leucite reinforced (IPS Empress CAD) and eighty specimens of lithium disilicate (IPS e.max CAD) ceramic material were divided into seven and eight groups of ten specimens respectively. A power analysis determined that ten specimens were necessary for each sample group. Each group of ten ceramic specimens had a different abrasive

and finishing protocol to simulate various types of clinical occlusal refinement situations. After the various finishing protocols were completed the samples were subjected to ultrasonic cleaning with distilled water and carefully analysed.

The surface finishing protocols included:

Leucite-reinforced ceramics (IPS Empress CAD, Ivoclar Vivadent)

- Group 1: 50µm grit diamond bur then over glazed with In-Ceram glaze paste
- Group 2: 50µm grit diamond bur and neither polished nor glazed
- Group 3: 50µm grit followed by 25µm grit bur
- Group 4: 50µm, 25µm grit bur, polished with Optrafine polishing system
- Group 5: 50µm, 25µm grit bur, polished with Optrafine, diamond polishing paste
- Group 6: 50µm, 25µm grit bur, polished with Optrafine, diamond paste, glazed
- Group 7: 50µm grit diamond bur and polished with Sof-Lex polishing discs

Lithium disilicate ceramics (IPS e.max CAD, Ivoclar Vivadent)

- Group 1: 50µm, 25µm grit bur, Optrafine system, crystallised and glazed
- Group 2: 50µm grit diamond bur, crystallised
- Group 3: 50µm, 25µm grit bur, crystallised
- Group 4: 50µm grit bur, crystallised, abraded again with 50µm grit bur
- Group 5: 50µm, 25µm grit bur, crystallised, Optrafine, diamond polishing paste
- Group 6: 50µm, 25µm grit bur, Optrafine polishing system, crystallised
- Group 7: 50µm, 25µm grit bur, Optrafine, diamond polishing paste, crystallised
- Group 8: 50µm grit diamond bur, crystallised, Sof-Lex polishing discs

9.1.3. Surface texture altitude parameters

Surface texture altitude parameters were analysed to assess the influence of various finishing protocols to the ceramic specimen surfaces. The same parameters were used to assess surface textures after the wear study was completed. The parameters include:

- R_a Arithmetical average of surface heights
- R_{pm} Magnitude of the peak to valley height in all cut off lengths
- R_z Average height difference between the five highest peaks and five lowest valleys within each cut off length.
- R_q Root Mean Square roughness (R_q) is the root mean square average of the roughness profile ordinates.

The means and standard errors were calculated and are reported and presented in the respective text and tables.

9.1.3.1. Double Determinations for surface texture analysis

Reliability of the research data for surface texture assessment was established by repeating surface texture parameters nine times for each individual specimen. This protocol was repeated for five randomly selected specimens from each group of ceramics at a different data collection occasion to ensure the validity of the measurements was as unbiased and reproducible.

The ANOVA two sample test confirmed that the differences between the surface texture parameter measurements were not statistically significant ($p=0.05$).

9.1.3.2. Programat CS Furnace

The Programat CS (Ivoclar Vivadent) (Figure 9.1.3) is ceramic furnace with a vacuum option. It allows crystallisation and glaze of IPS e.max CAD restorations in the dental office or laboratory. The specifications for crystallisation of IPS e.max CAD ceramic and In ceram glazing procedures are shown in Table 9.1.4.



Figure 9.1.3: Programat furnace.

Table 9.1.4: Programat CS furnace firing parameters. Source: Ivoclar Vivadent Programat CS furnace data sheet.

Crystallization/Glaze (max. 6 restorations)												
Furnace	Stand-by temperature B [°C/F]	Closing time S [min]	Closing time t ₁ [°C/F/min]	Firing temperature T ₁ [°C/F]	Holding time H ₁ [min]	Heating rate t ₂ [°C/F/min]	Firing temperature T ₂ [°C/F]	Holding time H ₂ [min]	Vacuum 1 T ₁ [°C/F]	Vacuum 2 T ₂ [°C/F]	Longterm cooling L [°C/F]	Longterm t ₃ [°C/F/min]
Programat CS Program 1	403 / 757	6:00	90 / 162	820 / 1508	0:10	30 / 54	840 / 1544	7:00	550/820 1022 / 1508	820/840 1508 / 1544	700 / 1292	0
Correction firing												
Furnace	Stand-by temperature B [°C/F]	Closing time S [min]	Closing time t ₁ [°C/F/min]	Firing temperature T ₁ [°C/F]	Holding time H ₁ [min]	Heating rate t ₂ [°C/F/min]	Firing temperature T ₂ [°C/F]	Holding time H ₂ [min]	Vacuum 1 T ₁ [°C/F]	Vacuum 2 T ₂ [°C/F]	Longterm cooling L [°C/F]	Longterm t ₃ [°C/F/min]
Programat CS Program 2	403 / 757	6:00	90 / 162	820 / 1508	0:10	30 / 54	840 / 1544	3:00	550/820 1022 / 1508	820/840 1508 / 1544	700 / 1292	0
Speed Crystallization/Glaze Spray (max. 2 restorations with Glaze Spray)												
Furnace	VZ Stand-by temperature B [°C/F]	Closing time S [min]	Closing time t ₁ [°C/F/min]	Firing temperature T ₁ [°C/F]	Holding time H ₁ [min]	Heating rate t ₂ [°C/F/min]	Firing temperature T ₂ [°C/F]	Holding time H ₂ [min]	Vacuum 1 T ₁ [°C/F]	Vacuum 2 T ₂ [°C/F]	Longterm cooling L [°C/F]	Longterm t ₃ [°C/F/min]
Programat CS Program 3	403 / 757	1:30	90 / 162	820 / 1508	0:10	30 / 54	840 / 1544	7:00	550/820 1022 / 1508	820/840 1508 / 1544	700 / 1292	0

9.1.3.3. Slow speed Saw

The IsoMet Low speed saw was used to section the ceramic CAD blocks (Figure

9.1.5). The IsoMetR Low Speed Saw is a precision sectioning saw of various materials. Its advantages include a low kept loss capacity and low risk of material deformation and damage. The Low Speed Saw consists of a 4" (102mm) Series 15H rim diamond wafering blade which functions at speeds between 0 and 5000 rpm. Techniques that allow low deformation sectioning include gravity specimen feed, dead weight load application and drag feed lubrication. Cutting loads can be applied to the holding arm in increments of 25 grams and the specimen weight can be tared through the use of a counter balance. Intermediate weight adjustments can be achieved by sliding the counter weight at the rear of the arm. This design allows reproducible cutting parameters from sample to sample. The sample holding arm incorporates a precise micrometer adjustment for alignment of the specimens prior to sectioning. Figure 9.1.6 shows the sectioning of a single IPS e.max CAD block into several 2mm thick specimens.



Figure 9.1.5: IsoMet Low Speed Saw.



Figure 9.1.6: Sectioned IPS e.max CAD block into 2mm thick slices.

9.1.3.4. Finishing diamonds

Finishing diamonds with 50 μ m and 25 μ m diamond impregnated grit drills were used to mimic clinical adjustment and occlusal refinement to the ceramic restorations (Figure 9.1.7). The diamond burs abraded the ceramic specimen in three plans for sixty seconds using a speed-increasing handpiece (1:3) under constant water coolant spray (120,000 rpm).

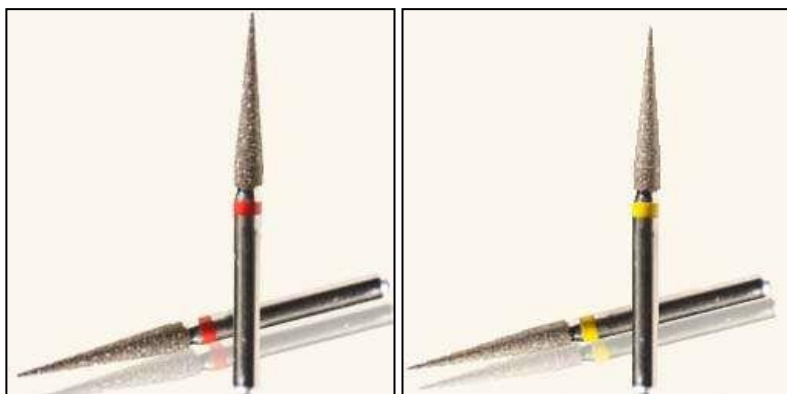


Figure 9.1.7: Red band 50 μ m grit diamond impregnated high speed bur (8879L, Komet, Gebr Brasseler, Lemgo, Germany (left). Yellow band 25 micron grit diamond impregnated high speed bur (S.sg CKEF, Komet) (right).

9.1.3.5. Optrafine polishing system

Optrafine polishing system is a specifically designed ceramic polishing system

developed by Ivoclar Vivadent (Figure 9.1.8). The system is autoclavable. It is available in the shapes "flame", "cup", and "disc". Polishing is carried out in three steps. Firstly, finishing and smoothing is completed with the light blue coloured 'Finisher F' bur, followed by polishing with the dark blue coloured 'Polisher P' and then finally the ceramic is finished to a high gloss using the high-gloss brush and diamond polishing paste HP. The polishing burs are recommended to be used in a slow speed contra angle hand piece at a maximum 15000 rpm. The manufacturer studies conclude polishing with Optrafine burs for 40-50 seconds each (20mm² area) results in a surface roughness of <0.2um for low fusing ceramics.

Diamond polishing paste HP is the final component of the Optrafine polishing system (Ivoclar Vivadent). The paste consists of diamond powder, glycerin, propylene glycol and sodium lauryl sulphate (Figure 9.1.8). The manufacturer recommends use of paste with a high gloss brush at a maximum 15 000 rpm.



Figure 9.1.8: Optrafine polishing system and diamond polishing paste (left) Source: R&D Ivoclar Vivadent AG / Schaan.

9.1.3.6. Sof-Lex discs

Sof-Lex discs (3M/ ESPE, St. Paul, MN, US) are a series of polishing discs of 12.7-mm or 8.5mm diameter (Figure 9.1.9). The series of essentially sand paper discs are impregnated with aluminium oxide of varying grit size. The discs are attached to a metallic mandrel and then inserted into an electric slow speed contra angle hand piece. The manufacturer recommends the discs to be used at a speed of 10,000 rpm for ten seconds for coarse and medium discs, and 30,000rpm for a minimum of ten

seconds for the fine and superfine discs. The operator must use all four grits to achieve optimal surface smoothness, ending with super fine

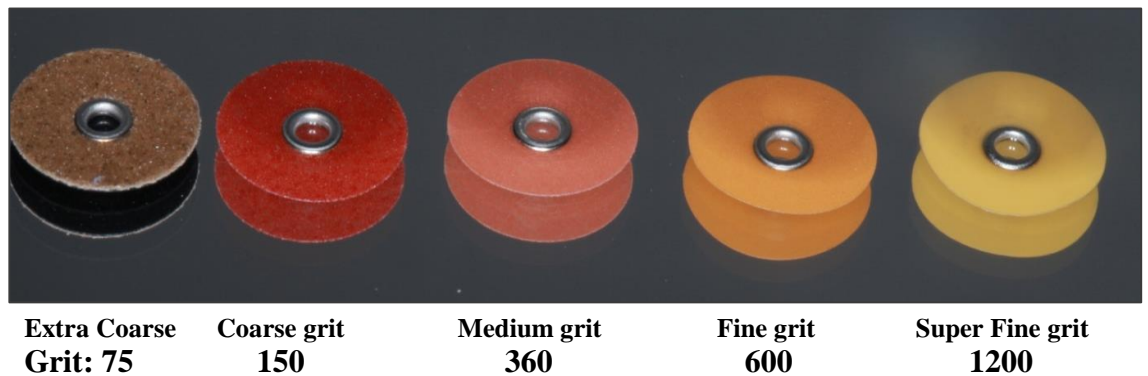


Figure 9.1.9: Sof-Lex discs (3M/ ESPE, St. Paul, MN, US) are essentially sand paper discs impregnated with aluminium oxide of varying grit size listed above. Note: "Grit" is a reference to the number of abrasive particles per square inch of sandpaper.

9.1.3.7. Glazing

Overglazing was completed with In-Ceram glaze paste (Figure 9.1.10). (Ivoclar-Vivadent) The glaze was applied to polished and non-polished ceramic specimens by an experienced ceramist. Two thin coats of glaze paste was applied to the ceramics and placed in the furnace for the appropriate period of time.



Figure 9.1.10: In-Ceram Glaze paste (Ivoclar-Vivadent, Lichtenstein).

9.2. STUDY B

9.2.1. Preparation of tooth specimens

Seventy five freshly extracted human teeth were obtained from various private dental

clinics in Western Australia and stored in thymol solution at 4⁰C for use. The teeth consisted of premolars and third molars, all of which were non-cariou with very little or no wear. The use of extracted human teeth followed an informed consent protocol that was reviewed and approved by the Committee on the Ethics of Human Experimentation, The University of Adelaide (H/27/90). The teeth were sectioned longitudinally in a mesio-distal direction so that each specimen consisted of a buccal or lingual half-crown with a root portion the pulp tissue was removed with a spoon excavator and the root tissue was removed along the cementum-enamel junction using a diamond disc attached to a high speed cutting machine under copious water coolant (Figure 9.2.1). Once the teeth specimen preparation was complete, the specimens were stored in distilled water for 7 days prior to testing. No wear facet was prepared in the enamel surface prior to the commencement of the wear cycles.

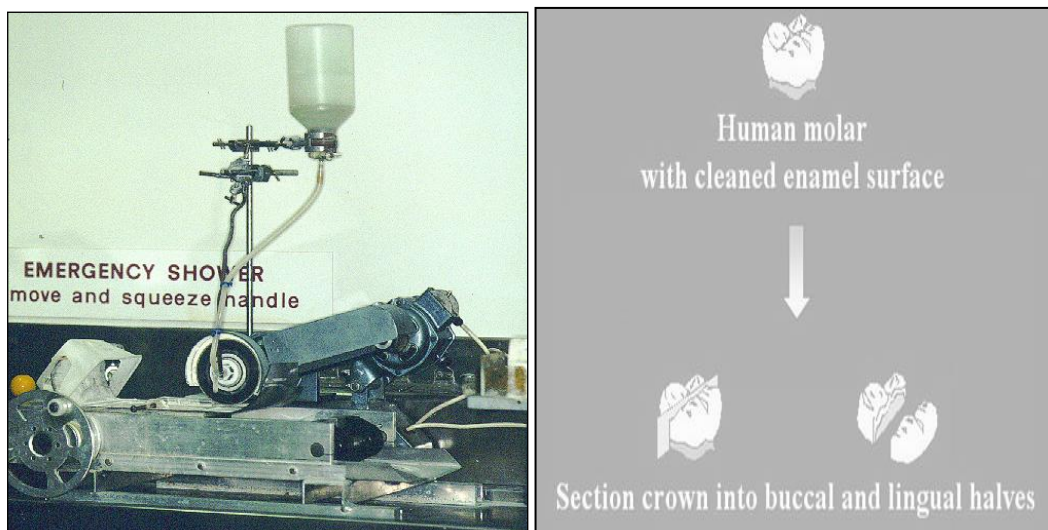


Figure 9.2.1: Tooth-sectioning machine, Adelaide Dental Hospital (left), Flow chart showing sequence of tooth sectioning (right).

9.2.2. Mounting specimens of Scanning Electron Microscopy (SEM) studs

The surface of SEM studs and the underlying unprepared surface of the ceramic specimens were sandblasted with aluminum powder 125 μ m (Argibond Australia) under pressure (2 bar) using a sandblasting unit (Renfert GmbH, Germany). The ceramic specimens were cemented to the SEM studs, using a chemically-cured resin

cement (Panavia F, Kuraray, Japan). The base and catalyst component of the cement was mixed with the ratio of 1:1, and applied to the roughened surface of the discs and they were attached to the sandblasted surface of the studs and light cured for forty seconds with a light cure unit (Visilux 2, 3MTMESPETM, Australia).

On each specimen, three titanium metal spheres of 2mm diameter were attached to the side of the stud with cold-cured resin (Vertex self-curing, Vertex Dental BV, the Netherlands) to act as reference points for the subsequent scanning process.

Tooth halves were mounted onto the sandblasted SEM studs in a different way. They were secured in cold-cured acrylic resin (Vertex self-curing, Vertex Dental BV, the Netherlands), which covered one half of the tooth specimen. Care was taken to ensure that the most prominent part of the enamel was positioned in the middle of the studs. The three reference metal balls were also partially embedded in resin, leaving the top part exposed. It was important that all the metal balls were equally spaced and were below the highest point of the enamel, porcelain or gold discs when the stud surfaces were horizontally positioned. This played an important role in the interpretation of the scanning images and for calculating the object volume above the reference plane formed by the metal balls (Figures 9.2.2 and 9.2.3).

Previous studies prepare 2mm wear facets in the enamel specimens prior to the wear simulation. In this study, the simulation of a wear facet to create positive contact between the opposing sample specimens was not necessary due to the significant number of simulated masticatory cycles, maximum amount of enamel was necessary.

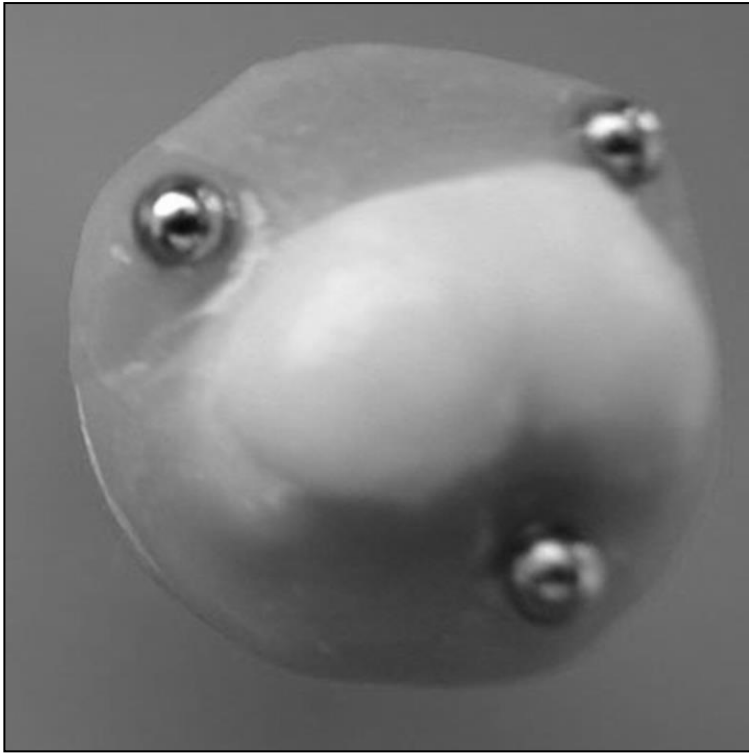


Figure 9.2.2: Enamel specimen on SEM stud with three reference metal balls.

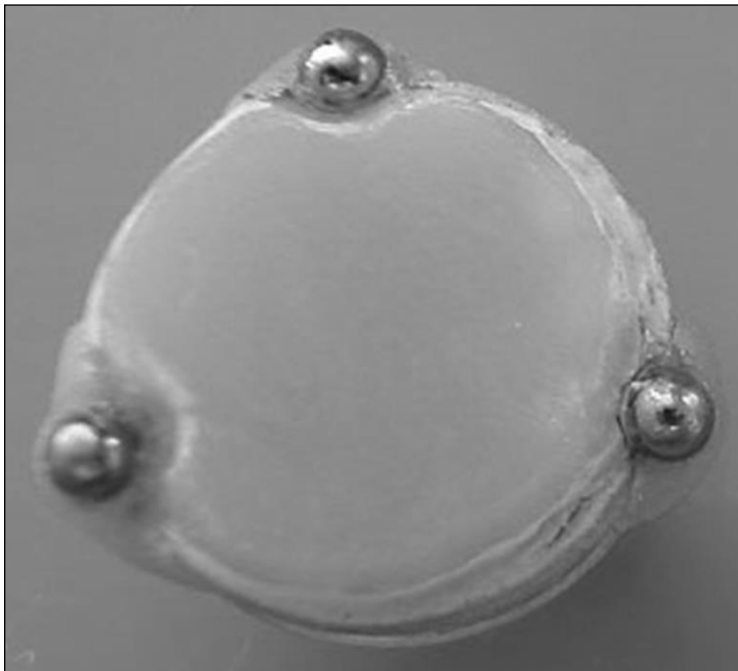


Figure 9.2.3: IPS Empress CAD ceramic specimen on SEM stud with three reference metal balls.

9.2.3. Assessment of tooth and ceramic wear

The degree of enamel wear can be calculated in a number of ways. Common methods in the literature include volume loss, depth of wear and weight loss of the enamel specimen. Height loss is described in wear studies because of its ease of measurement since no digital devices required and clinical relevance regarding the vertical dimension of occlusion [234].

Volume loss however is a more sensitive and accurate method because it changes linearly with time [201]. The difference between wear measured in volume and in height is largest when opposing surfaces feature cuspal morphologic structures. This difference is reduced as cuspal structure is removed and opposing surfaces become flat. The volume parameter of wear analysis has been shown to proceed in a linear manner [234] and has been shown to correlate with clinical data [30, 201] and thus can be used to predict clinical conditions.

9.2.3.1. Optical Microscope 3D assessment: Leica MZ16FA stereo microscope

The Leica MZ16FA stereo microscope (Leica Biosystems, Wetzlar, Germany) is a high-quality microscope with fluorescence capability (Figure 9.2.4). The fluorescence filters available on the MZ16Fa are: UV excitation – visible light emission, blue excitation – green emission, green excitation – red emission and a filter that is specifically designed for GFP3 imaging. Three objective lenses of different magnification are available for the MZ16FA allowing a magnification range of 3.5x to 230x thereby covering the sample size range from macro to micro. All functions on the MZ16FA such as zoom and focus are computer control which, when combined with the Leica IC 3D camera system on the microscope, enables a number of unique functionalities for the microscope. The camera system consists of two high quality cameras; one camera for each of the stereo light paths. These cameras are capable of recording 24-bit colour images with up to 2088 pixels by 1055 pixels and enable the full stereo functionality of the microscope to be used. In particular, it is possible to record true stereo pair images of a sample. The image capture software can be used to convert the stereo pair images to a relief map of the height variations in the surface of an object with a vertical accuracy of a few microns.

Another unique function of the microscope is to record a series of images where, under computer control, the image focus is changed by a small amount from one image to next. This image series can be combined using the image capture software to form a single image from which any depth of field effects have been removed. That is, an image that shows in-focus detail over the complete height of a sample.



Figure 9.2.4: Leica MZ16FA stereo microscope (Leica Biosystems, Wetzlar, Germany).

9.2.3.2. Three Dimensional Scanning and quantitative results

Accurate, reproducible three-dimensional (3D) data provide an important contribution to our ability to describe, compare and understand dental morphology. The existing technology however is often expensive or has technical limitations. Recently available, inexpensive 3D profilometers interfaced with standard personal

computers offer the potential to overcome some of these problems [351].

9.2.3.2.1. 3D PIX-4 scanner

For data acquisition a 3D scanner (PIX-4, Roland DG, Tokyo, Japan) interfaced with a personal computer was used to record the heights (Z) of surface mesh points (X and Y). An active piezo sensor detects contact between its stylus and the scanned surface. The X and Y mesh steps can be set between 50 μ m and 5.00 mm in 50 μ m steps and the Z-axis direction has a resolution of 25 μ m.

9.2.3.2.2. “Dr.PICZA” software

The “Dr.PICZA” software (Roland DG, Tokyo, Japan) provided with the scanner is a Windows or MAC OSX-based tool that allows the scan area to be defined to accommodate the dimensions of the specimen and the scanning resolution to be set according to the user’s needs. This decision involves balancing the need for high resolution against the size of the resultant data set and the scanning duration, both of which are increased with increasing resolution. In addition, a lower limit and the approximate X and Y coordinates of the highest point of the specimen can be defined to further optimise the size of the data set and shorten the scanner’s calibration and scanning times.

The software allows basic manipulation and visualization of the data (Figure 9.2.5) and has the facility to export data in a range of formats for subsequent analysis. In this study, the aim was to measure the changes in dental enamel volume resulting from simulated tooth wear. Therefore specimens were mounted (either the buccal or lingual halves of human tooth crowns) with three reference markers (2 mm diameter titanium spheres) equally spaced around the specimen. Specimens were subjected to the same scanning and calculating process to determine the volume of the specimens above the reference plane before and after the predetermined cycles in the chewing simulator. Wear volume in cubic millimetre was defined as the difference between

the two sets of data collected using the software Excel 2003 (Microsoft Corporation).

It was anticipated that the predicted changes were to be relatively small (expected to be of the order of 20 mm³) therefore the highest scanning resolution was used (i.e., 50µ for the X and Y matrix and 25µ for the height (Z)). The derived data set was exported as a text file for detailed analysis.

9.2.3.2.3. Matlab 6.5

For data analysis, a purpose-written software package was developed using MATLAB (version 6, The Mathworks Inc, Natick MA, U.S.A.). The package accepts data from “Dr PICZA” in the form of (X, Y, Z) triples, where the X values are the west-east coordinates and the Y values the north-south coordinates. To make optimum use of MATLAB and its graphic facilities, the data set was converted to a regular mesh grid and the Z-values were saved to a matrix (Z). The menu-driven software package then provides a series of options for defining the reference plane, graphing the data in 3D and deriving data describing the volume of the scanned object and the surface area and the height of the highest point on the object from the reference plane in cases where this is of interest.

For study B, the volume bounded by two surfaces: the tooth surface and a planar surface defined by the three external reference points were determined (Figure 9.2.6). The data transferred from Dr PICZA were plotted using the MATLAB routines and the maximum heights of the three reference points were identified (Figure 9.2.6 and Figure 9.2.7). The volume of the scanned object above the reference plane was analysed and calculated. The mean volume was determined after each data set was evaluated three times.



Figure 9.2.5: PIX-4 3D scanner, Roland DG, Tokyo, Japan.

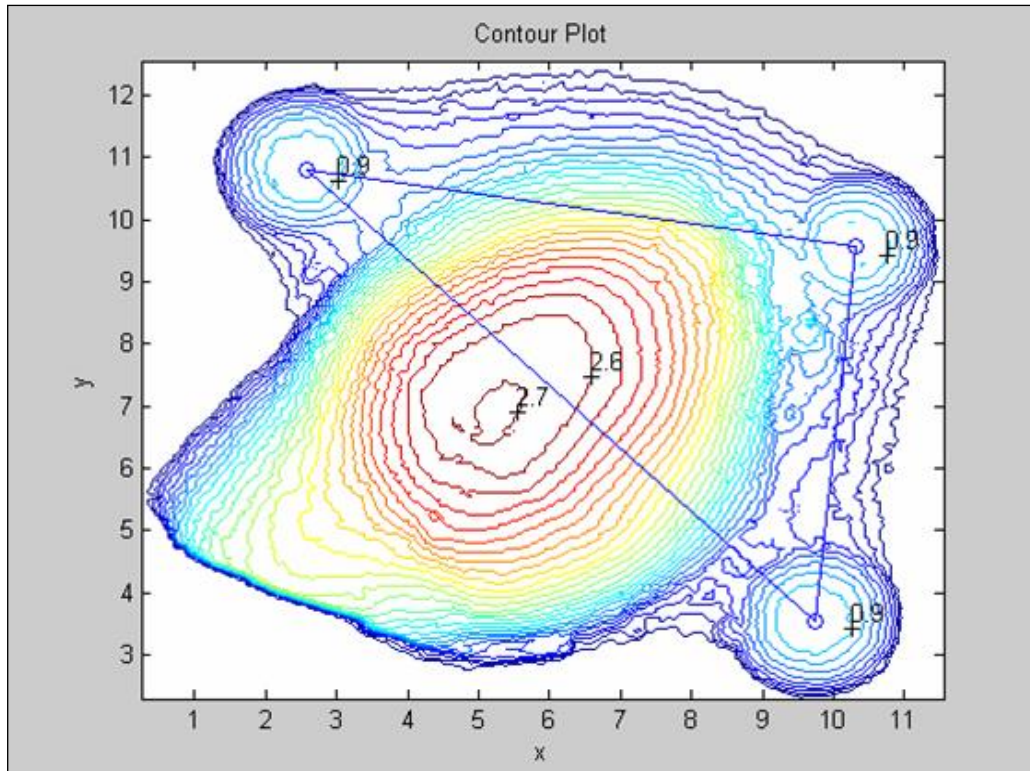


Figure 9.2.6: The graphic data in 3D.

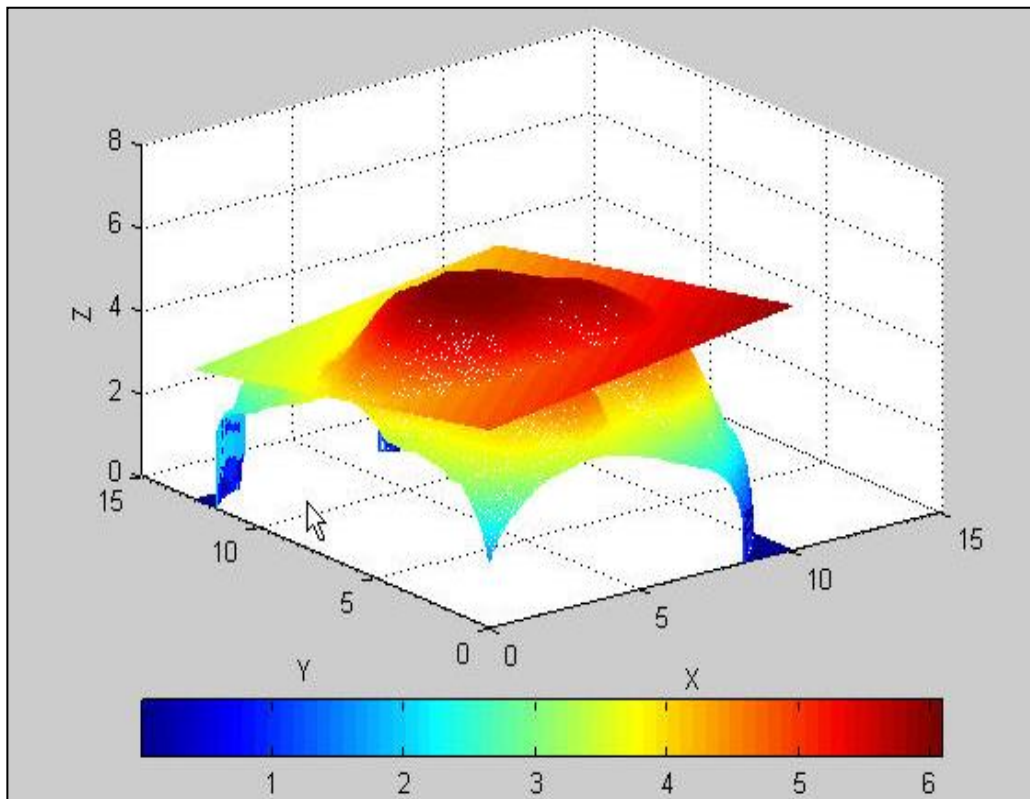


Figure 9.2.7: Reference plane defined for volume calculation with Matlab 6.5.

9.2.3.2.4. Validity and reliability of 3D Scanning and quantitative results

The Dr PICZA volumetric analysis has previously been validated by comparing calculated data with known dimensions and volumes of standard objects by different observers. The reproducibility of the derived data, both within and between observers has also been determined from repeated measurements [351]. The differences were less than 10% from objects which geometrically are difficult to scan and commonly less than 5%. The reproducibility, expressed as intra and inter-observer coefficients of variation was less than 1% for all scans and observers, and with no significant differences between observers or repeated scans [351].

Therefore the system described is an affordable, valid and reliable method for obtaining 3D data for the description and comparison of dental morphology.

9.2.3.3. Scanning Electron Microscopy (SEM) and qualitative results

9.2.3.3.1. Fabrication of specimen replicas

For each specimen, two resin replicas were fabricated, the first after the initial wear facet was created and the second after being subjected to the number of wear cycles required as part of each experimental protocol. Polyvinylsiloxane (ImprintTM, Quick Step, Light and Regular body 3MTM ESPETM) was used to make an impression of the specimens and the replicas were constructed in epoxy die material (Adelaide Epoxy Supplies, South Australia) according to the manufacturer's instructions. The replicas were mounted on standard SEM studs. These were subjected to subsequent scanning electron microscope examination.

9.2.3.3.2. Scanning Electron Microscopy (SEM) observations

The SEM has an electron gun at the top of an electron optical column. The beam is

focused into a small spot, which is scanned over the specimen in a raster pattern. The specimen is mounted in a vacuum chamber.

This signal is electronically converted into an image produced on a monitor screen. The magnification is determined by the area of the sample scanned by the beam.

Ceramic specimens and epoxy resin replicas on SEM studs were prepared for visual assessment using the Phillips 20XL Scanning Electron Microscope (Figure 9.2.8). The specimens were cleaned in an ultrasonic bath for thirty minutes prior to carbon coating. Ceramic specimens were assessed after completion of each finishing protocol and then again after completion of 600000 cycles against enamel in the Willytec chewing simulator.

For each group, two arbitrarily chosen ceramic specimens were selected and prepared for SEM observation (Figure 9.2.9). Observations of the overall surface were completed first under low magnification (20x) and subsequent details of the wear facet were closely observed under higher magnification (200-400x). At least two photographs were made for each chosen sample. To allow direct comparisons between the resulting photomicrographs, the acceleration voltage (kV) and the tilt angle were kept constant. Images were electronically stored for subsequent comparison and analysis.



Figure 9.2.8: Phillips 20XL Scanning Electron Microscope, Adelaide Microscopy laboratory

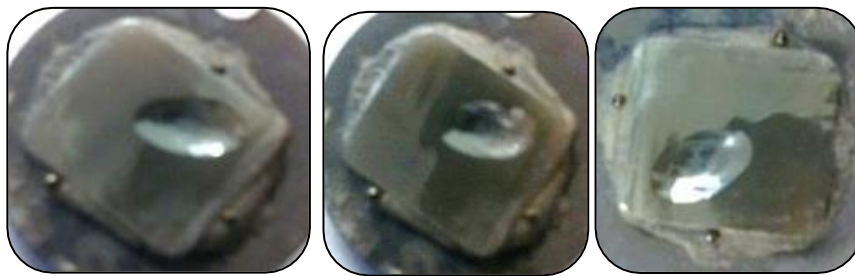


Figure 9.2.9: Ceramic specimens on SEM mount coated with Au/Pd for SEM surface analysis.

9.2.4. Tooth wear simulator protocol

The one hundred and fifty enamel specimens were attached to the superior component of the Willytec chewing simulator. The enamel specimens were abraded against the prepared ceramic specimen immersed in distilled water at neutral pH and at 37°C. The total number of cycles each specimen coupling completed was 600000 at a chewing rate of 4Hz. The occlusal force was 50N, lateral excursion 3 mm and cuspal contact time 0.46 seconds. These masticatory parameters are similar to those used in previous *in vitro* studies [234, 332].

According to the literature [349, 350] the wear produced by 240000 to 250000 masticatory cycles in a chewing simulator corresponds to the wear measured after 1 year of clinical service. Therefore, to simulate a service time of 5 years about 1200000 masticatory cycles have to be performed in a chewing simulator.

9.2.4.1. Willytec tooth wear design

Wear simulators aids researchers to assess the variables that influence rates of wear of enamel and restorative materials. Tooth specimens to be subjected to wear while controlling variables such as load, direction of movement, duration of contact, number of cycles, speed of each cycle, as well as the quantity and quality of selected lubricants (Figure 9.2.10).

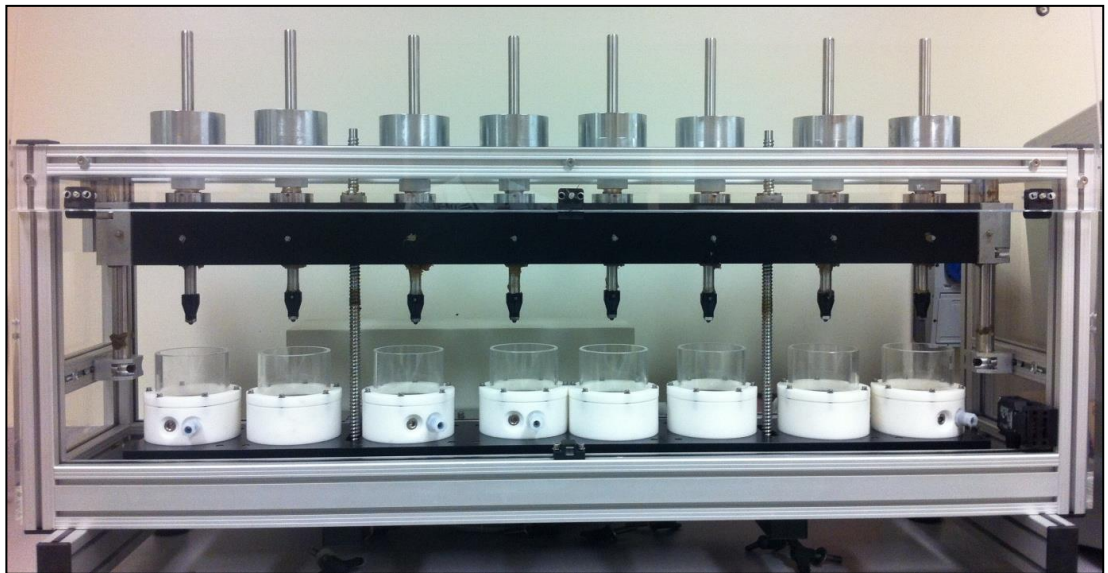


Figure 9.2.10: Willytec wear simulator, Dental School. University of Western Australia.

The Willytec chewing simulator has been commercially available since 1997. In principle, the load is produced by weights, which are mounted on a bar. Loads between 5 and 50 N can be applied in the vertical axis and an additional horizontal movement improves the clinical relevance by further creating a natural chewing pattern. This bar is driven by a computer controlled step motor by means of programmable logic controllers. After the specimens have been mounted in the test chambers, the chewing simulator is calibrated and the reference points (point “zero”) are defined. The chewing simulator contains eight test chambers and each test chamber has a bar and an individual weight; all bars are linked by a transverse bar that is driven by a step motor. When the stylus comes into contact with the specimen,

the whole mass of the weight is released. The step motor can also produce lateral movements. In addition, the simulator includes a thermocycling system, using magnetic valves in conjunction with a heating and cooling system controlled by PLCs (thermocycling is no longer available with the Willytec simulator).

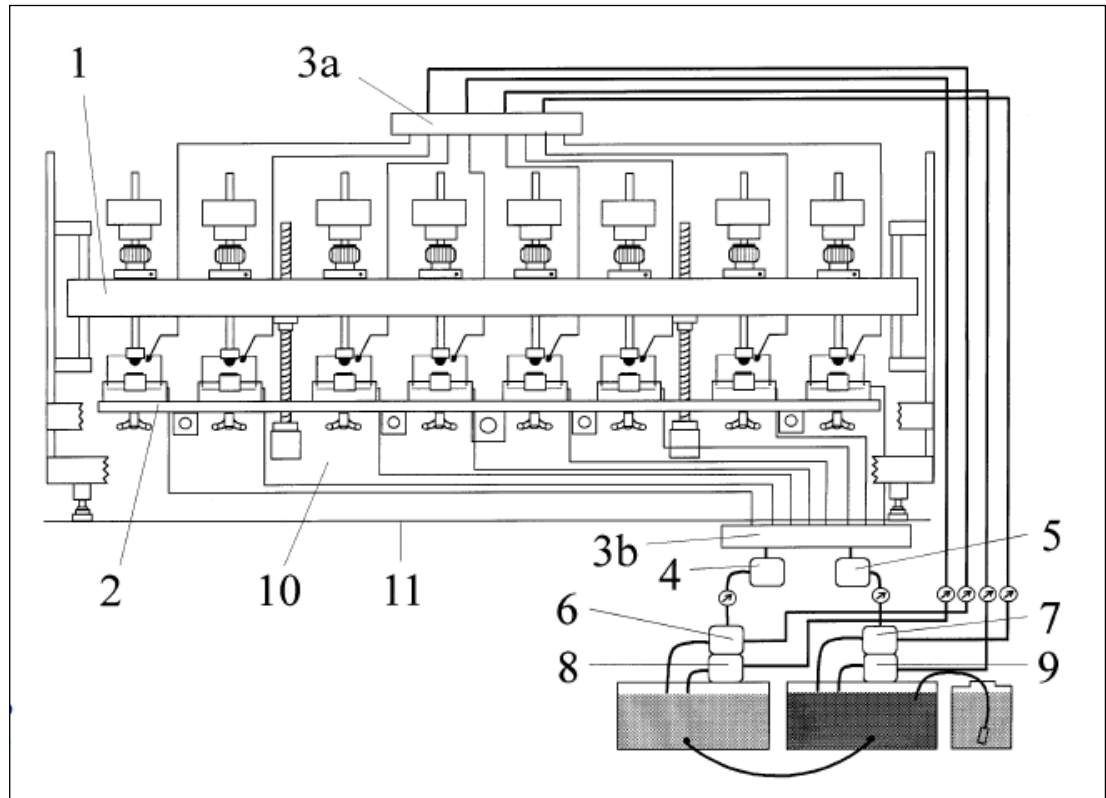


Figure 9.2.11: Schematic drawing of the dual-axis chewing simulator with eight sample chambers. (1) upper crossbeam, (2) lower crossbeam, (3a) water reservoir (in), (3b) water reservoir (out), (4) filter for cold water, (5) filter for warm water, (6) pump for removal of cold water, (7) pump for removal of warm water, (8) pump for application of cold water, (9) pump for application of warm water, (10) motor block, (11) table.

The chewing simulator was developed in co-operation with the Company Willytec*. It has eight identical sample chambers and two stepper motors which allow computer-controlled vertical and horizontal movements between two antagonistic specimens in each sample chamber (Figure 9.2.11). The masticatory load curve is programmed by the combination of the horizontal and vertical motion. The computer unit controls the mechanical motion and the water flow of the cold and warm water baths for the thermal cycling of the samples. Each of the eight sample chambers has a plastic sample holder which is adjustably fixed by a butterfly nut to the base of the

sample chamber and the underlying lower crossbeam. The samples are embedded into the lower sample holder. The lower crossbeam is moved by one stepper motor and allows a horizontal, sliding motion of the samples (Figure 9.2.12).

The antagonistic samples are embedded into the upper sample holders which are fixed at the lower end of the vertical guide rails (Figure 9.2.12). The guide rails are freely mounted within bearings in the upper crossbeam and the vertical height of the antagonistic sample is adjusted by the adjustment screw on top of the upper crossbeam. Adjustable weights are mounted on top of the guide rails and allow variation of the applied chewing force. The upper crossbeam is moved by the second stepper motor and moves the antagonistic samples vertically. When the upper crossbeam moves down and the antagonistic upper samples touch the lower samples, the upper crossbeam moves an additional 2 mm down. Because the guide rails are freely mounted within bearings in the crossbeam, their individual weight is fully transferred to each lower sample. The effective impact force is dependent on the antagonist's total weight and its velocity, which can both be precisely controlled. The chewing machine's computer unit calculates and displays the effective impact as kinetic energy.

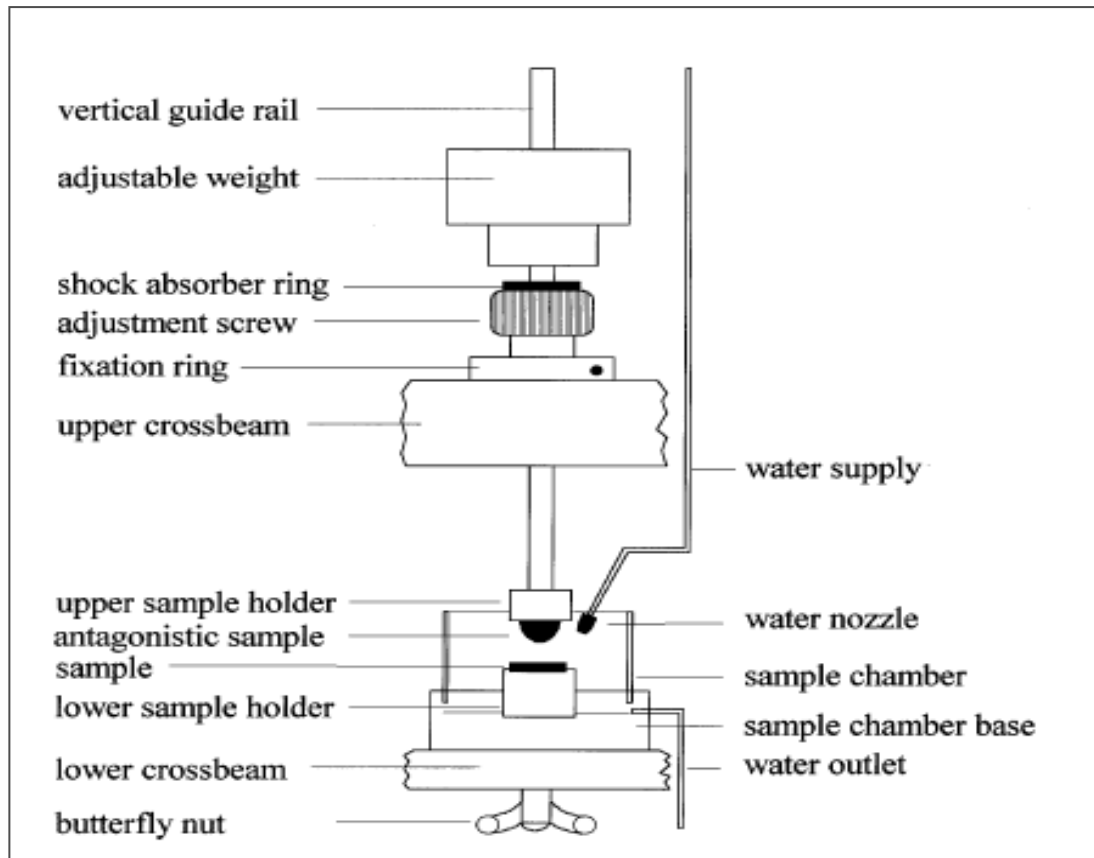


Figure 9.2.12: Schematic drawing of one chewing chamber. The sample rests on the sample holder which is fixed to the chamber base by a butterfly nut.

The Willytec chewing simulator has a number of variables that can be precisely adjusted as shown in Table 9.2.13. Such parameters allow ease of use and more accurate representation of oral tooth wear simulation.

Table 9.2.13: The Willytec chewing simulator with adjustable variables

Variable	Minmum-maximum	Ivoclar method
Number of cycles	1-9,999,999	120,000
Weight	1-11 kg	5 kg
Height	0-20 cm	3 mm
Lateral movement	0-±25 mm	-0.7 mm
Descent speed	8-90 mm/sec	60 mm/sec
Lifting speed	8-90 mm/sec	60 mm/sec
Feed speed	8-90 mm/sec	40 mm/sec
Return speed	8-90 mm/sec	40 mm/sec
Frequency	0.1-3 Hz	1.6 Hz
Thermocycling	Warm bath: 20-58 °C Length of warm bath: 0-999 s Cold bath: 3-20 °C Length of cold bath: 0-999 s Length for evacuation: 0-999 s	55 °C 105 s 5 °C 105 s 15 s

9.2.4.1.1. Method of lubrication

The lubrication system consisted of immersing the samples in a container filled with distilled water. The distilled water and specimens were checked to ensure correct working order and functioning in the chewing simulator every 5 hours. The level of the distilled water was approximately 5mm above the opposing tooth specimen (Figure 9.2.14).

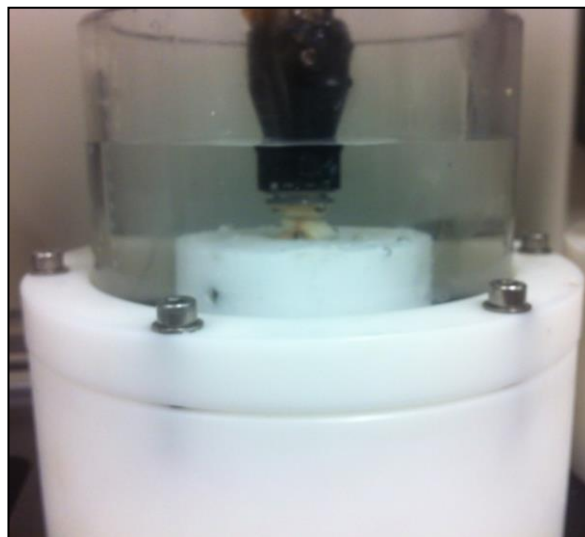


Figure 9.2.14: Willytec chewing simulator testing wear of enamel specimens, lubrication by immersing samples in distilled water.

9.2.5. Statistical analysis

The different null hypotheses were tested using one-way and two-way analysis of variance (ANOVA). One-way analysis of variance (ANOVA) was used to explore the surface texture characteristics for significant differences between the various ceramic groups and between the two ceramic materials. Post analysis paired comparisons of groups were then carried out using Tukey HSD multiple comparisons. The Tukey HSD test method is a follow-up multiple comparison test that is used after a significant one-way analysis of variance (ANOVA). It is one of the several tests that can be used to determine which mean among a set of means differ from the rest. It was used in this study to identify statistically significant group subsets identified by ANOVA. Statistical analyses were performed using SPSS Statistic software (IBM, USA).

Enamel and ceramic wear data were analysed using repeated measures ANOVA to explore the data for statistically significant effects of ceramic finishing surface, and number of cycles. The two factors analysed were the type of ceramic and finishing technique. After using ANOVA to determine the significance of ceramic type, finishing technique, and the interaction of ceramic type and finishing technique, the ceramic type was examined to determine why this effect was significant.

The number of observations per subgroup was nine and the statistical significance was set at the 0.05 probability level.

9.2.5.1. Double Determinations for volumetric analysis

The measuring accuracy and reproducibility of the 3D scanning instrument PICZA as well as the computer software Matlab 6.5 has previously been demonstrated to be satisfactory [352]. In this study, each enamel specimen was scanned once at the highest resolution using the PICZA 3D scanner. The Matlab 6.5 analysis was repeated three times for each enamel specimen and an average was taken. In order to

determine the reliability of the data, ten randomly selected enamel specimen data values were re assessed to determine if they were statistically similar to the previous results.

To assess the consistency and reliability of the volumetric data, two separate results per sample were acquired on different occasions. The ANOVA two sample test confirmed that the differences between the volumetric measurements were not statistically significant ($p=0.14$) (Appendix 7).

CHAPTER 10

RESULTS

STUDY A – SUFACE ROUGHNESS

10.1. SEM analysis

Qualitative surface texture characteristics for lithium disilicate, leucite-reinforced ceramics and tooth enamel specimens are presented (Figure 10.1.1-10.1.9)

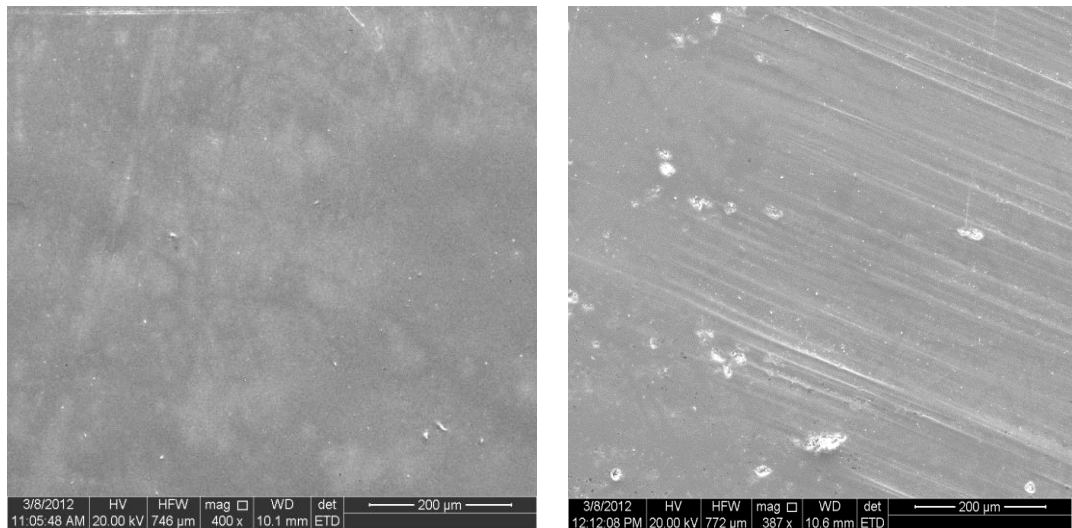


Figure 10.1.1: Leucite-reinforced ceramic, Glazed surface. LEFT: Surface texture Pre wear study, RIGHT: Surface texture Post wear study.

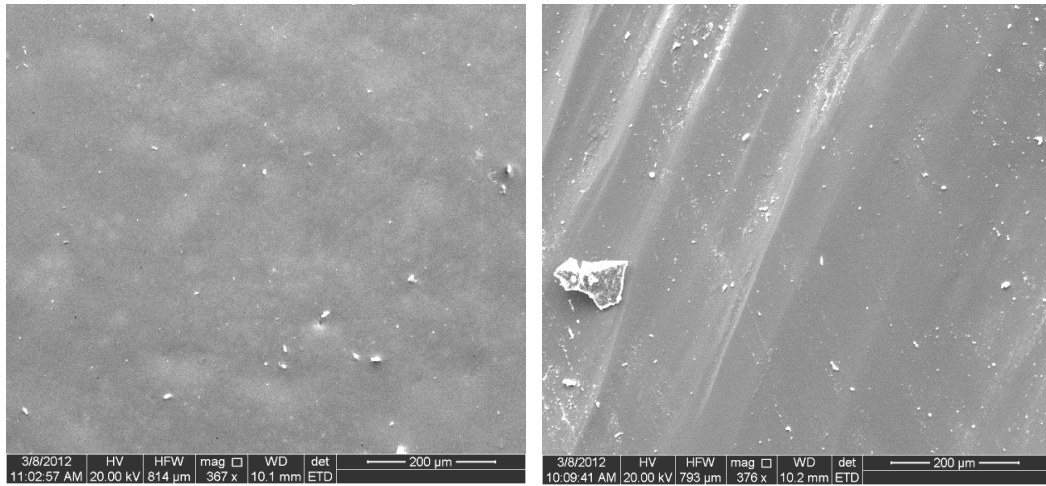


Figure 10.1.2: Lithium Disilicate Ceramic, Glazed surface. LEFT: Surface texture Pre wear study, RIGHT: Surface texture Post wear study.

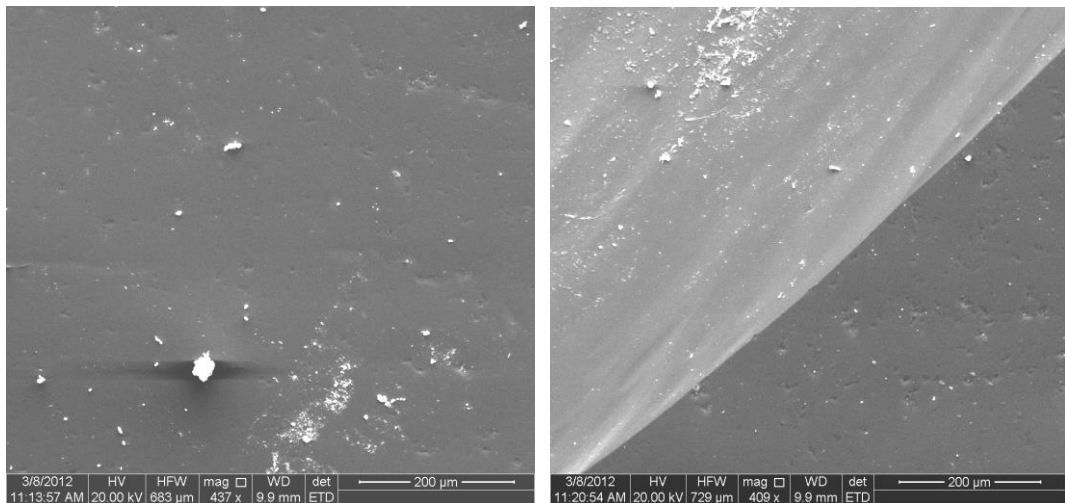


Figure 10.1.3: Leucite-reinforced ceramic, Optrafine and diamond polish paste. LEFT: Surface texture Pre wear study, RIGHT: Surface texture Post wear study.

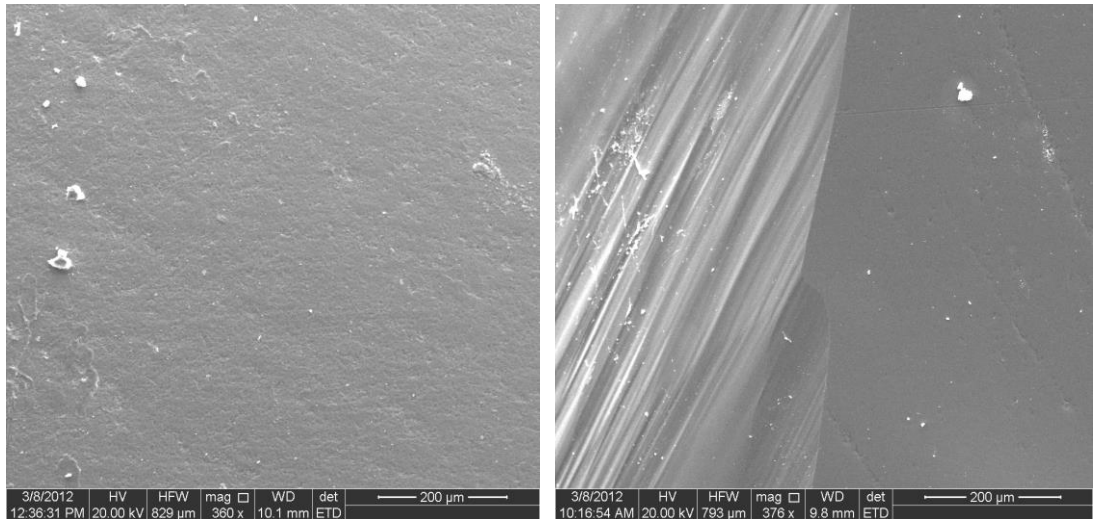


Figure 10.1.4: Lithium disilicate ceramic, Optrafine and diamond polish paste. LEFT: Surface texture Pre wear study, RIGHT: Surface texture Post wear study.

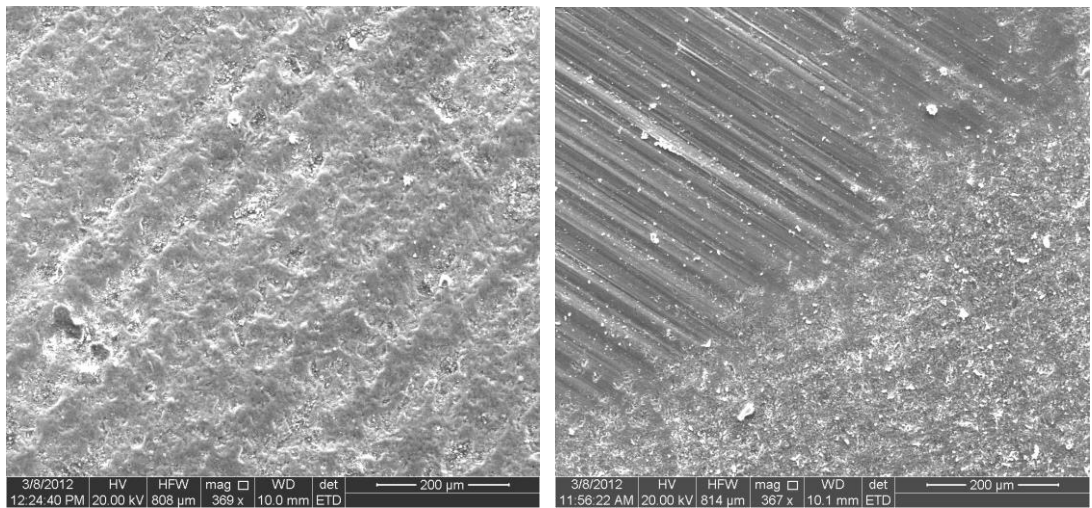


Figure 10.1.5: Leucite-reinforced ceramic High speed diamond 25µm grit. LEFT: Surface texture Pre wear study, RIGHT: Surface texture Post wear study..

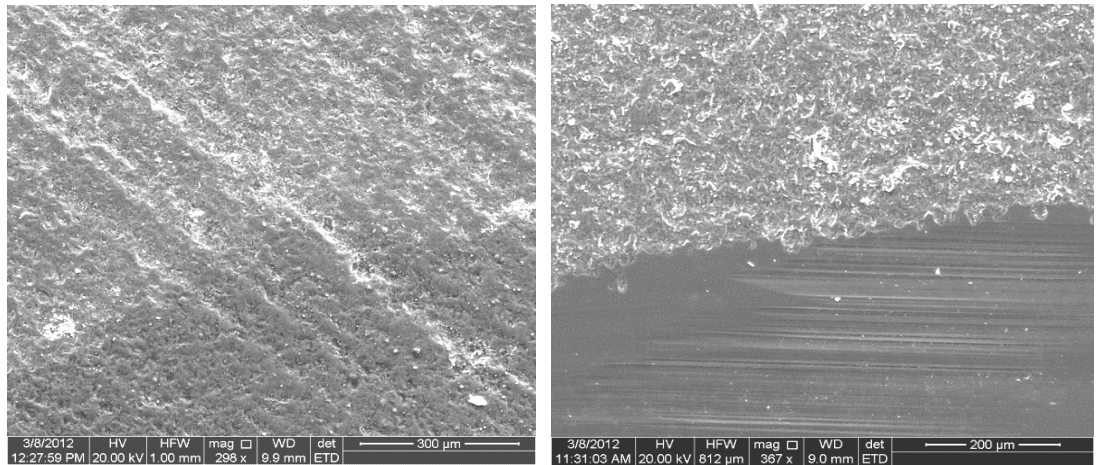


Figure 10.1.6: Lithium disilicate ceramic High speed diamond 25um grit. LEFT: Surface texture Pre wear study, RIGHT: Surface texture Post wear study.

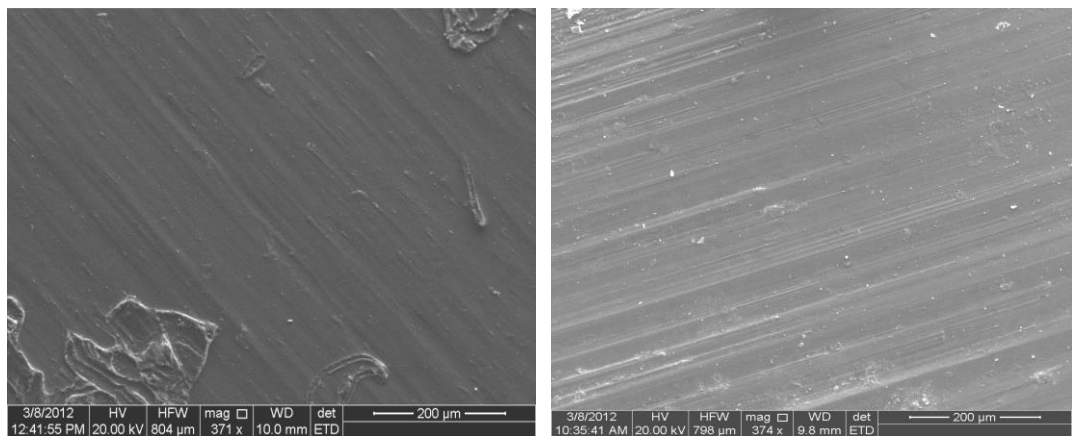


Figure 10.1.7: Leucite-reinforced ceramic Sof lex disc. LEFT: Surface texture Pre wear study, RIGHT: Surface texture Post wear study.

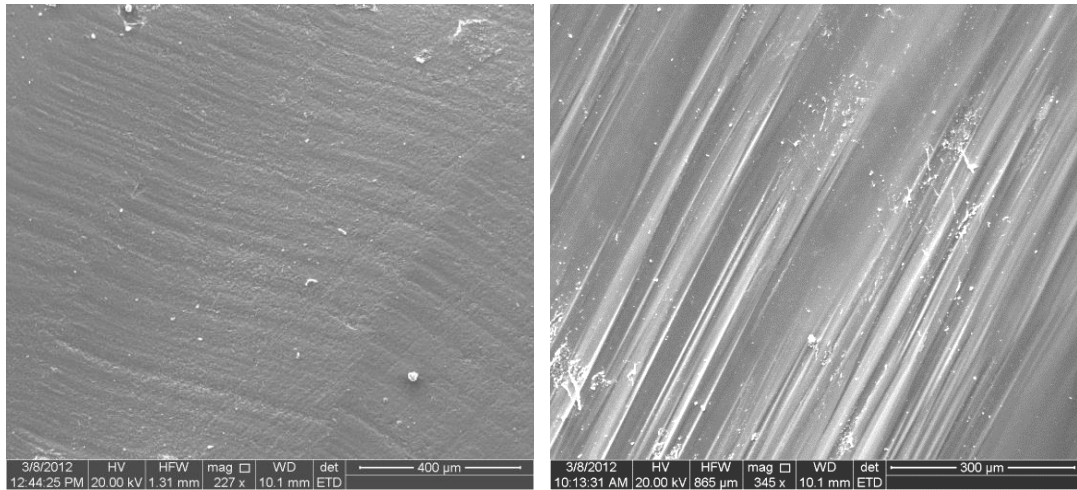


Figure 10.1.8: Lithium disilicate Ceramic Sof-Lex disc. LEFT: Surface texture Pre wear study, RIGHT: Surface texture Post wear study.

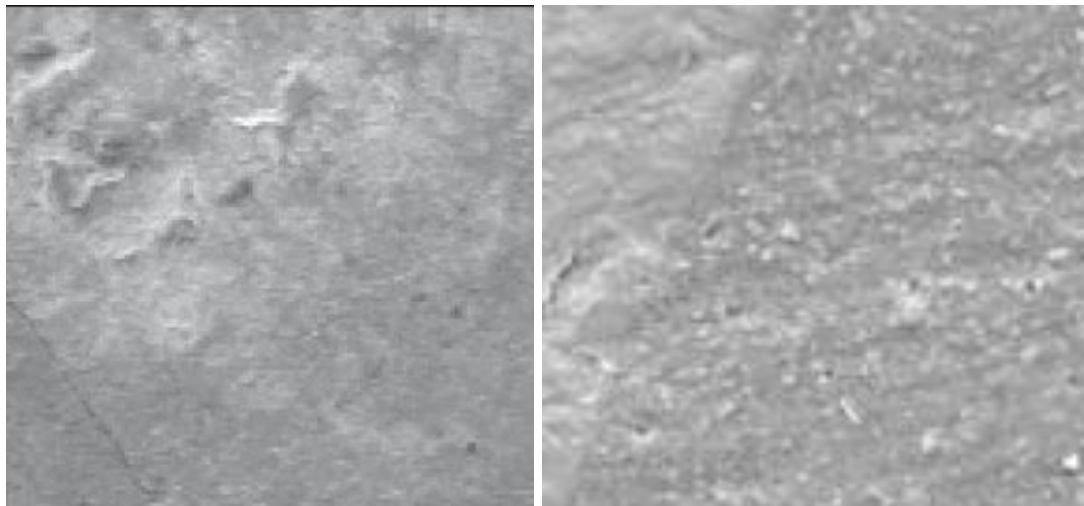


Figure 10.1.9: Enamel specimens. LEFT: Surface texture Pre wear study, RIGHT: Surface texture Post wear study.

No apparent visual difference could be determined at magnification 20x, 200x and 400x between lithium disilicate and leucite-reinforced ceramics when the same finishing protocol was completed. Both ceramic materials finished with as surface glaze or polished with Optrafine polishing system with or without diamond polishing paste had comparable surfaces. Ceramics finished with Sof-Lex under the same magnification as other ceramic specimens were notably different and have the appearance of a greater surface texture and roughness compared to glazed or Optrafine polished ceramic specimens. Ceramic specimens neither finished with a

glaze nor polishing system appeared visually to be significantly more abraded and rough in surface texture than the other ceramic specimens tested.

10.2. Leica MC 90 light microscope surface texture analysis

10.2.1. Surface characteristics before wear simulation

Leucite-reinforced ceramic specimens were glazed, abraded or mechanically polished as previously described. Multiple altitude surface texture parameters were assessed to reinforce the reliability and validity of the surface texture measurements.

The different altitude parameters analysed produced consistent results, therefore to aid simplicity, the most popular altitude parameter in the dental literature, Arithmetic average surface roughness (Ra) will only be described. The other altitude parameters analysed including Rpm, Rp, Rq support and improve the validity of the Ra parameter results however do not improve the relationship of the Ra parameter and its clinical significant. For comparison, the results of the surface texture parameters Rpm, Rq, Rz after various finishing protocols are presented in Appendix 1 and 2.

The surface texture of all ceramic and enamel specimens was analysed at completion of all surface finishing protocols which was prior to the commencement of the wear study.

10.2.1.1. Leucite-reinforced ceramic

According to the Tukey analysis, ceramic specimens finished with different finishing protocols resulted in different surface textures (Figure 10.2.1). Ceramics finished by Optrafine polishing system plus diamond polishing paste and glazed ceramics were statistically similar and had the lowest Ra values, while all other finishing protocols produced rougher ceramic surfaces.

Glazed specimens and specimens finished with Optrafine polishing system with or without diamond polishing paste presented with the lowest surface roughness measurements of ($0.26\mu\text{m} \pm 0.06$), ($0.30\mu\text{m} \pm 0.02$) and ($0.44\mu\text{m} \pm 0.09$) respectively. Specimens finished with Sof-Lex discs had a mean surface roughness measurement of ($0.70\mu\text{m} \pm 0.08$) and specimens which were only abraded with a $50\mu\text{m}$ grit diamond bur had a measurement of ($1.49\mu\text{m} \pm 0.16$).

The results of the surface texture parameters R_{pm} , R_q , R_z after various finishing protocols for leucite-reinforced ceramics are presented in Appendix 1 for comparison.

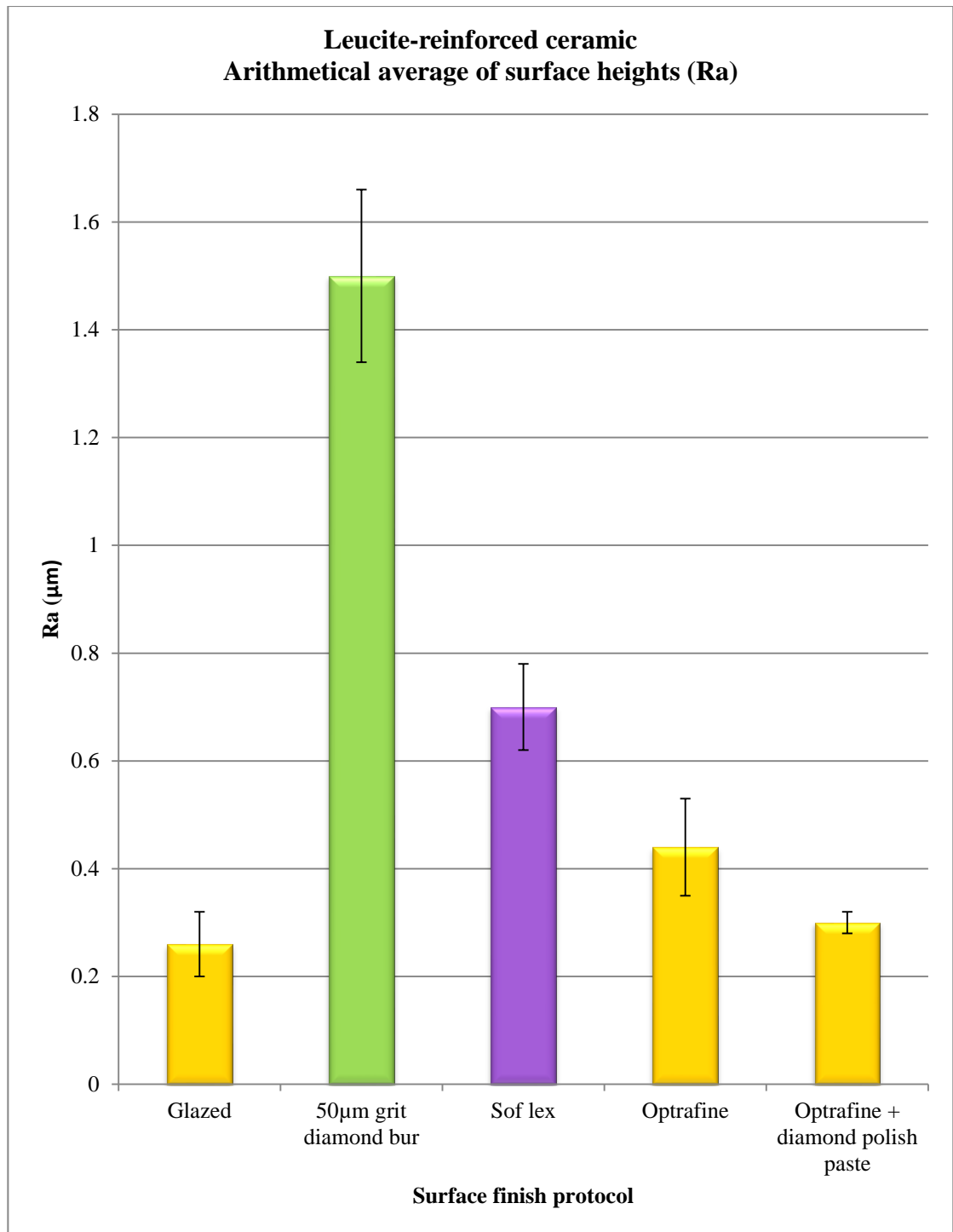


Figure 10.2.1: Arithmetical average of surface heights (Ra) measurement data values for leucite-reinforced ceramic after completion of different surface finishing protocols. Ceramic groups with statistically similar surface texture finishing protocols are shown in the same colour whereas surface finishing techniques which create statistically different surfaces are shown in different colours.

10.2.1.2. Lithium disilicate ceramic

According to the Tukey analysis, ceramic specimens finished with Optrafine

polishing system with ($0.41 \mu\text{m} \pm 0.08$) or without ($0.59 \mu\text{m} \pm 0.09$) diamond polishing paste were statistically but rougher than glazed ceramic specimens (Figure 10.2.2). Glazing lithium disilicate ceramic produced the lowest surface roughness Ra values ($0.22 \mu\text{m} \pm 0.08$). Sof-Lex discs produced a greater surface roughness ($0.82 \mu\text{m} \pm 0.15$) compared to glazing or the Optrafine polishing system. Specimens abraded with a $50 \mu\text{m}$ grit diamond bur after crystallisation had the highest Ra values compared to all other finishing protocols (1.59 ± 0.37).

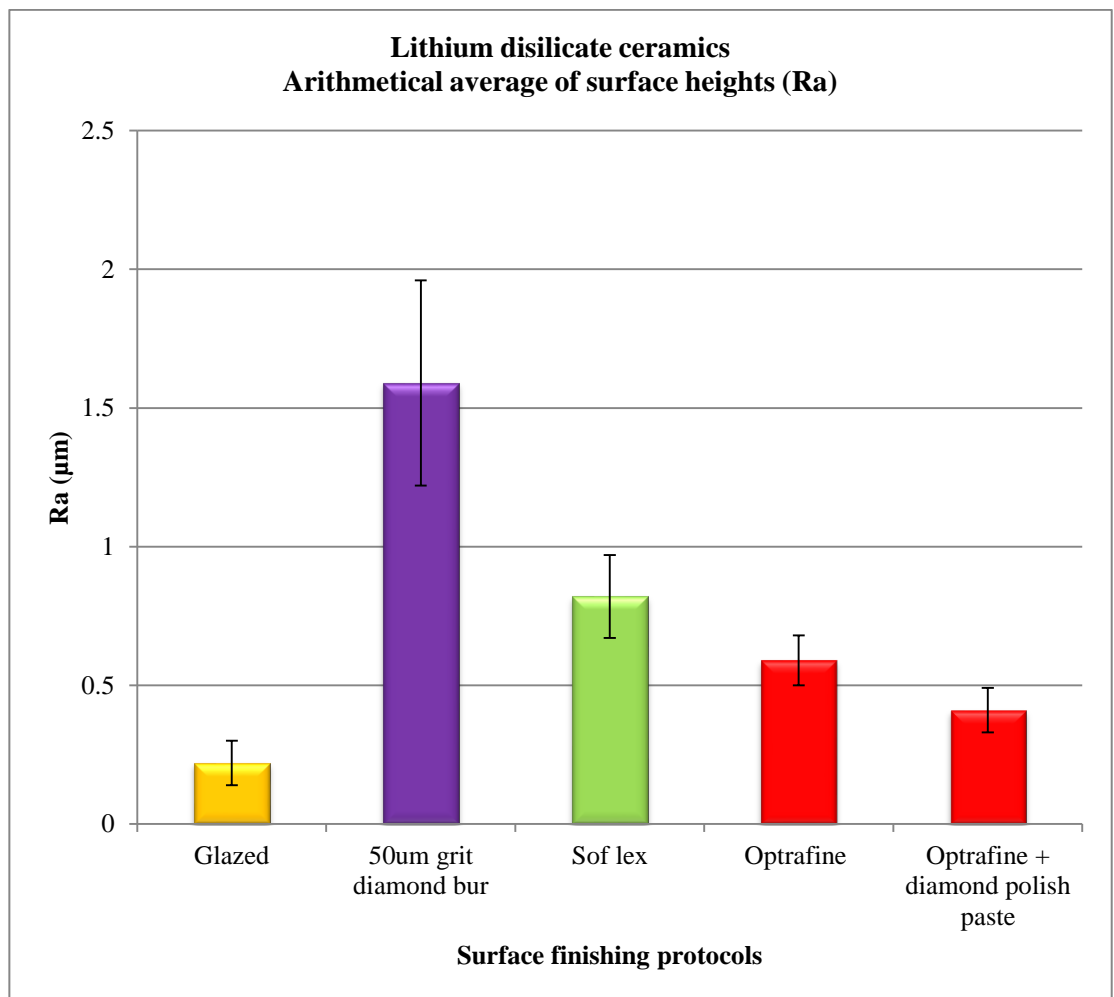


Figure 10.2.2: Arithmetical average of surface heights (Ra) data values (+/_S.E.) for lithium disilicate ceramic after the various surface finishing protocols. Ceramic groups with statistically similar surface texture finishing protocols are shown in the same colour.

The measurements and statistical analysis results of other surface texture altitude parameters tested for lithium disilicate ceramic specimens after the various surface finishing protocols were completed are shown in Appendix 2.

10.3. Surface finishing protocols and glass ceramics

There is no statistical difference in the surface roughness when the two different ceramics are finished by the same surface finishing protocol. Glazing produces a similar smooth surface texture regardless if the ceramic is lithium disilicate or leucite-reinforced (Table 10.3.1).

Table 10.3.1

Finishing Protocol	Leucite-reinforced			Lithium disilicate		
	<i>n</i>	<i>x</i>	<i>SD</i>	<i>n</i>	<i>x</i>	<i>SD</i>
Glazed	10	0.26	0.06	10	0.22	0.08
50um grit diamond bur	10	1.49	0.16	10	1.59	0.37
Sof-Lex polishing discs	10	0.7	0.08	10	0.82	0.15
Optrafine polish system	10	0.3	0.02	10	0.41	0.08
Optrafine and diamond polish paste	10	0.44	0.09	10	0.59	0.09

CHAPTER 11

RESULTS

STUDY B - WEAR

11.1. SEM analysis

Qualitative surface texture characteristics for lithium disilicate, leucite-reinforced ceramics and tooth enamel specimens after completion of the wear study was presented (Figure 10.1.1-10.1.9). The surface texture of ceramic specimens were analysed at magnification 20x, 200x and 400x. After the wear study was completed, all ceramic specimens visually were significantly abraded and consistent in appearance regardless of the initial surface finishing protocol or type of ceramic material.

11.2. Leica MC 90 light microscope surface texture post wear analysis

At completion of the wear study, the surface roughness of leucite-reinforced ceramics and lithium disilicate ceramic specimens was re-examined. The arithmetical average of surface heights (Ra) will be discussed. The remaining surface texture parameter measurements and the statistical analysis are presented in Appendix 3 and 4.

11.2.1. Leucite-reinforced ceramic

At completion of the wear study, the leucite-reinforced ceramic surface roughness according to the arithmetic average of surface heights parameter (Ra) is shown in Figure 11.1. The arithmetical average of surface height (Ra) values for the different ceramic specimen groups are as follows; Glazed ceramics ($1.86\mu\text{m}\pm 0.70$), 50 μm grit diamond bur ($2.01\ \mu\text{m} \pm 0.48$), Optrafine polishing system ($1.53\ \mu\text{m} \pm 0.68$), Optrafine polishing system and diamond polishing paste ($2.25\ \mu\text{m} \pm 0.49$) and Sof-

Lex discs ($2.14 \mu\text{m} \pm 0.59$). According to the Tukey analysis there are no statistical differences at $p= 0.05$ between any ceramic group. Based on this observation all the ceramic arithmetical average of surface height (Ra) values was pooled. The overall arithmetical average of surface height (Ra) value for all leucite-reinforced ceramic specimens after wear testing was $1.95 \mu\text{m} \pm 0.49$. For comparison, the other surface texture parameter measurements and the statistical analysis are presented in Appendix 3.

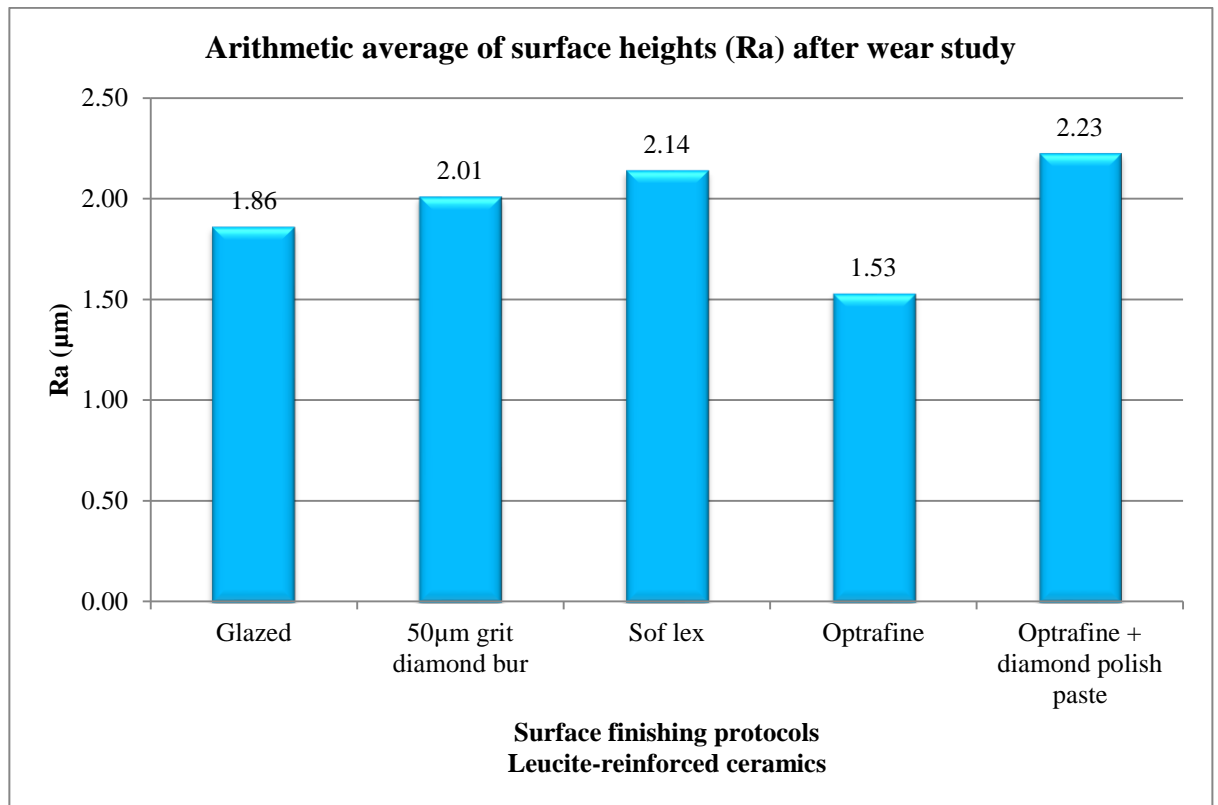


Figure 11.1: Arithmetical average of surface height (Ra) data values for the different leucite-reinforced ceramic specimen groups according to the surface finishing protocols, after subjected to 600000 wear cycles in the chewing simulator against enamel specimens. Ceramic groups with statistically similar surface texture finishing protocols are shown in the same colour

11.2.2. Lithium disilicate ceramics

According to the Tukey analysis, all lithium disilicate ceramic specimen groups had statistically similar arithmetic average of surface height (Ra) values at $p=0.05$. The

mean values for each group of ceramic specimens are as follows; Glazed $1.10 \mu\text{m} \pm 0.26$, $50\mu\text{m}$ grit diamond group $1.22 \mu\text{m} \pm 0.21$, Sof-Lex $1.50 \mu\text{m} \pm 0.15$, Optrafine polishing $1.54 \mu\text{m} \pm 0.18$ and Optrafine polishing with diamond polish paste $1.21 \mu\text{m} \pm 0.71$ (Figure 11.2). The total arithmetic average of surface height value when all the samples were pooled together was $1.31\mu\text{m} \pm 0.51$. For comparison, the remaining surface texture parameter measurements and the statistical analysis are presented in Appendix 4.

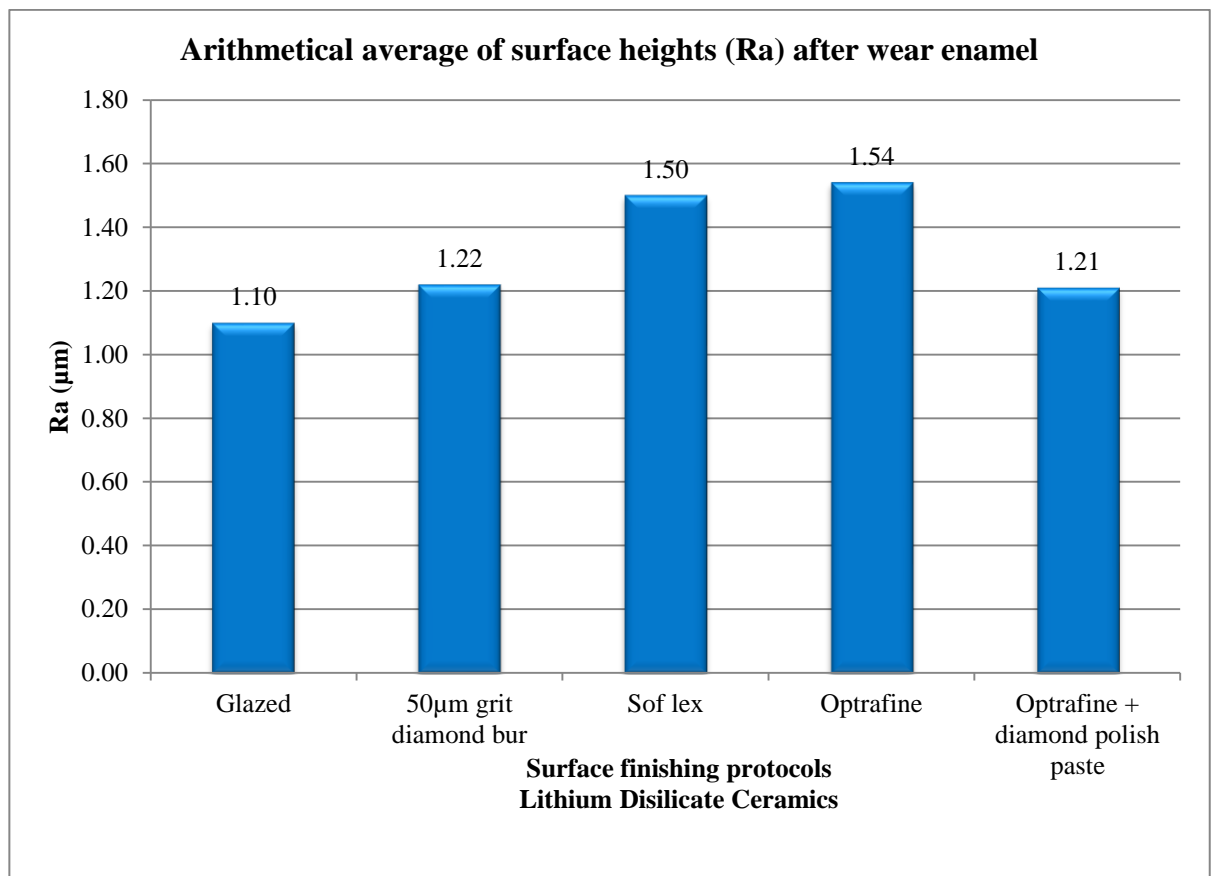


Figure 11.2: Arithmetical average of surface heights (Ra) after wear against enamel for the different lithium disilicate ceramic specimen groups according to the surface finishing protocols, after subjected to 600000 wear cycles in the chewing simulator against enamel specimens. Ceramic groups with statistically similar surface texture finishing protocols are shown in the same colour

11.2.3. Surface texture comparison between ceramics after wear simulation

For each ceramic material, all specimens were pooled together to determine the overall arithmetical average of surface heights (Ra) for each ceramic material after

two body wear simulation against enamel. This was justified since there was no statistical difference between ceramic specimen groups after the wear study was completed, regardless of the initial surface texture (Appendix 5). According to the two sample t test, the mean arithmetical average of surface heights (Ra) of pooled lithium disilicate ($1.31\mu\text{m} \pm 0.45$) is significantly lower ($p=0.01$) than the pooled leucite reinforced ceramics ($1.95\mu\text{m} \pm 0.33$) (Figure 11.3).

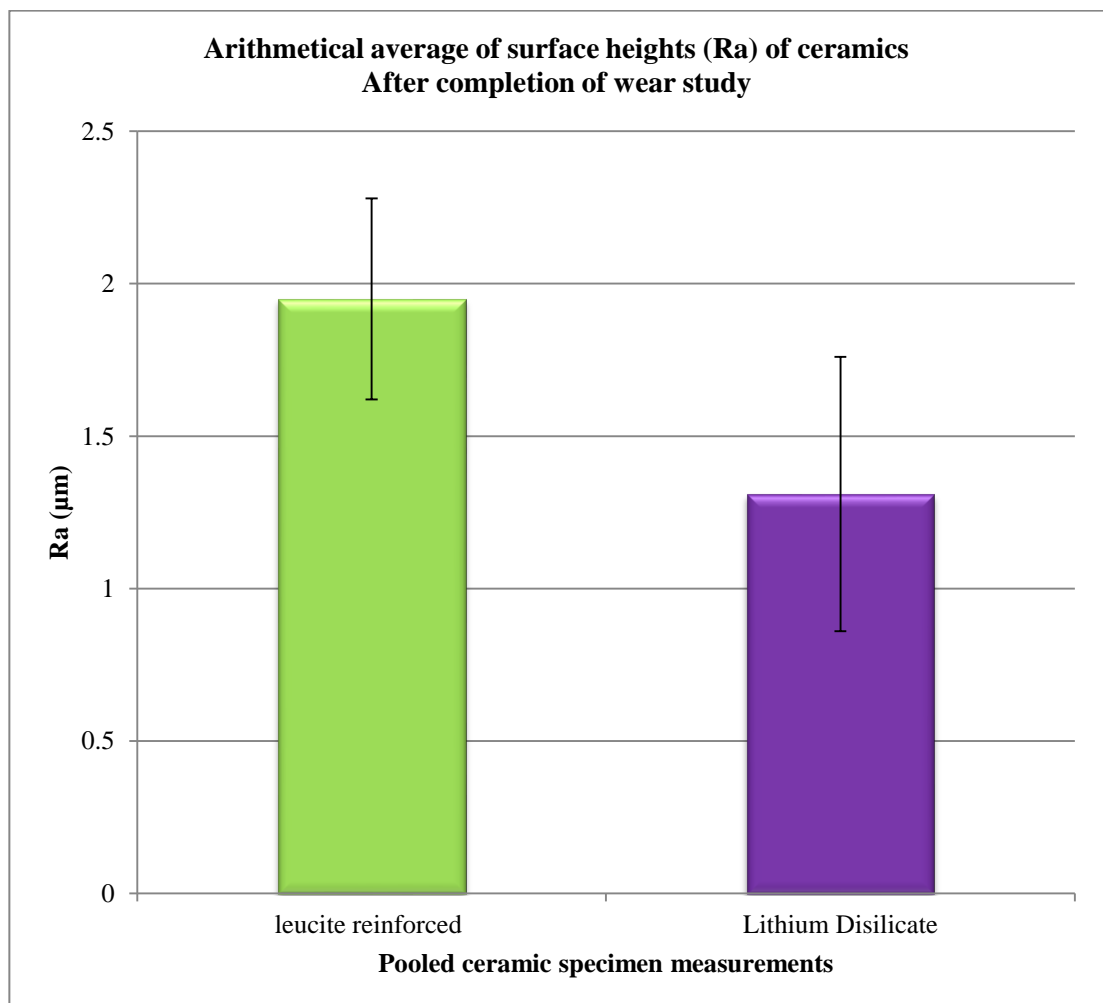


Figure 11.3: Comparison of mean surface texture altitude parameter Ra of leucite reinforced and lithium disilicate pooled ceramic specimens after two body wear simulation in the Willytec chewing simulator.

11.2.4. Enamel specimens

The Ra, Rpm, Rq and Rz surface texture parameter measurements taken before and

after the wear study which were calculated for comparison were statistically different to each other (Appendix 6).

The enamel surface roughness (Ra) was significantly greater ($1.1\mu\text{m} \pm 0.41$) after 600000 cycles of enamel-enamel wear than initially ($0.51\mu\text{m} \pm 0.29$) (Figure 11.4).

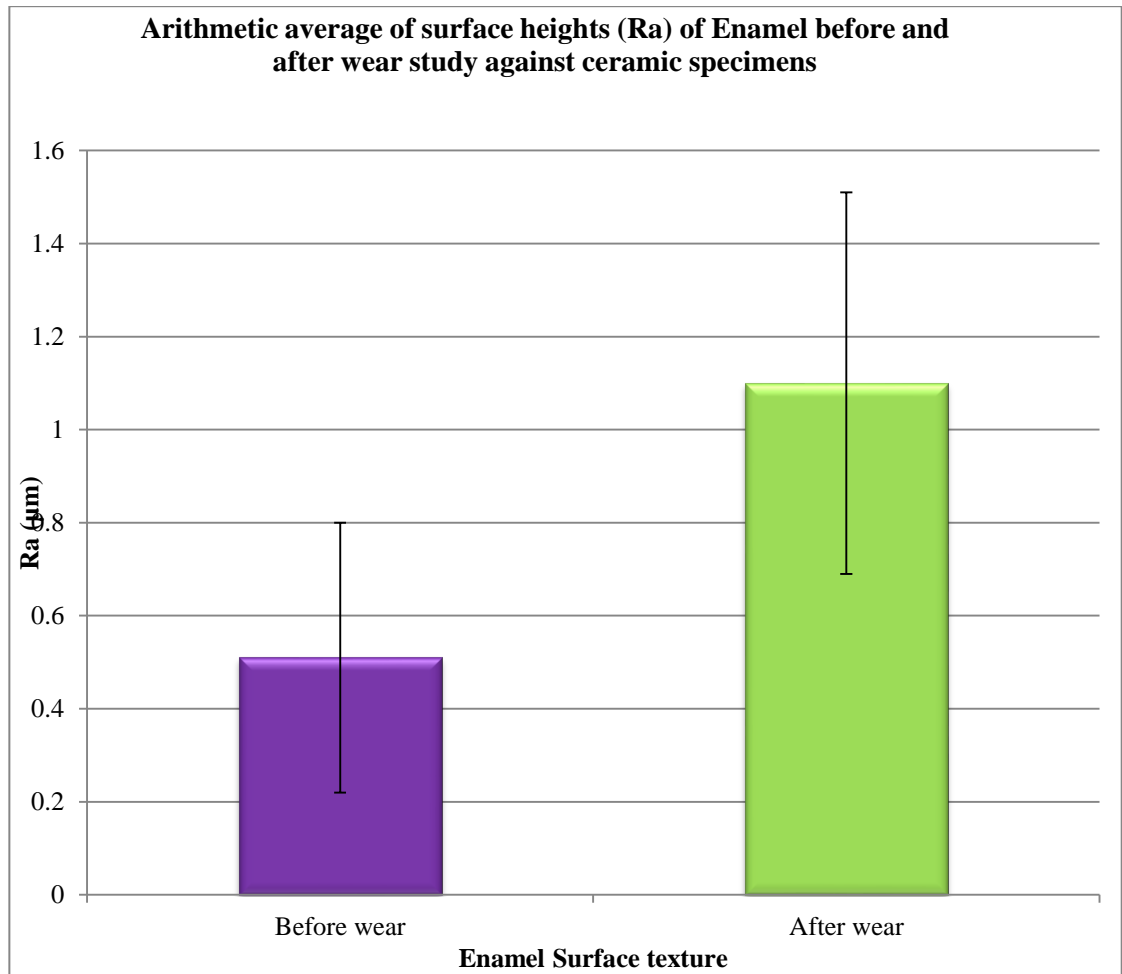


Figure 11.4: Mean values (μm) of enamel specimen surface texture altitude parameter Arithmetic average of surface heights (Ra) before and after *in vitro* wear simulation using a Willytec chewing simulator.

11.3. Volumetric analysis of enamel opposing leucite-reinforced ceramic

Paired occlusal surfaces were mapped and digitally recorded at the beginning and end of each masticatory test. Different surface finishing protocols did not influence

the wear rate of enamel at the completion of the wear study (Figure 11.5). For this reason enamel specimens worn against leucite-reinforced ceramics were pooled together.

A total of 23 enamel specimens were abraded against leucite-reinforced ceramic specimens. The average volumetric surface loss of enamel opposing leucite-reinforced ceramic specimens was $17.33\mu\text{m}\pm 1.97$ per 600000 cycles which correlates to a wear rate of $0.024\mu\text{m}$ per 1000 cycles of parafunctional wear simulation.

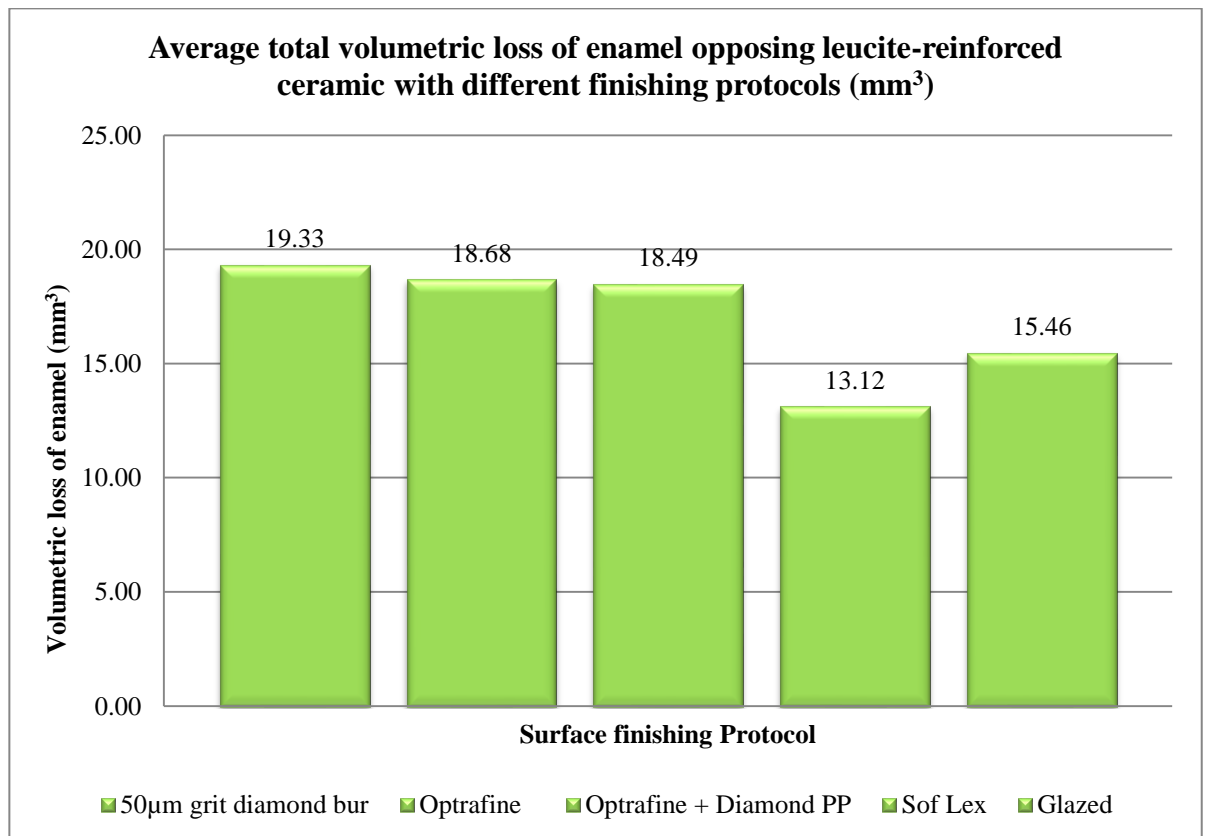


Figure 11.5: Average total volumetric loss of enamel opposing leucite-reinforced ceramic with different surface finishing protocols (mm³). Average total volumetric loss of enamel opposing leucite reinforced ceramic with different surface finishing protocols (mm³). The surface finishing protocol of the ceramic groups did not influence the rate of opposing enamel wear. The statistically similar ceramic groups are presented in the same colour.

11.4. Volumetric analysis of enamel opposing lithium disilicate ceramic

Different surface finishing protocols of lithium disilicate ceramics did not influence the wear rate of the opposing enamel at the completion of the wear study (Figure 11.6). Therefore enamel specimens worn against leucite-reinforced ceramics were pooled together.

A total of 27 enamel specimens were abraded against lithium disilicate ceramic specimens. The average volumetric surface loss of enamel opposing lithium disilicate ceramic specimens was $15.39\mu\text{m}\pm 1.08$ per 600000 cycles which correlates to a wear rate of $0.025\mu\text{m}$ per 1000 cycles of parafunctional wear simulation. There are no statistical differences between the rate of enamel wear and what the opposing ceramic specimen initial surface finish the specimen is abraded against.

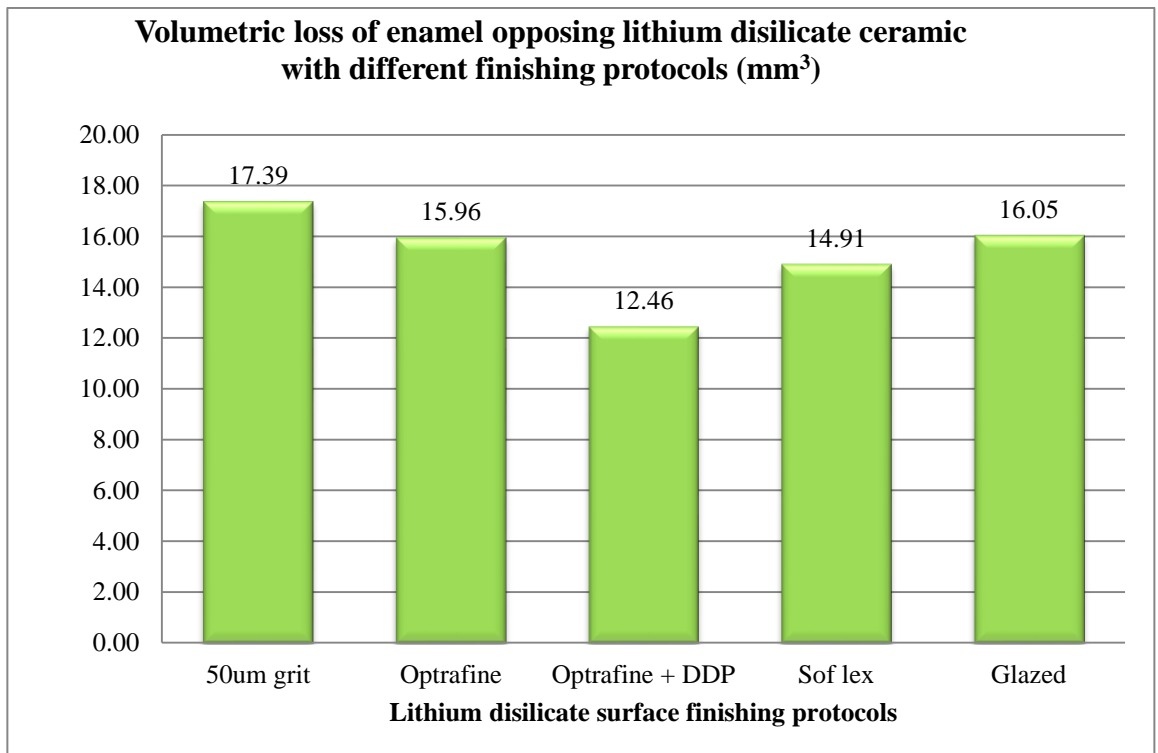


Figure 11.6: Average total volumetric loss of enamel opposing lithium disilicate ceramic specimens with various finishing protocols. Ceramic groups which resulted in statistically similar volumetric enamel loss are presented in the same colour.

11.5. Volumetric analysis of enamel when abraded against an enamel specimen

A total of 25 enamel specimens were abraded against enamel specimens. The group of enamel specimens was considered the control group and allowed the comparison of the enamel specimen wear rates when opposing ceramics. The average volumetric surface loss of enamel was $12.77\mu\text{m}\pm 1.32$ per 600000 cycles which correlates to a wear rate of $0.021\mu\text{m}$ per 1000 cycles of parafunctional wear simulation.

11.6. Volumetric loss of enamel when abraded against enamel, leucite-reinforced and lithium disilicate ceramic specimens

The wear rate of enamel opposing enamel compared to the wear rate of enamel when opposing lithium disilicate is not statistically different ($p=0.07$). However the wear rate of enamel opposing leucite-reinforced ceramic is significantly greater ($p=0.01$) according to the two sample t test (Figure 11.7).

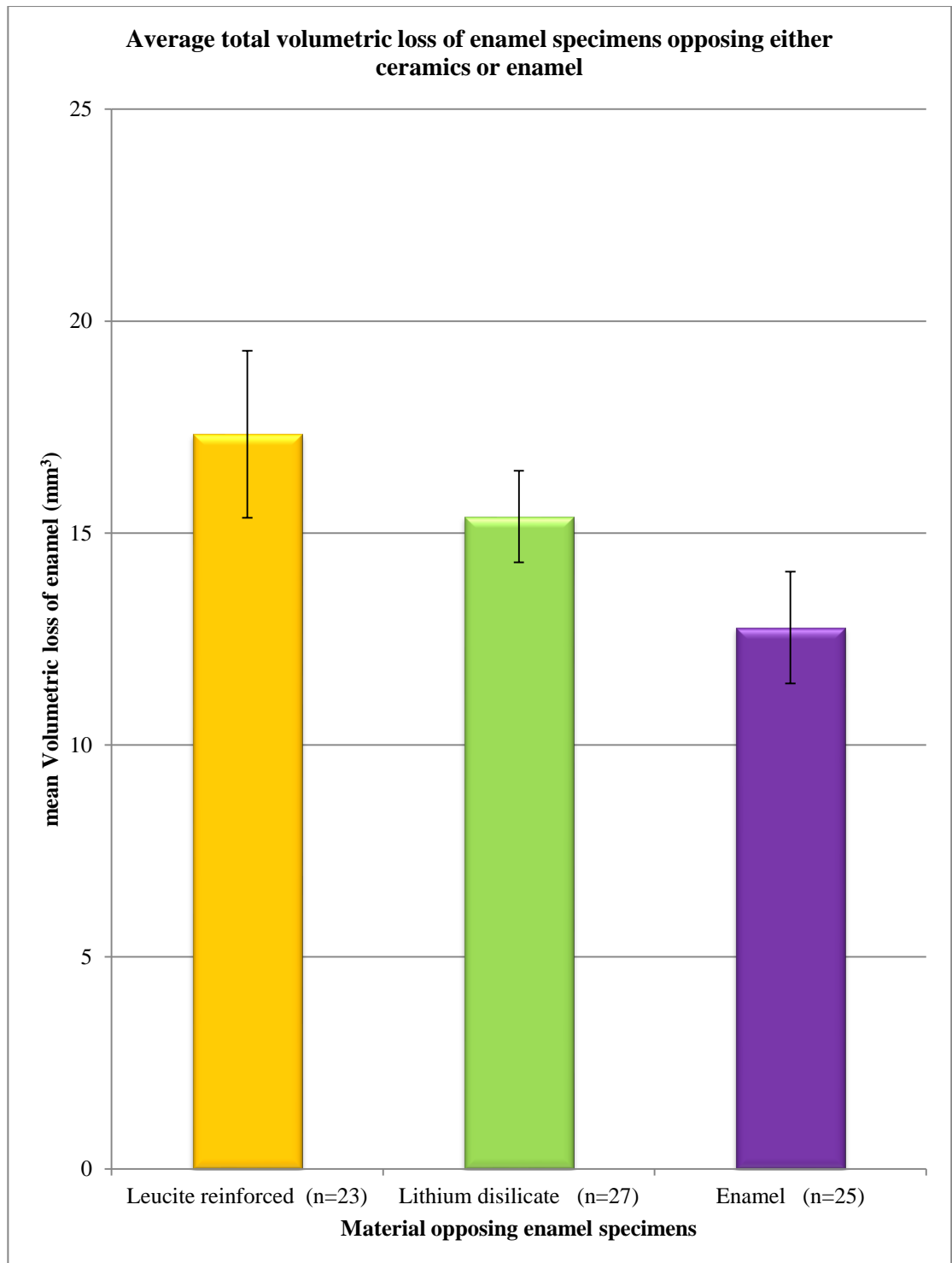


Figure 11.7: Mean volumetric loss of enamel specimen when opposing either enamel or ceramic specimens after wear study against enamel (mm³).

SECTION THREE

CHAPTER 12

DISCUSSION

12.1. Importance of ceramic surface texture and effectiveness of finishing methods

The surface texture of dental ceramics should be as smooth as possible to enhance the function, aesthetics, and biologic compatibility of a restoration [274, 275].

Mechanical polishing or glazing, are methods suitable to create a smooth ceramic surface.

The effectiveness of different polishing methods was assessed by comparing the resulting surface texture to glazed ceramic surfaces. Some types of polishing methods can produce a ceramic surfaces texture equal to that of glazing [308, 314, 315] or better than a glazed ceramic surface [264, 272, 302, 315-320]. The variation in conclusions between the different studies surface texture roughness is due to the variability in polishing protocols and variability of ceramic materials. Different methods and materials for polishing are more beneficial for some types of ceramics than others.

The clinical significance of the ceramic surface textures was analysed by comparing the wear rate of enamel specimens opposing enamel or ceramic specimens with various surface textures after 600 000 cycles in a Willytec chewing simulator.

12.2. Visual appearance of the effect of different finishing protocols

Traditional ceramic polishing techniques produced visually suboptimal ceramic surfaces compared to a glazed ceramic surface [353, 354]. The degree of success of any polishing technique for ceramics is dependent upon having a well condensed ceramic, because porosities in the ceramic are not completely eliminated by

polishing as they are in a natural or overglaze firing. With a well-condensed ceramic, the surface achieved by polishing can be as smooth as that of a glazed surface [337]. Modern dental ceramics such as leucite-reinforced and lithium disilicate ceramics are industrially manufactured and subsequently have a low percentage of flaws and porosities throughout the surface microstructure. This physical property is responsible for its advantageous mechanical polishability. This study has demonstrated mechanically polishing leucite-reinforced or lithium disilicate ceramics with Optrafine polishing system produces a visual ceramic surface lustre which, under SEM magnification, is comparable to a glazed surface. The use of aluminium oxide impregnated Sof- Lex discs did not produce a ceramic surface which was visually comparable to either Optrafine finished or glazed surfaces.

Researchers have recommended the combined use of glazing and polishing to improve surface characteristics of ceramics [234]. Qualitative SEM analysis showed the superiority of this technique [234] in relation to the appearance of a smooth surface finish and in relation to objective aesthetic parameters.

12.3. Efficacy of Optrafine finishing system and leucite-reinforced ceramics

Mechanical polishing leucite-reinforced ceramics with Optrafine polishing system produces a surface texture which is consistent with an over-glazed leucite-reinforced ceramic surface. This study did not find any statistical difference in the resultant surface texture of leucite-reinforced ceramic (Empress CAD) when it was finished by polishing with Optrafine or if the surface was glazed. Polishing with Sof-Lex aluminium impregnated discs produced a rougher surface texture. The results from the polishability of IPS Empress is consistent with Olivera et al [332] and Raimondo et al [131].

12.4. Efficacy of Optrafine finishing system and lithium disilicate ceramics

For lithium disilicate (e.max CAD), the Optrafine polishing system with diamond

polish paste did not produce as smooth a surface as overglazing in In-Ceram glaze paste. Therefore to achieve the smoothest surface texture for lithium disilicate ceramic, glazing is recommended rather than mechanical polishing.

12.5. Efficacy of Sof-Lex finishing method

The Sof-Lex polishing system resulted in a surface texture which was significantly rougher compared to Optrafine polishing system and glazing. The surface texture altitude parameters were reduced by an average of 50% from the initial abraded specimen after polishing with Sof-Lex discs. In this study, flat ceramic specimens were used and the disc contact with the ceramic was optimal. The functionality and practicality of polishing occlusal surfaces with Sof-Lex discs clinically, however, is further compromised by the undulating nature of the occlusal surfaces.

Martinez-Gomis et al [280] advocated the use of Sof-Lex finishing system and Yeti diamond polishing paste (Yeti Dental Produkte) for reducing IPS Classic ceramic surface roughness to an optimal smoothness. The results from the study concluded that the use of Sof-Lex polishing discs can reduce the surface texture parameters (Ra) to a mean of $0.3\mu\text{m}$ and $0.7\mu\text{m}$ for the Rpm parameter. In the present study completed, Sof-Lex discs resulted in surface texture parameters which were slightly, but statistically significantly higher. Specifically Sof-Lex disc polishing system produced mean Ra values of $0.7\mu\text{m}$ for leucite-reinforced ceramic and $0.82\mu\text{m}$ for lithium disilicate, and mean Rpm values of $3.30\mu\text{m}$ for leucite-reinforced and $3.88\mu\text{m}$ for lithium disilicate. These results are similar to data from Yilmaz et al [334] and [336] who reported Ra mean values of $0.5\text{-}1.0\mu\text{m}$. Al-ahadni [136] and Sassahara et al [128] stated that the polishing process outcome may largely depend on the nature of the material. Al-Wahadni [136] concluded that lithium disilicate and leucite-based ceramics have a resistance structure due to their crystal content which makes them difficult to polish with aluminium oxide discs. The present study appears to show that Sof-Lex aluminium discs are not as effective as other polishing methods such as the Optrafine Polishing system. As mentioned by Sasahara et al [128], it is commonly difficult to know what polishing method is most appropriate for a

particular ceramic.

12.6. Efficacy of diamond polishing paste finishing method

The current study concluded that diamond polishing paste reduced the surface roughness Ra parameter by approximately 0.1-0.2 μm which corresponds to findings by Martinez and Gomis et al [280] and Sarac et al [296]. This suggests that the use of diamond polish paste is effective regardless of the type of ceramic used or the previous polishing or finishing technique undertaken. Al-Wahadni and Martin [136] found that polishing with diamond paste is necessary to obtain a surface similar to glazed ceramic.

12.7. Surface texture comparison of leucite-reinforced and lithium disilicate ceramic before after wear simulation

The surface roughness of ceramics after completion of the wear study was not influenced by the initial surface roughness and finishing protocols of the ceramic specimens. Leucite-reinforced ceramic specimens had a mean Ra value of $1.95\mu\text{m} \pm 0.33$ and lithium disilicate ceramic specimens had a mean Ra value of $1.31\mu\text{m} \pm 0.45$. The resulting surface texture after abrasion against enamel may reflect the microstructure of the ceramic materials. The physical properties of ceramics have been shown to influence the surface characteristics and wear rate properties [265] [264]. No previous studies which analyses the surface roughness of ceramic surfaces after the completion of a wear study analysis are available for comparison.

12.8. Comparison of enamel specimen surface texture before and after wear simulation

The surface roughness of enamel was two times greater after the wear study compared to the beginning of the wear study. The surface texture of enamel was similar regardless of what ceramic it was abraded against. Again, there is no published data for comparison.

12.9. Limitations of *in vitro* wear studies

In vitro wear studies provide valuable information regarding the wear behaviour of dental materials in a short period of time. An ideal restorative material should not abrade the opposing enamel in function any more than the rate of wear when enamel is abraded against enamel [173]. However, when opposed by currently available ceramics, enamel may be subject to accelerated wear [294] and the pattern of which may vary according to the ceramic system and its surface characteristics [355].

A limitation in the wear-related literature is the lack of standardisation in the methodology [234]. The wide variety of abrasives, measuring instruments, methods of wear testing used and specimen preparation techniques [355] in studies make it difficult to compare different laboratory and clinical based studies [356], to the point where comparison is irrelevant [173]. Standardisation between wear studies is paramount to improve the quality of *in vitro* wear testing. Currently, there has been no consensus regarding the ideal method of laboratory wear testing restorative materials [234].

A study by Heitz et al [106] assessed the validity of various laboratory wear testing machines and the correlation of laboratory-based wear outcomes to clinical wear studies. The study concluded that different laboratory wear simulators were not comparable most likely because the laboratory wear methods followed different tribological concepts. As the clinical wear process is a complex mechanism with different tribological phenomena occurring at the same time, it can be assumed that there is no single laboratory wear method capable of showing a good correlation with clinical wear. Unfortunately wearing restorative materials in different laboratory wear machines did not improve the correlation of wear with observed clinical wear rates. Repeating the methodology of this study using a variety of laboratory wear simulators would provide little scientific benefit.

12.10. Current *in vitro* study parameters

Wear machines attempt to simulate the clinical masticatory cycle and oral environment [62, 357] however complete simulation by a machine may never be achieved [357]. Thus, this fact should always be considered in both the interpretation of results and any conclusions drawn from these *in vitro* studies.

The literature states that most occlusal contact areas are 1mm^2 and opposing teeth contact up to 500 times a day [358] and for less than thirty minutes per day [359]. The force during tooth contact is commonly less than 20N [360]. In the current *in vitro* wear study, the parameters are more aggressive in nature and correlate with heavy *in vivo* parafunctional activity. The area of abrasive contact between the specimens was 3mm^2 and the specimens were subject to a constant 50N force which has been used in previous studies [28, 355, 361]. Therefore the resulting wear rates of enamel opposing enamel, leucite-reinforced or lithium disilicate ceramics present a more negative image than what would be expected clinically.

12.11. Influence of ceramic initial surface texture and, finishing methods on opposing enamel wear rate

The initial ceramic surface texture recorded at the beginning of the wear study did not show any relationship with the overall wear rate and loss of enamel at the completion of the wear study. The initial ceramic surface texture may influence the wear rate of enamel in the short term however this was not assessed in the current study since samples were only measured at the beginning and end of the wear study. Therefore abrading or polishing ceramic does not result in a higher or lower rate of enamel wear compared to a glazed ceramic specimen. Glazing and/or polishing ceramic may influence the early stage of the wear process, but the suspected positive effect of a glazed/polished surface is quickly lost when the material is placed in function. Therefore the importance of the ceramic surface finishing method in terms of the wear rate of opposing enamel is low.

The importance of the surface texture and surface finishing protocols on the wear characteristics of opposing enamel specimens might not be as great as speculated [234]. Previous studies however have suggested that a polished ceramic surface is less abrasive than glazed porcelain [280], and others state a glazed surface is less abrasive [136]. A study by Olivera et al [332] also suggests that the wear rate of opposing enamel against different of glazed and polished ceramics tend to become more similar with an increasing number of wear cycles. Korber et al [362] reported that the abrasiveness of rough porcelain was initially greater than that of glazed porcelain, but fell to the same level after a 300-cycle wear-in period against enamel. DeLong et al stated that there is limited evidence that the ceramic surface finish influences enamel wear at all [227]. Krejci et al [209] demonstrated that after a glazed surface was worn away, the wear rate was nearly the same for the polished and the glazed ceramic. Jagger [256] and al-Hiyasat [245] also concluded that polished and glazed ceramic specimens resulted in similar wear rates in opposing enamel specimens. In relatively short-duration *in vitro* studies, Monasky et al [205] White et al [206] and Wiley [294] demonstrated that the smoothness of the ceramic glaze resulted in a reduction in the wear rate of the opposing enamel [205, 294]. Klausner et al [363] had similar findings in favour of polished porcelain in an *in vitro* investigation of the evaluation of four different porcelain polishing sequences. They reported no statistically significant difference in the average surface roughness between the final polished surfaces and the initial autoglazed surface.

Jagger and Harrison [364] concluded that there was no difference in the height loss of enamel when opposed to abraded, or glazed ceramic specimens. Jagger and Harrison used Sof-Lex discs and Shofu rubber points to polish Vita, Vitadur N ceramic specimens and noted that a polished ceramic surface resulted in less enamel wear. They suggested that the reason there is no difference in the wear rates of glazed and abraded ceramic is because after a short period of wear, the glaze surface is worn away. Therefore more recent studies recommend polishing prior to natural or overglazing ceramic. This is also in agreement with Jacobi et al [355] who referred to

Korber as stating that the surface roughness of 280-grit porcelain was initially greater than that of glazed porcelain but fell to the same level after a 300-wear cycle period against enamel.

This tends to suggest that in terms of enamel wear, the finishing protocol is not a significant factor for modern machinable glassy ceramics such as lithium disilicate and leucite-reinforced ceramics in a long term wear study. The positive effects of a glazed smooth surface may be lost soon after commencement of a wear study and thus not evident in long duration wear based studies such as the current study. In this study, periodic assessment of surface roughness was not completed therefore an appreciation of the rate of enamel wear throughout the study was not analysed.

After a relative short period of time in the wear simulator, the initial surface texture increases due to abrasion against enamel. The resulting inherent ceramic surface texture and roughness may correlate to the ceramic microstructure. Machinable ceramics such as leucite-reinforced and lithium disilicate ceramics are known to result in less abrasive wear against enamel [234] and this may likely be due to the improved microstructural properties [209].

The *resultant* ceramic surface texture recorded at the end of the wear study appears to influence the wear rate of the opposing enamel. The wear rate of enamel was higher when opposing leucite-reinforced when compared to lithium disilicate ceramic. Leucite-reinforced ceramic had a mean Ra value of $1.95\mu\text{m} \pm 0.33$ whereas lithium disilicate had a mean Ra value of $1.31\mu\text{m} \pm 0.45$ at the completion of the wear study.

12.12. Influence of ceramic hardness on opposing enamel wear rate

Hardness of leucite-reinforced and lithium disilicate ceramic is 6200 and 5800 VHN

respectively. This is significantly greater than the hardness of enamel which is approximately 420 VHN [201]. It was assumed that hardness was associated with the greater abrasiveness of ceramics [205, 256]. Recently however, hardness has been found not to correlate with opposing enamel wear [201] and thus is not a reliable predictor of opposing enamel wear [4]. Additional physical properties of the ceramic material may influence the wear rate but this is out of the scope of the current research.

The current study demonstrated that the wear rate of opposing enamel may be influenced by the inherent surface texture and the material hardness. The degree to which these properties influence opposing enamel wear is unknown.

12.13. Influence of the ceramic material on opposing enamel wear

The type of ceramic material influenced the rate of opposing enamel wear. In this study leucite-reinforced ceramic specimens inherently had a greater surface roughness and hardness compared to lithium disilicate ceramics. Subsequently, the wear rate of enamel opposing leucite-reinforced ceramics was significantly greater than when enamel opposed lithium disilicate ceramic specimens. The wear rate of enamel opposing lithium disilicate was not statistically different to the wear rate of enamel opposing enamel. Specifically the enamel wear rate was 35% higher when opposed against leucite-reinforced ceramic and 20% greater when opposed against lithium disilicate ceramics.

Krejci [203] reported CAD/CAM Vita specimens produced statistically similar vertical height loss when opposing enamel as enamel opposing enamel and significantly less wear on enamel than Dicor MGC ($\alpha=0.01$). Ratledge et al [361] reported no significant difference between *in vitro* wear data of unglazed IPS Empress opposing enamel from their control which was enamel opposing enamel [361]. Ramp et al speculated that IPS Empress and VitaMark II ceramic cause more

wear to opposing enamel because the ceramics are more brittle and it may be possible that ceramic fragments may act as a third body in the wear process [244]. A study by Olivera et al [332] reported that IPS Empress ceramic significantly increased the wear of opposing enamel. Since this study measured wear by height loss only, comparison with the current study is limited.

12.14. Influence of the ceramic microstructure porosity and flaws on opposing enamel wear

The micro-structural differences may be more important than their superficial roughness. In the present study, lithium disilicate and leucite-reinforced ceramics are glass ceramics which show some degree of correlation in their microstructures which may explain the similar effect on the degree of opposing enamel wear.

Machinable glass-ceramics are not free of porosity. Pores are caused by volume changes associated with thermal differences experienced during thermal processing. Pores impart undesirable characteristics to ceramics, including reduced strength and aesthetics [365]. The porosity of a ceramic may influence its wear characteristics to opposing enamel. For example, stress in a porous area of a ceramic can increase the risk of fracture. If a subsurface porosity is exposed during the wear process a circular fracture may result and the sharp edge of the defect produces more wear against the opposing dentition [201].

Machinable glass ceramics also have multiple flaws because of the inhomogeneous distribution of crystals in a glassy matrix. The flaws within the ceramic material may increase the wear of enamel [234]. Sealing of flaws by polishing and glazing can not only improve the strength but may also reduce the abrasiveness of dental ceramics. Previous studies have considered that glazing does not however reduce the rate of wear as once thought, since once the surface glaze is removed, the underlying and more abrasive ceramic is exposed. For such reasons, polishing of the ceramic surface

prior to glazing may further reduce the abrasiveness of the ceramic material when opposing natural tooth structure [205].

CHAPTER 13

CONCLUSIONS

- Polishing modern CAD glass ceramics with Optrafine polishing system produces a surface texture comparable to that of a glazed ceramic specifically for leucite reinforced ceramic and slightly less for lithium disilicate.
- Polishing with Sof-Lex discs results in a su-optimal surface texture compared to ceramic surfaces finished by Optrafine polishing and auto glazing
- The long term wear rate of opposing enamel appears to be more related to the inherent surface texture of modern CAD glass ceramics and not the initial surface texture measured after surface finishing procedures
- Surface texture increases after the initial glazed or polished surfaces is abraded and appears to correlate with the microstructure of the modern CAD glass ceramics
- Compared to the wear rate of enamel opposing enamel, the wear rate of enamel is 20% greater when opposing lithium disilicate and 35% greater when opposing leucite reinforced ceramics. The wear rate of enamel opposing is only statistically significant when opposing leucite reinforced ceramic compared to when it is opposing lithium discilicate,

SECTION FOUR

CHAPTER 14

REFERENCES

1. Anusavice, K.J., *Phillips' science of dental materials. 10th ed.* Philadelphia: WB Saunders Company, 2003. 598-600.
2. Oh, W.S., R. DeLong, and K.J. Anusavice, *Factors affecting enamel and ceramic wear: a literature review.* Journal of Prosthetic Dentistry, 2002. 87: p. 451-9.
3. Fuzzi, M., Z. Zaccheroni, and G. Vallania, *Scanning electron microscopy and profilometer evaluation of glazed and polished dental porcelain.* International Journal of Prosthodontics, 1996. 9(5): p. 452-458.
4. Seghi, R.R., F. Rosenstiel S, and B. P., *Abrasion of human enamel by different dental ceramics in vitro.* Journal of Dental Research, 1991. 70: p. 221-5.
5. Bessing, C. and A. Wiklorsson, *Comparison of two different methods of polishing porcelain.* Scandinavian Dental Research, 1983. 91: p. 482-487.
6. Lohbauer, U., F.A. Müller, and A. Petschelt, *Influence of surface roughness on mechanical strength of resin composite versus glass ceramic materials.* Dental Materials 2008. 24(1): p. 250-6.
7. Newitter, D.A., E.R. Schlissel, and M.S. Wolff, *An evaluation of adjustment and postadjustment finishing techniques on the surface of porcelain-bonded-to-metal crowns.* Journal of Prosthetic Dentistry, 1982. 43: p. 388-39.
8. Monasky, G.E. and D.F. Taylor, *Studies on the wear of porcelain, enamel, and gold.* Journal of Prosthetic Dentistry, 1971. 25: p. 299-306.
9. Raimondo, J., et al., *Polished versus autoglazed dental porcelain* Journal of Prosthetic Dentistry 1990. 64: p. 563-7.
10. Bollen, C.M.L., P. Lambrechts, and M. Quirynen, *Comparison of surface roughness of oral hard materials to the threshold surface roughness for bacterial plaque retention. A review of the literature.* Dental Materials 1997. 13: p. 258-269.
11. Clayton, J. and E. Green, *Roughness of pontic materials and dental plaque.* Journal of Prosthetic Dentistry, 1970. 23: p. 407-11.
12. Quirynen, M. and C.M.L. Bullen, *The influence of surface roughness and surface-free energy on supra- and subgingival plaque formation in man, A review of the literature.* Journal of Clinical Periodontology, 1995. 22: p. 1-14.
13. Quiryner, M., et al., *The influence of surface free energy and surface roughness*

- on early plaque formation*. Journal of Clinical Periodontology, 1990. 17: p. 138-14.
14. Leitaó, J. and T. Hegdahl, *On the measuring of roughness*. Acta Odontol Scand 1981. 39: p. 379-8.
15. Anusavice, K.J., *Phillips' science of dental materials. 10th ed.* Philadelphia: WB Saunders Company, 1996. 598-600.
16. Wiley, M.G., *Effects of porcelain on occluding surfaces of restored teeth*. . Journal of Prosthetic Dentistry, 1989. 61: p. 133-7.
17. Gwinnett, A.J., *Structure and composition of enamel*. . Operative Dentistry 1992. 17(Suppl 5): p. 10-7.
18. Ten Cate, A.R., *Oral histology: development, structure, and function*. St. Louis: Mosby, 1994.
19. Fernandez, C.P. and O. Chevitarese, *The orientation and direction of rods in dental enamel*. . Journal of Prosthetic Dentistry. 1991 65: p. 793-800.
20. Yamakoshi, Y., et al., *Proteomic analysis of enamel matrix using a two-dimensional protein fractionation system*. European Journal of Oral Science, 2006. 114: p. 266-71; discussion 285-6, 382.
21. Xu, H.H., et al., *Indentation damage and mechanical properties of human enamel and dentin*. . Journal of Dental Research, 1998. 77: p. 472-80.
22. Habelitz, S., S.J. Marshall, and G.W. Marshall, *Balooch M. Mechanical properties of human dental enamel on the nanometre scale*. Arch Oral Biol, 2001. 46: p. 173-83.
23. Eisenmann, D.R., *Enamel structure*. In: *Oral Histology. Development, Structure and Function*. AR. Ten Cate editor, 1998. St. Louis: Mosby: p. 218-235.
24. Marshall, G.W., *Dentin: microstructure and characterization*. Quintessence International 1993. 24: p. 606-17.
25. Torneck, C.D., *Dentin pulp complex*. In: *Oral Histology. Development, Structure and Function*. Ten Cate editor, 1998. St. Louis: Mosby: p. 150-196.
26. Garberoglio, R. and M. Brännström, *Scanning electron microscopic investigation of human dentinal tubules*. . Arch Oral Biol 1976. 21: p. 355-362.
27. Schindler, H.J., E. Stengel, and W.E. Spiess, *Feedback control during mastication of solid food textures--a clinical-experimental study*. Journal of Prosthetic Dentistry, 1998. 80: p. 330-6.
28. Bates, J.F., G.D. Stafford, and A. Harrison, *Masticatory function--a review of the literature. 1. The form of the masticatory cycle*. . Journal of Oral Rehabilitation 1975. 2: p. 281-301.

29. Bates, J.F., G.D. Stafford, and A. Harrison, *Masticatory function - a review of the literature. III. Masticatory performance and efficiency.* . Journal of Oral Rehabilitation 1976. 3: p. 57-67.
30. DeLong, R. and W.H. Douglas, *Development of an artificial oral environment for the testing of dental restoratives: bi-axial force and movement control.* . Journal of Dental Research, 1983. 62: p. 32-6.
31. Kohyama, K., et al., *Effects of sample hardness on human chewing force: a model study using silicone rubber.* . Arch Oral Biol 2004. 49: p. 805-16.
32. Gibbs, C.H., et al., *Chewing movements in relation to border movements at the first molar.* Journal of Prosthetic Dentistry, 1981. 46: p. 308-22.
33. Kaidonis, J.A., *Tooth wear: the view of the anthropologist.* Clinical Oral Investigations 2008. 12 (Suppl 1): p. S21-S26.
34. Hunter, J., *The Natural History of Human teeth. Explaining their Structure, Use, Formation, Growth and Diseases..* London: J Johnson 1778: p. 98-100.
35. Brace, C.L., *Occlusion to the anthropological eye.* In: McNamara JA Jr (ed) *The biology of occlusal development.* Monograph no. 7, Craniofacial Growth Series. The University of Michigan, Ann Arbor, , 1977: p. 179-20.
36. Molner, S., *Tooth wear and culture: a survey of tooth functions among some prehistoric populations.* . Current Anthropology 1962. 13: p. 511-26.
37. Sicher, H., *Oral Anatomy, rd 5.* . St. Louis, 1949. The C. I'. Mosby co. p p. 270.
38. Barrett, M.J., *Functioning occlusion.* Ann Aust Coll Dent Surg, 1969. 2: p. 68-80.
39. Kaifu, Y., et al., *Tooth wear and the "design" of the human dentition: a perspective from evolutionary medicine.* Am J Phys Anthropol, 2003. Suppl 37: p. 47-61.
40. Saitou, S., *Mastication and mechanocitology.* In: *Introduction to the masticatory system.* . Tokyo, Fujin-sha: , 1987 p. 115-129 (in Japanese).
41. Gatti, A.M., *Biocompatibility of micro- and nano-particles in the colon. Part II.* . Biomaterials, 2004. 25: p. 385-92.
42. Gatti, A.M. and F. Rivasi, *Biocompatibility of micro- and nanoparticles. Part I: in liver and kidney.* Biomaterials 2002. 23: p. 2381-7.
43. Heintze, S.D., et al., *Wear of ceramic and antagonist-A systematic evaluation of influencing factors in vitro.* Dental materials, 2008. 24: p. 433-449.
44. Genco, R.J., *Current view of risk factors for periodontal diseases.* Journal of Periodontology 1996. 67: p. 1041-9.

45. Carlsson, G.E., I. Egermark, and T. Magnusson, *Predictors of signs and symptoms of temporomandibular disorders: a 20-year follow-up study from childhood to adulthood.* . Acta Odontology Scandinavia 2002. 60: p. 180-5.
46. John, M.T., et al., *No association between incisal tooth wear and temporomandibular disorders.* Journal of Prosthetic Dentistry, 2002. 87: p. 197-203.
47. Seligman, D.A., A.G. Pullinger, and W.K. Solberg, *The prevalence of dental attrition and its association with factors of age, gender, occlusion, and TMJ symptomatology.* Journal of Dental Research, 1988. 67: p. 1323-33.
48. Smith, B.G. and N.D. Robb, *The prevalence of toothwear in 1007 dental patients.* Journal of Oral Rehabilitation, 1996. 23.
49. Smith, B.G.N., *Toothwear: aetiology and diagnosis.* Dentistry Update 1989 16: p. 204-212.
50. Lambrechts, P., et al., *Quantitative in vivo wear of human enamel.* Journal of Dental Research, 1989. 68: p. 1752-4.
51. Peschke, A., S.D. Heintze, and J.F. Roulet, *Two-year clinical evaluation and wear analysis of posterior composite restorations.* Journal of Dental Research 2007. 86 (Spec Issue A):Abstract No. 230.
52. Heintze, S.D., *How to qualify and validate wear simulation devices and methods.* Dental Materials 2006. 22: p. 712-34.
53. al-Hiyasat, A.S., et al., *Investigation of human enamel wear against four dental ceramics and gold.* Journal of Dentistry, 1998b. 26: p. 487-95.
54. DeLong, R., et al., *The wear of enamel when opposed by ceramic systems.* Dental Materials., 1989. 5(4): p. 266-271.
55. Khan, F., et al., *Dental cervical lesions associated with occlusal erosion and attrition.* Australian Dental Journal, 1999. 44(3): p. 176-86.
56. Halling, J., *Principles of tribology.* 1st ed. 1975, London: The Macmillan Press.
57. Smith, B.G.N. and J.K. Knight, *An index for measuring tooth wear.* British Dental Journal 1984. 156: p. 435-438.
58. Pugh, B., *Wear. In: Friction and Wear.* London Newnes-Butterworths, 1973: p. 141-172.
59. Khan, F., W.G. Young, and T.G. Daley, *Dental erosion and bruxism. A tooth wear analysis from South East Queensland.* Australian Dental Journal, 1998. 43(2): p. 117-127.
60. Grippo, J.O., *Abfractions: a new classification of hard tissue lesions of teeth.* . Journal of Esthetic Dentistry 1991. 3(1): p. 14-9.3.

61. Grippo, J.O. and M. Simring, *Dental 'erosion' revisited*. Journal of the American Dental Association, 1995. 126(5): p. 619-30.
62. Mair, L.H., et al., *Wear: mechanisms, manifestations and measurement. Report of a workshop*. Journal of Dentistry, 1996. 24: p. 141-8.
63. Lambrechts, P., et al., *Quantitative evaluation of the wear resistance of posterior dental restorations: a new three-dimensional measuring technique*. Journal of Dentistry 1984 12: p. 252-67.
64. Litonjua, L.A., et al., *Tooth wear: attrition, erosion, and abrasion*. Quintessence International 2003. 34: p. 435-46.
65. Cosme, D.C., et al., *Bruxism and voluntary maximal bite force in young dentate adults*. International Journal of Prosthodontics 2005. 18: p. 328-32.
66. Kaidonis, J.A., et al., *Tooth wear prevention: a quantitative and qualitative in vitro study*. Australian Dental Journal, 2003 48: p. 15-9.
67. Granada, S. and R.A. Hicks, *Changes in self-reported incidence of nocturnal bruxism in college students: 1966-2002*. Percept Mot Skills, 2003. 97: p. 777-8.
68. Kelleher, M. and K. Bishop, *The aetiology and clinical appearance of tooth wear*. European Journal of Prosthodont Restorartive Dentistry, 1997. 5(4): p. 157-60.
69. Abrahamsen, T.C., *The worn dentition-pathognomonic patterns of abrasion and erosion*. International Dentistry Journal, 2005. 55(4 Suppl 1): p. 268-76.
70. Dahl, B.L., G.E. Carlsson, and A. Ekfeldt, *Occlusal wear of teeth and restorative materials. A review of classification, etiology, mechanisms of wear, and some aspects of restorative procedures*. Acta Odontology Scandinavia, 1993. 51(5): p. 299-311.
71. Bernhardt, O., et al., *Risk factors for high occlusal wear scores in a population-based sample: results of the Study of Health in Pomerania (SHIP)*. International Journal of Prosthodontics, 2004. 17(3): p. 333-9.
72. Dahl, B.L., F. Floystrand, and K. Karlsen, *Pathologic attrition and maximal bite force*. Journal of Oral Rehabilitation, 1985. 12(4): p. 337-42.
73. Poynter, M.E. and P.S. Wright, *Tooth wear and some factors influencing its severity*. Restorative Dentistry, 1990. 6(4): p. 8-11.
74. Richards, L.C. and T. Brown, *Dental attrition and age relationships in Australian Aborigines*. Archaeol Phys Anthropol Ocean, 1981. 16: p. 94-8.
75. Litonjua, L.A., et al., *Tooth wear: attrition, erosion, and abrasion*. Quintessence International, 2003. 34(6): p. 435-46.
76. Whitehead, S.A., A.C. Shearer, and D.C. Watts, *Comparison of methods for*

measuring surface roughness of ceramic. Journal of Oral Rehabilitation, 1995. 22(6): p. 421-427.

77. Hattab, F.N. and O.M. Yassin, *Etiology and diagnosis of tooth wear: a literature review and presentation of selected cases.* International Journal of Prosthodontics, 2000. 13(2): p. 101-7.

78. Addy, M. and R.P. Shellis, *Interaction between attrition, abrasion and erosion in tooth wear.* Monogr Oral Sci, 2006. 20: p. 17-31.

79. Lee, W.C. and W.S. Eakle, *Possible role of tensile stress in the etiology of cervical erosive lesions of teeth.* Journal of Prosthetic Dentistry 1984. 52(3): p. 374-80.

80. McCoy, G., *On the longevity of teeth.* . Journal of Oral Implantology, 1983. 11(2): p. 248-252.

81. Jahanmir, S. and T.E. Fischer, *Friction and wear of ceramics.* In: Booser ER, editor. *CRC handbook of lubrication and tribology, vol. III, Monitoring, materials, synthetic lubricants and applications.* Boca Raton, FL: CRC Press; , 1994: p. 103-20.

82. Suh, N.P., *The delamination theory of wear.* . Wear 25, 1973: p. 111-124.

83. American Society for Testing and Materials, C.o.S.D., *Terminology relating to wear and erosion.* Philadelphia: American Society for Testing and Materials, 2002. G 40-02.

84. Pindborg, J.J., *Pathology of the dental hard tissues.* 1970, Munksgaard: Copenhagen.

85. Smith, B.G., *Toothwear: aetiology and diagnosis.* Dent Update, 1989. 16(5): p. 204-12.

86. *THE GLOSSARY OF PROSTHODONTIC TERMS.* Journal of Prosthetic Dentistry. , 2005. 94(1): p. 15.

87. Eccles, J.D., *Dental erosion of nonindustrial origin: a clinical survey and classification.* Journa of Prosthetic Dentistry, 1979. 42: p. 649-53.

88. Kaidonis, J.A., *Tooth wear: the view of the anthropologist.* Clinal Oral Investigations, 2008. 12 (Suppl 1)(Suppl 1): p. S21-26.

89. Smales, R.J. and J.A. Kaidonis, *Definitions, appearances, prevalence and etiology,* in *Tooth erosion: prevalence and treatment,* K.H. Yip, R.J. Smales, and J.A. Kaidonis, Editors. 2006, Jaypee Brothers: New Delhi. p. 1-10.

90. Verrett, R.G., *Analyzing the etiology of an extremely worn dentition.* Journal of Prosthodontics, 2001. 10: p. 224-33.

91. Milosevic, A., D.A. Brodie, and P.D. Slade, *Dental erosion, oral hygiene, and*

nutrition in eating disorders. International Journal of Eatings Disorders, 1997. 21(2): p. 159-9.

92. Zero, D.T. and A. Lussi, *Erosion-chemical and biological factors of importance to the dental practitioner*. International Dental Journal, 2005. 55 (Suppl 1)(4 Suppl 1): p. 285-90.

93. Ali, D.A., et al., *Dental erosion caused by silent gastroesophageal reflux disease* Journal of the American Dental Association 2002. 133: p. 734-7.

94. Stephan, R.M., *Changes in the hydrogen-ion concentration on tooth surfaces and in carious lesions*. Journal of the American Dental Association 1940. 27(47): p. 718-23.

95. Gray, J.A., *Kinetics of the dissolution of human dental enamel in acid*. Journal of Dental Research 1962. 412(48): p. 633-45.

96. Zero, D.T., *Cariology*. Dent Clin North Am 1999. 43(4): p. 655.

97. Milosevic, A., *Tooth wear: an aetiological and diagnostic problem*. European Journal of Prosthodontic Restorative Dentistry, 1993. 1(4): p. 173-8.

98. Wiegand, A. and T. Attin, *Occupational dental erosion from exposure to acids: a review*. Occup Med (Lond), 2007. 57(3): p. 169-76.

99. Meyers, I.A., *Diagnosis and management of the worn dentition: risk management and pre-restorative strategies for the oral and dental environment*. Ann R Australas Coll Dent Surg, 2008. 19: p. 27-30.

100. Shaw, L., *The epidemiology of tooth wear*. European Journal of Prosthodontic Restorative Dentistry, 1997. 5(4): p. 153-6.

101. Al-Omiri, M.K., P.J. Lamey, and T. Clifford, *Impact of tooth wear on daily living*. International Journal of Prosthodontics 2006. 19: p. 601-5.

102. Azzopardi, A., et al., *A literature review of the techniques to measure tooth wear and erosion*. Eur J Prosthodont Restor Dent European Journal of Prosthodontic Restorative Dentistry, 2000. 8(3): p. 93-7.

103. Cvar, J.F. and G. Ryge, *Criteria for the clinical evaluation of dental restorative materials*. In: US Public Health Service. San Francisco: US, Government Printing Office, 1971: p. 244.

104. Taylor, D.F., et al., *Comparison of direct and indirect methods for analyzing wear of posterior composite restorations*. Dental Materials 1989. 5: p. 157-60.

105. Hickel, R., et al., *Recommendations for conducting controlled clinical studies of dental restorative materials (Science Committee Project 2/98 - FDI World Dental Federation)*. Journal of Adhesive Dentistry 2007. 9 (Supplement 1).

106. Heintze, S.D., et al., *Correlation of wear in vivo and six laboratory wear methods*. Dental Materials, 2012. 28: p. 961–973.
107. Leinfelder, K.F., et al., *Quantitative wear measurement of posterior composite resins*. Dental Materials, 1986. 2: p. 198-201.
108. Moffa, J.P. and A.A. Lugassy, *Calibration of evaluators utilizing the M-L occlusal loss scale*. Journal of Dental Research 1986. 65: p. 302, Abstract No. 1197.
109. Bryant, R.W., *Comparison of three standards for quantifying occlusal loss of composite restorations*. Dental Materials, 1990. 6: p. 60-2.
110. Perry, R., et al., *Composite restoration wear analysis: conventional methods vs. three-dimensional laser digitizer*. J Am Dent Assoc, 2000. 131: p. 1472-7.
111. Barbour, M.E. and J.S. Rees, *The laboratory assessment of enamel erosion: a review*. Journal of Dentistry, 2004. 32(8): p. 591-602.
112. Attin, T., *Methods for assessment of dental erosion*. Monogr Oral Sci, 2006. 20: p. 152-72.
113. Finke, M., et al., *Mechanical properties of *in situ* demineralised human enamel measured by AFM nanoindentation*. Surf Sci, 2001. 491: p. 456-67.
114. Azzopardi, A., et al., *A literature review of the techniques to measure tooth wear and erosion*. . European Journal of Prosthodontic Restorative Dentistry 2000. 8: p. 93-7.
115. Peschke, A., S.D. Heintze, and J.F. Roulet, *Comparison of two impression methods for clinical wear measurement*. Journal of Dental Research (Spec Iss B) 2005. 84:Abstract No 350 (Continental European and Scandinavian Divisions).
116. DeLong, R., *Intra-oral restorative materials wear: rethinking the current approaches: how to measure wear*. Dental Materials, 2006. 22(8): p. 702-11.
117. Mehl, A., et al., *A new optical 3-D device for the detection of wear*. Journal of Dental Research, 1997. 76(11): p. 1799-807.
118. Wennerberg, A. and T. Albrektsson, *Suggested guidelines for the topographic evaluation of implant surfaces*. International Journal of Oral and Maxillofacial Implants, 2000. 15: p. 331-344.
119. Thomas, T.R., *Trends in surface roughness*. International Journal of Machine Tools and Manufacture, 1998. 38(5-6): p. 405-411
120. Bai, C., J. Li, and L. Zhang, *AFM as a surface probe-beyond structural information*. Surface and Interface Analysis, 1999. 28(1): p. 44-48.
121. Heintze, S.D., et al., *A comparison of three different methods for the quantification of the *in vitro* wear of dental materials*. Dental Materials, 2006.

22(11): p. 1051-62.

122. Demirel, F., G. Yüksel, and M. Muhtaroğulları, *Effect of topical fluorides and citric acid on heat-pressed all-ceramic material*. International Journal of Periodontics and Restorative Dentistry, 2005. 25(3): p. 277-281.

123. Folwaczny, M., A. Mehl, and C. Haffner, *Polishing and coating of dental ceramic materials with 308 nm XeCl excimer laser radiation*. Dental Materials, 1998. 14(3): p. 186-193.

124. Tholt de Vasconcellos, B., W.G. Miranda-Júnior, and R. Prioli, *Surface roughness in ceramics with different finishing techniques using atomic force microscope and profilometer*. Operative Dentistry, 2006. 31(4): p. 442-449.

125. Silikas, N., D.C. Watts, and K.E. England, *Surface fine structure of treated dentine investigated with tapping mode atomic force microscopy (TMAFM)*. Journal of Dentistry, 1999. 27(2): p. 137-144.

126. Teixeira, E.C.N., J.I. Thompson, and J.R. Piasek, *In vitro toothbrush-dentifrice abrasion of two restorative composites*. Journal of Esthetic and Restorative Dentistry, 2005. 17(3): p. 172-182.

127. Lodding, A., *SIMS of biomineralized tissues: present trends and potentials*. Advanced Dental Research, 1997. 11(4): p. 364-79.

128. Sasahara, R.M.C., F.C. Riberio, and P.F. Cesar, *Influence of the finishing technique on surface roughness of dental porcelains with different microstructures*. Operative Dentistry 2006. 31(5): p. 557-583.

129. Goldstein, G.R., B.R. Barnhard, and B. Penugonda, *Profilometer, SEM, and visual assessment of porcelain polishing methods*. Journal of Prosthetic Dentistry, 1991. 65(5): p. 627-634.

130. Klausner, L.H., C.B. Cartwright, and G.T. Charbeneau, *Polished versus autoglazed porcelain surfaces*. Journal of Prosthetic Dentistry, 1989. 47(2): p. 157-167.

131. Raimondo, R.L., J.T. Richardson, and B. Wiedner, *Polished versus autoglazed dental porcelain*. Journal of Prosthetic Dentistry, 1990. 64(5): p. 553-557.

132. Campbell, S.D., *Evaluation of surface roughness and polishing techniques for new ceramic materials*. Journal of Prosthetic Dentistry, 1989. 61(5): p. 563-568.

133. Brewer, J.D., D.A. Garlapo, and E.A. Chipps, *Clinical discrimination between autoglazed and polished porcelain surfaces*. Journal of Prosthetic Dentistry, 1990. 64(6): p. 631-634.

134. Shearer, A.C., R.P. Kusy, and J.Q. Whitley, *Finishing of MGC Dicor material*. International Journal of Prosthodontics, 1994. 7(2): p. 167-173.

135. Camacho, G.B., D. Vinha, and H. Panzeri, *Surface roughness of a dental ceramic after polishing with different vehicles and diamond pastes*. *Brazilian Dental Journal*, 2006. 17(3): p. 191-194.
136. Al-Wahadni, A.M. and D.M. Martin, *An in vitro investigation into the wear effects of glazed, unglazed and refinished dental porcelain on an opposing material*. *Journal of Oral Rehabilitation*, 1999. 26: p. 538-546.
137. Mair, L.H., *Understanding wear in dentistry*. *Compendium*, 1999 20(1): p. 19-30.
138. Gadelmawla, E.S., et al., *Roughness parameters*. *Journal of Materials Processing Technology*, 2002. 123: p. 133-14.
139. Poon, C.Y. and B. Bhushan, *Comparison of surface roughness measurements by stylus profiler, AFM, and non-contact optical profiler*. *Wear*, 1995. 190 p. 76-88.
140. Leitao, J. and T. Hegdahl, *On the measuring of roughness*. *Acta Odontol Scand* 1981. 39: p. 379-8.
141. Mair, L.H., *Wear in dentistry-current terminology*. *Journal of Dental Research*, 1992. 20(3): p. 140-4.
142. Whitley, J.Q., et al., *Surface roughness of stainless steel and electroformed nickel standards using a HeNe laser*. *Optics and Laser technology*, 1987. 19: p. 18.
143. Jost, H.P., *Lubrication (tribology) education and research*. *Department of Education and Science*. HMSO, 1969.
144. Archard, J.F., *Wear theory and mechanisms*. *Wear Control Handbook*, ed. M. B. Peterson and W. O. Winer, 1980. ASME, New York.: p. 35-80.
145. Bhushan, B. and B.K. Gupta, *Handbook of Tribology: Materials, Coatings, and Surface Treatments*. McGraw-Hill, New York., 1991.
146. Zum-Gahr, K.H., *Classification of wear processes*. In: *Microstructure and Wear of Materials*.. Amsterdam, Elsevier, 1987(80-90).
147. Czichos, H., *Introduction to friction and wear*. In: *Friction and wear of polymer composites*. K Friedrich editor. Amsterdam: Elsevier, 1986: p. 1-22.
148. Kragelskii, I.V., *Friction and wear*. 1965, London: Butterworths.
149. Zum-Gahr, K.-H., *Microstructure and wear of materials*. 1987, Amsterdam: Elsevier.
150. Mair, L.H., *Wear in dentistry-current terminology*. *J Dent*, 1992. 20(3): p. 140-4.
151. Mair, L.H., et al., *Wear: mechanisms, manifestations and measurement*.

- Report of a workshop.* J Dent, 1996. 24(1-2): p. 141-8.
152. Abebe, M. and F.C. Apple, *Theoretical analysis of the basic mechanics of abrasvie processes. Part I: general model.* Wear, 1988. 126: p. 251-266.
153. Sinmazcelik, T. and I. Taskiran, *Erosive wear behaviour of polyphenylenesulphide (PPS) composites* Materials in engineering 2007. 28(9): p. 2471-2477.
154. Mair, L.H., *Understanding wear in dentistry.* Compendium, 1999. 20(1): p. 19-30.
155. Kingery, W.D. and P.B. Vandiver, *Ceramic masterpieces. Art, structure, technology.* 1986, New York: The Free Press.
156. Craig, R.G., *Ceramics*, in *Craig's restorative dental materials*, J.M. Powers and R.L. Sakaguchi, Editors. 2006, Elsevier Mosby: London. p. 444-64.
157. Jones, D.W., *Development of dental ceramics. An historical perspective.* Dent Clin North Am, 1985. 29(4): p. 621-44.
158. van Noort, R., *Introduction to dental materials.* 1994, London: Mosby.
159. Ring, M.E., *Dentistry: An Illustrated History* New York: Harry N Abrams Inc, 1985: p. 108–211.
160. Kelly, J., I. Nishimura, and S.D. Campbell, *Ceramics in Dentistry. Historical roots and current perspectives.* Journal of Prosthetic Dentistry 1996, 1996. 75(1): p. 18-32.
161. Zeilgler, H., *The father of porcelain dental art.* . Dominion Dent J, 1905
162. Rosenblum, M.A. and A. Schulman, *A review of all-ceramic restorations.* Journal of the American Dental Association, 1997. 128(3): p. 297-307.
163. Giordano, R.A., *Dental ceramic restorative systems.* Compendium Continuing Education Dentistry, 1996. 17(8): p. 779-82, 784-6 passim; quiz 794.
164. Naylor, W.P., *Introduction to metal ceramic technology* Quintessence publishing, 2009
165. McLean, J.W., *The Science and Art of Dental Ceramics. Volume I: The Nature of Dental Ceramics and Their Clinical Use.* Chicago, IL: Quintessence Publishing Co; Monograph 1, 1979.
166. McLean, J., *Perspectives on dental ceramics. In: Dental Ceramics. Proceedings of the First International Symposium on Dental Ceramics.* Chicago: Quintessence, 1984: p. 13-40.
167. Weber, H., et al., *Glaskeramikkronen klinisch betrachtet.* Zahnarztl Mit,

1987. 77: p. 2416-2421.

168. Pröbster, L., *Erfahrung mit vollkeramischem Zahnersatz-Ein Rückblick. In: Kappert HF (ed).* Berlin: Quintessence, 1996. Vollkeramik: Werkstoffkunde-Zahntechnik-Klinische Erfahrung. : p. 103-116.

169. Zheng, J. and Z.R. Zhou, *Friction and wear behavior of human teeth under various wear conditions.* Tribology International, 2007. 40(2): p. 278-284.

170. Zheng, J. and Z.R. Zhou, *Effect of age on the friction and wear behaviors of human teeth.* . Tribology International, 2006. 39(3): p. 266-273.

171. Anusavice, K.J., *Phillips' Science of Dental Materials, ed 11.* . Philadelphia: Saunders,, 2003.

172. McLean, J.W., *The nature of dental ceramics, in The Science and Art of Dental Ceramics.* 1979, Quintessence Publishing Co., Inc.: Chicago. p. 23-51.

173. Oh, W.S., R. DeLong, and K.J. Anusavice, *Factors affecting enamel and ceramic wear: A literature review.* The Journal of Prosthetic Dentistry., 2002. 87(4): p. 451-459.

174. Denry, I., *Recent advances in ceramics for dentistry.* Crit review Oral boil Med 1996. 131: p. 47s-51s.

175. Kelly, J.R., I. Nishimura, and S.D. Campbell, *Ceramics in dentistry: historical roots and current perspectives.* Journal Prosthetic Dentistry, 1996. 75(1): p. 18-32.

176. Kelly, J.R. and P. Benetti, *Ceramic materials in dentistry: historical evolution and current practice.* Australian Dental Journal 2011. 56(1 Suppl): p. 84-96.

177. Muia, P.J., *The four Dimensional tooth colour system.* Chicargo Quintessence, 1982.

178. Ritter, R., *Dental ceramics.* Journal of Esthetic and Restorative Dentistry, 2010. 22(5).

179. Jung, Y.G., et al., *Lifetime- limiting strength degradation from contact fatigue in dental ceramics.* Journal of Dental Research, 2000. 79: p. 722-31

180. Höland, W., et al., *A comparison of the microstructure and properties of the IPS Empress 2 and the IPS Empress glassceramics.* Journal of Biomedical Material Research, 2000. 53(4): p. 297-303.

181. Studer, S., C. Lehner, and P. Schrer, *Seven-year results of leucite-reinforced glass-ceramic inlays and onlays.* IADR, 1998. Nice(abstract 1375).

182. Dong, J.K., et al., *Heatpresse ceramics: Technology and Strength.*

International Journal of Prosthodontics, 1992. 9(5): p. 9-16.

183. Van Dijken, J.W., *All-ceramic restorations: classification and clinical evaluations*. Compend Contin Educ Dent, 1999. 20(12): p. 1115-24, 1126 passim; quiz 1136.

184. Conrad, H.J., W.J. Seong, and I.J. Pesun, *Current ceramic materials and systems with clinical recommendations: a systematic review*. Journal of Prosthetic Dentistry, 2007. 98(5): p. 389-404.

185. Fradeani, M. and M. Regemagni, *An 11 year clinical evaluation of leucite-reinforced glass-ceramic crowns: A retrospective study*. Quintessence International, 2002. 33: p. 503-10.

186. Guess, P.C.Z., et al., "*Monolithic CAD/CAM Lithium Disilicate Versus Veneered Y-TZP Crowns: Comparison of Failure Modes and Reliability After Fatigue*". International Journal of Prosthodontics 2010. 23(151-159).

187. Kelly, J.R., P. Bernetti, and A. Della Bona, *The slippery slope - Critical perspectives on in vitro research methodologies*. Dental Materials, 2012. 28: p. 41-51.

188. Mormann, W.H. and A. Bindl, *All-ceramic, chair-side computer-aided design/computer-aided machining restorations*. Dent Clin North Am, 2002. 46(2): p. 111-116.

189. Denry, I. and J.R. Kelly, *State of the art of zirconia for dental applications*. Dental Materials, 2008. 24(3): p. 299-307.

190. Thompson, V. and D. Rekow, *Dental Ceramics and the Molar Crown Testing Ground*. Journal of Applied Science, 2004. 12 p. 26-36.

191. Bindl, A. and W.H. Mormann, *An up to 5-year clinical evaluation of posterior in-ceram CAD/CAM core crowns*. International Journal of Prosthodontics, 2002. 15(5): p. 451-6.

192. McLean, J.W., *Evolution of dental ceramics in the twentieth century*. Journal of Prosthetic Dentistry, 2001. 85(1): p. 61-6.

193. Garvie, R.C., R.H. Hannink, and R.T. Pascoe, *Ceramic steel?* . Nature 1975. 258: p. 703-706.

194. Kelly, J.R., J.A. Tesk, and J.A. Sorensen, *Failure of all-ceramic fixed partial dentures in vitro and in vivo: analysis and modelling*. Journal of Dental Research 1995. 74(6): p. 125.

195. Della Bona, D. and J.R. Kelly, *The clinical success of all-ceramic restorations*. Journal of the American Dental Association 2008. 139(8S-13S).

196. Kosmac, T., et al., *The effect of surface grinding and sandblasting on flexural*

- strength and reliability of Y-TZP zirconia ceramic*. Dental Materials, 1999. 15(6): p. 426-33.
197. Luthardt, R.G., O. Sandkuhl, and B. Reitz, *Zirconia-TZP and alumina-advanced technologies for the manufacturing of single crowns*. European Journal of Prosthodontic Restorative Dentistry, 1999. 7(4): p. 113-9.
198. Ghazal, M., J. Hedderich, and M. Kern, *Wear of feldspathic ceramic, nano-filled composite resin and acrylic resin artificial teeth when opposed to different antagonists*. European Journal of Oral Science, 2008. 116(6): p. 585-92.
199. Lawn, B.R., S.M. Wiederhorn, and D.E. Roberts, *Effect of sliding friction forces on the strength of brittle materials*. Journal of Material Science 1984. 19: p. 2561-9.
200. Fisher, R.M., et al., *The effects of enamel wear on the metal-porcelain interface*. Journal of Prosthetic Dentistry 1983. 50: p. 627-31.
201. DeLong, R., et al., *The wear of dental porcelain in an artificial mouth*. Dental Materials, 1986. 2: p. 214-9.
202. Hacker, C.H., W.C. Wagner, and M.E. Razzoog, *An in vitro investigation of the wear of enamel on porcelain and gold in saliva*. Journal of Prosthet Dentistry 1996. 75: p. 14-7.
203. Krejci, I., F. Lutz, and M. Reimer, *Wear of CAD/CAM ceramic inlays: restorations, opposing cusps, and luting cements*. Quintessence International 1994. 25(3).
204. Mahalick, J.A., F.J. Knap, and E.J. Weiter, *Occlusal wear in prosthodontics*. Journal of the American Dental Association, 1971. 82: p. 154-9.
205. Monasky, G.E., *Studies on the wear of porcelain, enamel and gold*. Journal of Prosthetic Dentistry, 1971. 25(299-306).
206. White, S.N., *Mechanical fatigue of a feldspathic dental porcelain*. Dental Materials 1993. 9: p. 260-4.
207. Haywood, V.B., H.O. Heymann, and M.S. Scurria, *Effects of water, speed, and experimental instrumentation on finishing and polishing porcelain intra-orally*. Dental Materials, 1989. 5: p. 185-188.
208. Hedegård, B., *Need for correlation between laboratory testing and clinical research*. In: National Bureau of Standards Special Publication 354. Dental materials research proceedings of the 50th anniversary symposium, October 6-8, 1968. U.S. Department of Commerce; , 1972: p. 187-9.
209. Krejci, I., F. Lutz, and C. Zedler, *Effect of contact area size on enamel and composite wear*. Journal of Dental Research 1992. 71(7): p. 1413-6.

210. ISO, D.m., *Guidance on testing of wear. Part 2: Wear by two-and/or three body contact*. Techn Specific 2001. No. 14569-2.
211. al-Hiyasat, A.S., et al., *Investigation of human enamel wear against four dental ceramics and gold*. Journal of Dentistry, 1998b. 26(5-6): p. 487-95.
212. Elmaria, A., et al., *An evaluation of wear when enamel is opposed by various ceramic materials and gold*. Journal of Prosthetic Dentistry, 2006. 96(5): p. 345-53.
213. Esquivel-Upshaw, J.F., et al., *In vivo wear of enamel by a lithia disilicate-based core ceramic used for posterior fixed partial dentures: first-year results*. International Journal of Prosthodontics, 2006. 19(4): p. 391-6.
214. Etman, M.K., M. Woolford, and S. Dunne, *Quantitative measurement of tooth and ceramic wear: in vivo study*. International Journal of Prosthodontics, 2008. 21(3): p. 245-52.
215. Fisher, R.M., et al., *The effects of enamel wear on the metal-porcelain interface*. Journal of Prosthetic Dentistry, 1983. 50(5): p. 627-31.
216. Kadokawa, A., S. Suzuki, and T. Tanaka, *Wear evaluation of porcelain opposing gold, composite resin, and enamel*. Journal of Prosthetic Dentistry, 2006. 96(4): p. 258-65.
217. O'Kray, H.P. and W.J. O'Brien, *In vitro human enamel wear by a hydrated high-alkali porcelain*. Quintessence International, 2005. 36(8): p. 617-22.
218. Ramp, M.H., L.C. Ramp, and S. Suzuki, *Vertical height loss: an investigation of four restorative materials opposing enamel*. Journal of Prosthodontics, 1999. 8(4): p. 252-7.
219. Ramp, M.H., et al., *Evaluation of wear: enamel opposing three ceramic materials and a gold alloy*. Journal of Prosthetic Dentistry, 1997. 77(5): p. 523-30.
220. Alarcon, J.V., et al., *Wear testing of composite, gold, porcelain, and enamel opposing a removable cobalt-chromium partial denture alloy*. Journal of Prosthodontics, 2009. 18: p. 421-6.
221. Metzler, K.T., et al., *In vitro investigation of the wear of human enamel by dental porcelain*. Journal of Prosthetic Dentistry, 1999. 81(3): p. 356-64.
222. Palmer, D.S., et al., *Wear of human enamel against a commercial castable ceramic restorative material*. Journal of Prosthetic Dentistry, 1991. 65(2): p. 192-5.
223. Monasky, G.E. and D.F. Taylor, *Studies on the wear of porcelain, enamel, and gold*. Journal of Prosthetic Dentistry, 1971. 25(3): p. 299-306.
224. Clelland, N.L., et al., *Relative wear of enamel opposing low-fusing dental porcelain*. Journal of Prosthodontics, 2003. 12(3): p. 168-75.

225. Condon, J.R. and J.L. Ferracane, *Evaluation of composite wear with a new multi-mode oral wear simulator*. Dental Materials, 1996. 12(4): p. 218-26.
226. Grossman, D.G., *Structure and physical properties of Dicor/MGC glass-ceramic*. In: *Proceedings of the International Symposium on Computer Restorations*,. Mo'rmann WH, editor. Quintessence Publishing. Co., Chicago, 1991: p. 103-115.
227. DeLong, R.P., M.R. and W.H. Douglas, *The wear of enamel opposing shaded ceramic restorative materials. An in vitro study*. Journal of Prosthetic Dentistry., 1992. 68: p. 42-48.
228. Alarcon, J.V., et al., *Wear testing of composite, gold, porcelain, and enamel opposing a removable cobalt-chromium partial denture alloy*. Journal of Prosthodontics 2009. 18: p. 421-6.
229. Clelland, N.L., et al., *Relative wear of enamel opposing low-fusing dental porcelain*. Journal of Prosthodontics 2003. 12: p. 168-75.
230. Kadokawa, A., S. Suzuki, and T. Tanaka, *Wear evaluation of porcelain opposing gold, composite resin, and enamel*. Journal of Prosthetic Dentistry 2006. 96: p. 258-65.
231. Ramp, M.H., L.C. Ramp, and S. Suzuki, *Vertical height loss: an investigation of four restorative materials opposing enamel*. Journal of Prosthodontics 1999. 8: p. 252-7.
232. Clelland, N.L., et al., *Wear of enamel opposing low-fusing and conventional ceramic restorative materials*. Journal of Prosthodontics, 2001. 10(1): p. 8-15.
233. Ghazal, M., M. Steiner, and M. Kern, *Wear resistance of artificial denture teeth*. International Journal of Prosthodontics, 2008. 21: p. 166-8.
234. Magne, P., et al., *Wear of enamel and veneering ceramics after laboratory and chairside finishing procedures*. Journal of Prosthetic Dentistry 1999. 82: p. 669-79.
235. Willytec., *Multifunctional chewing simulator-Instructions of use* 2001: p. 1-39.
236. Heintze, S.D., G. Zappini, and V. Rousson, *Wear of 10 dental restorative materials in five wear simulators-Results of a round robin test*. Dental Materials 2005. 21: p. 304-17.
237. Ranjitkar, S., et al., *An in vitro assessment of the effect of load and pH on wear between opposing enamel and dentine surfaces*. Arch Oral Biol, 2008. 53(11): p. 1011-6.
238. Shabanian, M. and L.C. Richards, *In vitro wear rates of materials under different loads and varying pH*. Journal of Prosthetic Dentistry, 2002. 87(6): p. 650-

6.

239. O'Kray, H.P. and W.J. O'Brien, *In vitro human enamel wear by a hydrated high-alkali porcelain*. Quintessence International 2005. 36: p. 617-22.

240. Palmer, D.S., et al., *Wear of human enamel against a commercial castable ceramic restorative material*. Journal of Prosthetic Dentistry 1991. 65: p. 192-5.

241. Gibbs, C.H., et al., *Occlusal forces during chewing and swallowing as measured by sound transmission*. J Prosthet Dent 1981. 46: p. 443-9.

242. Lutz, F., I. Krejci, and F. Barbakow, *Chewing pressure vs. wear of composites and opposing enamel cusps*. Journal of Dental Research 1992. 71: p. 1525-9.

243. Elmaria, A., et al., *An evaluation of wear when enamel is opposed by various ceramic materials and gold*. Journal of Prosthetic Dentistry 2006. 96: p. 345-53.

244. Ramp, M.H., et al., *Evaluation of wear: Enamel opposing three ceramic materials and a gold alloy*. The Journal of Prosthetic Dentistry, 1997. 77: p. 523-30.

245. al-Hiyasat, A.S., et al., *The abrasive effect of glazed, unglazed, and polished porcelain on the wear of human enamel, and the influence of carbonated soft drinks on the rate of wear*. International Journal of Prosthodontics, 1997. 10: p. 269-82.

246. Al-Hiyasat, A.S., W.P. Saunders, and G.M. Smith, *Three-body wear associated with three ceramics and enamel*. Journal of Prosthetic Dentistry, 1999. 82: p. 476-48.

247. Metzler, K.T., et al., *In vitro investigation of the wear of human enamel by dental porcelain*. Journal of Prosthetic Dentistry 1999. 81: p. 356-64.

248. Richards, L.C., *Tooth wear and temporomandibular joint change in Australian Aboriginal populations*. American Journal Physical Anthropology, 1990. 82: p. 377-84.

249. Derand, P. and P. Vereby, *Wear of low-fusing dental porcelains*. Journal of Prosthetic Dentistry, 1999. 81(4): p. 460-3.

250. al-Hiyasat, A.S., W.P. Saunders, and G.M. Smith, *Three-body wear associated with three ceramics and enamel*. Journal of Prosthetic Dentistry, 1999. 82(4): p. 476-81.

251. Magne, P., et al., *Wear of enamel and veneering ceramics after laboratory and chairside finishing procedures*. Journal of Prosthetic Dentistry, 1999. 82(6): p. 669-79.

252. Hacker, C.H., W.C. Wagner, and M.E. Razzoog, *An in vitro investigation of the wear of enamel on porcelain and gold in saliva*. Journal of Prosthetic Dentistry, 1996. 75(1): p. 14-7.

253. Kaidonis, J.A., et al., *Wear of human enamel: a quantitative in vitro assessment*. Journal of Dental Research, 1998. 77(12): p. 1983-90.
254. al-Hiyasat, A.S., et al., *The effect of a carbonated beverage on the wear of human enamel and dental ceramics*. Journal of Prosthodontics, 1998a. 7(1): p. 2-12.
255. al-Hiyasat, A.S., et al., *The abrasive effect of glazed, unglazed, and polished porcelain on the wear of human enamel, and the influence of carbonated soft drinks on the rate of wear*. International Journal of Prosthodontics, 1997. 10(3): p. 269-82.
256. Jagger, D.C. and A. Harrison, *An in vitro investigation into the wear effects of selected restorative materials on enamel*. Journal of Oral Rehabilitation 1995. 22: p. 275-81.
257. de Silva, M.F.A., R.M. Davies, and B. Stewart, *Effect of whitening gels on the surface roughness of restorative materials in situ* Dental Materials, 2006. 22(10): p. 919-924.
258. Sarikaya, I. and A.U. Guler, *Effects of different polishing techniques on surface roughness on the surface roughness of dental porcelains*. Journal of Applied Science, 2010. 18(1): p. 10-16.
259. Etman, M.K., M. Woolford, and S. Dunne, *Quantitative measurement of tooth and ceramic wear: in vivo study* International Journal of Prosthodontics 2008. 21: p. 245-52.
260. Esquivel-Upshaw, J.F., et al., *In vivo wear of enamel by a lithia disilicate-based core ceramic used for posterior fixed partial dentures: first-year results*. International Journal of Prosthodontics 2006. 19: p. 391-6.
261. Derand, P. and P. Vereby, *Wear of low-fusing dental porcelains*. The Journal of Prosthetic Dentistry. , 1999. 81(4): p. 460-463.
262. Fischer, T.E., M.P. Anderson, and S. Jahanmir, *Influence of fracture toughness on the wear resistance of yttria-doped zirconium oxide*. Journal of the American Ceramic Society 1989. 72: p. 252-7.
263. Seghi, R.R., S.F. Rosenstiel, and P. Bauer, *Abrasion of human enamel by different dental ceramics in vitro*. Journal of Dental Research, 1991. 70(3): p. 221-5.
264. Martinez-Gomis, J., et al., *Comparative evaluation of four finishing systems on one ceramic surface*. International Journal of Prosthodontics, 2003. 16: p. 74-77.
265. Al-Wahadni, A.M. and D.M. Martin, *An in vitro investigation into the wear effects of glazed, unglazed and refinished dental porcelain on an opposing material*. . Journal of Oral Rehabilitation 1999. 26: p. 538-546.
266. Monasky, G.E. and D.F. Taylor, *Studies on the wear of porcelain, enamel, and gold*. The Journal of Prosthetic Dentistry, 1971. 25(3): p. 299-306.

267. Oh, W.-s., R. DeLong, and K.J. Anusavice, *Factors affecting enamel and ceramic wear: A literature review*. The Journal of Prosthetic Dentistry, 2002. 87(4): p. 451-459.
268. Suputtamongkol, K., et al., *Surface roughness resulting from wear of lithia-disilicate-based posterior crowns*. Wear.
269. Metzler, K.T., et al., *In vitro investigation of the wear of human enamel by dental porcelain*. The Journal of Prosthetic Dentistry, 1999. 81(3): p. 356-364.
270. DeLong, R., et al., *The wear of enamel when opposed by ceramic systems*. Dental Materials, 1989. 5(4): p. 266-271.
271. Hulterström, A.K. and M. Bergman, *Polishing systems for dental ceramics*. Acta Odontol Scand 1993. 51: p. 229-234.
272. Saraç, D., et al., *Comparison of 3 Polishing Techniques for 2 All-Ceramic Materials*. International Journal of Prosthodontics, 2007. 20: p. 465-468.
273. DeLong, R., et al., *The wear of dental porcelain in an artificial mouth*. Dental Materials, 1986. 2(5): p. 214-219.
274. Cook, P.A., W.H. Griswold, and A.C. Post, *The effect of superficial colorant and glaze on the surface texture of vacuum fired porcelain*. Journal of Prosthetic Dentistry. , 1984. 51(4): p. 476-484.
275. Ma, T., G.H. Johnson, and G.E. Gordon, *Effects of chemical disinfectants on surface characteristics and color of three fixed prosthodontic crown materials*. . Journal of Prosthetic Dentistry. , 1999. 82(5): p. 600-607.
276. Rosenblum, M.A. and A. Schulman, *A review of all-ceramic restorations*. Journal of the American Dental Association, 1997. 128(3): p. 297-307.
277. Wright, M.D., R. Masri, and C.F. Driscoll, *Comparison of three systems for the polishing of an ultra-low fusing dental porcelain*. Journal of Prosthetic Dentistry, 2004. 92(5): p. 486-49.
278. Clayton, J.A. and E. Green, *Roughness of pontic materials and dental plaque*. Journal of Prosthetic Dentistry, 1970. 23(4): p. 407-411.
279. Kawai, K., M. Urano, and S. Ebisu, *Effect of surface roughness of porcelain on adhesion of bacteria and their synthesizing glucans*. Journal of Prosthetic Dentistry, 2000. 83(6): p. 664-667.
280. Martinez-Gomis, J., J. Bizar, and J.M. Anglada, *Comparative evaluation of four finishing systems on one ceramic surface*. International Journal of Prosthodontics., 2003. 16(1): p. 74-77.
281. Bollen, C.M.L., P. Lambrechts, and M. Quirynen, *Comparison of surface roughness of oral hard materials to the threshold surface roughness for bacterial*

- plaque retention: a review of the literature.* Dental Materials, 1997. 13(4): p. 258-269.
282. Kramer, N., et al., *Antagonist enamel wears more than ceramic inlays.* Journal of Dental Research, 2006. 85(12): p. 1097-100.
283. Lambrechts, P., et al., *Quantitative in vivo wear of human enamel.* Journal of Dental Research, 1989. 68(12): p. 1752-4.
284. Grossman, D., *Structure and physical properties of DICO/MGC glass-ceramic.* In: Mörmann WH, editor. *International symposium on computer restorations.* Chicago: Quintessence Publ. Co, 1991. DICOR MGC report. York, PA: Caulk/Dentsply; : p. 103-15
285. Ghazal, M., M. Steiner, and M. Kern, *Wear resistance of artificial denture teeth.* International Journal of Prosthodontics, 2008. 21(2): p. 166-8.
286. Malkin, S., *Theory and applications of machining with abrasives. Grinding Technology.* Chichester, England. Ellis Horwood Limited 1989: p. 107-245.
287. Eliades, G.C., J.G. Tzoutzas, and G.J. Vougiouklakis, *Surface alterations on dental restorative materials subjected to an air-powder abrasive instrument.* Journal of Prosthetic Dentistry, 1991. 65(1): p. 27-33.
288. Alkhiary, Y.M., S.M. Morgano, and R.A. Giordano, *Effects of acid hydrolysis and mechanical polishing on surface residual stresses of low-fusing dental ceramics.* Journal of Prosthetic Dentistry., 2003. 90(2): p. 133-142.
289. *THE GLOSSARY OF PROSTHODONTIC TERMS.* journal of Prosthetic Dentistry, 2005. 94(1): p. 15.
290. Ahmad, R., B. Wu, and S.M. Morgano, *Polishing mechanisms and its effects on the mechanical properties of ceramic restorations- A review of the literature. .* Annal Dent Univ Malaya, 2001. 8: p. 57-61.
291. Kalpakjian, S., *Manufacturing Engineering and Technology. Third Edition.* Reading, Mass. Addison-Wesley Publishing Company Inc. , 1995(781-824).
292. McLean, J.W., *The science and art of dental ceramics. A collection of monographs. .* Louisiana State University. School of Dentistry, Continuing Education Programme, 1974.
293. Craig, R.G. and J.M. Powers, *Restorative Dental Materials.* 11th ed. St. Louis, MO: Mosby Company, 2002.
294. Wiley, M.G., *Effects of porcelain on occluding surfaces of restored teeth. .* Journal of Prosthetic Dentistry t, 1989. 61(2): p. 133-137.
295. Sarac, D. and S. Sarac, *The effects of porcelain systems on the color and surface texture of feldspathic porcelain.* Journal of Prosthetic Dentistry, 2006.

96(20): p. 122-128.

296. Saraç, D., et al., *Comparison of 3 Polishing Techniques for 2 All-Ceramic Materials*. International Journal of Prosthodontics, 2007. 20: p. 465-468.

297. Tamura, K., *Essentials of Dental Technology*. Chicago: Quintessence Publishing Co., 1987: p. 390-392.

298. Klausner, L.H., C.B. Cartwright, and C.T. Charbeneau, *Polished versus autogiazed porcelain surfaces*. Journal of Prosthetic Dentistry, 1982. 47(): p. 157-162.

299. Sasahara, R.M.C., et al., *Influence of the finishing technique on surface roughness of dental porcelains with different microstructures*. Operative Dentistry, 2006. 31: p. 557-583.

300. Stoll, R., et al., *The use of polishing systems on the surface of different ceramic materials*. In: Mormann WH (ed). *CAD/CAM in Aesthetic Dentistry - CEREC 10 year anniversary symposium*. Quintessence. 1996. 589-97.

301. Glavina, D., et al., *Surface quality of Cerec CAD/CAM ceramic veneers treated with four different polishing systems*. European Journal of Peadiatric Dentistry, 2004. 30: p. 31-34.

302. Jagger, D.C. and A. Harrison, *An in vitro investigation into the wear effects of unglazed, glazed, and polished porcelain on human enamel*. Journal of Prosthetic Dentistry, 1994. 72: p. 320-326.

303. Naylor, W.P., *Introduction to metal ceramic technology*. Chicago: Quintessence, 2010: p. 157-161.

304. Zalkind, M., S. Lauer, and N. Stern, *Porcelain surface texture after reduction and natural glazing*. Journal of Prosthetic Dentistry, 1986. 55: p. 30-33.

305. Jacobi, R., H.T. Shillingburg, and M.G. Duncanson, *A comparison of the abrasiveness of six ceramic surfaces and gold*. Journal of Prosthetic Dentistry, 1991. 66: p. 303-9.

306. Barghi, N., C.J. King, and R.A. Draughn, *A study of porcelain surfaces as utilised in fixed prosthodontics*. Journal of Prosthetic Dentistry, 1975. 34: p. 314-9.

307. Magne, P., et al., *Wear of enamel and veneering ceramics after laboratory and chairside finishing procedures*. Journal of Prosthetic Dentistry, 1999. 82.

308. Brewer, J.D., et al., *Clinical discrimination between autoglazed and polished porcelain surfaces*. Journal of Prosthetic Dentistry, 1990. 64: p. 631-4.

309. Zalkind, M., S. Lauer, and N. Stern, *Porcelain surface texture after reduction and natural glazing*. Journal of Prosthetic Dentistry, 1986. 55: p. 30-3.

310. Fuzzi, M., Z. Zaccheroni, and G. Vallania, *Scanning electron microscopy and profilometer evaluation of glazed and polished dental porcelain*. International Journal of Prosthodontics 1996. 9: p. 452-458.
311. Rosenstiel, S.F., M.A. Balker, and W.M. Johnston, *A comparison of glazed and polished dental porcelain*. International Journal of Prosthodontics 1989. 2: p. 524-52.
312. Metzler, K.T., et al., *In vitro investigation of the wear of human enamel by dental porcelain*. Journal of Prosthetic Dentistry 1999(81): p. 356-36.
313. Patterson, C.J., et al., *Efficacy of a porcelain refinishing system in restoring surface finish after grinding with fine and extra-fine diamond burs*. Journal of Prosthetic Dentistry, 1992. 68: p. 402-406.
314. Sulik, W.D. and E. Plekavich, *Surface finishing of dental porcelain*. Journal of prosthetic dentistry 1981. 46: p. 217-221.
315. Patterson, C.J.W., et al., *Efficacy of a porcelain refinishing system in restoring surface finish after grinding with fine and extra-fine diamond burs*. . Journal of Prosthetic Dentistry, 1992. 68: p. 402-406.
316. Goldstein, G.R., B.R. Barnhard, and B. Penugonda, *Profilometer, SEM, and visual assessment of porcelain polishing methods*. Journal of Prosthetic Dentistry, 1991. 65: p. 627-34.
317. Haywood, V.B., H.O. Heymann, and M.S. Scurria, *Effects of water, speed and experimental instrumentation on finishing and polishing porcelain intra-orally*. Dental Materials, 1989. 5: p. 185-8.
318. Klausner LH, C.C., Charbeneau CT., *Polished versus autogiazed porcelain surfaces*. Journal of Prosthetic Dentistry, 1982. 47: p. 157-162.
319. Patterson, C.J.W., et al., *Refinishing of porcelain by using a refinishing kit*. Journal of Prosthetic Dentistry, 1991. 65: p. 383-8.
320. Wright, M.D., et al., *Comparison of three systems for the polishing of an ultra-low fusing dental porcelain*. Journal of Prosthetic Dentistry, 2004. 92: p. 486-90.
321. Al-Hiyasat, A.S., W.P. Saunders, and G.M. Smith, *Three-body wear associated with three ceramics and enamel*. Journal of Prosthetic Dentistry 1999. 82: p. 476-48.
322. Scurria, M.S. and M. Powers, *Surface roughness of two polished ceramic materials*. Journal of Prosthetic Dentistry 1994. 71: p. 174-177.
323. Haywood, V.B., et al., *Polishing porcelain veneers: an SEM and specular reflectance analysis*. Dental Materials, 1988. 4: p. 116-121.

324. Glavina, D., et al., *Surface quality of Cerec CAD/CAM ceramic veneers treated with four different polishing systems*. European Journal of Paediatric dentistry, 2004. 30: p. 31-34.
325. Stoll, R., et al., *The use of polishing systems on the surface of different ceramic materials*. In: Mormann WH (ed). *CAD/CAM in Aesthetic Dentistry - CEREC 10 year anniversary symposium*. Quintessence 1996: p. 589-97.
326. Karapetian, V.S., V. Jockel, and M.A. Baumann, *Comparison of different polishing systems for dental inlay ceramics*. In: Mormann WH (ed). *CAD/CAM in Aesthetic Dentistry - CEREC 10 year anniversary symposium*. Quintessence., 1996: p. 553-9. .
327. Mormann, W.H. and A. Bindl, *All-ceramic, chair-side computer-aided design/computer-aided machining restorations*. Dent Clin North Am, 2002. 46(2): p. 405-26.
328. Jung, M., O. Wehlen, and J. Klimek, *Finishing and polishing of indirect composite and ceramic inlays in vivo: Occlusal surfaces*. Operative Dentistry, 2004. 29(2): p. 131-141.
329. Elmaria, A., et al., *An evaluation of wear when enamel is opposed by various ceramic materials and gold*. Journal of Prosthetic Dentistry, 2006. 96: p. 345-5.
330. Flury, S., A. Lussie, and B. Zimmerli, *Performance of Different polishing techniques for Direct CAD/CAM ceramic restorations*. Operative Dentistry, 2010. 35(4): p. 470-481.
331. Flury, S., A. Lussie, and B. Zimmerli, *Performance of Different polishing techniques for Direct CAD/CAM ceramic restorations*. Operative Dentistry, 2010. 35(4): p. 470-481.
332. Olivera, E.A., M. E., and M.M. Marques, *The Effect of Glazed and Polished Ceramics on Human Enamel Wear*. International Journal of Prosthodontics, 2006. 19: p. 547-548.
333. Jacobi, R., H.T. Shillingburg, and M.G. Duncanson, *A comparison of the abrasiveness of six ceramic surfaces and gold*. Journal of Prosthetic Dentistry, 1991. 66(303-30).
334. Yilmaz, K. and P. Ozkan, *Profilometer evaluation of the effect of various polishing methods on the surface roughness in dental ceramics of different structures subjected to repeated firings*. Quintessence International., 2010. 41: p. 125-131.
335. Ward, M.T., W.H. Tate, and J.M. Powers, *Surface roughness of opalescent porcelains after polishing*. Operative Dentistry 1995. 20: p. 106-11.
336. Hultstrom, A.K. and M. Bergma, *Polishing systems for dental ceramics*. . Acta Odontol Scand 1993. 51: p. 229-234.

337. Sulik, W.D. and E. Plekavich, *Surface finishing of dental porcelain*. Journal of Prosthetic Dentistry 1981. 46: p. 217-221.
338. Hulterstrom, A.K. and M. Bergma, *Polishing systems for dental ceramics*. Acta Odontol Scand 1993. 51: p. 229-234.
339. Tholt, B., et al., *Surface roughness in Ceramics with Different finishing techniques using atomic force microscope and profilometer*. Operative Dentistry, 2006. 31(4): p. 422-449.
340. Wang, F. and J. Chen, *Surface Roughness of a Novel Dental Porcelain Following Different Polishing Procedures*. International Journal of Prosthodontics, 2009. Mar-Apr(22(2)): p. 178-80.
341. Levy, H., *Effects of laboratory finishing techniques on the mechanical properties of dental ceramics*. International Dental Journal 1987. 69: p. 1039-1045.
342. Brackett, S., et al., *An evaluation of porcelain strength and the effect of surface treatment*. Journal of Prosthetic Dentistry 1989. 61: p. 446-451.
343. Fairhurst, C.W., et al., *The effect of glaze on porcelain strength*. Dental Materials, 1992. 8: p. 203-207.
344. Griggs, I.A., I.Y. Thompson, and K.I. Anusavice, *Effects of flaw size and auto-glaze treatment on porcelain strength*. Journal of Dental Research 1996. 75: p. 1414-1417.
345. Chen, X., et al., *Crystallization and flexural strength optimization of fine-grained leucite glass-ceramics for dentistry*. Dental Materials 2011 27(11): p. 1153-61.
346. Chu, F.C., N. Frankel, and R.J. Smales, *Surface roughness and flexural strength of self glazed, polished and reglazed Inceram/Vitadur Alpha porcelain laminates*. International Journal of Prosthodontics. 2000. 13(1): p. 66-71.
347. Patterson, C.J.W., et al., *Refinishing of porcelain by using a refinishing kit*. Journal of Prosthetic Dentistry, 1991. 65: p. 383-8.
348. Zalkind, M.M., et al., *Accumulation of Streptococcus mutans on light-cured composites and amalgam: an in vitro study*. Journal of Esthetic Dentistry 1998. 10: p. 187-190.
349. Sakaguchi, R.L., et al., *The wear of Posterior composites in an artificial mouth: a Clinical Correlation*. Dental Materials, 1986. 2: p. 235-240.
350. Delong, R., et al., *The wear of dental amalgam in an artificial mouth. A clinical correlation*. Dental Materials, 1985. 1: p. 238.
351. Liu, P., et al., *A System for the Acquisition and Analysis of Three-Dimensional Data Describing Dental Morphology*. Dental Anthropology, 2004. 17:

p. 70-74.

352. Liu, P.R.S., et al., *A system for the acquisition and analysis of three-dimensional data describing dental morphology*. Dental Anthropology 2004. 17: p. 70-4.
353. Morrow, R.M., et al., *Evaluation of methods for denture teeth*. Journal of Prosthetic Dentistry, 1973. 30: p. 222.
354. Barghi, W. and C.J. King, *Porcelain surfaces utilized in fixed prosthodontics* Journal of Prosthetic Dentistry, 1975. 34: p. 314.
355. Jacobi, R., H.T. Shillingburg, and M.G. Duncanson, *A comparison of the abrasiveness of six ceramic surfaces and gold*. Journal of Prosthetic Dentistry., 1991. 66: p. 303-9.
356. Eichhold, W.A. and D.T. Brown, *Wear rates of various artificial tooth materials: a literature review*. Compendium Continuing Educational Dentistry 1996. 17: p. 1074-8.
357. de Gee, A. and P. Pallav, *Occlusal wear simulation with the ACTA wear machine*. Journal of Dentistry 1994. 22: p. 521-527.
358. Profitt, W.R., *Intra-oral pressures in a young and adult group*. Journal of Dental Research, 1966. 43: p. 555.
359. Picton, D.C., R.B. Johns, and D.J. Wills, *Oral Sci Rev*. 5, 1971: p. 3-21.
360. Graf, H., *Occlusal forces during function*. In: *Occlusion: research on form and function*. University of Michigan 1975. Ann Arbor: p. 90.
361. Ratledge, D.K., B.G.N. Smith, and R.F. Wilson, *The effect of restorative materials on the wear of human enamel*. Journal of Prosthetic Dentistry, 1994. 72: p. 194-203.
362. Korber, K.H., K. Ludwig, and P. Dunner, *Experimental studies of the abrasion effect between dental enamel and dental ceramic*. [in German]. Dtsch Zahnärztl Z 1984. 39: p. 2-11.
363. Klausner, L.H., C.B. Cartwright, and G.T. Charbeneau, *Polished versus autoglazed porcelain surfaces*. Journal of Prosthetic Dentistry, 1982. 47(2): p. 157-167.
364. Jagger, D.C. and A. Harrison, *An in vitro investigation into the wear effects of unglazed, glazed, and polished porcelain on human enamel*. Journal of Prosthetic Dentistry 1994. 72: p. 320-3.
365. Oilo, G., *Flexural strength and internal defects of some dental porcelains*. Acta Odontol Scand., 1988. 46(313-22).

SECTION FIVE

CHAPTER 15

APPENDICES

APPENDIX 1

STUDY A

Leucite-Reinforced Ceramics

Surface texture altitude parameter analysis

After completion of Surface finishing protocols

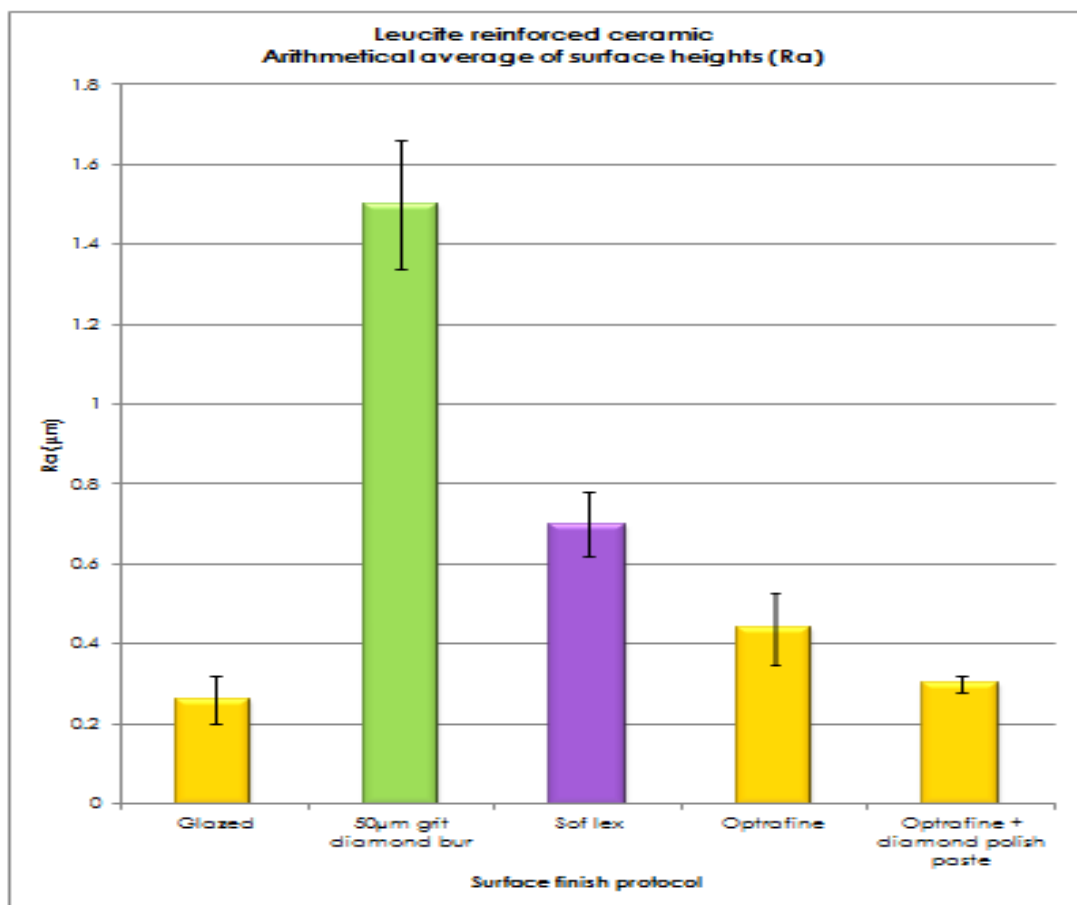


Figure A1.1: Arithmetical average of surface heights (Ra) data values for leucite-reinforced ceramic after the various surface finishing protocols.

According to the Tukey analysis, specimens abraded with 50 μm grit diamond bur had the highest surface roughness measurement ($1.50 \mu\text{m} \pm 0.16$). Specimens finished with a 25 μm grit diamond bur and specimens finished with Sof-Lex polishing discs had statistically similar surface texture results ($0.72 \mu\text{m} \pm 0.13$) and ($0.70 \mu\text{m} \pm 0.08$) respectively. Ceramic specimens finished with Optrafine polishing system had the third highest Ra values ($0.44 \mu\text{m} \pm 0.09$) which were statistically significant from the other finishing protocols. Specimens finished with Optrafine polishing system and diamond polishing paste and ceramic specimens finished with an overglaze presented with the lowest surface roughness measurements ($0.30 \mu\text{m} \pm 0.02$) and ($0.22 \mu\text{m} \pm 0.060$) respectively. Statistical differences between the groups finished by difference clinical procedures was measured at $p=0.05$. Ceramic groups with statistically similar surface texture finishing protocols are shown in the same colour.

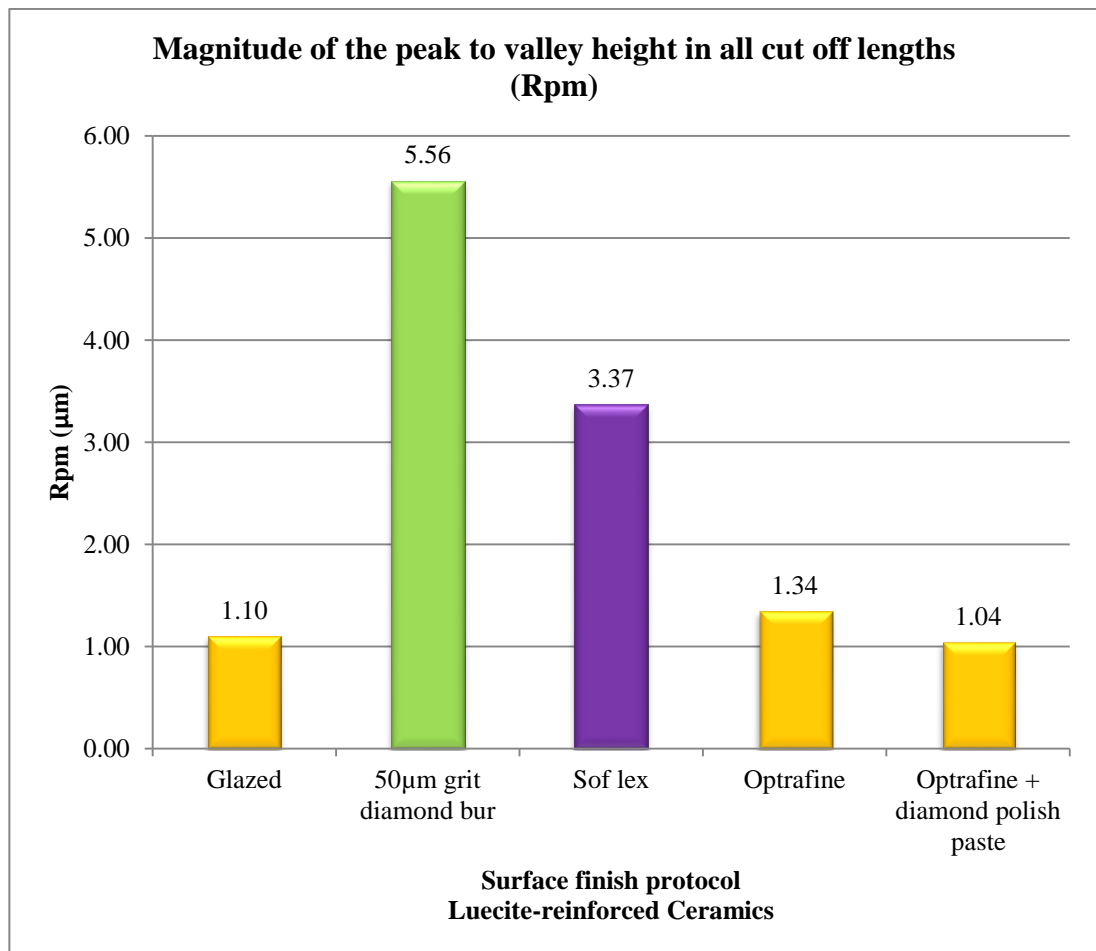


Figure A1.2: Magnitude of the peak to valley height in all cut off lengths (Rpm) for leucite-reinforced ceramic after the various surface finishing protocols.

According to the Tukey analysis ceramic specimens abraded with a 50 μm grit diamond bur had the highest Rpm value ($5.62 \mu\text{m} \pm 0.86$). Ceramics polished with Sof-Lex discs ($3.32 \mu\text{m} \pm 1.18$) had the second highest Rpm value. Ceramics finished either by Optrafine polishing system ($1.34 \mu\text{m} \pm 0.47$), or with diamond polish paste ($1.10 \mu\text{m} \pm 0.43$) or glazed ($1.04 \mu\text{m} \pm 0.29$) had the lowest Rpm values which were not statistically significant from each other at $p=0.05$. Ceramic groups with statistically similar surface texture finishing protocols are shown in the same colour.

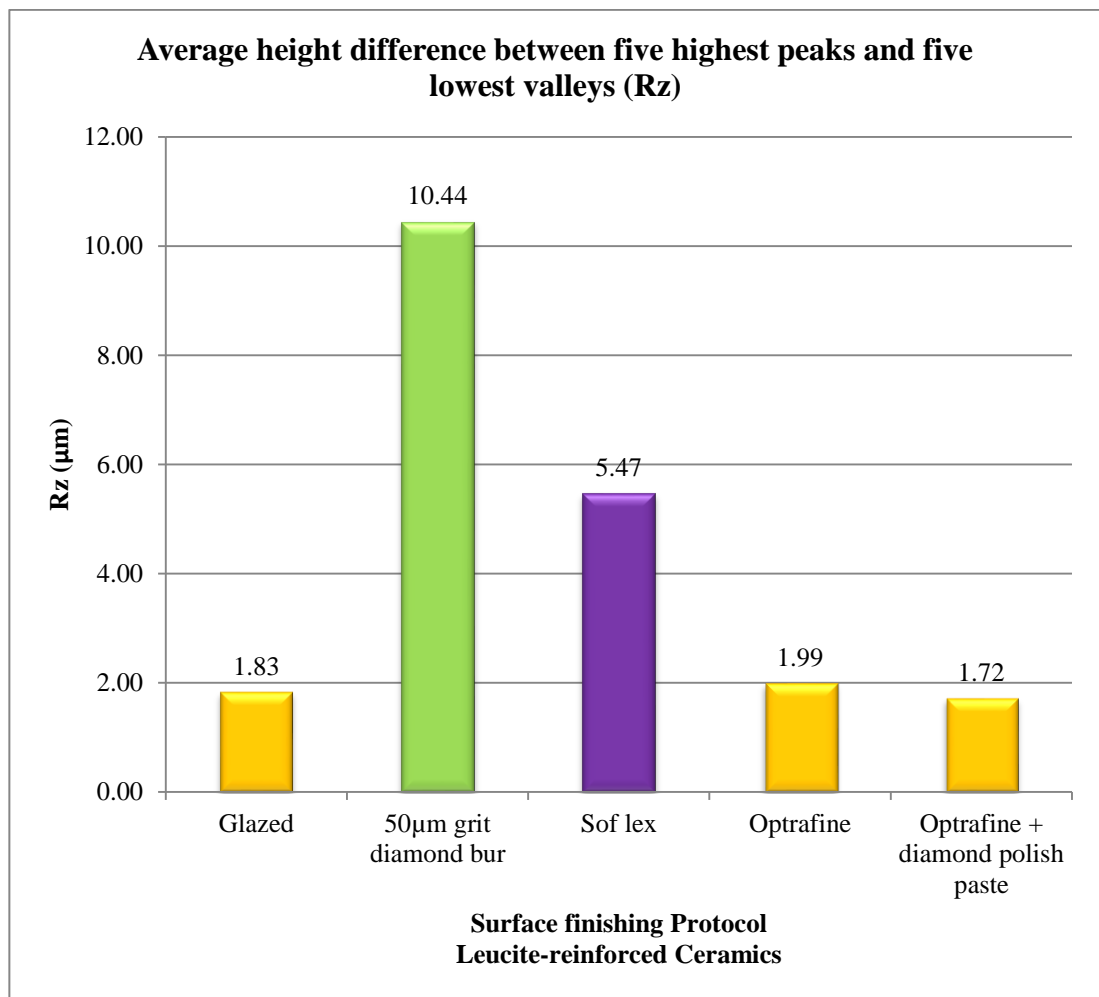


Figure A1.3: Average height difference between five highest peaks and five lowest valleys (Rz) for leucite-reinforced ceramic after the various surface finishing protocols.

According to the Tukey analysis ceramics abraded with a 50 μm grit diamond bur had the highest Rz values ($10.4 \mu\text{m} \pm 2.3$). Ceramics finished with Sof-Lex discs had Rz values of $5.47 \mu\text{m} \pm 1.381$. Ceramics finished with Optrafine polishing system

($1.9 \mu\text{m} \pm 0.16$), diamond polish paste ($1.71 \mu\text{m} \pm 0.43$) or glazed ($1.80 \mu\text{m} \pm 0.27$) had the lowest Rz values. There were no statistical differences specimens finished with a glaze or Optrafine polishing kit with or without diamond polish paste. Ceramic groups with statistically similar surface texture finishing protocols are shown in the same colour.

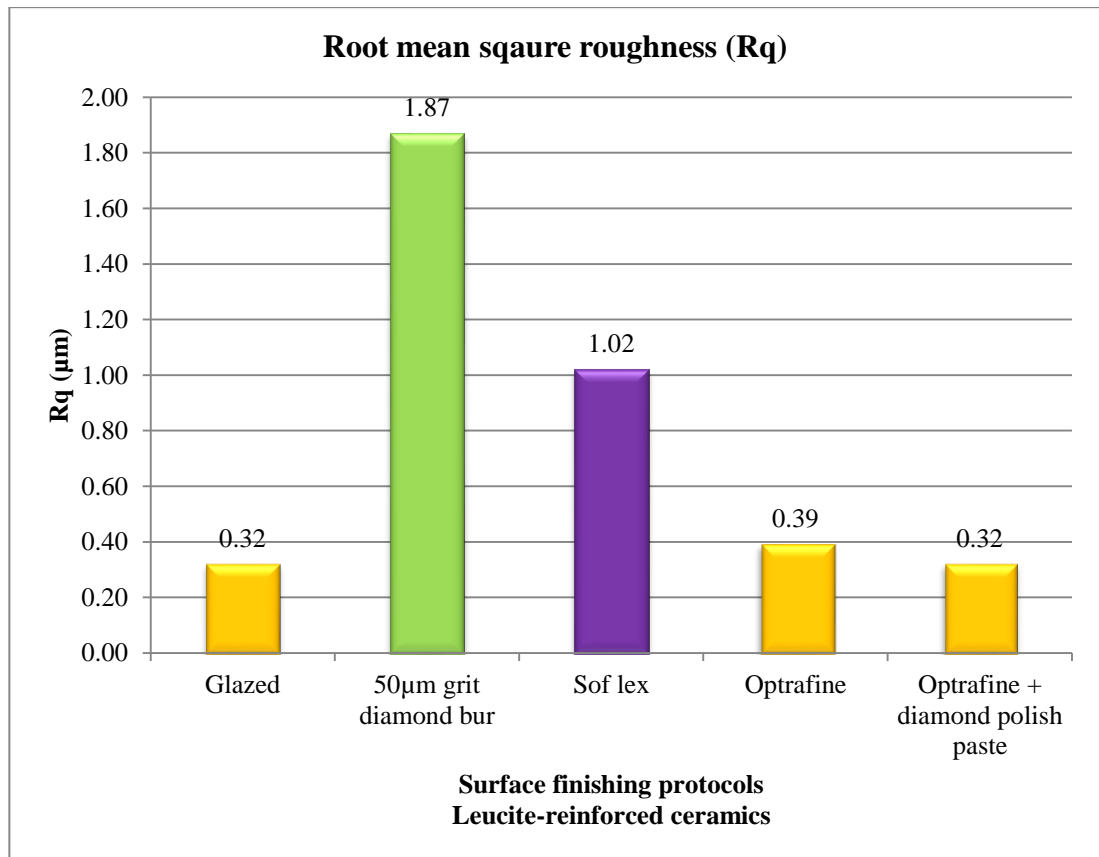


Figure A1.4: Root mean square roughness (Rq) for leucite-reinforced ceramic after the various surface finishing protocols.

According to the Tukey analysis Ceramics abraded with a $50 \mu\text{m}$ grit diamond bur had the highest Rq value ($1.86 \mu\text{m} \pm 0.27$). Ceramics finished by Sof-Lex discs had an average Rz value of $0.97 \mu\text{m} \pm 0.20$. The lowest Rq values were achieved by ceramics that were surface finished by Optrafine polishing system ($0.39 \pm 0.04 \mu\text{m}$), diamond polish paste ($0.31 \mu\text{m} \pm 0.83$) or by glazing the surface ($0.32 \mu\text{m} \pm 0.58$). The Rq values of glazed and Optrafine polished ceramics are not statically significant from one another at $p=0.05$. Ceramic groups with statistically similar surface texture finishing protocols are shown in the same colour.

APPENDIX 2

STUDY A

Lithium Disilicate Ceramics

Surface texture altitude parameter analysis

After completion of Surface finishing protocols

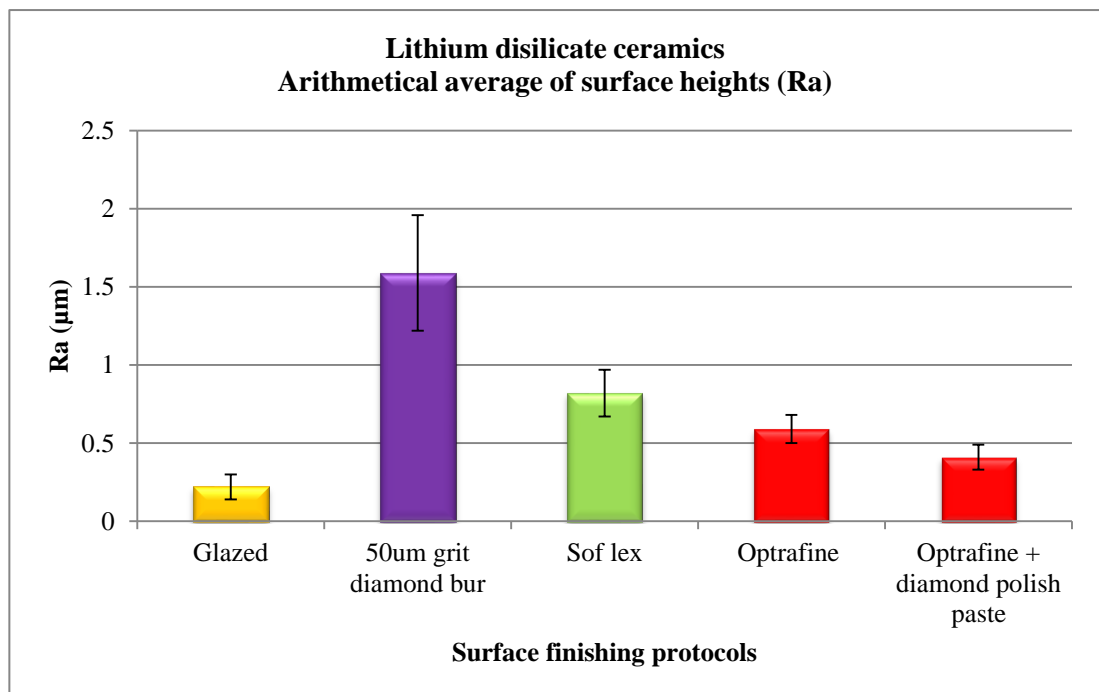


Figure A2.1: Arithmetical average of surface heights (Ra) for lithium disilicate ceramic after the various surface finishing protocols.

According to the Tukey analysis, specimens abraded with a 50 µm grit diamond bur after crystallisation had the highest Ra values compared to all other finishing protocols (1.59 µm ± 0.37). Specimens abraded with 50µm grit diamond bur then polished with Sof-Lex polishing discs had the second highest Ra values (0.82 µm ± 0.15). Specimens finished with 50µm grit then 25µm grit diamond burs (0.64 µm ± 0.01), specimens finished with Optrafine polishing system (0.59 ± 0.09) and

ceramic specimens finished with Optrafine polishing system and diamond polishing paste (0.40 ± 0.42) produced statistically similar surface texture altitude parameter results. Surface texture of specimens finished with Optrafine polishing and diamond polish paste was not influenced by whether it was completed either before or after the crystallisation of the ceramic. The crystallisation step did however reduce the surface texture altitude parameters of specimens abraded with 50 μm grit diamond burs. The surface texture of glazed lithium disilicate ceramic was ($0.21 \mu\text{m} \pm 0.58$). This was the lowest value recorded and statistically significant compared to other ceramic groups at $p=0.05$. Ceramic groups with statistically similar surface texture finishing protocols are shown in the same colour.

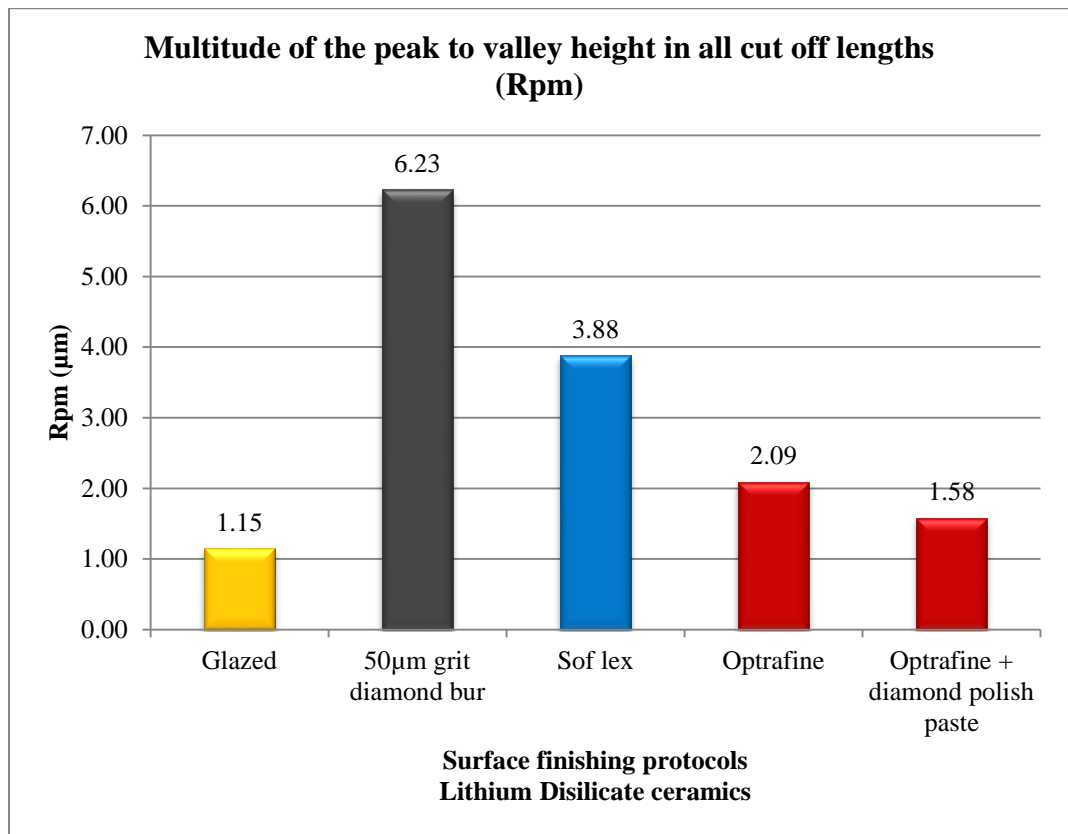


Figure A2.2: Multitude of the peak to valley height in all cut off lengths (Rpm) for lithium disilicate ceramic after the various surface finishing protocols

According to the Tukey analysis specimens abraded with 50 μm grit diamond had the highest Rpm values ($6.23 \mu\text{m} \pm 0.81$) had the highest Rpm values. Sof-Lex specimens had Rpm values of $3.88 \mu\text{m} \pm 0.09$. Ceramics finished with Optrafine polishing system ($2.09 \mu\text{m} \pm 0.12$) with diamond polish paste ($1.58 \mu\text{m} \pm 0.07$) or

glazed ($1.15 \mu\text{m} \pm 0.57$) had the lowest statistically similar Rpm values when tested at $p=0.05$. Ceramic groups with statistically similar surface texture finishing protocols are shown in the same colour.

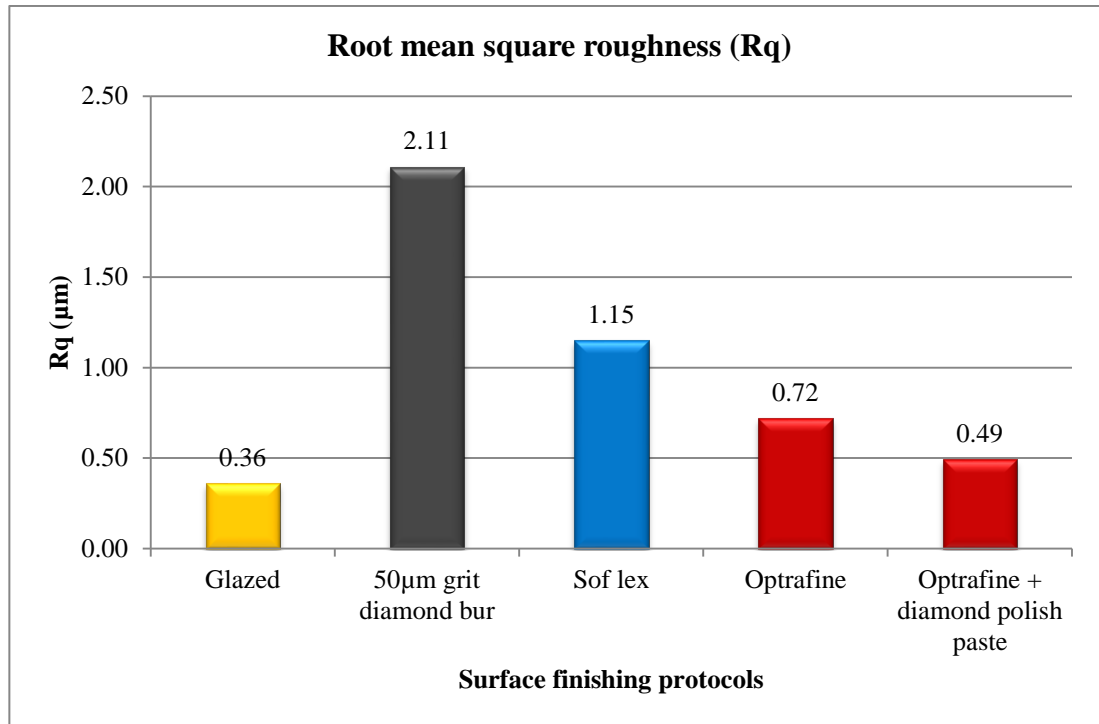


Figure A2.3: Root mean square roughness (Rq) for lithium disilicate ceramic after the various surface finishing protocols.

According to the Tukey analysis, ceramic specimens abraded with a 50 µm grit diamond bur had the highest Rq values ($2.18 \mu\text{m} \pm 0.81$). Sof-Lex discs had an Rq value of $1.15 \mu\text{m} \pm 0.09$. This was statistically higher than ceramics finished with Optrafine polishing system or glazing. Optrafine finished ceramics resulted in Rq values of $0.72 \mu\text{m} \pm 0.11$, Optrafine polishing followed by diamond polishing paste produced Rq values of $0.49 \mu\text{m} \pm 0.12$ and glazed ceramic specimens produced Rq values of $0.36 \mu\text{m} \pm 0.07$. The Rq values of the three lowest groups were not statistically significant to one another at $p=0.05$. Ceramic groups with statistically similar surface texture finishing protocols are shown in the same colour.

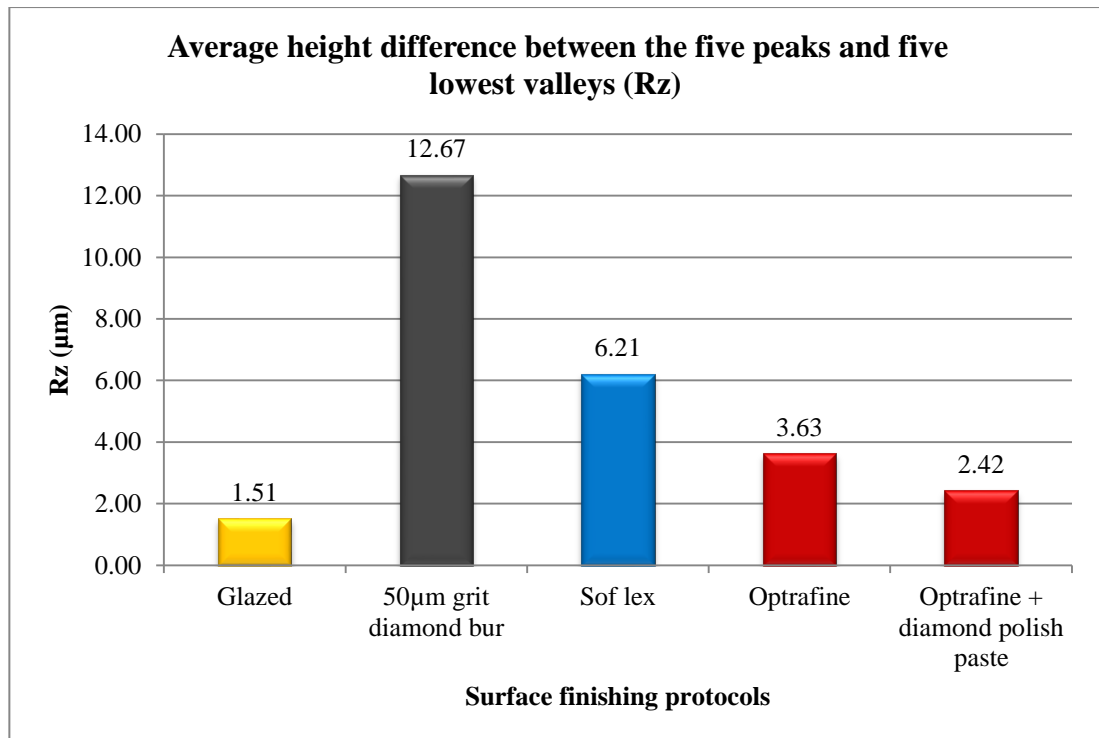


Figure A2.4: Average height difference between the five peaks and five lowest valleys (Rz) for lithium disilicate ceramic after the various surface finishing protocols.

According to the Tukey analysis, ceramic specimens abraded with a 50 µm grit diamond bur had the highest Rq values ($12.67 \mu\text{m} \pm 6.07$). Sof-Lex discs had an Rq value of $6.21 \mu\text{m} \pm 1.12$. This was statistically higher than ceramics finished with Optrafine polishing system or glazing. Optrafine finished ceramics resulted in Rq values of $3.63 \mu\text{m} \pm 0.69$, Optrafine polishing followed by diamond polishing paste produced Rq values of $2.42 \mu\text{m} \pm 0.68$ and glazed ceramic specimens produced Rz values of $1.51 \mu\text{m} \pm 0.39$. The Rq values of the three lowest groups were not statistically significant to one another at $p=0.05$.

APPENDIX 3

STUDY B

Leucite-reinforced Ceramics

Surface texture altitude parameter analysis

Post wear simulation

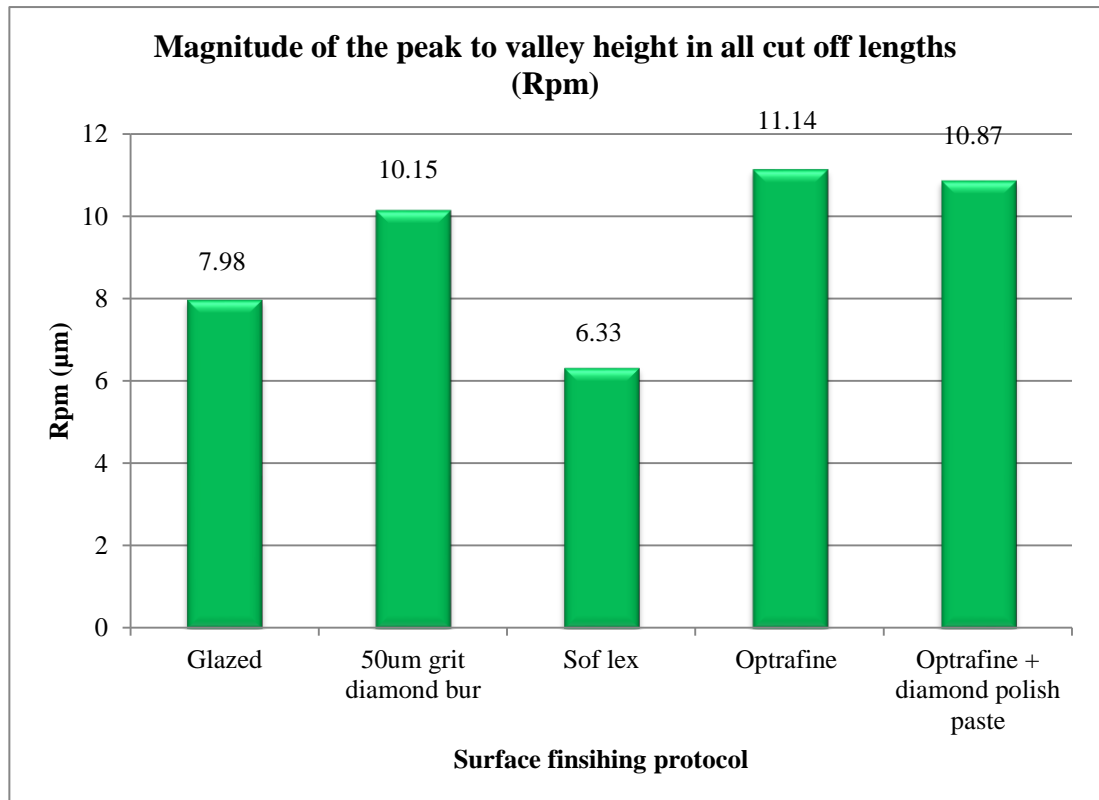


Figure A3.1: Magnitude of the peak to valley height in all cut off lengths (Rpm) for the different leucite-reinforced ceramic specimen groups according to the surface finishing protocols, after subjected to 600000 wear cycles in the chewing simulator against enamel specimens.

According to the Tukey analysis there are no statistically differences at $p= 0.05$ between any of the group Rpm values after the ceramic specimens were subjected to 600000 cycles in the chewing simulator against natural human enamel. The Rpm values for glazed ceramics was $7.98 \mu\text{m} \pm 1.89$, 50 μm grit diamond bur $10.15 \mu\text{m}$

± 2.12 , Sof-Lex 6.33 ± 1.82 , Optrafine polishing system 11.14 ± 2.24 and Optrafine polishing system with diamond polishing paste was 10.87 ± 1.86 .

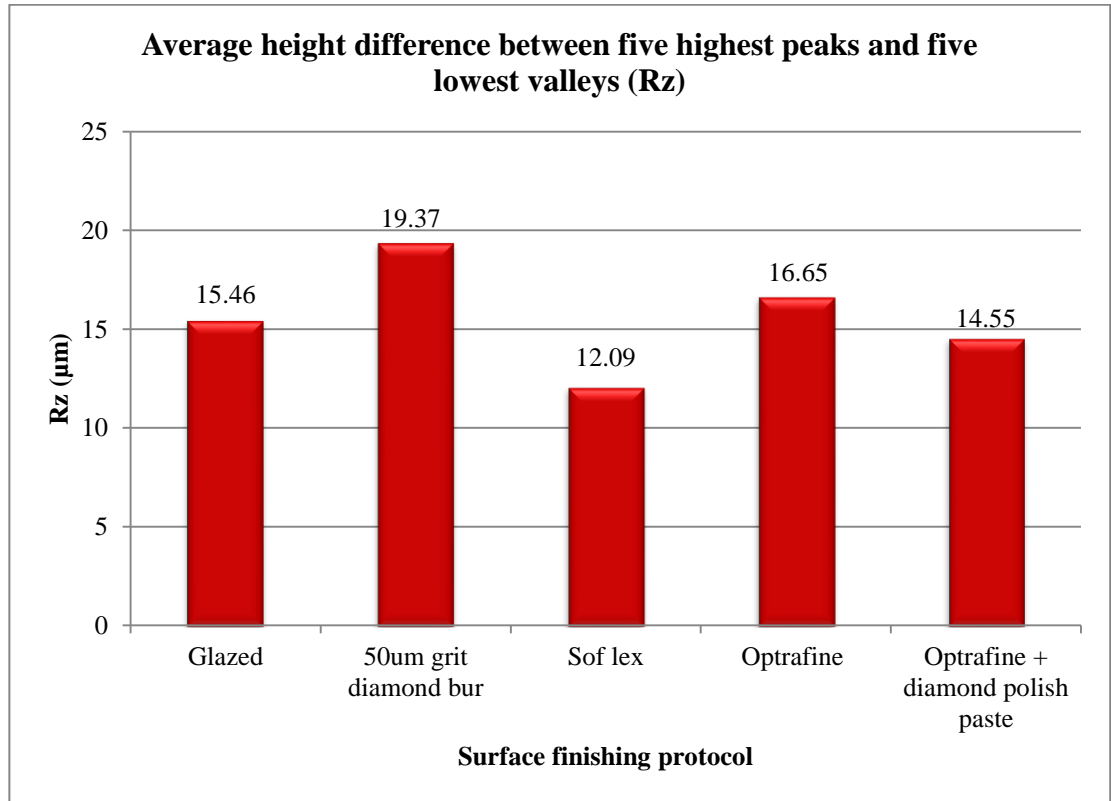


Figure A3.2: Average height difference between five highest peaks and five lowest valleys (Rz) for the different leucite-reinforced ceramic specimen groups according to the surface finishing protocols, after subjected to 600000 wear cycles in the chewing simulator against enamel specimens.

According to the Tukey analysis there are no statistical differences at $p = 0.05$ between any ceramic group. The Average height difference between five highest peaks and five lowest valleys (Rz) values for the different ceramic specimen groups are as follows; Glazed ceramics ($15.46 \mu\text{m} \pm 2.13$), $50 \mu\text{m}$ grit diamond bur ($19.37 \mu\text{m} \pm 4.89$), Sof-Lex ($12.09 \mu\text{m} \pm 4.89$), Optrafine polishing system ($16.65 \mu\text{m} \pm 3.34$), Optrafine polishing system and diamond polishing paste ($14.55 \mu\text{m} \pm 8.074$).

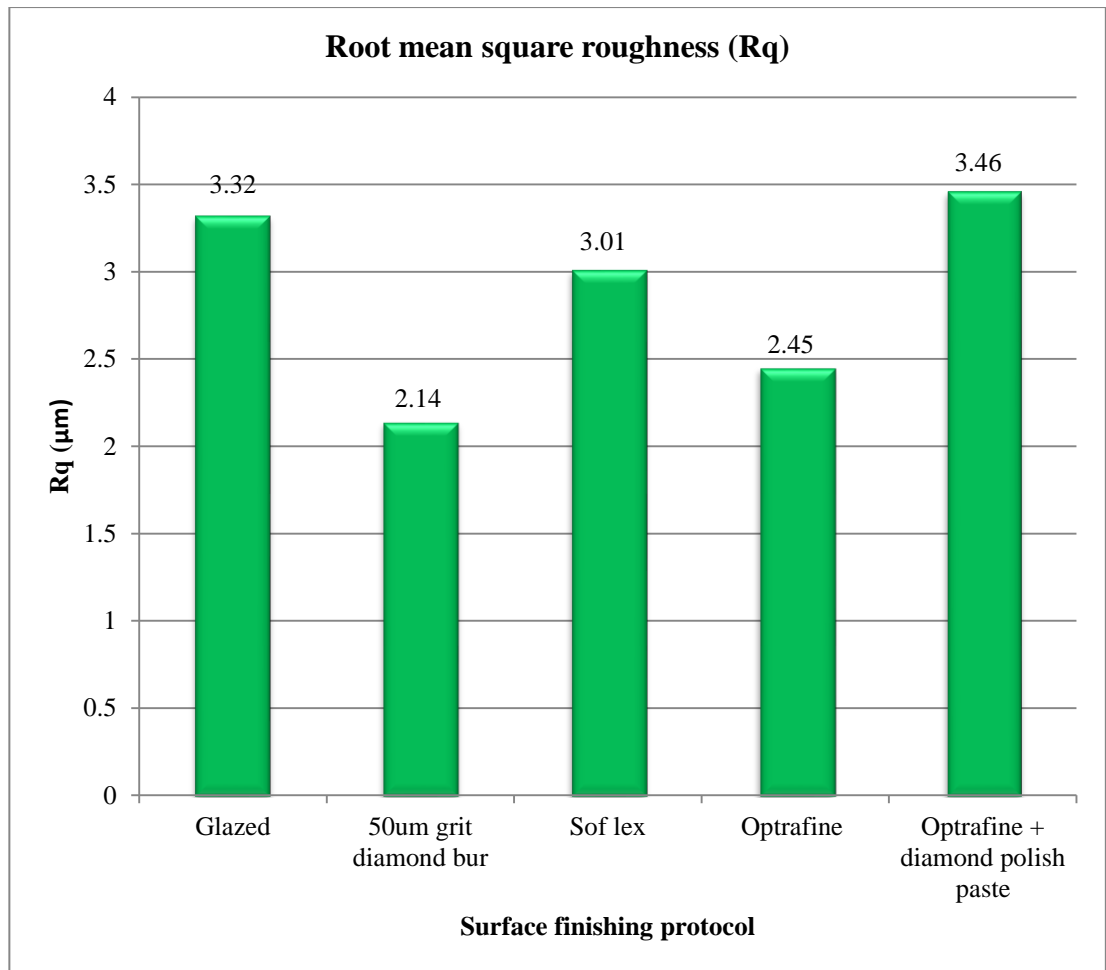


Figure A3.3: Root mean square roughness (Rq) for the different leucite-reinforced ceramic specimen groups according to the surface finishing protocols, after subjected to 600000 wear cycles in the chewing simulator against enamel specimens.

According to the Tukey analysis there are no statistical differences at $p= 0.05$ between any ceramic group. The root mean square roughness (Rq) values for the different ceramic specimen groups are as follows; Glazed ceramics (3.32 ± 0.45), 50 µm grit diamond bur ($2.14 \mu\text{m} \pm 1.12$), Sof-Lex ($3.01 \mu\text{m} \pm 0.99$), Optrafine polishing system ($2.45 \mu\text{m} \pm 0.075$), Optrafine polishing system and diamond polishing paste ($3.46 \mu\text{m} \pm 2.12$).

APPENDIX 4

STUDY B

Lithium Disilicate

Surface texture altitude parameter analysis

Post wear simulation

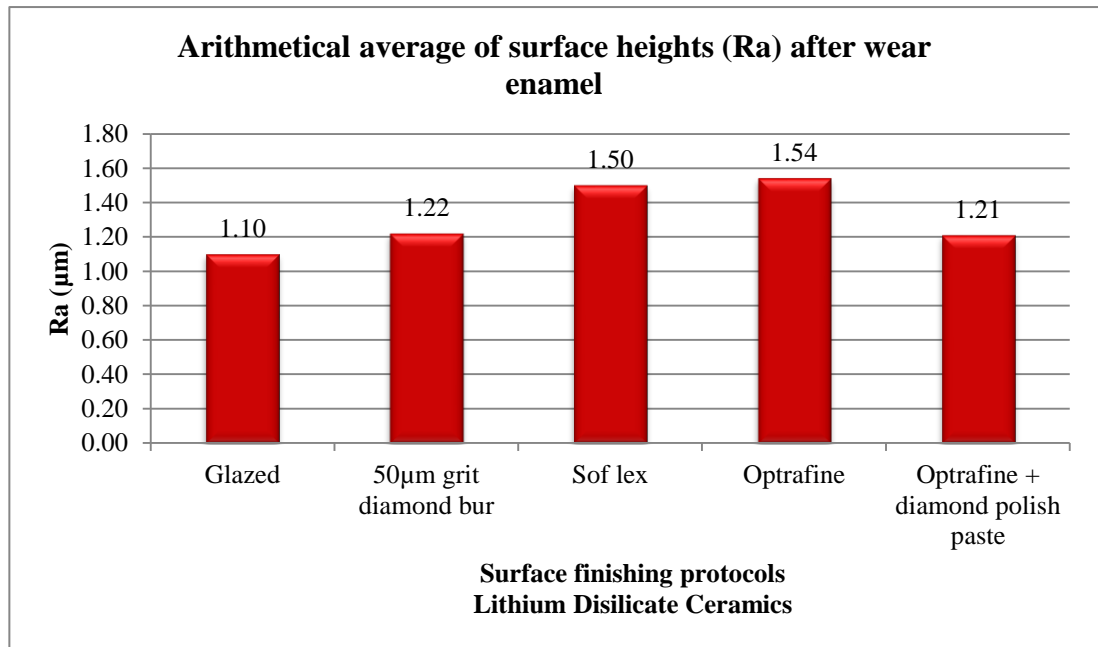


Figure A4.1: Arithmetical average of surface heights (Ra) after wear against enamel for the different lithium disilicate ceramic specimen groups according to the surface finishing protocols, after subjected to 600000 wear cycles in the chewing simulator against enamel specimens.

According to the Tukey analysis, all specimen groups had statistically similar arithmetic average of surface height (Ra) values at $p=0.05$. The mean values for each group of ceramic specimens are as follows; Glazed $1.10 \mu\text{m} \pm 0.26$, 50µm grit diamond group $1.22 \mu\text{m} \pm 0.21$, Sof-Lex $1.50\mu\text{m} \pm 0.15$, Optrafine polishing $1.54 \mu\text{m} \pm 0.18$ and Optrafine polishing with diamond polish paste $1.21 \mu\text{m} \pm 0.71$. Ceramic groups with statistically similar surface texture finishing protocols are shown in the same colour.

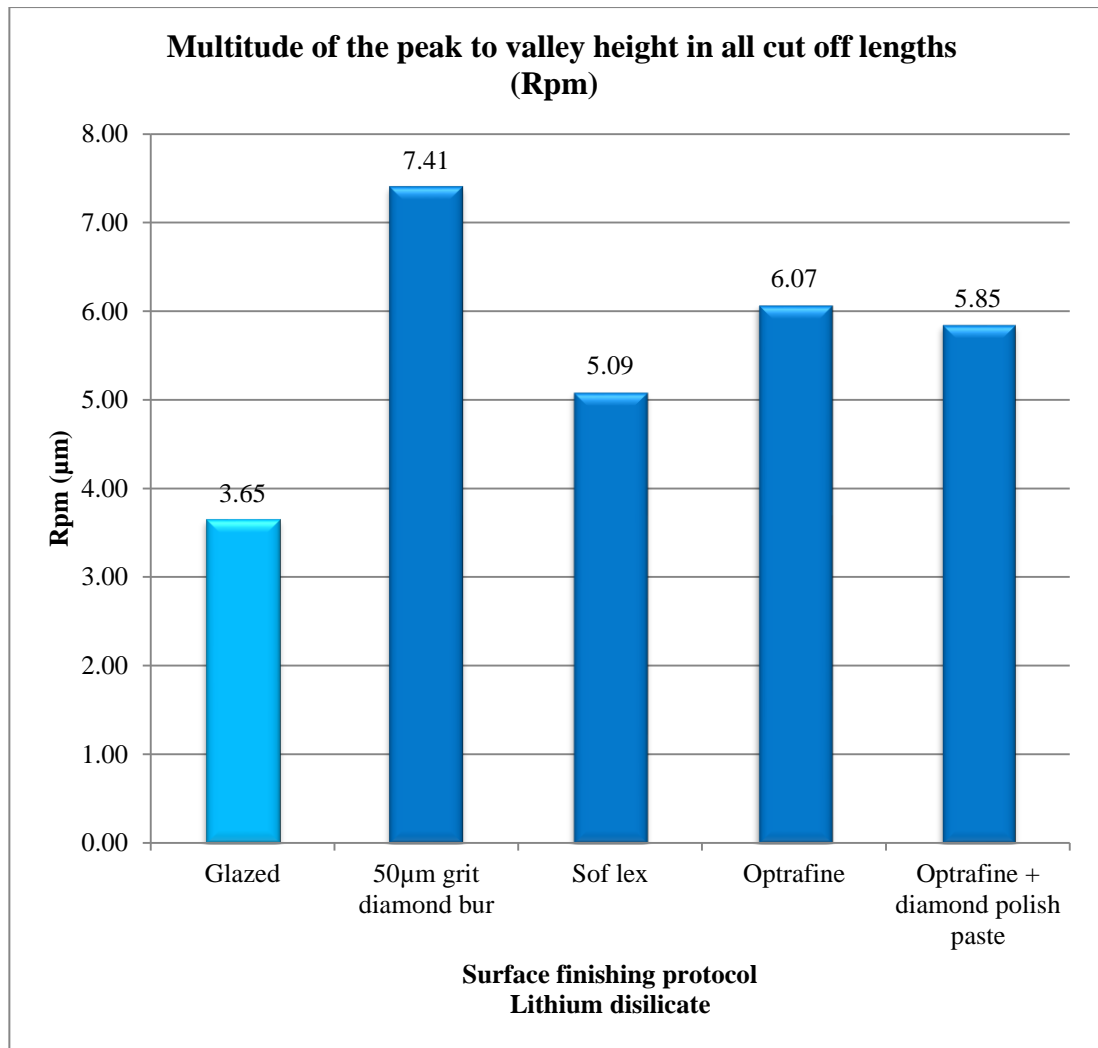


Figure A4.2: Multitude of the peak to valley height in all cut off lengths (Rpm) after wear against enamel for the different lithium disilicate ceramic specimen groups according to the surface finishing protocols, after subjected to 600000 wear cycles in the chewing simulator against enamel specimens

According to the Tukey analysis, all specimen groups had statistically similar Rpm values at $p=0.05$. The mean values are as follows. Glazed ($3.65\mu\text{m} \pm 0.96$), 50 μm grit diamond bur ($7.41 \mu\text{m} \pm 1.62$), Sof-Lex polishing discs ($5.09 \mu\text{m} \pm 1.62$), Optrafine polishing system ($6.07 \mu\text{m} \pm 0.97$) and Optrafine polishing system plus diamond polish paste ($5.85 \mu\text{m} \pm 1.45$). Ceramic groups with statistically similar surface texture finishing protocols are shown in the same colour.

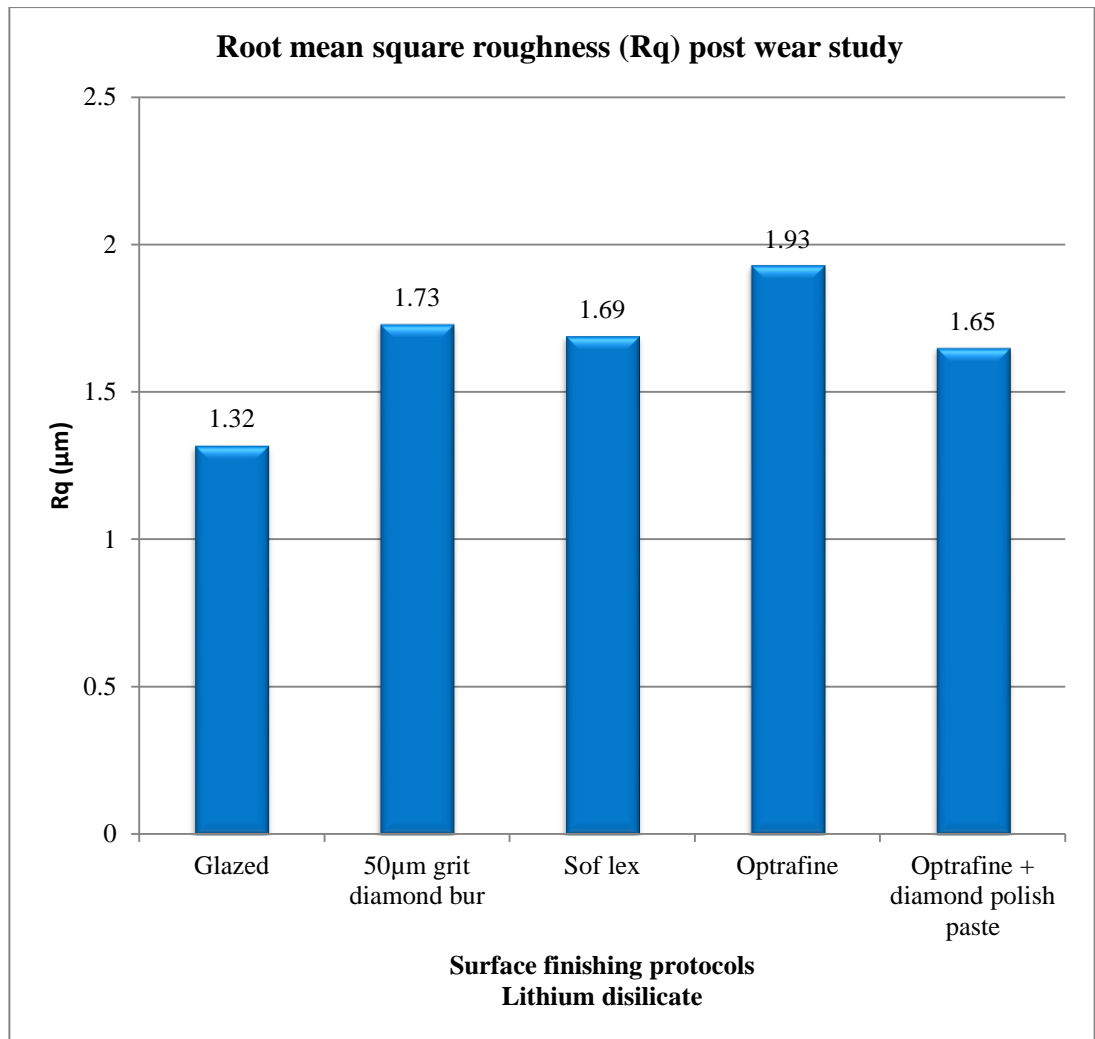


Figure A4.3: Root mean square roughness (Rq) post wear study after wear against enamel for the different lithium disilicate ceramic specimen groups according to the surface finishing protocols, after subjected to 600000 wear cycles in the chewing simulator against enamel specimens.

According to the Tukey analysis, all specimen groups had statistically similar Rpm values at $p=0.05$. The mean values are as follows. Glazed ($1.32\mu\text{m} \pm 0.96$), 50 µm grit diamond but ($1.73\mu\text{m} \pm 3.45$), Sof-Lex polishing discs ($1.69\mu\text{m} \pm 0.75$), Optrafine polishing system ($1.93\mu\text{m} \pm 0.235$) and Optrafine polishing system plus diamond polish paste ($1.65\mu\text{m} \pm 0.217$). Ceramic groups with statistically similar surface texture finishing protocols are shown in the same colour.

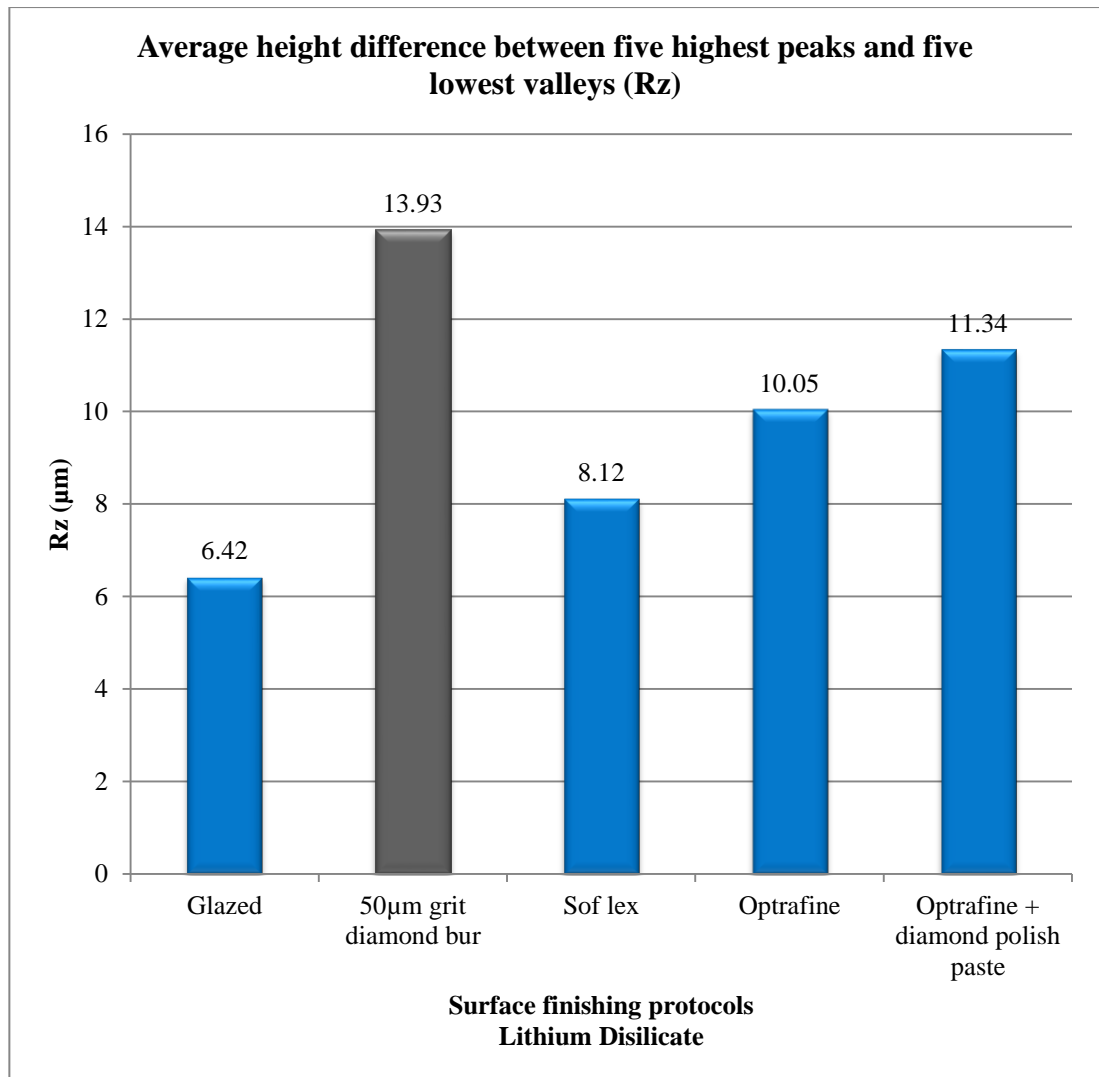


Figure A4.4: Average height difference between five highest peaks and five lowest valleys (Rz) after wear against enamel for the different lithium disilicate ceramic specimen groups according to the surface finishing protocols, after subjected to 600000 wear cycles in the chewing simulator against enamel specimens.

According to the Tukey analysis ceramics finished with 50µm grit diamond bur had the highest Rz values which were statistically different from the other groups (13.93µm±2.51). Glazed (6.42 µm ±1.56), Sof-Lex (8.12 µm ±1.43), Optrafine (10.05 µm ±3.06) and diamond polish paste groups (11.34 µm ±2.65) all had statistically similar Rz values to one another at p=0.05.

APPENDIX 5

STUDY B

Comparison of ceramic surface texture

Surface texture post wear simulation

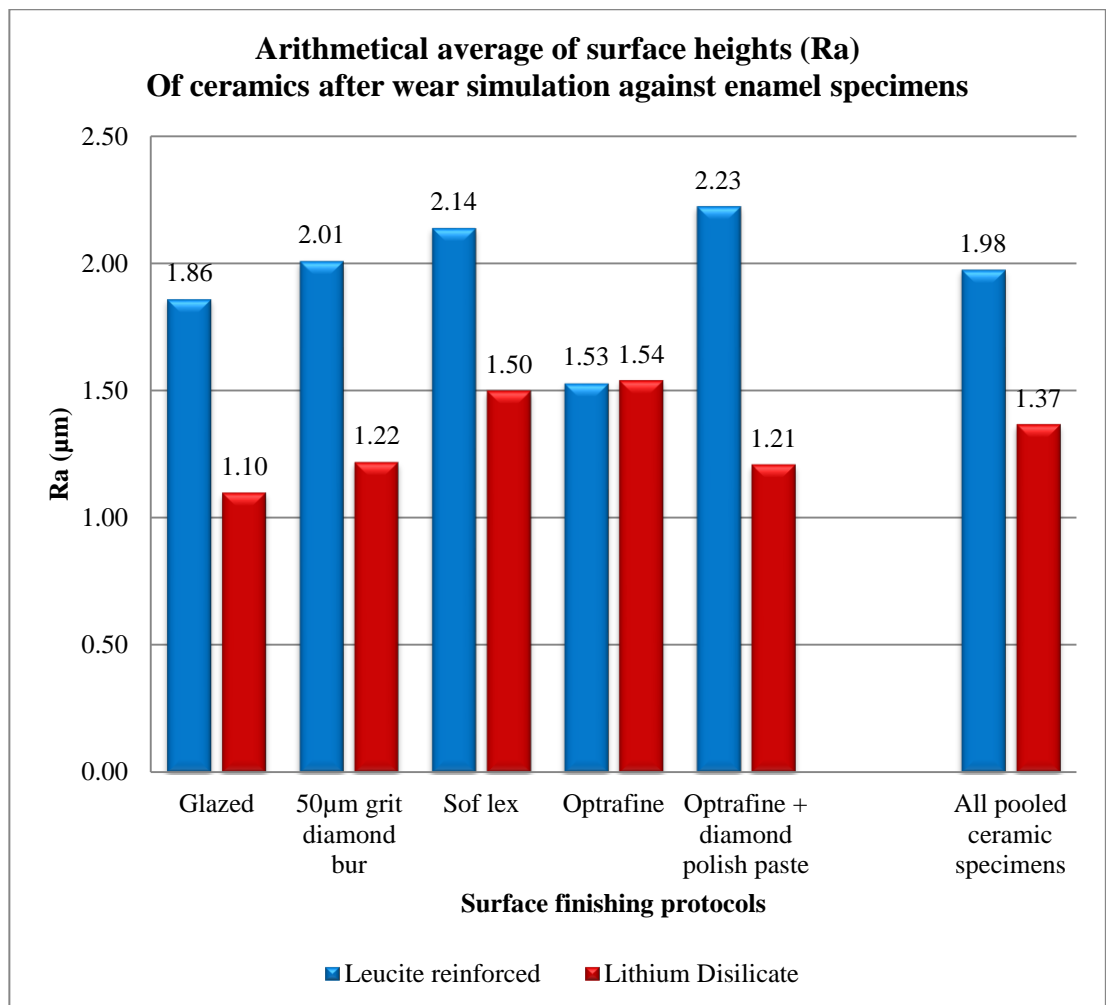


Figure A5.1: Surface texture comparison between leucite-reinforced and lithium disilicate ceramic after two body wear simulation in the Willytec chewing simulator for 600000 cycles.

Surface texture comparison between leucite-reinforced and lithium disilicate ceramic after two body wear simulation in the Willytec chewing simulator for 600000 cycles.

The arithmetic average surface roughness values for leucite-reinforced ceramic are consistently statistically higher than the values for lithium disilicate ceramics except with the ceramic surface finish protocol is by the Optrafine polishing system.

APPENDIX 6

STUDY A & B

Enamel specimens

Surface texture analysis

The enamel surface texture altitude parameter measurements taken before and after the wear study are presented. No statistical differences were noted in the surface texture altitude parameters of enamel when they were abraded against either leucite-reinforced or lithium disilicate ceramics.

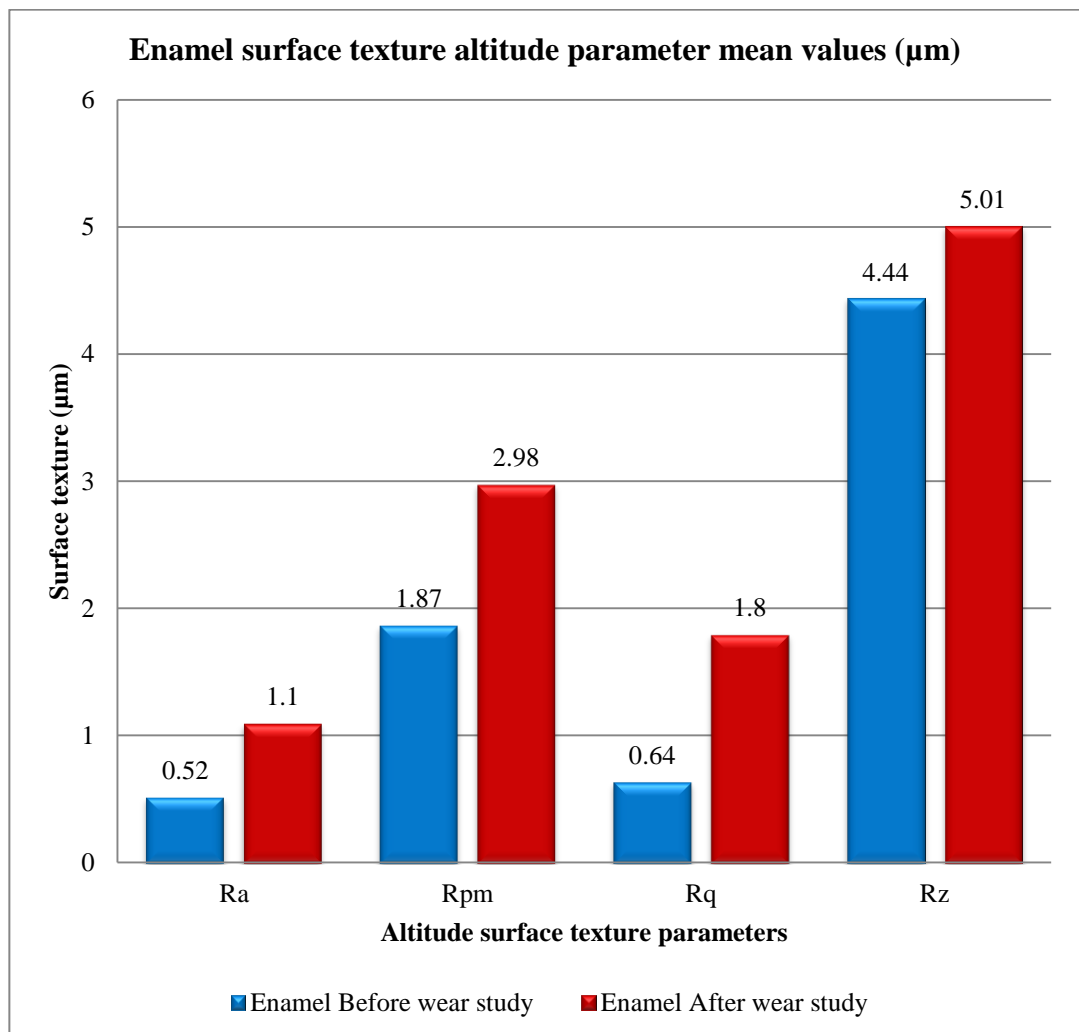


Figure A6.1: Enamel surface texture altitude parameter measurements taken before and after the wear study.

APPENDIX 7

**Summation of references for various materials
and polishing systems**

	Reflex	IPS classic shade guide ceramic	Empress I	Empress II	Dicor	Vitadur N	Vitamark I	Vitamark II	Vita In-Ceram Alumina	Vita In-Ceram Zirconia
Sof-Lex discs	1	2, 9,15, 21	2,7,15	6,15	7	7,8	7	5,6,7,16, 21	6	6
Diamond polishing paste		9, 21	7,	19, 20	7	4,7, 19	7	7,16, 21		
Rubber silicon point polishing kits		2, 9, 21, 23	7, 18	2,7, 18, 19, 20	3,7	7,8, 19	7	5,7,16, 21		
Diamond drills		2	2	6		4		5,6	6	6
Rubber felt wheels			17							
Glazing	1	9,15, 21, 23	7,15,18	7,15, 18, 19, 20	3,7	4,7,8, 19	7	7,16, 21		

	Procera AllCeram	Denzir	VMK68 porcelain	Vita VMK 6	ceramo II porcelain	Finess (dentsply)	Biobond and ceramco (dentsply)	VMK 95	duracem	symbio
Sof-Lex discs	6	6			16	13		16		
Diamond polishing paste	20		10	11	12,16	22	14	16		22
Rubber silicon point polishing kits	20, 23				16	22, 23	14	16	18	18, 22
Diamond drills	6, 20	6		11	12					
Rubber felt wheels			10	11						
Glazing	20, 23			11	16	13, 22, 23	14	16	18	18, 22

Figure A7.1: Summation of materials and various polishing systems.

Figure A7.1 References

1. Wang F, Chen J. Surface Roughness of a Novel Dental Porcelain Following Different Polishing Procedures. *International journal of Prosthodontics*. 2009;Mar-Apr(22(2)):178-80.
2. Martinez-Gomis J, Bizar J, Anglada JM, Samsó J, Peraire M. Comparative evaluation of four finishing systems on one ceramic surface. *International Journal of Prosthodontics*. 2003;16:74-77.
3. Magne P, Oh WS, Pintado MR, DeLong R. Wear of enamel and veneering ceramics after laboratory and chairside finishing procedures. *Journal of Prosthetic Dentistry*. 1999;82.
4. Patterson CJ, McLundie AC, Stirrups DR, Taylor WG. Efficacy of a porcelain refinishing system in restoring surface finish after grinding with fine and extra-fine diamond burs. . *Journal of Prosthetic Dentistry*. 1992;68:402-406.
5. Aykent F, Yondem I, Ozyesil A, Gunal K, Mustafa C, Ozkan S. Effect of different finishing techniques for restorative materials on surface roughness and bacterial adhesion. *Journal of Prosthetic Dentistry*. 2010;103:221-227.
6. Kou W, Molin M, Sjögren G. Surface roughness of five different dental ceramic core materials after grinding and polishing. . *Journal of Oral Rehabilitation*. 2006;33:117-24.
7. Hultström AK, Bergman M. Polishing systems for dental ceramics. *Acta Odontol Scand* 1993;51:229-23.
8. Jagger DC, Harrison A. An in vitro investigation into the wear effects of unglazed, glazed, and polished porcelain on human enamel. *Journal of Prosthetic*

Dentistry. 1994;72:320-326.

9. Raimondo J, Richard L, Richardson T, Wiedner B. Polished versus autoglazed dental porcelain Journal of prosthetic Dentistry

1990;64:563-7.

10. Brewer J, Garlapo DA, Chipps EA, Tedesco LA. Clinical discrimination between autoglazed and polished porcelain surfaces Journal of Prosthetic Dentistry. 1990;64:631-4.

11. Fuzzi M, Zaccheroni Z, Vallania G. Scanning electron microscopy and profilometer evaluation of glazed and polished dental porcelain. International Journal of Prosthodontics 1996;9:452-458.

12. Haywood VB HH, Scurria MS. . Effects of water, speed and experimental instrumentation on finishing and polishing porcelain intra-orally. Dental Materials. 1989;5:185-8.

13. Wright MD, Masri R, Driscoll CF, Romberg E, Geoffrey A, Thompson M. Comparison of three systems for the polishing of an ultra-low fusing dental porcelain. Journal of Prosthetic Dentistry. 2004;92:486-90.

14. Goldstein GR, Barnhard BR, Penugonda B. Profilometer, SEM, and visual assessment of porcelain polishing methods. Journal of Prosthetic Dentistry. 1991;65:627-34.

15. Yilmaz K, Ozkan P. Profilometer evaluation of the effect of various polishing methods on the surface roughness in dental ceramics of different structures subjected to repeated firings. Quintessence international. 2010;41:e:125-131.

16. Sarikaya I, Guler AU. Effects of different polishing techniques on surface roughness on the surface roughness of dental porcelains. Journal of applied science. 2010;18(1):10-16.

17. Al-Wahadni AM, Martin DM. An in vitro investigation into the wear effects of glazed, unglazed and refinished dental porcelain on an opposing material. . Journal of Oral Rehabilitation 1999;26:538-546.

18. Olivera EA, Matson E, Marques MM. The Effect of Glazed and Polished Ceramics on Human Enamel Wear. *International Journal of Prosthodontics*. 2006;19:547-548.
19. Saraç D, Turk T, Elekdag-Turk S, Saraç S. Comparison of 3 Polishing Techniques for 2 All-Ceramic Materials. *international journal of Prosthodontics*. 2007;20:465-468.
20. Tholt B, Miranda WG, Prioli R, Thompson J. Surface roughness in Ceramics with Different finishing techniques using atomic force microscope and profilometer. *Operative Dentistry*. 2006;31(4):422-449.
21. Flury, A. Lussi and B. Zimmerli (2010) Performance of Different Polishing Techniques for Direct CAD/CAM Ceramic Restorations. *Operative Dentistry*: July 2010, Vol. 35, No. 4, pp. 470-481
22. Sasahara RMC, Riberio FC, Cesar PF, Yoshimura HN. Influence of the finishing technique on surface roughness of dental porcelains with different microstructures. *Operative Dentistry*. 2006;31:557-583.
23. Elmaria A, Goldstein G, Vijayaraghavan T, Legeros R, Hittelman E. An evaluation of wear when enamel is opposed by various ceramic materials and gold. *Journal of Prosthetic Dentistry*. 2006;96:345-5.

FIGURES

FIGURE 1.1 SCANNING ELECTRON MICROGRAPH OF ETCHED ENAMEL. THE ENAMEL RODS HAVE BEEN CUT LONGITUDINALLY (LEFT). THE ENAMEL RODS HAVE BEEN CUT DIAGONALLY (RIGHT) [23].	3
TABLE 1.1: PHYSICAL PARAMETERS (MEAN VALUE) OF ENAMEL AND DENTINE. [17,21, 22]	4
FIGURE 2.1.1: CLINICAL IMAGE OF MALE PATIENT, 22 YEARS OF AGE. SEVERE ATTRITION ASSOCIATED WITH PARAFUNCTIONAL HABIT.	9
FIGURE 2.1.2: OCCLUSAL VIEW OF UPPER TEETH. NOTE LOSS OF CUSP TIPS AND FLATTENED OCCLUSAL SURFACES.	10
FIGURE 2.1.3: OCCLUSAL VIEW OF LOWER TEETH.	10
FIGURE 2.1.4: RIGHT LATERAL VIEW. NOTE EQUAL DENTINE AND ENAMEL TISSUE HEIGHT AND COMMUNICATION OF OPPOSING TEETH WEAR FACETS IN LATERAL MANDIBULAR MOVEMENT	10
FIGURE 2.1.5: LEFT LATERAL VIEW.	11
FIGURE 2.2: SCANNING ELECTRON MICROSCOPE IMAGE OF WEAR FACET SHOWING PARALLEL STRIATIONS. THE DENTINE (D) IS NOT SCOOPED OUT AND IS AT THE SAME LEVEL AS THE ENAMEL (E)[33].	11
FIGURE 2.3: AN EXAMPLE SHOWING THE EFFECT OF AN ABRASIVE DIET ON THE TEETH OF A PRE-CONTEMPORARY AUSTRALIAN ABORIGINAL. NOTE THE GOUGED AND PITTED ENAMEL AND THE SCOOPING OF THE DENTINE [33].	13
FIGURE 2.4: MICROWEAR DETAIL OF AN ABRASION AREA SHOWING HAPHAZARD SCRATCH MARKS [33].	14
FIGURE 2.5: CLINICAL IMAGE OF ABRASION LESIONS ON OCCLUSAL SURFACES. PATIENT IS 43 YEARS OLD WITH HISTORY OF GASTRIC OESOPHAGEAL REFLUX DISEASE, SEVERE PARAFUNCTIONAL ACTIVITY AND HARD BRISTLE TOOTH BRUSH. NOTE STRIATIONS OF ENAMEL AND SCOOPING OF THE DENTINE.	14
FIGURE 2.6: CLINICAL IMAGE OF 65 YEAR OLD PATIENT WITH NON CARIOUS CERVICAL LESIONS. SELF-PERFORMED PLAQUE CONTROL WITH HARD BRISTLE TOOTHBRUSH.	15
FIGURE 2.7: MULTIFACTORIAL AETIOLOGY OF NCCLS RESULTING IN VARIATION IN NCCL MORPHOLOGY.	16
FIGURE 2.8: MICROGRAPH OF EROSION LESION (COURTESY OF DR S. RANJITKAR). NOTE THE LACK OF MECHANICAL WEAR.	18
FIGURE 2.9: MAXILLARY LEFT FIRST INCISOR SHOWING EROSION ON THE INCISAL EDGE AND ON THE PALATAL SURFACE. PALATAL ENAMEL IS MOSTLY ERODED, EVEN INTO THE GINGIVAL SULCUS. PALATAL DENTINE IS FINELY STRIATED. THIS TOOTH WAS FROM A PATIENT WITH <i>BULIMIA NERVOSA</i> [59].	19

FIGURE 3.1: DISTORTION OF A SURFACE PROFILE DUE TO THE EFFECT OF STYLUS SIZE [119].	27
FIGURE 3.2: MODES OF REFLECTION[119]: (A) COMBINED SPECULAR AND DIFFUSE; (B) SPECULAR ONLY; (C) DIFFUSE ONLY.	28
FIGURE 3.3: WORKING PRINCIPLES OF AFM[120].	31
FIGURE 3.4: SURFACE TEXTURE PARAMETER [119]	33
FIGURE 3.5: THE LIMITATIONS OF AVERAGE MEAN ROUGHNESS. VARIATIONS IN WAVELENGTH ARE NOT EVIDENT WITH SURFACE TEXTURE PARAMETER 'AVERAGE MEAN ROUGHNESS.' ALL GRAPHICAL REPRESENTATIONS SHOWING SURFACE ROUGHNESS HAVE THE SAME RA VALUE.	35
FIGURE 3.6: MATHEMATICAL DEFINITION AND THE DIGITAL IMPLEMENTATION OF ARITHMETIC AVERAGE HEIGHT PARAMETER (RA). L = EVALUATION LENGTH, Y = HEIGHT, X = DISTANCE ALONG MEASUREMENT, Z(X) = PROFILE ORDINATES OF ROUGHNESS PROFILE.	35
FIGURE 3.7: RA IS THE ARITHMETIC MEAN OF THE ABSOLUTE DEPARTURES OF THE ROUGHNESS PROFILE FROM THE MEAN LINE. IT IS UNIVERSALLY RECOGNISED AS THE MOST OFTEN USED INTERNATIONAL PARAMETER OF ROUGHNESS [137].	35
FIGURE 3.8: MATHEMATICAL DEFINITION AND THE DIGITAL IMPLEMENTATION OF THE ROOT MEAN SQUARE ROUGHNESS (RMS OR RQ) L = EVALUATION LENGTH, Y = HEIGHT, X = DISTANCE ALONG MEASUREMENT, Z(X) = PROFILE ORDINATES OF ROUGHNESS PROFILE [140].	36
FIGURE 3.9: RMS MEAN LINE DIVIDES THE PROFILE SO THAT THE SUM OF THE SQUARES OF THE DEVIATIONS OF THE PROFILE HEIGHT FROM IT IS EQUAL TO ZERO [140].	37
FIGURE 3.10: THE MATHEMATICAL AND GRAPHICAL DEFINITION OF MEAN ROUGHNESS PARAMETER RZ WHERE N IS THE NUMBER OF SAMPLES ALONG THE ASSESSMENT LINE [140].	38
FIGURE 3.11: THE MEAN WIDTH OF PROFILE ELEMENTS (RSM) IS THE ARITHMETIC MEAN VALUE OF THE WIDTHS OF THE PROFILE ELEMENTS OF THE ROUGHNESS PROFILE, WHERE A PROFILE ELEMENT IS A PEAK AND VALLEY IN THE ROUGHNESS PROFILE [139].	39
FIGURE 3.12: MEAN LEVELLING DEPTH PARAMETER MEASURES THE MEAN VALUE OF THE LEVELLING DEPTHS OF FIVE CONSECUTIVE SAMPLING LENGTHS. THE LEVELLING DEPTH (RP) IS ALSO THE LARGEST OF THE FIVE LEVELLING DEPTHS. THE MAXIMUM ROUGHNESS DEPTH (RT), PEAK TO VALLEY HEIGHT IS THE VERTICAL DISTANCE BETWEEN THE HIGHEST PEAK AND THE LOWEST VALLEY OF THE ROUGHNESS PROFILE R WITHIN THE EVALUATION LENGTH L. [139, 141] RPM = 1/5 (RP1 + RP2 + RP3 + RP4 + RP5).	40
FIGURE 4.1: TRIBOLOGICAL INTERACTIONS AND WEAR MECHANISMS [147].	42

- FIGURE 4.2: ADHESIVE WEAR PROCESS. NOTE THE TRANSFER OF MATERIAL FROM ONE SURFACE TO ANOTHER [62]. 43
- FIGURE 4.3: ABRASIVE WEAR. THE SURFACE CAN BE PLOUGHED AND PLASTICALLY DEFORMED WITHOUT REMOVAL OF MATERIAL OR REMOVAL CAN OCCUR BY A LOW-CYCLE FATIGUE MECHANISM [62]. 44
- FIGURE 4.4: TWO-BODY ABRASIVE WEAR. IF BOTH SURFACES ARE BRITTLE, THERE IS FRACTURE OF THE ASPERITIES (UPPER RIGHT DIAGRAM). IF ONE SURFACE IS HARDER THAN THE OTHER, THE HARDER SURFACE ‘PLOWS’ INTO THE SOFTER SURFACE (LOWER RIGHT IMAGE) [141]. 45
- FIGURE 4.5: THREE-BODY ABRASIVE WEAR. AS THE ABRASIVE PARTICLES IN THE SLURRY FLOW UNDER PRESSURE, THEY CUT AWAY THE SURFACES [141]. 45
- FIGURE 4.6: THE PROCESS OF FATIGUE WEAR [62]. ROLLING ACTION OF TWO SURFACES RESULTS IN SHEAR STRESS AT THE SUBSURFACE WHICH RESULT IN NUCLEATION OF CRACKS. CRACKS PROPAGATE Laterally TO SURFACE WITH REPEATED ROLLING ACTION RESULTING IN DELAMINATION AND FATIGUE FAILURE. 47
- FIGURE 4.7: CORROSIVE WEAR OCCURS WHEN THERE IS SLIDING MOVEMENT IN A CORROSIVE ENVIRONMENT. THE LAYER OF PROTECTIVE OXIDES FORMED DUE TO THE EFFECTS OF CORROSION ARE WORN AWAY WITH SLIDING MOVEMENT [62]. 48
- FIGURE 5.1: DIAGRAM OF A SILICATE UNIT WITH EACH SiO_4 TETRAHEDRAL SHARING AN OXYGEN ATOM (UPPER LEFT). THREE DIMENSIONAL DRAWING OF A SILICATE UNIT IN WHICH THE SILICON ATOM Si IS SURROUNDED BY FOUR OXYGEN ATOMS (UPPER RIGHT). THREE DIMENSIONAL DRAWING OF LINKED SILICATE UNITS WHICH FORM THE CONTINUOUS NETWORK IN GLASS (LOWER) [165]. 52
- FIGURE 5.2: SCHEMATIC REPRESENTATION OF THREE BASIC CLASSES OF DENTAL CERAMICS. PREDOMINANTLY GLASS-BASED CERAMICS ARE LIGHTLY FILLED WITH COLORANTS AND OPACIFIERS TO MIMIC NATURAL AESTHETICS AND ARE THE WEAKEST CERAMICS (LEFT). GLASSES CONTAINING 35 TO 70 PERCENT FILLER PARTICLES FOR STRENGTH CAN BE MODERATELY AESTHETIC AS FULL-THICKNESS RESTORATIONS (MIDDLE). COMPLETELY POLYCRYSTALLINE CERAMICS (NO GLASS), WHICH ARE USED TO CREATE STRONG SUBSTRUCTURES AND FRAMEWORKS VIA COMPUTER-AIDED DESIGN/COMPUTER-AIDED MANUFACTURING PROCESSES (RIGHT). 55
- FIGURE 5.3: CLASSIFICATION OF CERAMICS BASED ON PHYSICAL PROPERTIES- FRACTURE TOUGHNESS AND BENDING STRENGTH [176]. 56
- FIGURE 5.4: THE SEM IMAGES OF POLISHED AND ETCHED SURFACES REVEAL THE MICROSTRUCTURE OF IPS EMPRESS CAD (LEFT). ETCHING TECHNIQUE USING 40% HF VAPOUR, 20 SECONDS, DISSOLVES THE LEUCITE CRYSTALS MORE

QUICKLY THAN THE GLASS (RIGHT). TYPICAL LEUCITE STRUCTURE OF IPS EMPRESS ESTHETIC VENEER EXPOSED WHEN ETCHED WITH 3% HF FOR 10 SECONDS. SOURCE: R&D IVOCLAR VIVADENT AG, SCHAAN, LIECHTENSTEIN.	58
TABLE 5.5: STANDARD CHEMICAL COMPOSITION IN PERCENTAGE BY WEIGHT OF LEUCITE-REINFORCED GLASS CERAMIC, IPS EMPRESS CAD. (IVOCLAR VIVADENT, SCHAAN, LIECHTENSTEIN) SOURCE: R&D IVOCLAR VIVADENT AG, SCHAAN, LIECHTENSTEIN	59
TABLE 5.6: PHYSICAL PROPERTIES OF IPS EMPRESS CAD (IVOCLAR VIVADENT AG, SCHAAN, 2005/2006)	59
TABLE 5.7: STANDARD CHEMICAL COMPOSITION IN % BY WEIGHT OF LITHIUM DISILICATE GLASS CERAMIC, IPS E.MAX PRESS (LEFT) AND CAD BLOCK (RIGHT). (IVOCLAR VIVADENT, SCHAAN, LIECHTENSTEIN) SOURCE: R&D IVOCLAR VIVADENT AG, SCHAAN, LIECHTENSTEIN	60
TABLE 5.8: PHYSICAL PROPERTIES OF IPS E.MAX PRESS AND CAD BLOCKS	61
FIGURE 5.9: THE TRANSLUCENCY OF IPS E.MAX. (IVOCLAR VIVADENT, SCHAAN, LIECHTENSTEIN) AIDS EASE OF QUALITY CONTROL SINCE POROSITIES CAN BE EASILY DETECTED. SOURCE: R&D IVOCLAR VIVADENT AG, SCHAAN, LIECHTENSTEIN.	62
FIGURE 5.10: THE IPS E.MAX CAD “BLUE BLOCK” USES A TWO-STAGE CRYSTALLISATION PROCESS. SOURCE: R&D IVOCLAR VIVADENT AG, SCHAAN, LIECHTENSTEIN.	64
FIGURE 5.11. SEM IMAGE OF PARTIALLY CRYSTALLISED LITHIUM METASILICATE IPS E.MAX CAD (IVOCLAR VIVADENT) ETCHED WITH 0.5% HF FOR 10 SEC. THE ETCHED-OUT AREAS REPRESENT THE LITHIUM METASILICATE CRYSTALS (LEFT). FULLY CRYSTALLISED LITHIUM DISILICATE IPS E.MAX CAD (IVOCLAR VIVADENT) ETCHED WITH 0.5% HF VAPOUR FOR 30 SEC (RIGHT). SOURCE: R&D IVOCLAR VIVADENT AG, SCHAAN, LIECHTENSTEIN.	64
FIGURE 5.12: IPS E.MAX CAD “BLUE BLOCK” (IVOCLAR VIVADENT) (RIGHT), IPS E.MAX CAD COMPLETELY CRYSTALLISED LITHIUM DISILICATE CERAMIC (LEFT). SOURCE: R&D IVOCLAR VIVADENT AG, SCHAAN, LIECHTENSTEIN.	65
FIGURE 5.13: FOLLOWING THE GLASS FORMATION, THE INGOTS ARE THEN NUCLEATED AND CRYSTALLISED IN ONE HEAT TREATMENT TO PRODUCE THE FINAL INGOTS (LEFT). THE INGOTS ARE AVAILABLE IN TWO DEGREES OF OPACITY (RIGHT). SOURCE: R&D IVOCLAR VIVADENT AG, SCHAAN, LIECHTENSTEIN.	66
FIGURE 5.14: MICROSTRUCTURE OF IPS E.MAX PRESS GLASS CERAMIC. NOTE THE LONG (3-6µM) LITHIUM DISILICATE CRYSTALLINE STRUCTURE (IVOCLAR VIVADENT, SCHAAN, LIECHTENSTEIN) SOURCE: R&D IVOCLAR VIVADENT AG, SCHAAN, LIECHTENSTEIN.	66
FIGURE 5.15: POLYCRYSTALLINE 3Y TZP CERAMIC. NOTE THE DENSE ARRAY OF	

ATOMS, IRREGULAR NETWORK AND ABSENCE OF GLASS MATRIX [176].	67
TABLE 5.16: TETRAGONAL ZIRCONIA POLYCRYSTALS 3Y-TZP: MECHANICAL AND PHYSICAL PROPERTIES.	68
FIGURE 7.1: SCHEMATIC ILLUSTRATION OF THE POLISHING PROCESS SHOWING PROCESS VARIABLES. THE FIGURE DEPICTS CONVENTIONAL GRINDING. A STRAIGHT GRINDING WHEEL OF DIAMETER D REMOVES A LAYER OF MATERIAL TO A DEPTH D. AN INDIVIDUAL GRAIN ON THE PERIPHERY OF THE WHEEL MOVES AT AN ANGULAR VELOCITY [290].	88
FIGURE 7.2: SCHEMATIC REPRESENTATION OF COMPRESSIVE STRESS AS A RESULT OF MECHANICAL INTERACTIONS OF ABRASIVE GRAINS WITH THE WORKPIECE. FOR CRACKS TO PROPAGATE , ENERGY MUST BE CONSUMED TO OVERCOME THE COMPRESSIVE STRESSES [290].	89
FIGURE 9.1.1: IPS E.MAX CAD PARTIALLY CRYSTALLISED BLOCKS (IVOCLAR-VIVADENT).	103
FIGURE 9.1.2: IPS EMPRESS CAD BLOCKS (IVOCLAR VIVADENT).	103
FIGURE 9.1.3: PROGROMAT FURNACE.	106
TABLE 9.1.4: PROGRAMAT CS FURNACE FIRING PARAMETERS. SOURCE: IVOCLAR VIVADENT PROGRAMAT CS FURNACE DATA SHEET.	106
FIGURE 9.1.5: ISOMET LOW SPEED SAW.	107
FIGURE 9.1.6: SECTIONED IPS E.MAX CAD BLOCK INTO 2MM THICK SLICES.	108
FIGURE 9.1.7: RED BAND 50 μ M GRIT DIAMOND IMPREGNATED HIGH SPEED BUR (8879L, KOMET, GEBR BRASSELER, LEMGO, CERMANY (LEFT). YELLOW BAND 25 MICRON GRIT DIAMOND IMPREGNATED HIGH SPEED BUR (S.SG CKEF, KOMET) (RIGHT).	108
FIGURE 9.1.8: OPTRAFINE POLISHING SYSTEM AND DIAMOND POLISHING PASTE (LEFT) SOURCE: R&D IVOCLAR VIVADENT AG / SCHAAN.	109
FIGURE 9.1.9: SOF-LEX DISCS (3M/ ESPE, ST. PAUL, MN, US) ARE ESSENTIALLY SAND PAPER DISCS IMPREGNATED WITH ALUMINIUM OXIDE OF VARYING GRIT SIZE LISTED ABOVE. NOTE: "GRIT" IS A REFERENCE TO THE NUMBER OF ABRASIVE PARTICLES PER SQUARE INCH OF SANDPAPER.	110
FIGURE 9.1.10: IN-CERAM GLAZE PASTE (IVOCLAR-VIVADENT, LICHTENSTEIN).	110
FIGURE 9.2.1: TOOTH-SECTIONING MACHINE, ADELAIDE DENTAL HOSPITAL (LEFT), FLOW CHART SHOWING SEQUENCE OF TOOTH SECTIONING (RIGHT).	111
FIGURE 9.2.2: ENAMEL SPECIMEN ON SEM STUD WITH THREE REFERENCE METAL BALLS.	113
FIGURE 9.2.3: IPS EMPRESS CAD CERAMIC SPECIMEN ON SEM STUD WITH THREE REFERENCE METAL BALLS.	113
FIGURE 9.2.4: LEICA MZ16FA STEREO MICROSCOPE (LEICA BIOSYSTEMS, WETZLAR, GERMANY).	115
FIGURE 9.2.5: PIX-4 3D SCANNER, ROLAND DG, TOKYO, JAPAN.	118

FIGURE 9.2.6: THE GRAPHIC DATA IN 3D.	119
FIGURE 9.2.7: REFERENCE PLANE DEFINED FOR VOLUME CALCULATION WITH MATLAB 6.5.	119
122	
FIGURE 9.2.8: PHILLIPS 20XL SCANNING ELECTRON MICROSCOPE, ADELAIDE MICROSCOPY LABORATORY	122
FIGURE 9.2.9: CERAMIC SPECIMENS ON SEM MOUNT COATED WITH AU/PD FOR SEM SURFACE ANALYSIS.	122
FIGURE 9.2.10: WILLYTEC WEAR SIMULATOR, DENTAL SCHOOL. UNIVERSITY OF WESTERN AUSTRALIA.	123
FIGURE 9.2.11: SCHEMATIC DRAWING OF THE DUAL-AXIS CHEWING SIMULATOR WITH EIGHT SAMPLE CHAMBERS. (1) UPPER CROSSBEAM, (2) LOWER CROSSBEAM,(3A) WATER RESERVOIR (IN), (3B) WATER RESERVOIR (OUT), (4) FILTER FOR COLD WATER, (5) FILTER FOR WARM WATER, (6) PUMP FOR REMOVAL OF COLD WATER, (7) PUMP FOR REMOVAL OF WARM WATER, (8) PUMP FOR APPLICATION OF COLD WATER, (9) PUMP FOR APPLICATION OF WARM WATER, (10) MOTOR BLOCK, (11) TABLE.	124
FIGURE 9.2.12: SCHEMATIC DRAWING OF ONE CHEWING CHAMBER. THE SAMPLE RESTS ON THE SAMPLE HOLDER WHICH IS FIXED TO THE CHAMBER BASE BY A BUTTERFLY NUT.	126
TABLE 9.2.13: THE WILLYTEC CHEWING SIMULATOR WITH ADJUSTABLE VARIABLES	127
FIGURE 9.2.14: WILLYTEC CHEWING SIMULATOR TESTING WEAR OF ENAMEL SPECIMENS, LUBRICATION BY IMMERSING SAMPLES IN DISTILLED WATER.	127
FIGURE 10.1.1: LEUCITE-REINFORCED CERAMIC, GLAZED SURFACE. LEFT: SURFACE TEXTURE PRE WEAR STUDY, RIGHT: SURFACE TEXTURE POST WEAR STUDY.	130
FIGURE 10.1.2: LITHIUM DISILICATE CERAMIC, GLAZED SURFACE. LEFT: SURFACE TEXTURE PRE WEAR STUDY, RIGHT: SURFACE TEXTURE POST WEAR STUDY.	131
FIGURE 10.1.3: LEUCITE-REINFORCED CERAMIC, OPTRAFINE AND DIAMOND POLISH PASTE. LEFT: SURFACE TEXTURE PRE WEAR STUDY, RIGHT: SURFACE TEXTURE POST WEAR STUDY.	131
FIGURE 10.1.4: LITHIUM DISILICATE CERAMIC, OPTRAFINE AND DIAMOND POLISH PASTE. LEFT: SURFACE TEXTURE PRE WEAR STUDY, RIGHT: SURFACE TEXTURE POST WEAR STUDY.	132
FIGURE 10.1.5: LEUCITE-REINFORCED CERAMIC HIGH SPEED DIAMOND 25UM GRIT. LEFT: SURFACE TEXTURE PRE WEAR STUDY, RIGHT: SURFACE TEXTURE POST WEAR STUDY..	132
FIGURE 10.1.6: LITHIUM DISILICATE CERAMIC HIGH SPEED DIAMOND 25UM GRIT. LEFT: SURFACE TEXTURE PRE WEAR STUDY, RIGHT: SURFACE TEXTURE POST WEAR STUDY.	133

FIGURE 10.1.7: LEUCITE-REINFORCED CERAMIC SOF LEX DISC. LEFT: SURFACE TEXTURE PRE WEAR STUDY, RIGHT: SURFACE TEXTURE POST WEAR STUDY.	133
FIGURE 10.1.8: LITHIUM DISILICATE CERAMIC SOF-LEX DISC. LEFT: SURFACE TEXTURE PRE WEAR STUDY, RIGHT: SURFACE TEXTURE POST WEAR STUDY.	134
FIGURE 10.1.9: ENAMEL SPECIMENS. LEFT: SURFACE TEXTURE PRE WEAR STUDY, RIGHT: SURFACE TEXTURE POST WEAR STUDY.	134
FIGURE 10.2.1: ARITHMETICAL AVERAGE OF SURFACE HEIGHTS (RA) MEASUREMENT DATA VALUES FOR LEUCITE-REINFORCED CERAMIC AFTER COMPLETION OF DIFFERENT SURFACE FINISHING PROTOCOLS. CERAMIC GROUPS WITH STATISTICALLY SIMILAR SURFACE TEXTURE FINISHING PROTOCOLS ARE SHOWN IN THE SAME COLOUR WHEREAS SURFACE FINISHING TECHNIQUES WHICH CREATE STATISTICALLY DIFFERENT SURFACES ARE SHOWN IN DIFFERENT COLOURS.	137
FIGURE 10.2.2: ARITHMETICAL AVERAGE OF SURFACE HEIGHTS (RA) DATA VALUES (+/_S.E.) FOR LITHIUM DISILICATE CERAMIC AFTER THE VARIOUS SURFACE FINISHING PROTOCOLS. CERAMIC GROUPS WITH STATISTICALLY SIMILAR SURFACE TEXTURE FINISHING PROTOCOLS ARE SHOWN IN THE SAME COLOUR.	138
TABLE 10.3.1	139
FIGURE 11.1: ARITHMETICAL AVERAGE OF SURFACE HEIGHT (RA) DATA VALUES FOR THE DIFFERENT LEUCITE-REINFORCED CERAMIC SPECIMEN GROUPS ACCORDING TO THE SURFACE FINISHING PROTOCOLS, AFTER SUBJECTED TO 600000 WEAR CYCLES IN THE CHEWING SIMULATOR AGAINST ENAMEL SPECIMENS. CERAMIC GROUPS WITH STATISTICALLY SIMILAR SURFACE TEXTURE FINISHING PROTOCOLS ARE SHOWN IN THE SAME COLOUR	141
FIGURE 11.2: ARITHMETICAL AVERAGE OF SURFACE HEIGHTS (RA) AFTER WEAR AGAINST ENAMEL FOR THE DIFFERENT LITHIUM DISILICATE CERAMIC SPECIMEN GROUPS ACCORDING TO THE SURFACE FINISHING PROTOCOLS, AFTER SUBJECTED TO 600000 WEAR CYCLES IN THE CHEWING SIMULATOR AGAINST ENAMEL SPECIMENS. CERAMIC GROUPS WITH STATISTICALLY SIMILAR SURFACE TEXTURE FINISHING PROTOCOLS ARE SHOWN IN THE SAME COLOUR	142
FIGURE 11.3: COMPARISON OF MEAN SURFACE TEXTURE ALTITUDE PARAMETER RA OF LEUCITE REINFORCED AND LITHIUM DISILICATE POOLED CERAMIC SPECIMENS AFTER TWO BODY WEAR SIMULATION IN THE WILLYTEC CHEWING SIMULATOR.	143
FIGURE 11.4: MEAN VALUES (μM) OF ENAMEL SPECIMEN SURFACE TEXTURE ALTITUDE PARAMETER ARITHMETIC AVERAGE OF SURFACE HEIGHTS (RA) BEFORE AND AFTER <i>IN VITRO</i> WEAR SIMULATION USING A WILLYTEC CHEWING SIMULATOR.	144

FIGURE 11.5: AVERAGE TOTAL VOLUMETRIC LOSS OF ENAMEL OPPOSING LEUCITE-REINFORCED CERAMIC WITH DIFFERENT SURFACE FINISHING PROTOCOLS (MM ³). AVERAGE TOTAL VOLUMETRIC LOSS OF ENAMEL OPPOSING LEUCITE REINFORCED CERAMIC WITH DIFFERENT SURFACE FINISHING PROTOCOLS (MM ³). THE SURFACE FINISHING PROTOCOL OF THE CERAMIC GROUPS DID NOT INFLUENCE THE RATE OF OPPOSING ENAMEL WEAR. THE STATISTICALLY SIMILAR CERAMIC GROUPS ARE PRESENTED IN THE SAME COLOUR.	145
FIGURE 11.6: AVERAGE TOTAL VOLUMETRIC LOSS OF ENAMEL OPPOSING LITHIUM DISILICATE CERAMIC SPECIMENS WITH VARIOUS FINISHING PROTOCOLS. CERAMIC GROUPS WHICH RESULTED IN STATISTICALLY SIMILAR VOLUMETRIC ENAMEL LOSS ARE PRESENTED IN THE SAME COLOUR.	146
FIGURE 11.7: MEAN VOLUMETRIC LOSS OF ENAMEL SPECIMEN WHEN OPPOSING EITHER ENAMEL OR CERAMIC SPECIMENS AFTER WEAR STUDY AGAINST ENAMEL (MM ³).	148
FIGURE A1.1: ARITHMETICAL AVERAGE OF SURFACE HEIGHTS (RA) DATA VALUES FOR LEUCITE-REINFORCED CERAMIC AFTER THE VARIOUS SURFACE FINISHING PROTOCOLS.	190
FIGURE A1.2: MAGNITUDE OF THE PEAK TO VALLEY HEIGHT IN ALL CUT OFF LENGTHS (RPM) FOR LEUCITE-REINFORCED CERAMIC AFTER THE VARIOUS SURFACE FINISHING PROTOCOLS.	191
FIGURE A1.3: AVERAGE HEIGHT DIFFERENCE BETWEEN FIVE HIGHEST PEAKS AND FIVE LOWEST VALLEYS (RZ)FOR LEUCITE-REINFORCED CERAMIC AFTER THE VARIOUS SURFACE FINISHING PROTOCOLS.	192
FIGURE A1.4: ROOT MEAN SQUARE ROUGHNESS (RQ) FOR LEUCITE-REINFORCED CERAMIC AFTER THE VARIOUS SURFACE FINISHING PROTOCOLS.	193
FIGURE A2.1: ARITHMETICAL AVERAGE OF SURFACE HEIGHTS (RA) FOR LITHIUM DISILICATE CERAMIC AFTER THE VARIOUS SURFACE FINISHING PROTOCOLS.	194
FIGURE A2.2: MULTITUDE OF THE PEAK TO VALLEY HEIGHT IN ALL CUT OFF LENGTHS (RPM) FOR LITHIUM DISILICATE CERAMIC AFTER THE VARIOUS SURFACE FINISHING PROTOCOLS	195
FIGURE A2.3: ROOT MEAN SQUARE ROUGHNESS (RQ) FOR LITHIUM DISILICATE CERAMIC AFTER THE VARIOUS SURFACE FINISHING PROTOCOLS.	196
FIGURE A2.4: AVERAGE HEIGHT DIFFERENCE BETWEEN THE FIVE PEAKS AND FIVE LOWEST VALLEYS (RZ) FOR LITHIUM DISILICATE CERAMIC AFTER THE VARIOUS SURFACE FINISHING PROTOCOLS.	197
FIGURE A3.1: MAGNITUDE OF THE PEAK TO VALLEY HEIGHT IN ALL CUT OFF LENGTHS (RPM) FOR THE DIFFERENT LEUCITE-REINFORCED CERAMIC SPECIMEN GROUPS ACCORDING TO THE SURFACE FINISHING PROTOCOLS, AFTER SUBJECTED TO 600000 WEAR CYCLES IN THE CHEWING SIMULATOR AGAINST ENAMEL SPECIMENS.	198

FIGURE A3.2: AVERAGE HEIGHT DIFFERENCE BETWEEN FIVE HIGHEST PEAKS AND FIVE LOWEST VALLEYS (RZ) FOR THE DIFFERENT LEUCITE-REINFORCED CERAMIC SPECIMEN GROUPS ACCORDING TO THE SURFACE FINISHING PROTOCOLS, AFTER SUBJECTED TO 600000 WEAR CYCLES IN THE CHEWING SIMULATOR AGAINST ENAMEL SPECIMENS.	199
FIGURE A3.3: ROOT MEAN SQUARE ROUGHNESS (RQ) FOR THE DIFFERENT LEUCITE-REINFORCED CERAMIC SPECIMEN GROUPS ACCORDING TO THE SURFACE FINISHING PROTOCOLS, AFTER SUBJECTED TO 600000 WEAR CYCLES IN THE CHEWING SIMULATOR AGAINST ENAMEL SPECIMENS.	200
FIGURE A4.1: ARITHMETICAL AVERAGE OF SURFACE HEIGHTS (RA) AFTER WEAR AGAINST ENAMEL FOR THE DIFFERENT LITHIUM DISILICATE CERAMIC SPECIMEN GROUPS ACCORDING TO THE SURFACE FINISHING PROTOCOLS, AFTER SUBJECTED TO 600000 WEAR CYCLES IN THE CHEWING SIMULATOR AGAINST ENAMEL SPECIMENS.	201
FIGURE A4.2: MULTITUDE OF THE PEAK TO VALLEY HEIGHT IN ALL CUT OFF LENGTHS (RPM) AFTER WEAR AGAINST ENAMEL FOR THE DIFFERENT LITHIUM DISILICATE CERAMIC SPECIMEN GROUPS ACCORDING TO THE SURFACE FINISHING PROTOCOLS, AFTER SUBJECTED TO 600000 WEAR CYCLES IN THE CHEWING SIMULATOR AGAINST ENAMEL SPECIMENS	202
FIGURE A4.3: ROOT MEAN SQUARE ROUGHNESS (RQ) POST WEAR STUDY AFTER WEAR AGAINST ENAMEL FOR THE DIFFERENT LITHIUM DISILICATE CERAMIC SPECIMEN GROUPS ACCORDING TO THE SURFACE FINISHING PROTOCOLS, AFTER SUBJECTED TO 600000 WEAR CYCLES IN THE CHEWING SIMULATOR AGAINST ENAMEL SPECIMENS.	203
FIGURE A4.4: AVERAGE HEIGHT DIFFERENCE BETWEEN FIVE HIGHEST PEAKS AND FIVE LOWEST VALLEYS (RZ) AFTER WEAR AGAINST ENAMEL FOR THE DIFFERENT LITHIUM DISILICATE CERAMIC SPECIMEN GROUPS ACCORDING TO THE SURFACE FINISHING PROTOCOLS, AFTER SUBJECTED TO 600000 WEAR CYCLES IN THE CHEWING SIMULATOR AGAINST ENAMEL SPECIMENS.	204
FIGURE A5.1: SURFACE TEXTURE COMPARISON BETWEEN LEUCITE-REINFORCED AND LITHIUM DISILICATE CERAMIC AFTER TWO BODY WEAR SIMULATION IN THE WILLYTEC CHEWING SIMULATOR FOR 600000 CYCLES.	205
FIGURE A6.1: ENAMEL SURFACE TEXTURE ALTITUDE PARAMETER MEASUREMENTS TAKEN BEFORE AND AFTER THE WEAR STUDY.	208
FIGURE A7.1: SUMMATION OF MATERIALS AND VARIOUS POLISHING SYSTEMS.	208